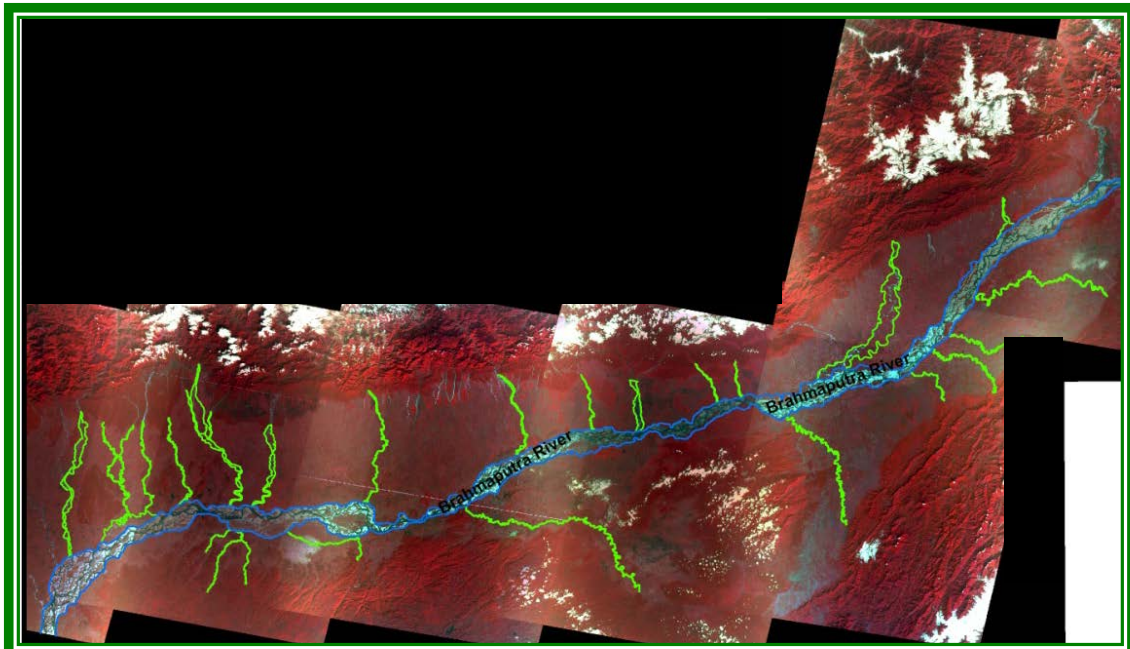


FINAL REPORT
ON
STUDY OF BRAHMAPUTRA RIVER EROSION
AND ITS CONTROL



Study Conducted

By

Department of Water Resources Development and Management
Indian Institute of Technology Roorkee

For

National Disaster Management Authority of India

May -2012

PHASE – I

**SATELLITE DATA BASED ASSESSMENT
OF
STREAM BANK EROSION OF MAIN STEM BRAHMAPUTRA
AND ITS MAJOR TRIBUTARIES**

TEAM OF INVESTIGATORS

- 1. Prof. Dr. Nayan Sharma**
- 2. Dr. R. D. Garg**
- 3. Ms. Archana Sarkar**
- 4. Md. Parwez Akhtar**
- 5. Mr. Neeraj Kumar**

TABLE OF MAJOR CONTENTS

Sl. No.	Subject	Page No.
CHAPTER -I:	SATELLITE DATA BASED ANALYSIS OF CHANNEL MORPHO-DYNAMIC STUDY FOR EROSION CONTROL OF BRAHMAPUTRA RIVER SYSTEM	
	[A] BRAHMAPUTRA RIVER MAIN STEM	3
	[B] MAJOR TRIBUTARIES OF BRAHMAPUTRA RIVER SYSTEM	46
CHAPTER - II	SATELLITE DATA BASED ANALYSIS FOR MORIGAON SITE ON BRAHMAPUTRA RIVER	60
CHAPTER - III	FINDINGS OF PHASE - I STUDY	71
	REFERENCES	75

CHAPTER - I

SATELLITE DATA BASED

ANALYSIS OF CHANNEL MORPHO-

DYNAMIC STUDY FOR EROSION

CONTROL OF BRAHMAPUTRA

RIVER SYSTEM

[A] BRAHMAPUTRA MAIN STEM

CHAPTER – I [A]

BRAHMAPUTRA MAIN STEM

SATELLITE DATA BASED ANALYSIS OF CHANNEL MORPHO-DYNAMIC STUDY FOR EROSION CONTROL OF BRAHMAPUTRA RIVER SYSTEM

INTRODUCTION

The river Brahmaputra has been the lifeline of northeastern India since ages. This mighty river runs for 2880 kms through China, India and Bangladesh. Any alluvial river of such magnitude has problems of sediment erosion-deposition attached with it; the Brahmaputra is no exception. The problems of flood, erosion and drainage congestion in the Brahmaputra basin are gigantic. The Brahmaputra river is characterized by its exceedingly large flow, enormous volume of sediment load, continuous changes in channel morphology, rapid bed aggradations and bank line recession and erosion. The river has braided channel in most of its course in the alluvial plains of Assam. The lateral changes in channels cause severe erosion along the banks leading to a considerable loss of good fertile land each year. Bank oscillation also causes shifting of outfalls of its tributaries bringing newer areas under waters. Thousands of hectares of agricultural land is suffering from severe erosion continuously in the Brahmaputra basin covering parts of states like Assam, Arunachal Pradesh, Meghalaya, Nagaland and Manipur.

In order to tackle the problem of floods and erosion various agencies including state, central government and autonomous institutions are engaged in planning and execution of flood management programs in the north eastern region. To achieve effective flood management programs a variety of structural and non structural measures are adopted. These result in reasonable degree of protection to the flood prone areas in the Brahmaputra valley. However, due to the inherent widening characteristic of the Brahmaputra river they do not sustain and adversely affect the benefits anticipated while implementing the flood control and anti-erosion works. High floods cause large scale breaches in the existing embankments bringing vast areas under flood inundation.

Stream-bank erosion and its effects on channel evolution are essential geomorphic research problems with relevance to many scientific and engineering fields. Stream-bank erosion can damage infrastructure such as highway and bridges, can cause significant problems in adjusting water-discharge rating curves, and may represent up to 80 to 90% of the sediment load in streams and rivers (Simon and Rinaldi, 2000). It contributes to total maximum daily loads (TMDLs), can be a significant source of nonpoint-source sediment and nutrient pollution, and can have adverse effects on water quality and fish spawning habitat. However, bank erosion also is beneficial and an integral part of many river ecosystem processes (Florsheim *et al.*, 2008). For example, coarse sediment from bank erosion can provide substrate for fish spawning (Flosi *et al.*, 1998) and sediment for crane roosting habitat (Johnson 1994; U.S. Geological Survey, 2005). Irregular banks provide habitat for invertebrates, fish, and birds (Florsheim *et al.*, 2008), and areas disturbed by erosion and deposition provide substrate for the establishment of riparian vegetation (Miller and Friedman, 2009). Moreover, knowledge of the dynamics of bank erosion is essential for planning dam removal projects and for designing river restoration

projects that accommodate the natural river migration processes that erode banks and build floodplains (Moody and Meade, 2008) on various time scales (Couper, 2004). Therefore, a better understanding on river channel changes is of great importance for river engineering and environmental management.

LITERATURE REVIEW

Several investigators have used remotely sensed data for ascertaining channel changes of Brahmaputra River and its tributaries. NRSA (1980) has done the river migration study of the Brahmaputra using airborne scanner survey and to carry out repetitive survey to monitor changes in landuse, river channels and banks to provide a base for estimating the response of the rivers to flood events. Sarma and Basumallick (1980) studied the bankline migration of the Burhi Dihing River (southern tributary of Brahmaputra river) using topographic maps and field survey. Bardhan (1993) studied the channel behavior of the Barak river using satellite imagery and other data to identify the river stretches, if any, which remained reasonably stable during the period 1910-1988. SAC (Space Application Centre), Ahmedabad and Brahmaputra Board (1996) jointly took up a study to access the extent of river erosion in Majuli island in order to identify and delineate the areas of the island which have undergone changes along the bankline due to dynamic behaviour of the river. Based on this report and other collateral data, Brahmaputra Board (1997) has prepared a status report on the erosion problem of Majuli Island. Naik *et al.* (1999) studied the erosion at Kaziranga National Park using remote sensing data. Goswami *et al.* (1999) carried out a study on river channel changes of the Subansiri (northern tributary of Brahmaputra River) in Assam, India using information of topographic sheet and satellite data. Mani *et al.* (2003) studied the erosion in Majuli island using remote sensing data. Bhakal *et al.* (2005) have quantified the extent of bank erosion in Brahmaputra River near Agyathuri in Assam, India over a period of thirty years (1973-2003) using remote sensing data integrated with GIS. Kotoky *et al.* (2005) studied selected reach of Brahmaputra with two sets of Survey of India toposheets (1914 and 1975) and a set of IRS satellite images (1998, IRS-1B, LISS II B/W geocoded data by dividing the 270 km channel configuration from Panidihing Reserve Forest to Holoukonda Bil of the Brahmaputra River into ten segments. Sarma *et al.* (2007) studied the nature of bankline migration as well as made a quantitative assessment of the total amount of bank area subjected to erosion at different parts of Burhi Dihing River (southern tributary of Brahmaputra river) course during a period of time from 1934 to 2004 using Survey of India (SOI) toposheets, aerial photographs and IRS satellite data. Das and Saraf (2007) made a study in respect to a trend in river course changes of Brahmaputra river and influence of various surrounding geotectonic features for varying period between 1970-2002 for different sections of the river using Landsat-MSS, TM and ETM images. However, a comprehensive study of the bank erosion and channel migration of the entire Brahmaputra in India including its major tributaries with most recent satellite data has not yet been reported in the literature.

Fluvial landforms are produced by the action of flowing water in the terrestrial environment, whereas fluvial geomorphic processes are those natural processes that produce, maintain and change fluvial landforms. The channel pattern or landform of a reach of an alluvial river reflects the hydrodynamics of flow within the channel and the associated processes of sediment transfer and energy dissipation. Channel

patterns form a continuum in response to varying energy conditions ranging from straight and meandering to braided forms. Generally, braiding is favoured by high energy fluvial environments with steeper gradients, large and variable discharges, dominant bed load transport and non-cohesive banks lacking stabilization by vegetation (Richards, 1982). The secondary flow component also contributes to the growth of channel deformations (Bathurst et al., 1979).

Kotoky et al (2005) studied selected reach of Brahmaputra with two sets of Survey of India toposheets (1914 and 1975) and a set of IRS satellite images covering the cloud-free period. For assessing rate of erosion, the channel configuration was divided for a distance of 270 km from Panidihing Reserve Forest to Holoukonda Bil of the Brahmaputra River into ten segments (I to X) at an interval of 15 minute east longitude in downstream direction. The bank-lines were superimposed upon each other and the areas subjected to erosion and deposition were measured with the help of a digital planimeter. Kotoky et al (2005) reported that the activity of erosion/deposition processes that operated was not similar for the periods 1914–75 and 1975–98.

However, Kotoky's(2005) work was restricted to some of the limited stretches of river Brahmaputra and lacks a representative braiding tendency of the river in Assam flood plains, moreover braiding phenomenon which has been the major stakeholder of causative erosion and deposition was not dealt with. The remote sensing data used for study pertained to previous IRS sensor namely LISS I with coarse resolution resulting in possibilities of enhanced discrepancy while conducting analysis for studying bank shifting trend of River Brahmaputra.

Existing Braiding Indicators

Several past studies had presented discrimination between the straight, meandering, and braided streams on the basis of discharge and channel slope. Lane (1957) suggested the following criterion for the occurrence of braiding.

$$S > 0.004 (Q_m)^{-0.25} \quad (1)$$

Where, Q_m = mean annual discharge; and S = channel slope.

Using bank full discharge Q_b , Leopold and Wolman in 1957 (Richards, 1982) proposed the relationship for braiding to occur, which also predicts braids at higher slopes and discharges:

$$S > 0.013 Q_b^{-0.44} \quad (2)$$

Where, Q_b = bank full discharge.

Antropovskiy (1972) developed the following criterion for the occurrence of braiding

$$S > 1.4Q_b^{-1} \quad (3)$$

Leopold and Wolman (1957) also indicated that braided and meandering streams can be separated by the relationship:

$$S = 0.06 Q^{0.44} \quad (4)$$

Where, S = channel; and Q = water discharge.

However, these indicators have been criticized by Schumm and Khan (1972) as none of these recognizes the importance of sediment transport. These results imply a higher power expenditure rate in braided streams, a conclusion reinforced by Schumm and Khan's (1972) flume experiments. However, none of these investigators recognizes the control of channel pattern by sedimentology. Since, bed material transport and bar formation are necessary in both meander and braid development processes, the threshold between the patterns should relate to bed load.

Henderson (1961) re-analyzed Leopold and Wolman's data to derive an expression including d_{50} , median grain size (mm):

$$S > 0.002 d_{50}^{1.15} Q_b^{-0.46} \quad (5)$$

Where, d_{50} = median grain size

According to equation (5), a higher threshold slope is necessary for braiding in coarse bed materials. Bank material resistance affects rate of channel migration and should also influence the threshold, although its effect may be difficult to quantify and also be non-linear since greater stream power is required to erode clays and cobbles than sands.

Parker's stability analysis (1976) indirectly illustrates the effects of bank material resistance by defining the meander - braid threshold as:

$$S/F_r = D/B \quad (6)$$

Where, D = mean depth of the flow; B = width of the stream, and Fr = Froude number. However, depth, width and Froude number may be expressed in terms of discharge and bank silt-clay percentage, as suggested by Schumm (Richards, 1982). Meandering occurs when $S/F_r \leq D/B$, braiding occurs when $S/F_r \geq D/B$, and transition occurs in between $S/F_r \sim D/B$.

Ferguson (1981) suggested for braiding to occur, which predicts steeper threshold slopes for braiding in channels with resistant silty banks.

$$S > 0.0028 (Q_b)^{-0.34} B_c^{0.90} \quad (7)$$

Where, B_c = percentage of silty clay content in the bank material.

Measures of the degree of braiding generally fall into two categories: (i) the mean number of active channels or braid bars per transect across the channel belt; and (ii) the ratio of sum of channel lengths in a reach to a measure of reach length (total sinuosity). The sinuosity, P is thalweg length / valley length.

Smith (1970) illustrated the measurement of cross - section bed relief, measured by the index.

$$BRI = \frac{2[(T_1+T_2+\dots+T_n) - (t_1+t_2+t_3+\dots+t_n)] \pm T_{e_1}, T_{e_2}}{B_L} \quad (8)$$

Where, T_i = height maxima between hollows; t_i = minima between peaks; B_L = transect length; and T_e = end heights.

Sharma (2004) developed Plan Form Index (PFI), Flow Geometry Index (FGI), and Cross-Slope ratio for identifying the degree of braiding of highly braided river. The PFI, FGI and Cross- Slope formulae have been given below:

$$\text{Plan Form Index} = \frac{\frac{T}{B} \times 100}{N} \quad (9)$$

$$\text{Flow Geometry Index} = \left[\frac{\sum d_i x_i}{WxD} \right] \times N \quad (10)$$

$$\text{Cross-Slope} = \frac{\frac{B_L}{2}}{(Bank\ level - Av.\ bed\ level)} \quad (11)$$

where, T = flow top width; B = overall width of the channel; B_L = Transect length across river width; N = number of braided channel; d_i and x_i are depth and top lateral distance of submerged sub-channel; and D = hydraulic mean depth.

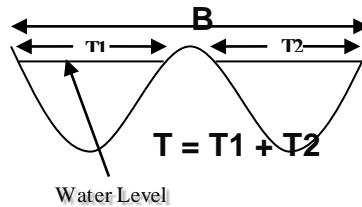


Fig. 1 Definition sketch of PFI

Plan Form Index (PFI) in Equation 9 (Definition sketch as shown in Fig. 1) reflects the fluvial landform disposition with respect to a given water level and its lower value is indicative of higher degree of braiding. For providing a broad range of classification of the braiding phenomenon, the following threshold values for PFI are proposed by Sharma (2004).

Highly Braided:	$PFI < 4$
Moderately Braided:	$19 > PFI > 4$
Low Braided:	$PFI > 19$

STUDY OBJECTIVE

The present paper briefly describes a study of the Brahmaputra river - its entire course in Assam from upstream of Dibrugarh up to the town Dhubri near Bangladesh border for a stretch of around 620 kms and its major tributaries (13 northern and 10 southern) for a period of recent 18 years (1990-2008) using an integrated approach of Remote Sensing and Geographical Information System (GIS). The satellite data has provided the information on the channel configuration of the river system on repetitive basis revealing much needed data on the changes in river morphology, erosion pattern and its influence on the land, stable and unstable reaches of the river banks, changes in the main channel of the Brahmaputra river, changes in the major tributaries of the Brahmaputra river, etc

In this study, it is endeavored to assess the channel morphological changes actuated by stream bank erosion process. The newer braiding indicator PFI for Brahmaputra River formulated by Sharma (2004) has been adopted in the study to analyze the braiding behavior. Attempt has been made to assess the temporal and spatial variation of braiding intensities along the whole stretch of Brahmaputra in Assam plains of Indian Territory based on the remote sensing image analyses, which is the forcing function of erosion and thereby causing severe yearly land loss.

THE STUDY AREA

The Brahmaputra river, termed a moving ocean, is an antecedent snow fed river which flows across the rising young Himalayan Range. Geologically, the Brahmaputra is the youngest of the major rivers of the world. It originates at an altitude of 5,300 m about 63 Km south-east of the Mansarowar lake in Tibet. The river is known as Psangpo in Tibet. Flowing eastward for 1,625 km. over the Tibetan plateau, the Tsangpo enters a deep narrow gorge at Pe (3,500 m.) and continues southward across the east-west trending ranges of the Himalayas, viz. the Greater

Himalayas, Middle Himalayas and sub-Himalayas. After crossing the Indo-China border near Pasighat the river is called as the Siang or the Dihang. Two major rivers namely the Dibang and the Lohit join the Dihang at a short distance upstream of Kobo to form the river Brahmaputra. The river flows westward through Assam for about 700 Km distance from Dhola until downstream of the town Dhubri, where it abruptly turns south and enters Bangladesh. The gradient of the Brahmaputra river is as steep as 4.3 to 16.8 m./km. in the gorge section upstream of Pasighat, but near Guwahati it is as flat as 0.1m./km. The dramatic reduction in the slope of the Brahmaputra as it cascades through one of the world's deepest gorges in the Himalayas before flowing in to the Assam plains explains the sudden dissipation of the enormous energy locked in it and the resultant unloading of large amounts of sediments in the valley downstream.

In the course of its 2,880 km. journey, the Brahmaputra receives as many as 22 major tributaries in Tibet, 33 in India and three in Bangladesh. The northern and southern tributaries differ considerably in their hydro-geomorphological characteristics owing to different geological, physiographic and climatic conditions. The north bank tributaries generally flow in shallow braided channels, have steep slopes, carry a heavy silt charge and are flashy in character, whereas the south bank tributaries have a flatter gradient, deep meandering channels with beds and banks composed of fine alluvial soils, marked by a relatively low sediment load.

Due to the colliding Eurasian (Chinese) and Indian tectonic plates, the Brahmaputra valley and its adjoining hill ranges are seismically very unstable. The earthquakes of 1897 and 1950, both of Richter magnitude 8.7, are among the most severe in recorded history. These earthquakes caused extensive landslides and rock falls on hill slopes, subsidence and fissuring in the valley and changes in the course and configuration of several tributary rivers as well as the main course

The drainage basin of the Brahmaputra extends to an area of about 580,000 km², from 82°E to 97° 50' E longitudes and 25° 10' to 31° 30' N latitudes. The basin spans over an area of 293,000 km² (50.51%) in Tibet (China), 45,000 km² (7.75%) in Bhutan, 194,413 km² (33.52%) in India and 47,000 km² (8.1%) in Bangladesh. Its basin in India is shared by six states namely, Arunachal Pradesh (41.88%), Assam (36.33%), Nagaland (5.57%), Meghalaya (6.10%), Sikkim (3.75%) and West Bengal (6.47%) (59).

For the present study, a reach of 620 Km on the main stem of Brahmaputra River, i.e., its entire course in Assam from upstream of Dibrugarh up to the town Dhubri near Bangladesh border has been considered. Twenty three major tributaries (13 northern and 10 southern) within India have also been considered.

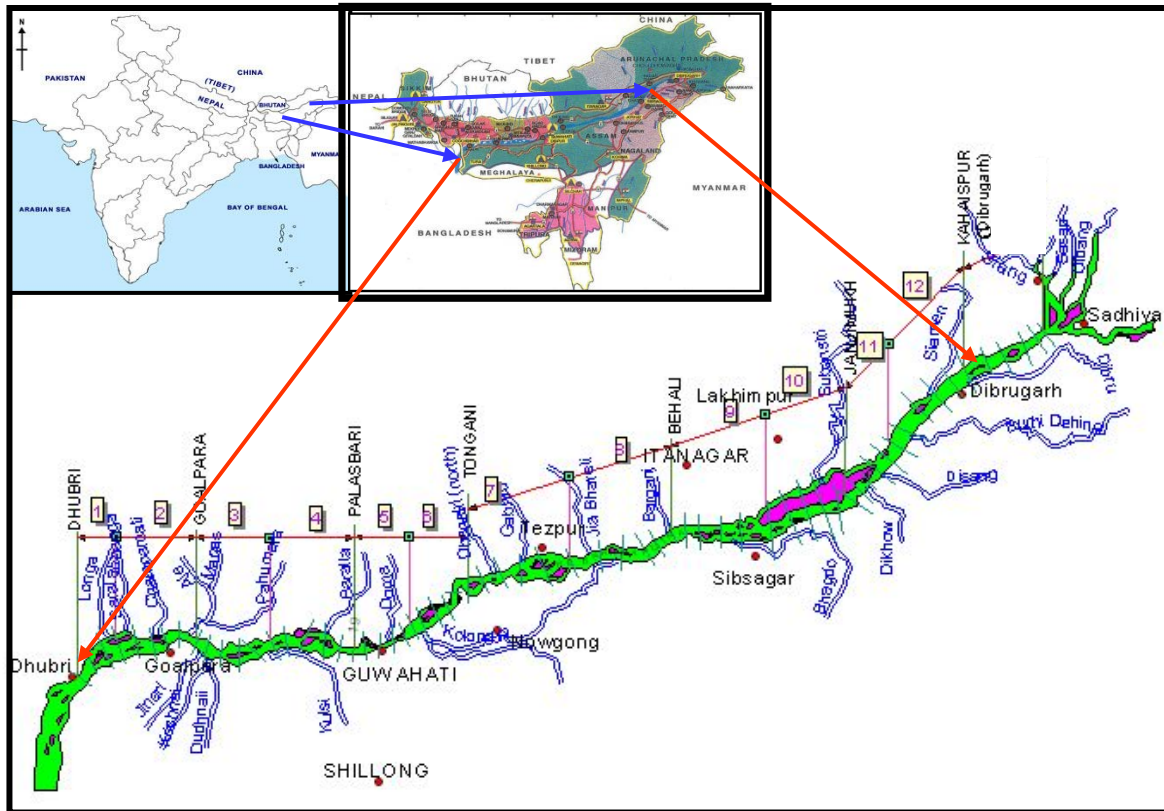


Fig. 2: Study Area

DATA USED

The basic data used in this study are digital satellite images of Indian Remote Sensing (IRS) LISS-I and LISS-III sensor, comprising of scenes for the years 1990, 1997, and 2008. In order to bring all the images under one geometric co-ordinate system, these are geo-referenced with respect to Survey of India (1:50,000 scale) topo-sheets using second order polynomial. IRS P6 LISS images of 1990, 1997 and 2008 years are geometrically rectified with reference to the Landsat images of the same area. The UTM projection and WGS 84 datum has been taken for geo-referencing. Rectification of the images was done with a residual RMS (root mean square error) of less than 1. Subsequently the re-sampling was performed at 23.5 m resolution using Nearest Neighborhood technique.

The entire river from Dhubri to upper Assam beyond Dibrugarh has been divided into 12 reaches. Each reach comprised of 10 cross sections. The bank line of the Brahmaputra River is demarcated from each set of imageries and the channel patterns are digitized using Arc GIS software. Cross sections are shown Fig. 2.

The spatial resolution of LISS-III is 23.5 m. The data used in the analysis have been presented in Table 1. ERDAS IMAGINE 8.6 image processing software has been used to perform the image processing works. Then satellite images of the other years were co-registered using image-to-image registration technique.

TABLE 1: CHARACTERISTICS OF THE REMOTE SENSING DATA USED

Satellite /sensor	Path/row	Acquisition	Spatial resolution	Spectral bands and channels
IRS 1C and D/ LISS-III (Standard Product)	112/52	1990, 1997, 2007-08	23.5m	Visible band- (Green channel) (0.52-0.59 μ m)
IRS 1C and D/ LISS-III (Standard Product)	112/53	1990, 1997,2007- 08	23.5m	Visible band- Red channel (0.62-0.68 μ m) Near infrared (NIR) (0.77 - 0.86 μ m)

For convenience in computing, the study area of around 622.73 km from Dhubri to Kobo beyond Dibrugarh in Upper Assam is considered as shown in Figs 2.

METHODOLOGY

Appropriate GIS applications are done to precisely extract bank line information. Segment wise satellite-derived plan-form maps have been developed for the discrete years i.e. 1990, 1997 and 2007-08.

Data Geo Referencing and Image Processing

One set of Survey of India topo-sheets (1965) and digital satellite images of IRS LISS-I and LISS-III sensors, comprising scenes for the years 1990, 1997 and 2007-08 are used for the present study. In order to assess the rate of erosion, maps and imagery are registered and geo-referenced with respect to Survey of India (1:50,000 scale) toposheets using second order polynomial. Using ERDAS imagine software, the satellite data have been geo-referenced with respect to 1:50,000 Survey of India topo-sheets.

The geo-referencing was done by the hardcopy map on digitizing table using second order equation with root mean square error less than 1.0 and nearest neighborhood re-sampling technique to create a geo-referenced image of pixel size 23.5m x 23.5m. Subsequently other images were also registered with the geo-referenced image using image-to-image registration technique. The registered images for different dates pertaining to study area were used for further analysis.

Delineation of River Bank Line

For convenience, the main river has been divided into 120 strips, and reference cross sections were drawn at the boundary of each strip. Each ten cross sections are grouped as a reach with numbering from downstream to upstream of the river (of equal base length (Fig. 3; Table -2). Base line of Latitude 25.966° and Longitude 90° E has been taken as permanent reference line. The derived data for each cross section from satellite images of years 1990, 1997, 2008 have been analyzed and the bank lines are also digitized for all the years. The length of arcs of both the left and right banks for all the above years are found out using GIS software. The years 1990 , 1997 and 2008 have been taken for analyzing erosion and deposition along the river left bank as well as right bank.

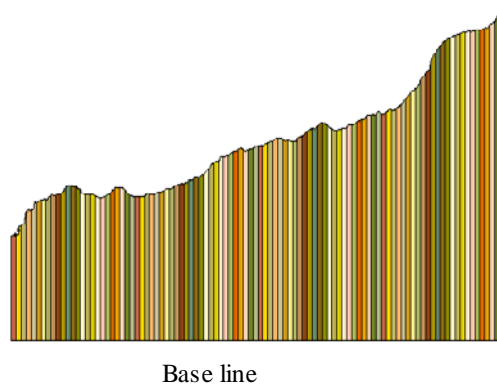


Fig.3: 120 strips of left bank

Intermediate channel widths, and total widths of channel at each predefined cross sections are measured using GIS software tools for computing Plan Form Indices for each cross sections for further analysis.

Erosion in north and south banks of the river area during the study period (that is 1990-2007-08 and 1997-2007-08) is estimated by GIS software tools through delineating the river bank lines and drawing polygons within bank line variations within the study period

Remote sensing satellite data having ability to provide comprehensive, synoptic view of fairly large area at regular interval with quick turn around time integrated with GIS techniques makes it appropriate and ideal for studying and monitoring river erosion and its bank line shifting. Various studies in this regard have been carried out for some major rivers all over the world. Surian (1999) reported the channel changes of the Piave River in the Eastern Alps, Italy, which occurred in response to human interventions in the fluvial system through a historical analysis using maps and aerial photographs. A typical study of channel migration by Yang *et al.* (1999) in Yellow river (China) made use both analog and digital data with a time sequential imageries of 19 dates from 1976 to 1994. Rinaldi (2003) presented changes in channel width of the main alluvial rivers of Tuscany (central Italy) during the 20th century by comparing available aerial photographs (1954 and 1993-98). Surian and Rinaldi (2003) reviewed all existing published studies and available data on most Italian rivers that experienced considerable channel adjustment during the last centuries due to various types of human disturbance. Fuller et al (2003) quantified three-dimensional morphological adjustment in a chute cutoff (breach) alluvial channel using Digital Elevation Model (DEM) analysis for a 0.7 km reach of the River Coquet, Northumberland, UK. Li et al (2007) examined human impact on channel change in Jianli reach of the middle Yangtze River of China employing 1:100,000 channel distribution maps from 1951, 1961 and 1975 and 1:25,000 navigation charts from 1981 and 1997 to reconstruct channel change in the study reach. Kummur et al (2008) assessed bank erosion problems in the Vientiane–Nong Khai section of the Mekong River, where the Mekong borders Thailand and Lao PDR using two Hydrographic Atlases dated 1961 and 1992, and SPOT5 satellite images of 2004 and 2005 with a resolution of 2.5m in natural colours.

PLAN FORM INDEX (PFI)

Plan Form Index (PFI) reflects the fluvial landform disposition with respect to a given water level and its lower value is indicative of higher degree of braiding.

The computed Plan Form Index for each reference cross-section totalling 120 in numbers across the study reaches are plotted against reach cross-section number in Fig. 7 for three discrete years. From the plot, it can be readily inferred that from 1990 to 2007-08, the PFI values by and large decreases significantly indicating the increase in braiding intensities in majority of cross sections considering the fixed threshold values of PFI given for measuring braiding intensity mentioned in Sec. 2 (Sharma, 2004) of this paper.

The analysis can further be extended by computing mean PFI values for reach-1 to reach 12 comprising of ten cross-sections each, shown in tables 3, 4, 5 for the discrete years. Similarly, extreme values that are maximum PFI (indicating least braiding within the reach) and minimum PFI (indicating highest braiding within the reach) for each reach are computed and shown in Table-6. The corresponding plot for Mean, Minimum and Maximum PFI against reach numbers are plotted and shown in Fig. 4, 5 and 6 respectively. Mean PFI enveloping with maximum and minimum cross-sectional PFI suggest the ranges of variation in braiding intensities within a reach. It can be easily figured out that maximum values are predominant in the year 1990, whereas in 2007-08 minimum values are predominant. All three statistically measured PFIs are registering little changes or similar trend in three to four identified reaches with rock-outcrops numbered 2, 4, 6-7 and 9, which are in the vicinity of Jogighopa, Guwahati, Tezpur and Bessamora in Majuli.

It strongly suggests that irrespective of the time, the aforementioned four discrete reaches show little changes in braiding intensity and pattern. It confirms the existence of the aforesaid four geological control points which hold the river, and in between there are intermittent fanning out of the river with time. Other than these river control points, more braiding is expected where bank line configurations and characteristics are conducive for braiding to occur in other reaches.

As discussed, the graphical plots of Plan Form Index for the Brahmaputra River shows increasing trend thereby registering an increasing level of braiding, as can be seen from the threshold limits as described in Sec. 2 of this paper. Plots for all reference cross sections for the years 1990, 1997 and 2007-08 between PFI's and cross section numbers shows the increasing trend of braiding with time. These plots clearly demonstrate the rationality of using the Plan Form Index as a measure of braiding and closely conform to the actual physical situation of the occurrence of braiding vividly depicted in satellite images. In light of the threshold values of Plan Form Index, it can be readily inferred from graphical plots showing maximum, minimum and mean values of PFIs of cross sections that have heavy with moderate and low braiding characteristics resulting in a very complex channel hydrodynamics.

TABLE 2: IDENTIFICATION OF REACHES IN RESPECT OF THE LOCATION IN THE VICINITY

Reach	Locations in Vicinity
1	Dhubri
2	Goalpara
3	Palasbari
4	Guwahati
5	Morigaon (Near Mangaldai)
6	Morigaon (Near Dhing)
7	Tezpur
8	U/s of Tezpur (Near Gohpur)
9	Majuli
10	U/s of Majuli (Near Sibsagar)
11	Dibrugarh
12	U/s of Dibrugarh

TABLE 3: PLAN FORM INDEX (PFI) ESTIMATION OF BRAHMAPUTRA RIVER FOR 1990 YEAR

Reach	Plan Form Index	Threshold Indicator
1	22.69	Low Braided
2	15.39	Moderately Braided
3	10.55	Moderately Braided
4	55.97	Low Braided
5	14.19	Moderately Braided
6	28.34	Low Braided
7	31.94	Low Braided
8	19.12	Low Braided
9	10.14	Moderately Braided
10	13.61	Moderately Braided
11	12.38	Moderately Braided
12	20.95	Low Braided

**TABLE 4: PLAN FORM INDEX (PFI) ESTIMATION OF
BRAHMAPUTRA RIVER FOR 1997 YEAR**

Reach	Plan Form Index	Threshold Indicator
1	8.94	Moderately Braided
2	8.60	Moderately Braided
3	7.71	Moderately Braided
4	33.62	Low Braided
5	13.55	Moderately Braided
6	14.74	Moderately Braided
7	17.21	Moderately Braided
8	10.77	Moderately Braided
9	10.69	Moderately Braided
10	7.87	Moderately Braided
11	6.81	Moderately Braided
12	4.89	Moderately Braided

**TABLE 5: PLAN FORM INDEX (PFI) ESTIMATION OF
BRAHMAPUTRA RIVER FOR 2008 YEAR**

Reach	Plan Form Index	Threshold Indicator
1	15.66	Moderately Braided
2	20.30	Low Braided
3	9.99	Moderately Braided
4	73.64	Low Braided
5	8.08	Moderately Braided
6	7.78	Moderately Braided
7	18.50	Moderately Braided
8	6.89	Moderately Braided
9	6.34	Moderately Braided
10	6.54	Moderately Braided
11	5.41	Moderately Braided
12	2.61	Heavily Braided

TABLE 6: COMPARISON OF PLAN FORM INDEX (PFI) FOR THE YEAR 1990, 1997 AND 2008 FOR THE RIVER BRAHMAPUTRA

Reach No.	PFI(1990)			PFI(1997)			PFI(2008)			Remarks
	Mean	Minimum	Maximum	Mean	Minimum	Maximum	Mean	Minimum	Maximum	
1	22.69	9.90	45.16	8.94	13.22	4.37	15.66	5.74	38.65	Highly Braided: PFI < 4 Moderately Braided: 19 > PFI > 4 Low Braided: PFI > 19
2	15.39	5.23	48.67	8.60	3.50	21.09	20.30	4.42	98.05	
3	10.55	3.50	31.15	7.71	2.83	16.22	9.99	3.75	24.79	
4	55.97	8.46	113.89	33.62	8.94	124.48	73.64	16.47	136.85	
5	14.19	6.18	20.92	13.55	4.52	38.39	8.08	4.88	19.67	
6	28.34	9.98	108.61	14.74	7.73	30.46	7.78	3.40	31.30	
7	31.94	18.23	82.47	17.21	7.48	37.27	18.50	4.37	100.00	
8	19.12	3.28	83.19	10.77	4.39	32.43	6.89	3.84	14.95	
9	10.14	5.25	22.71	10.69	3.64	48.37	6.34	2.00	17.55	
10	13.61	6.09	34.31	7.87	5.25	10.65	6.54	3.77	12.57	
11	12.38	7.65	27.93	6.81	3.36	12.23	5.41	3.52	10.91	
12	20.95	4.27	87.05	4.89	2.76	7.57	2.61	1.63	3.70	

Note: There is considerable increase in braiding intensity during the period 1990-2008 as can be seen from Table -5

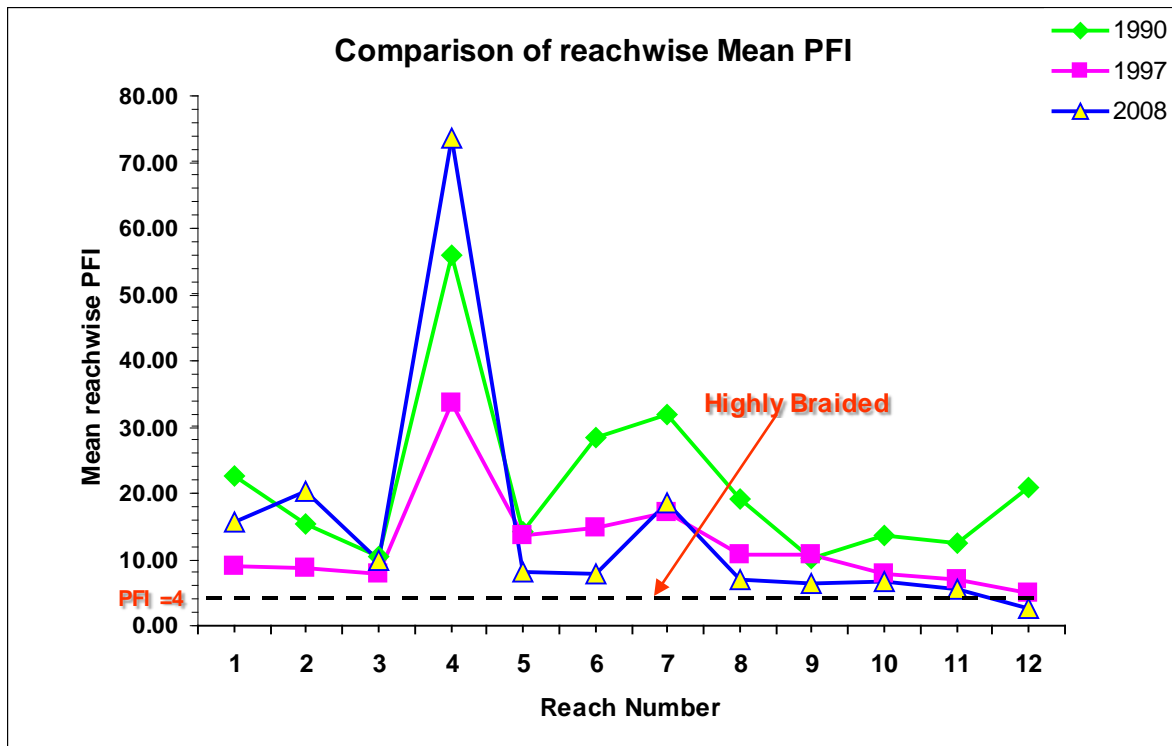


Fig. 4: Change in the Reach wise MEAN Plan Form Index (PFI) Values in different reaches of the Brahmaputra River in 1990, 1997 and 2008 year

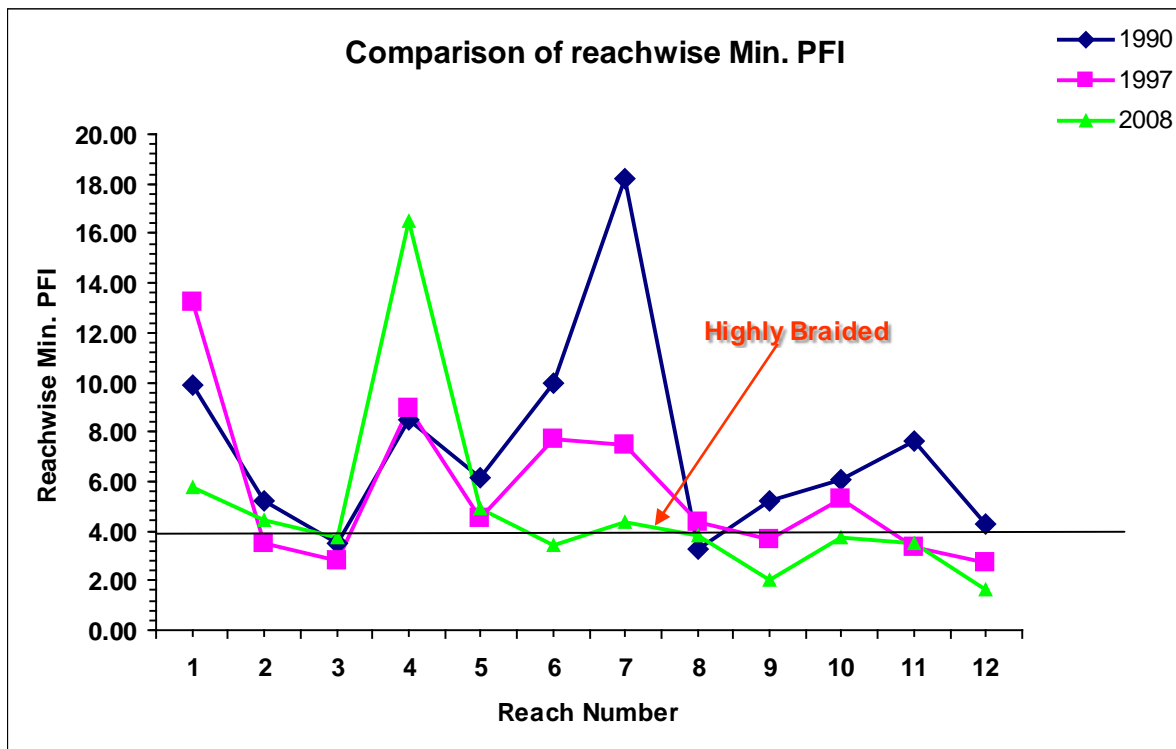


Fig. 5: Change in the Reach wise MINIMUM Plan Form Index (PFI) Values in different reaches of the Brahmaputra River in 1990, 1997 and 2008 year

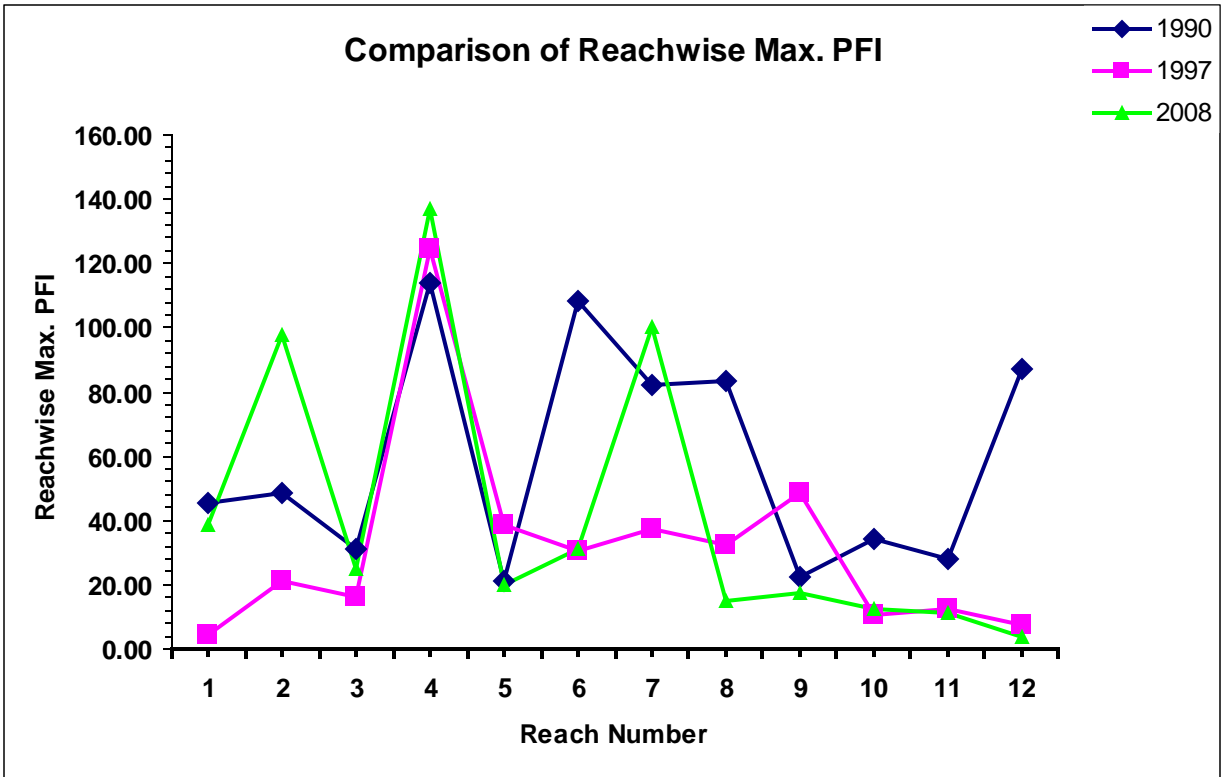


Fig. 6: Change in the Reach wise MAXIMUM Plan Form Index (PFI) Values in different reaches of the Brahmaputra River in 1990, 1997 and 2008 year

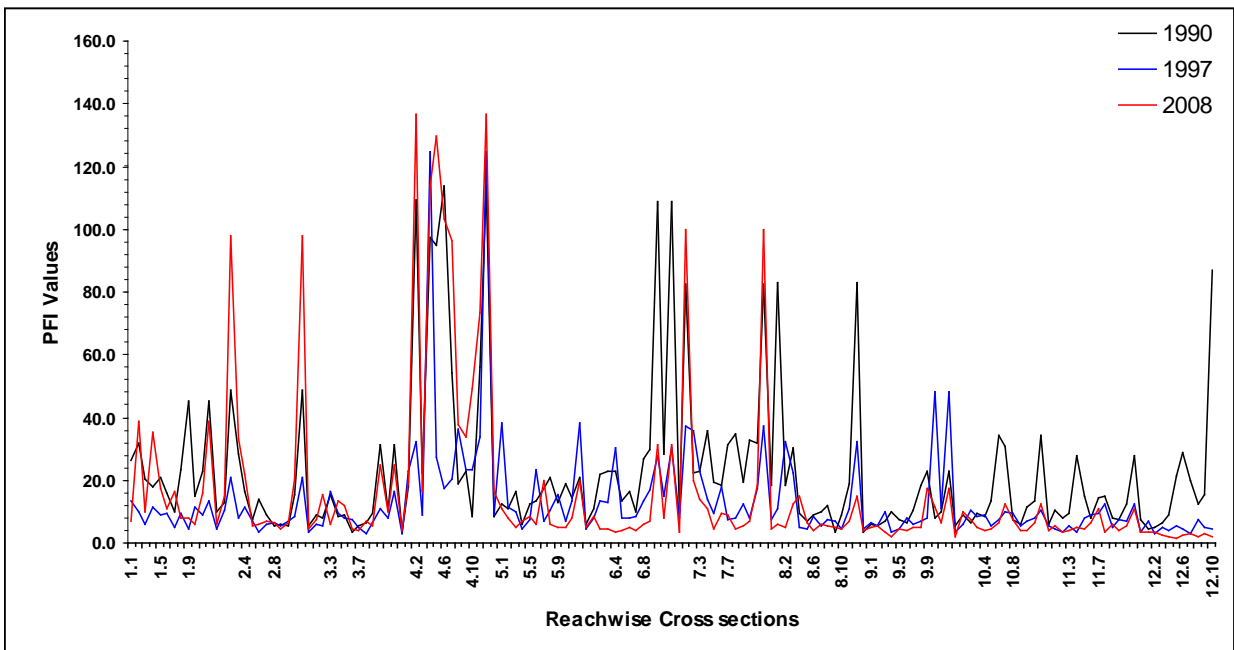


Fig. 7: Cross-section wise Plan Form Index (PFI) Values in different reaches of the Brahmaputra River in 1990, 1997 and 2008 year

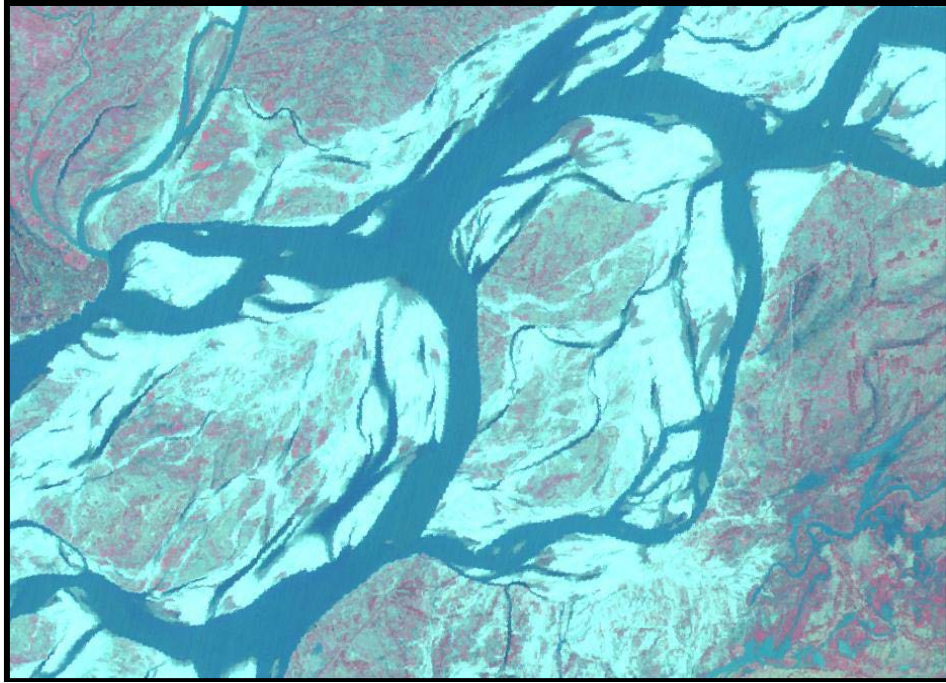


Fig. 8: The Moderately Braided Channels (Reach 1 - Near Dhubri) in IRS 1C LISS - III image of 1997 year with Plan Form Index value 11.2

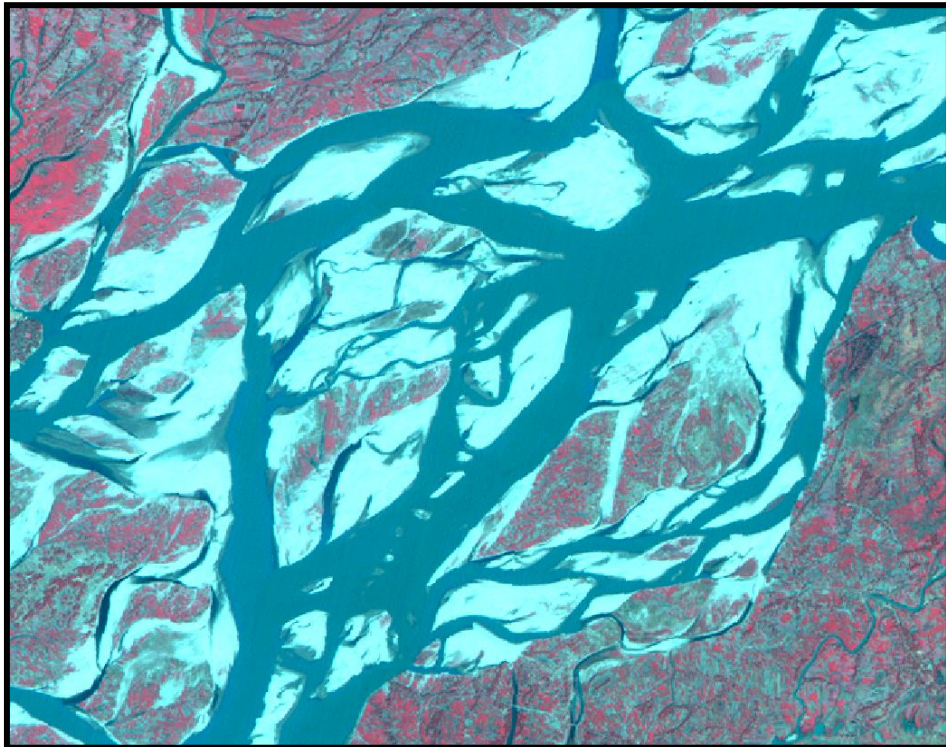


Fig. 9: The Highly Braided Channels (Reach 1 - Near Dhubri) in IRS P6 LISS - III image of 2008 year with Plan Form Index value 3.7



Fig. 10: The Moderately Braided Channels (Reach 2 – Near Barpeta) in IRS 1C LISS - III image of 1997 year with Plan Form Index value 4.1

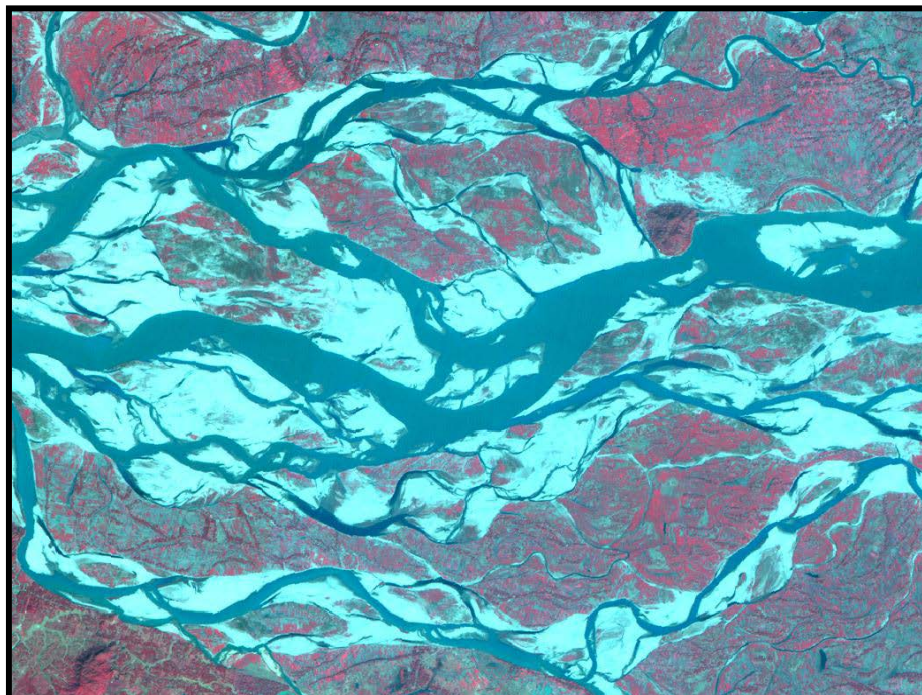


Fig. 11: The Highly Braided Channels (Reach 2 – Near Barpeta) in IRS P6 LISS - III image of 2008 year with Plan Form Index value 1.9



Fig. 12: The Moderately Braided Channels (Reach 3 - Palashbari Gumi) in IRS 1C LISS - III image of 1997 year with Plan Form Index value 2.4

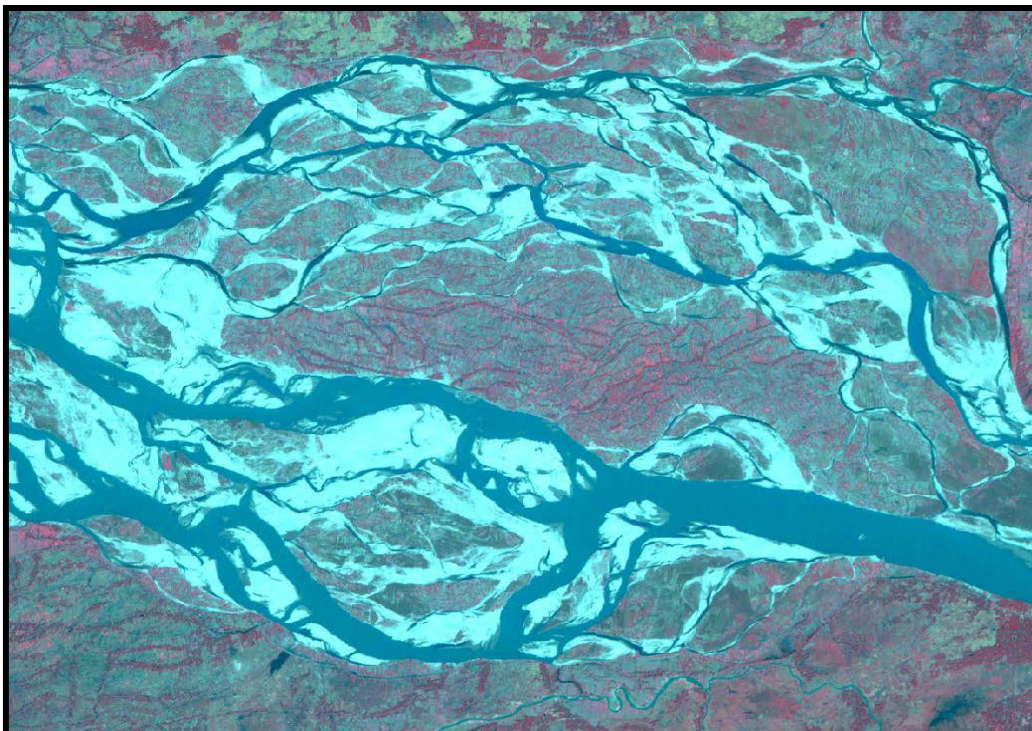


Fig. 13: The Highly Braided Channels (Reach 3 - Palashbari Gumi) in IRS P6 LISS - III image of 2008 year with Plan Form Index value 1.6

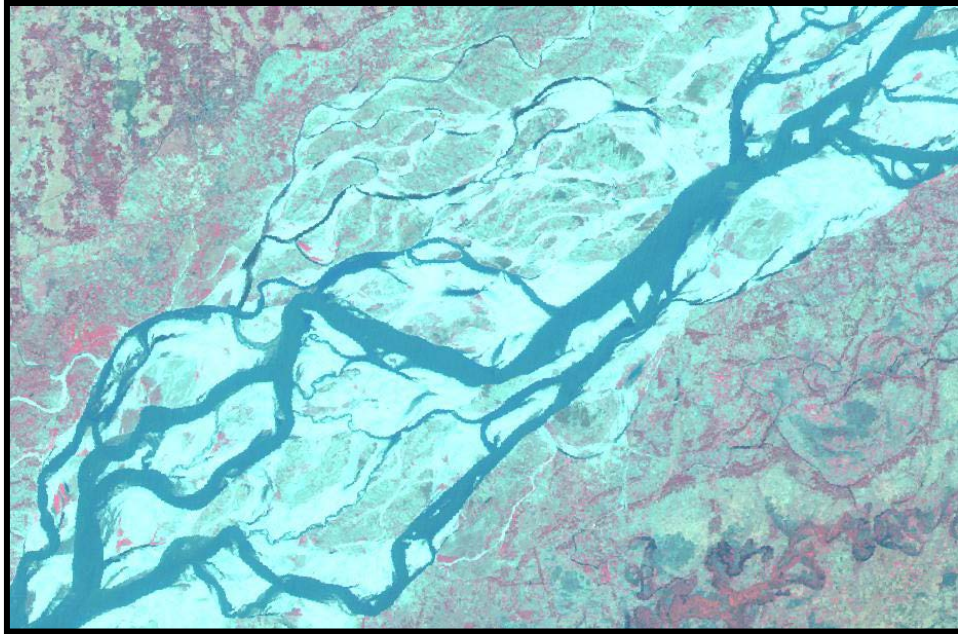


Fig. 14: The Highly Braided Channels (Reach 5 – Near Mangaldai) in IRS 1C LISS - III image of 1997 year with Plan Form Index value 2.1

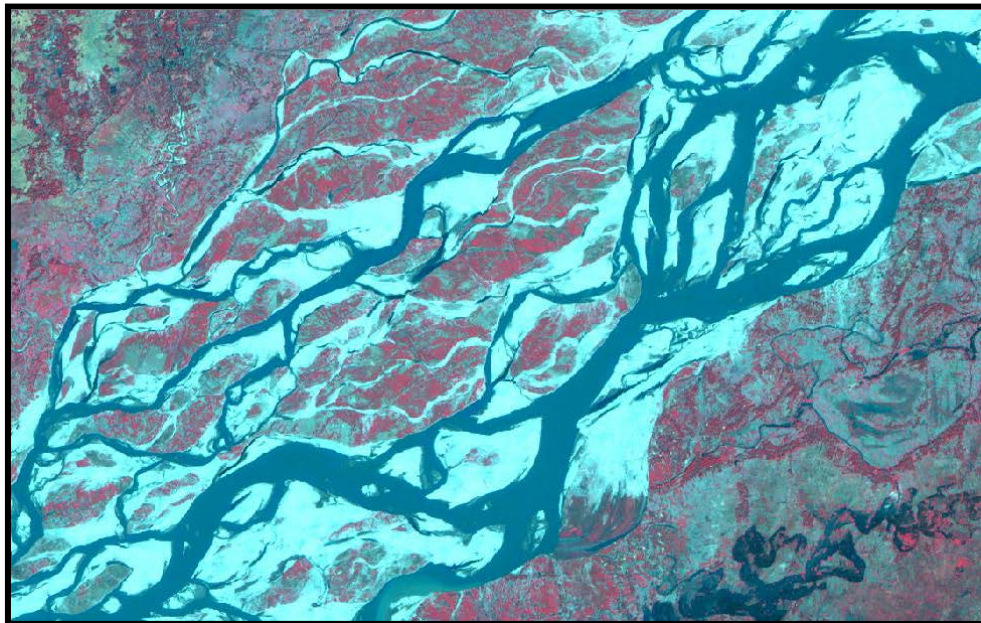


Fig. 15: The Highly Braided Channels (Reach 5 – Near Mangaldai) in IRS P6 LISS - III image of 2008 year with Plan Form Index value 2.7

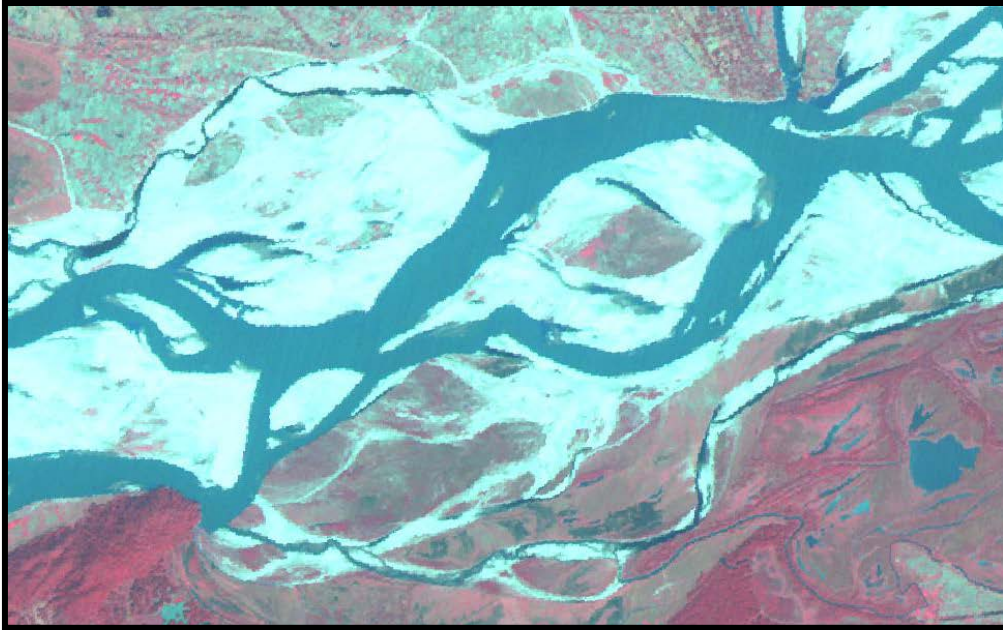


Fig. 16: The Moderately Braided Channels (Reach 7 – Upstream Silghat) in IRS 1C LISS - III image of 1997 year with Plan Form Index value 5.5

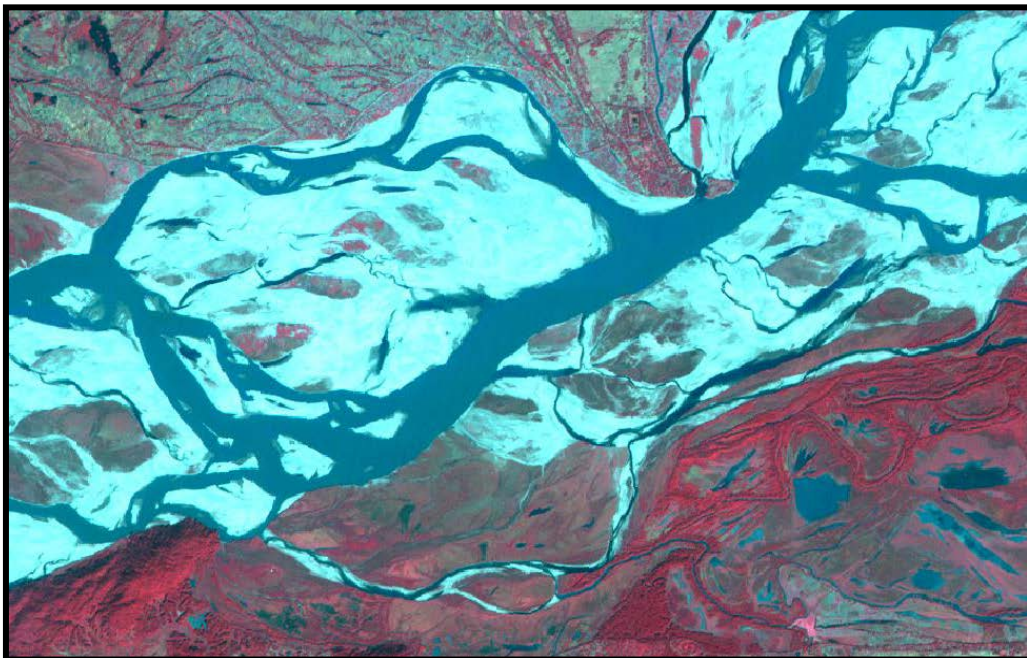


Fig. 17: The Highly Braided Channels (Reach 7 – Upstream Silghat) in IRS P6 LISS - III image of 2008 year with Plan Form Index value 3.7

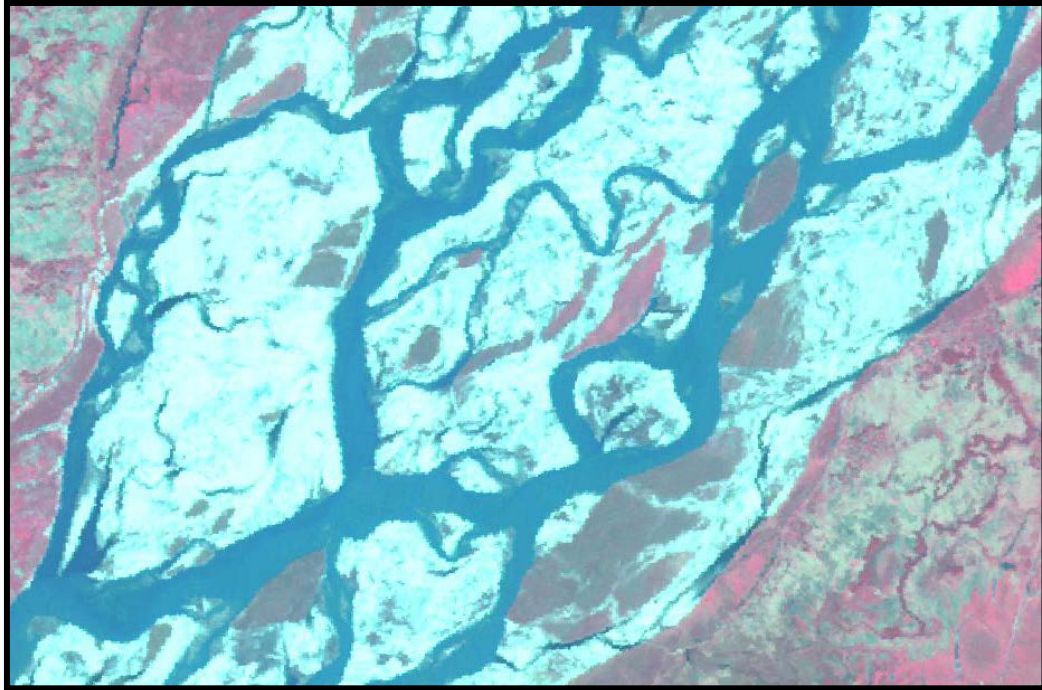


Fig. 18: The Moderately Braided Channels (Reach 10 – Upstream Sibsagar) in IRS 1C LISS - III image of 1997 year with Plan Form Index value 5.2

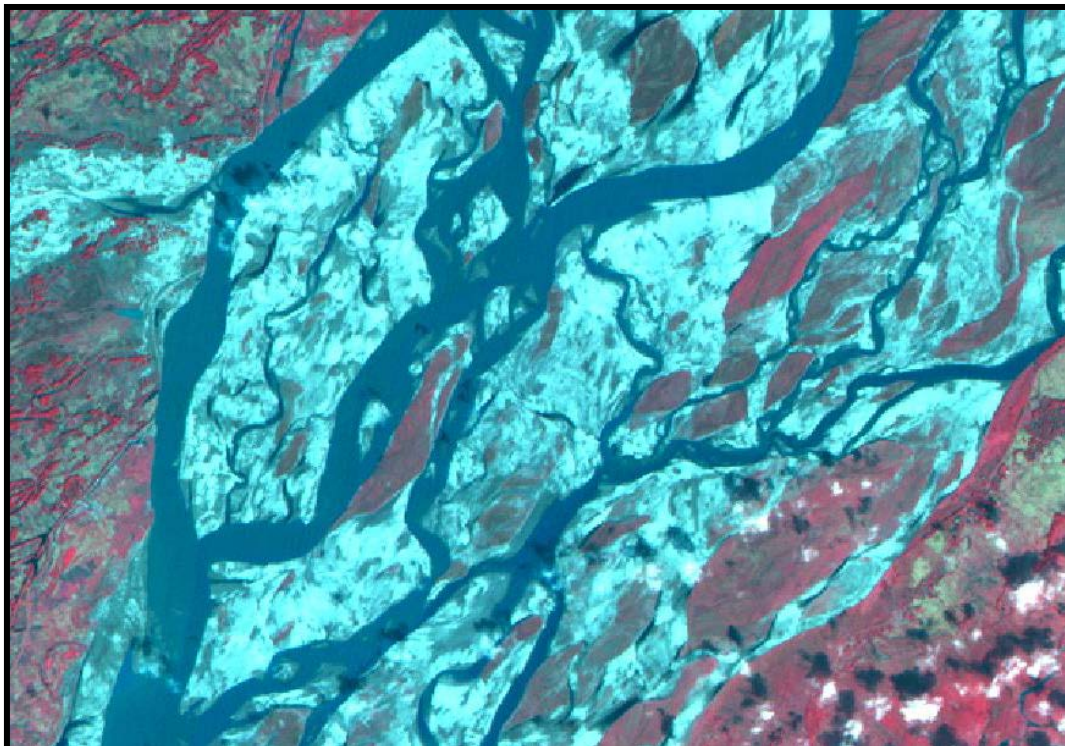


Fig. 19: The Highly Braided Channels (Reach 10) in IRS P6 LISS - III image of 2008 year with Plan Form Index value 3.8

RIVER BANK EROSION / MIGRATION

The bank lines of the river were demarcated from the Satellite Imageries of 1990, 1997 and 2008 year using ERDAS and ArcMap Software Tools. Mosaic images of year 1990, 1997 and 2007-08 with digitized bank lines and reference cross-sections are presented in Fig. 20, 21 and 22 respectively.

The satellite image based estimation of area eroded in Brahmaputra during periods 1990 to 2007-08 and 1997 to 2007-08 is presented in tabular form (Table 7), which shows the eroding tendency along the river banks of Brahmaputra in the entire study area. For the period of 17 years, the total land loss per year excluding forest area is found out to be 62km²/year. For more recent period of 1997 to 2007-08 the total land loss per year (excluding avulsion) is found out to be 72.5km²/year which is registering sharp increase in land lost due to river erosion in recent years. This calls for a robust and efficient river management action plan to arrest huge valuable land losses to erosion.

TABLE 7 SATELLITE BASED ESTIMATION AND COMPARISON OF AREA ERODED IN BRAHMAPUTRA DURING THE PERIOD 1990 TO 2007-08 AND 1997 TO 2007-08

Reach Number	North Bank			South Bank			Minimum PFI Values	
	Total Erosion Length (Km)	1990 to 2007-08 (in Sq.Km)	1997 to 2007-08 (in Sq. Km)	Total Erosion Length (Km)	1990 to 2007-08 (Sq. Km)	1997 to 2007-08 (in Sq. Km)	1997	2007-08
1(Dhubri)	40.19	124.461	94.129	7.05	194.983	10.791	13.22	5.74
2(Goalpara)	39.5	79.046	40.902	4.85	17.816	5.052	3.50	4.42
3(Palasbari)	54.87	48.668	42.914	14.02	23.006	15.859	2.83	3.75
4(Guwahati)	21.02	7.92	1.654	24.38	5.385	12.079	8.94	16.4
5(Morigaon-Mangaldai)	6	35.606	2.138	47.91	96.979	103.7	4.52	4.88
6(Morigaon-Dhing)	24.86	29.057	7.275	47.8	10.795	56.72	7.73	3.40
7(Tezpur)	8.58	38.758	4.733	52.95	16.628	44.774	7.48	4.37
8(Tezpur-Gohpur)	8.85	31.187	5.794	44.16	26.098	71.227	4.39	3.84
9(Majuli-Bessamora)	24.69	25.562	12.327	47.17	32.788	28.998	3.64	2.00
10(Majuli-Sibsagar)	16.93	60.657	16.878	54.95	44.018	42.118	5.25	3.77
11(Dibrugarh)	37.86	37.506	43.529	43.89	46.595	6.066	3.36	3.52
12(U/s Dibrugarh)	70.5	20.376	55.454	57.54	399.529	333.416	Forest Area Excluded southern side	
TOTAL	353.85	538.805	327.726	389.13	914.62	730.8		

Moreover, vulnerability of the stream bank erosion is significant as evident from Table 7. Almost 750 km of bank line in both side of the river has potential erosion tendency. The table also shows that downstream of Guwahati (Reach Number 4), erosion tendency is considerably high in north bank line whereas in the upstream of Guwahati erosion tendency is considerably high in south bank-line, indicating that river geological control point at Guwahati in respect to other control points has significant causative impact on the morphological behavior of River Brahmaputra as a whole in Assam flood plains. It urgently warrants attention for undertaking the integrated river management planning of Brahmaputra on holistic approach.

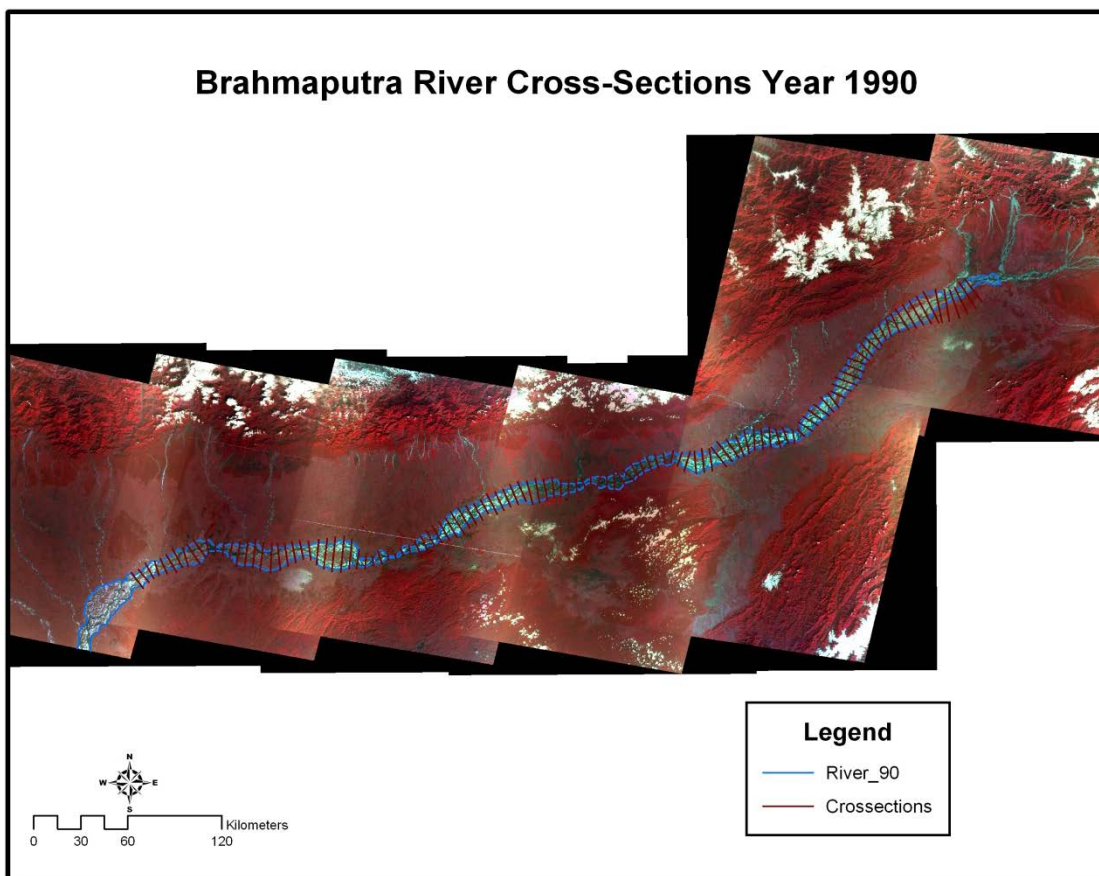


Fig. 20: Brahmaputra River Cross-Sections Year 1990

Mosaic of IRS 1C LISS – III Satellite Images of Brahmaputra River Cross-Sections Year 1997

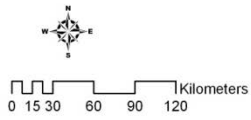
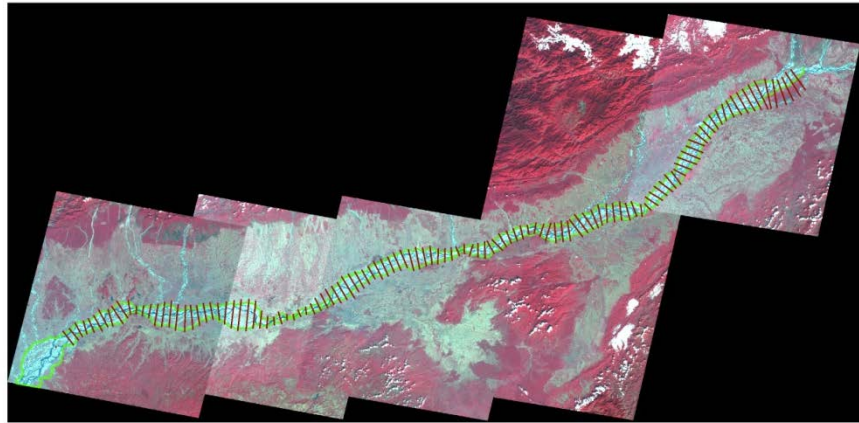


Fig. 21: Mosaic of IRS 1C LISS – III Satellite Image of Brahmaputra River Year 1997

Mosaic of IRSP6: LISS – III Satellite Images of Brahmaputra River Cross-Sections Year 2007-08

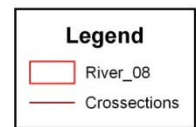
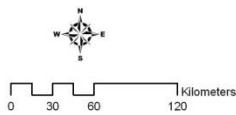
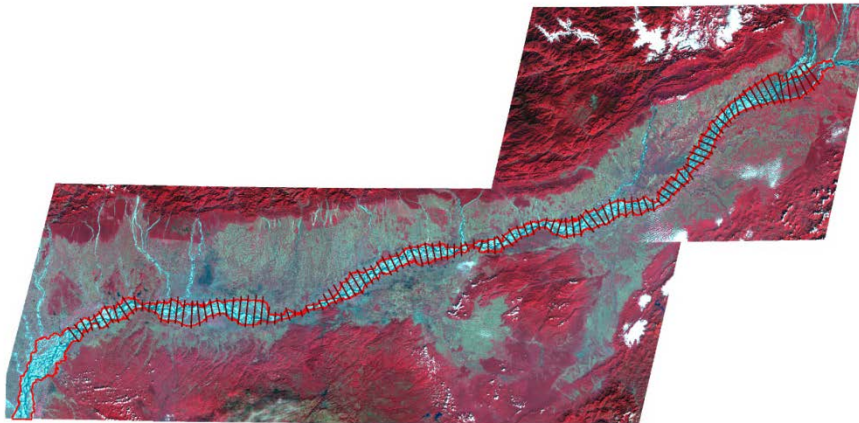


Fig. 22: Mosaic of IRS P6 LISS – III Satellite Image of Brahmaputra River Cross-Sections Year 2007-08

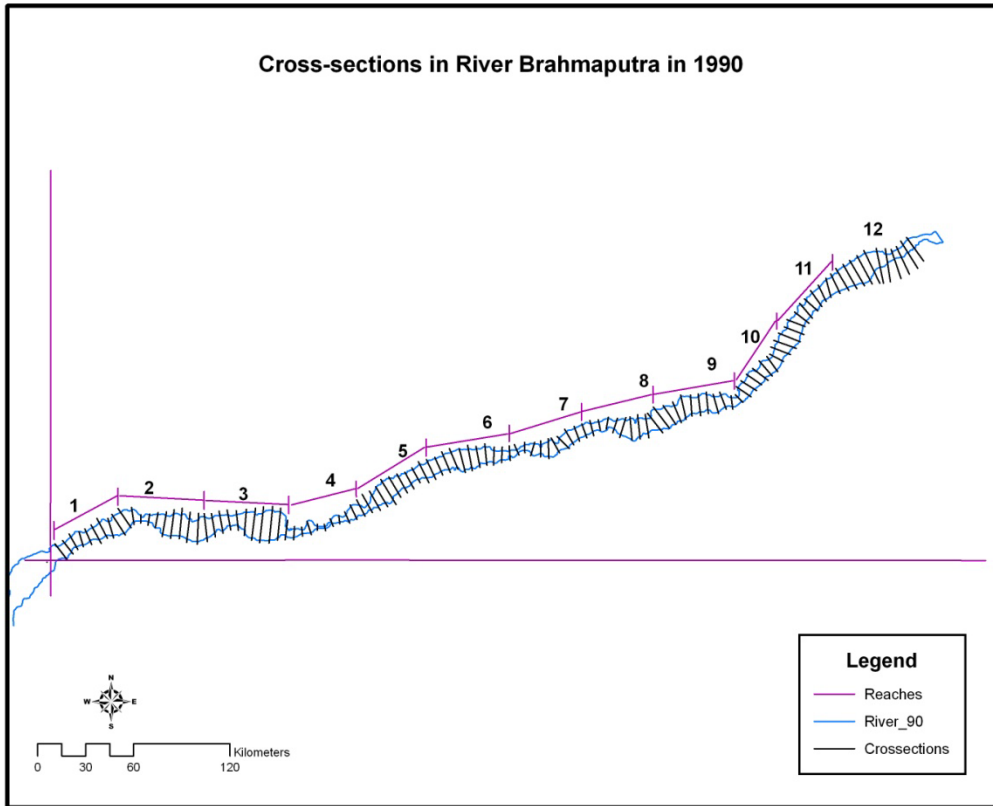


Fig. 23: Cross-sections in River Brahmaputra in 1990

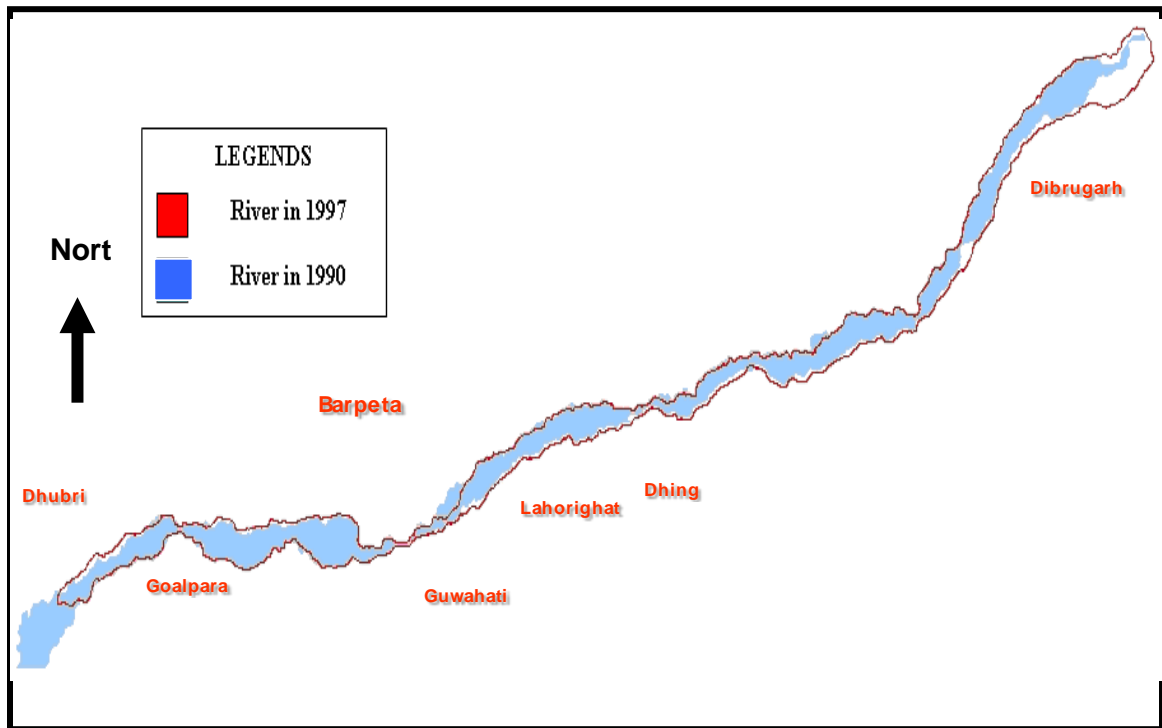


Fig. 24: Comparison in River Brahmaputra Years 1990 & 1997

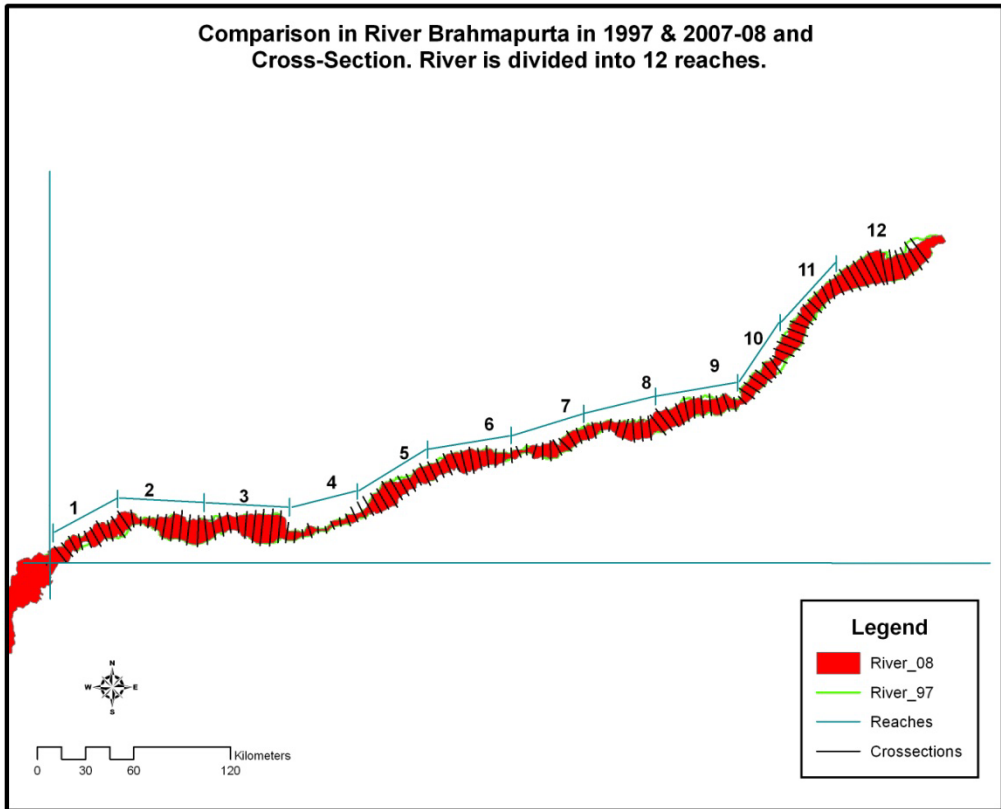


Fig. 25: Comparison in River Brahmaputra in 1997 & 2007-08 and Cross-Section. River is divided into 12 reaches

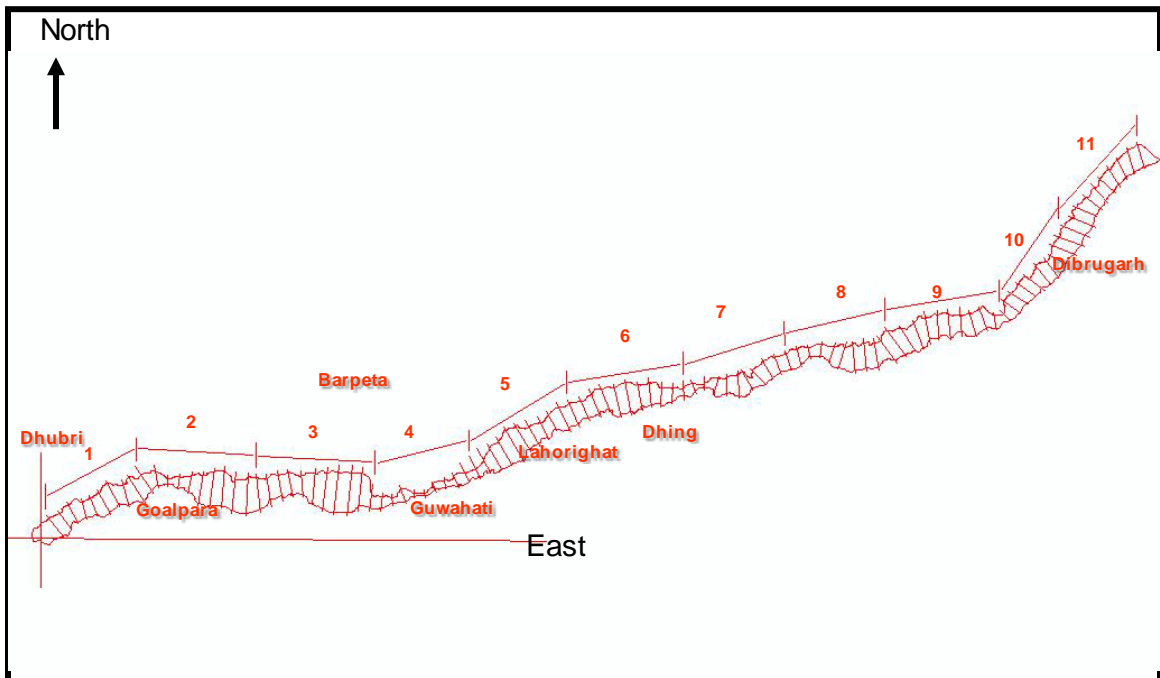


Fig. 26: The River channel demarcated from the IRS P6 LISS III image of 2008 year

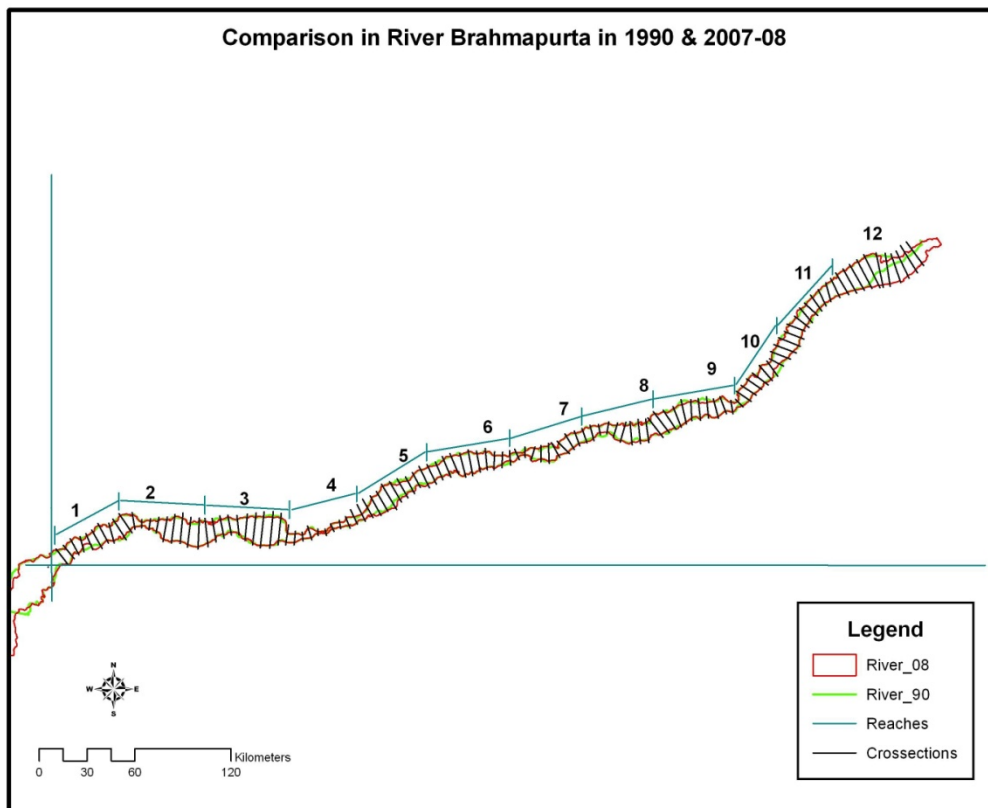


Fig. 27: Comparison in River Brahmaputra in 1990 & 2008 and Cross-Section. River is divided into 12 reaches

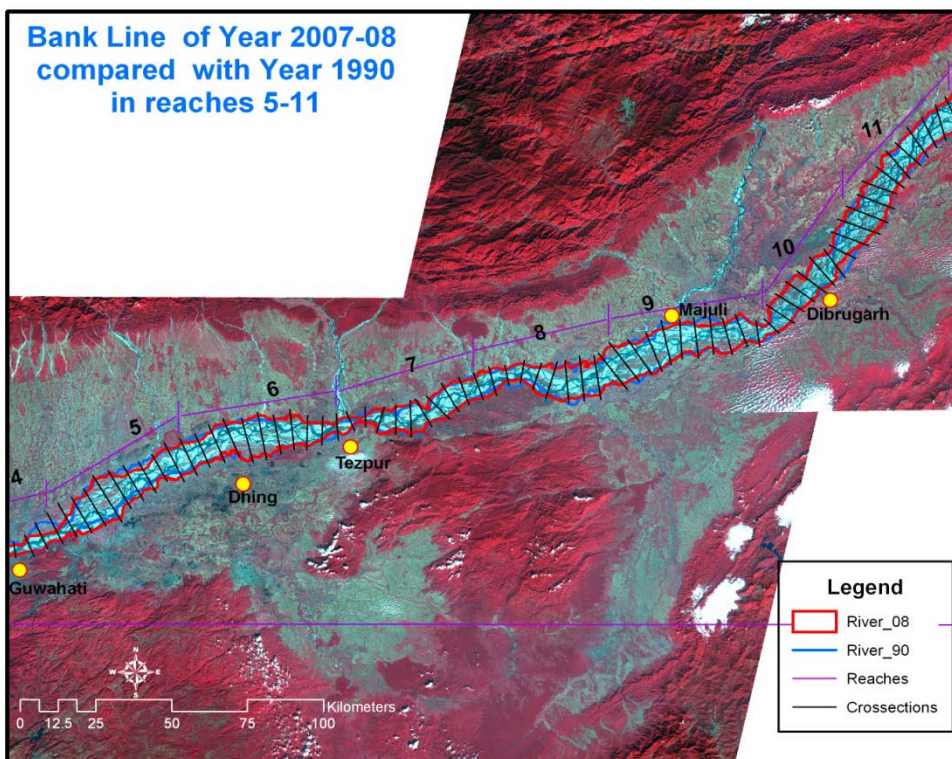


Fig. 28: Bank Line of Year 2007-08 compared with year 1990 in reaches 5-11

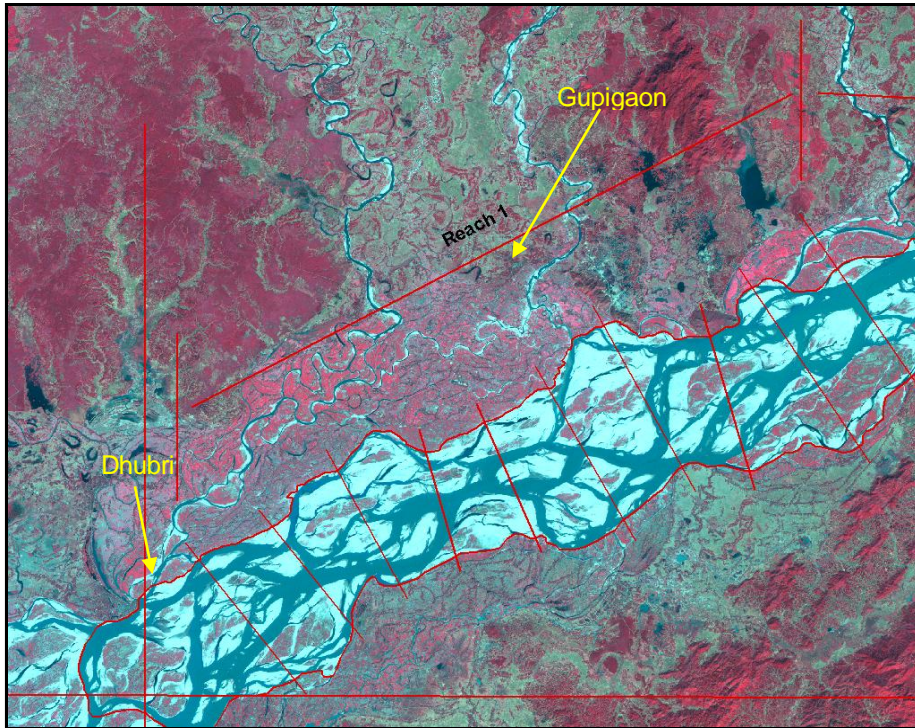


Fig. 29: The River channel in Reach 1 demarcated from the IRS P6 LISS III image of 2008 year

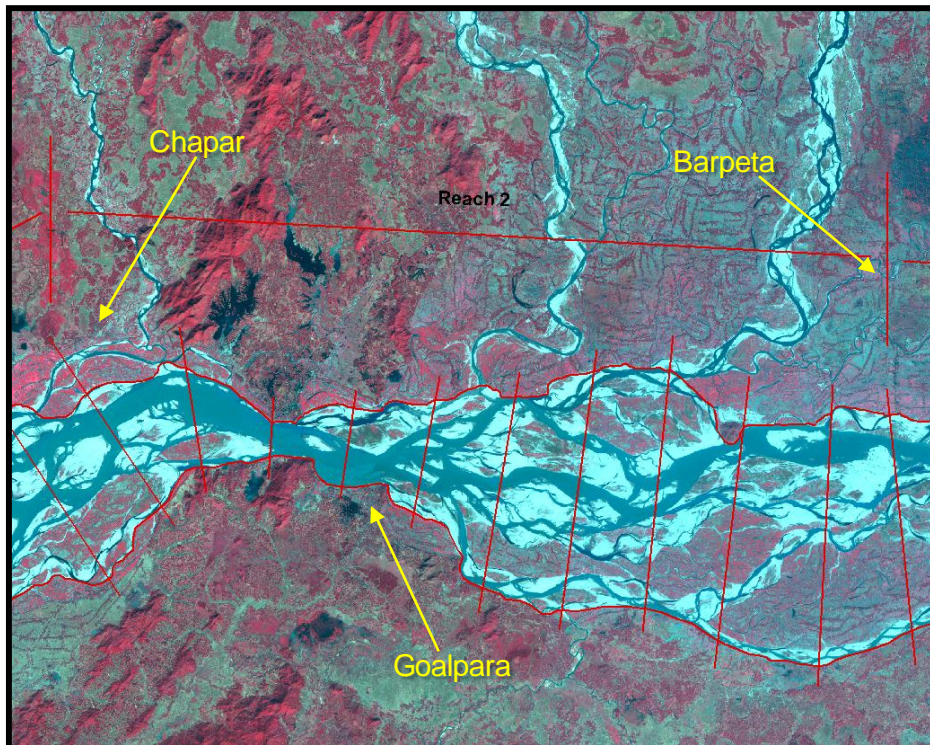


Fig. 30: The River channel in Reach 2 demarcated from the IRS P6 LISS III image of 2008 year.

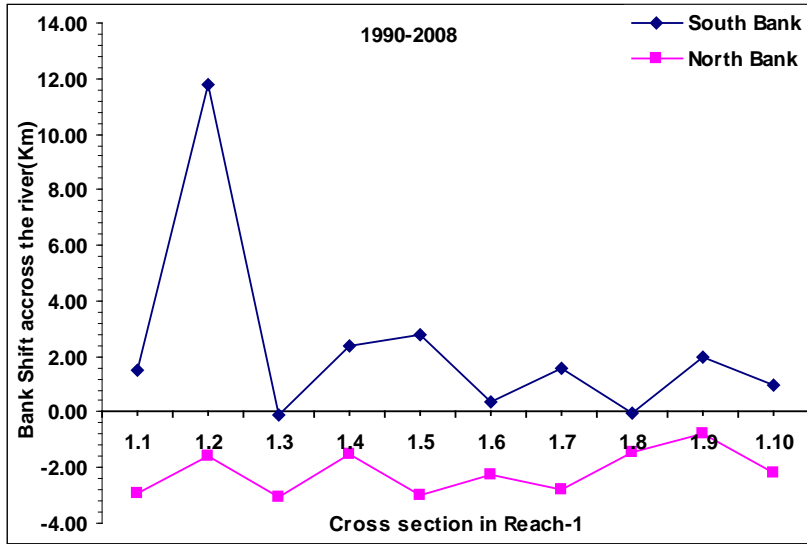


Fig. 31: Shift of Left and Right Bank between 1990 and 2008 year in Reach 1

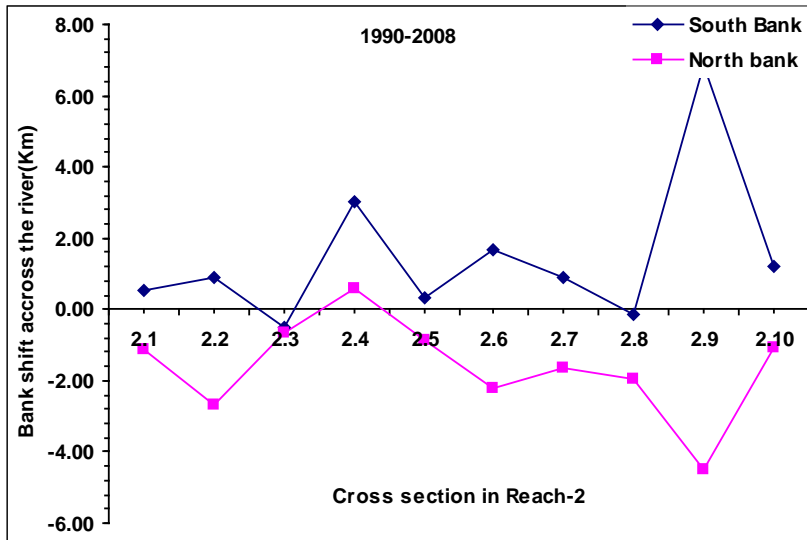


Fig. 32: Shift of Left and Right Bank between 1990 and 2008 year in Reach 2

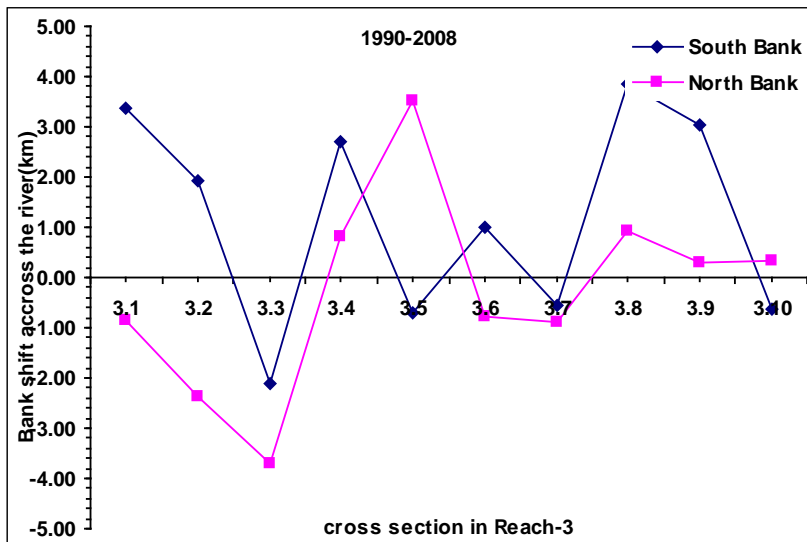


Fig. 33: Shift of Left and Right Bank between 1990 and 2008 year in Reach 3

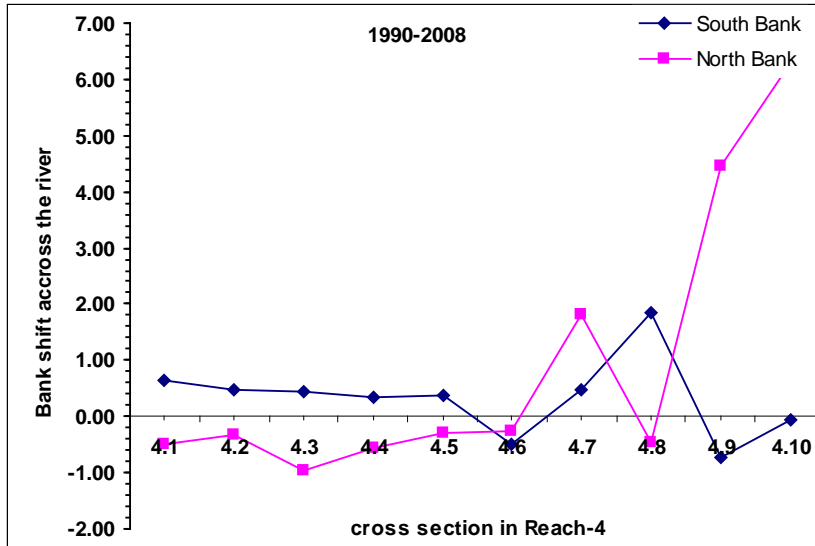


Fig. 34: Shift of Left and Right Bank between 1990 and 2008 year in Reach 4

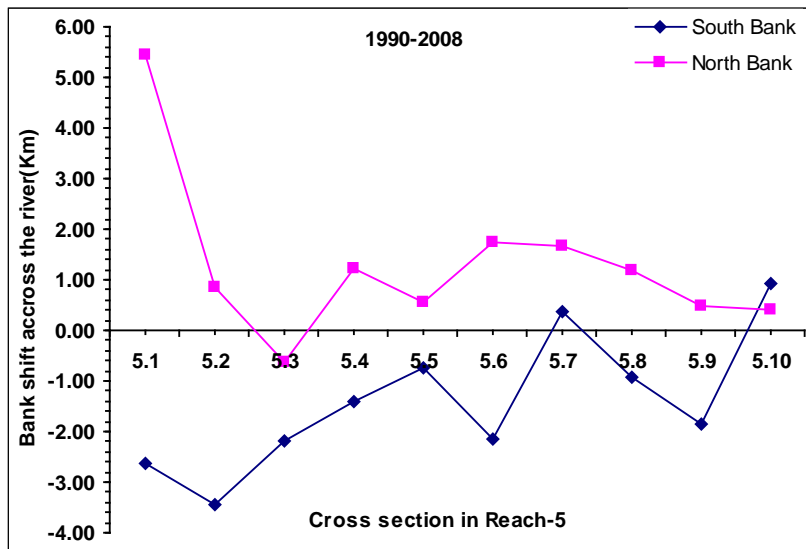


Fig. 35: Shift of Left and Right Bank between 1990 and 2008 year in Reach 5

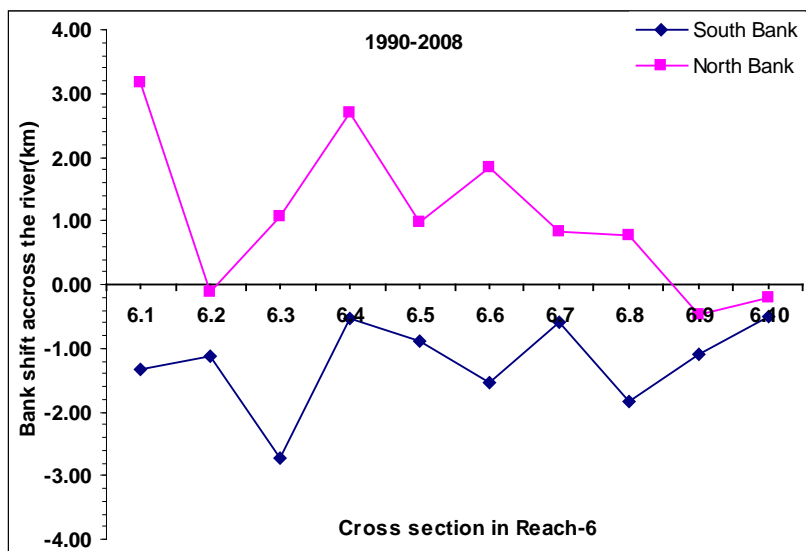


Fig. 36: Shift of Left and Right Bank between 1990 and 2008 year in Reach 6

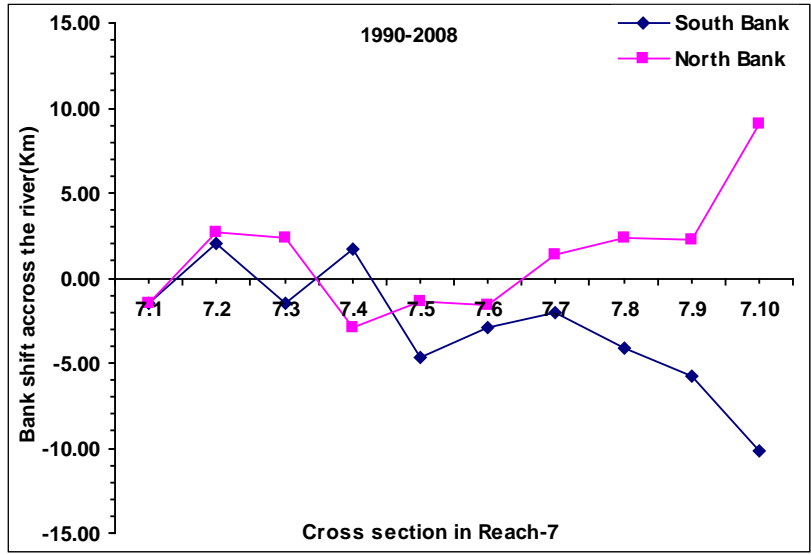


Fig. 37: Shift of Left and Right Bank between 1990 and 2008 year in Reach 7

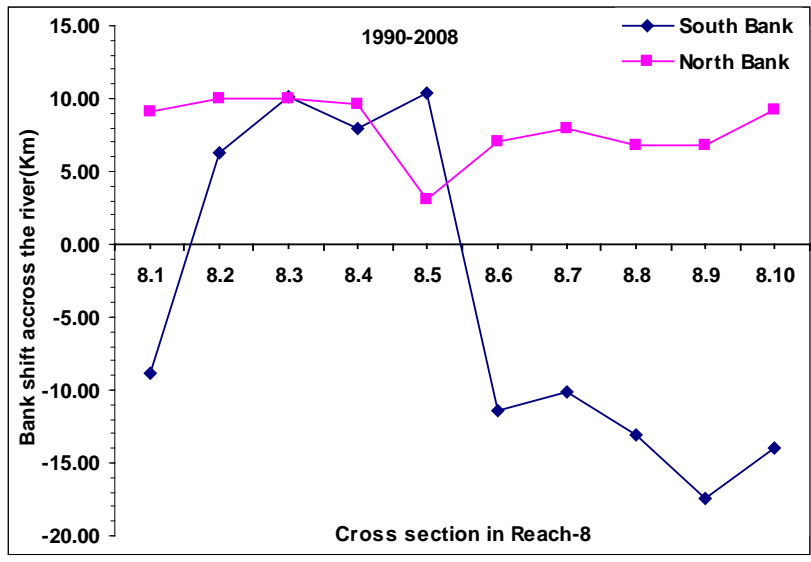


Fig. 38: Shift of Left and Right Bank between 1990 and 2008 year in Reach 8

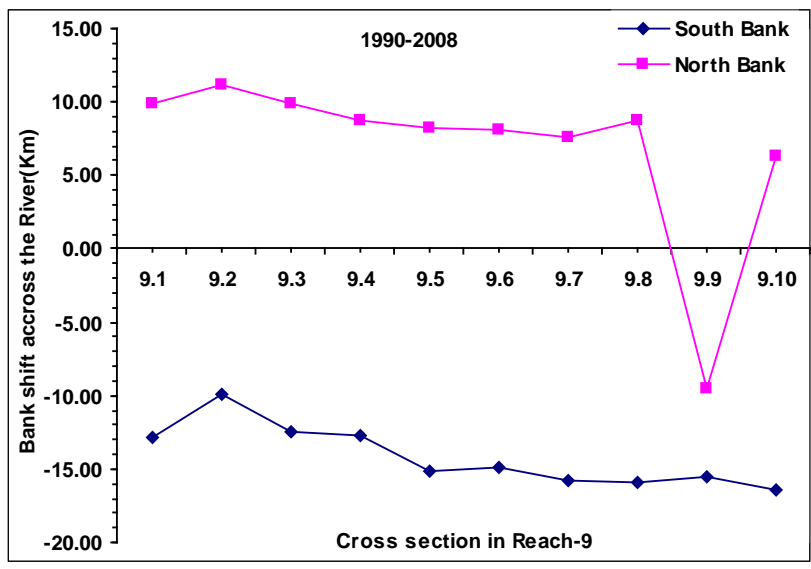


Fig. 39: Shift of Left and Right Bank between 1990 and 2008 year in Reach 9

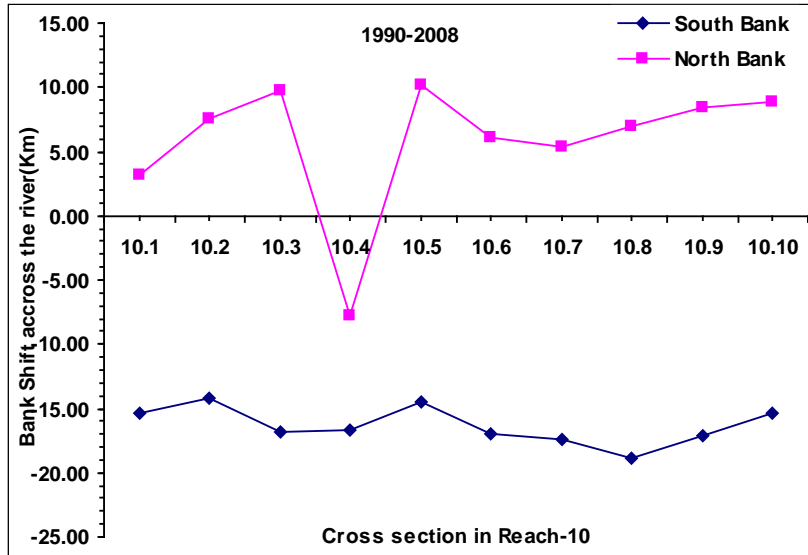


Fig. 40: Shift of Left and Right Bank between 1990 and 2008 year in Reach 10

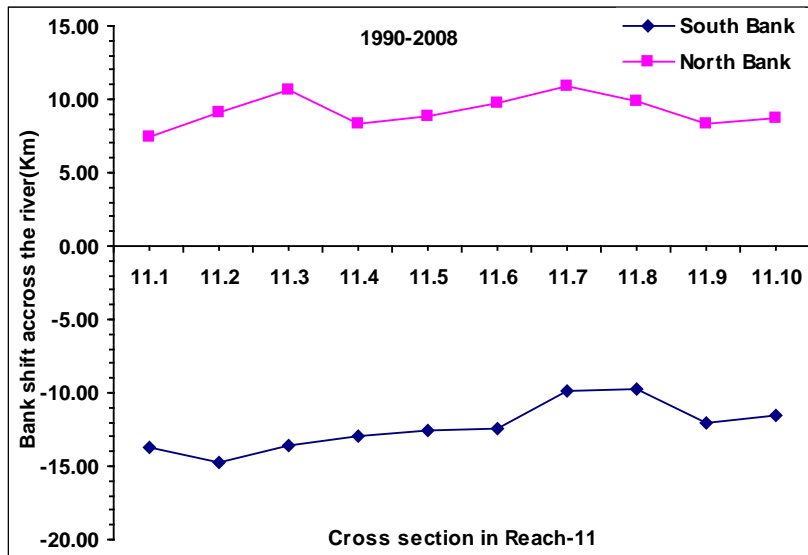


Fig. 41: Shift of Left and Right Bank between 1990 and 2008 year in Reach 11

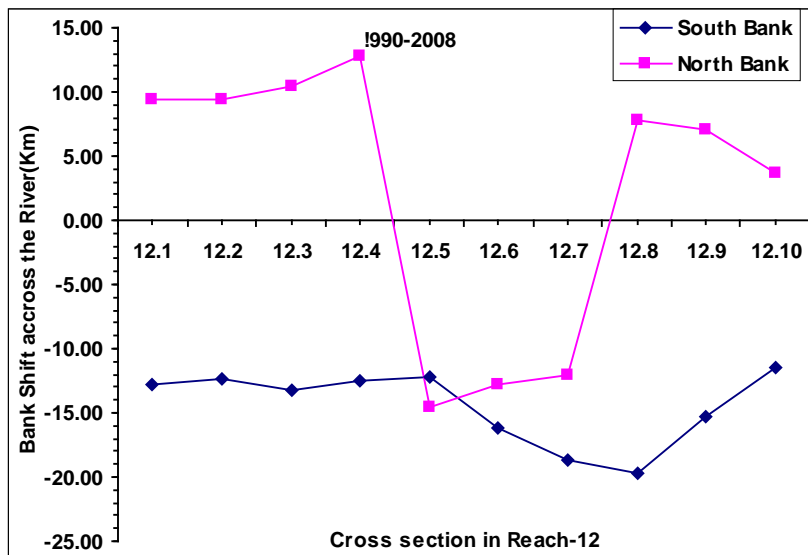


Fig. 42: Shift of Left and Right Bank between 1990 and 2008 year in Reach 12

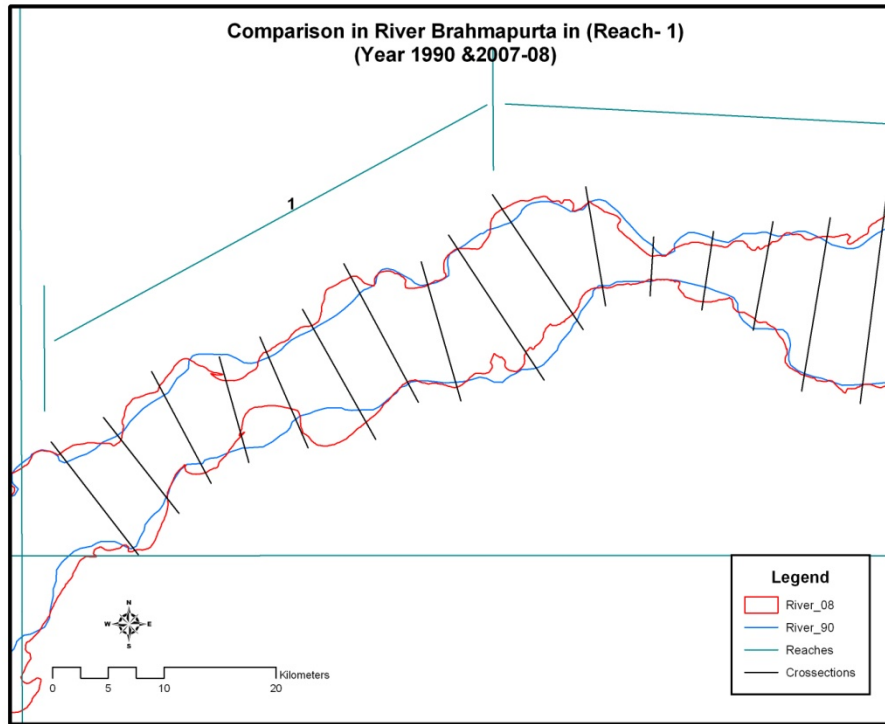


Fig. 43: Comparison in River Brahmaputra in (Reach- 1) (Year 1990 & 2008)

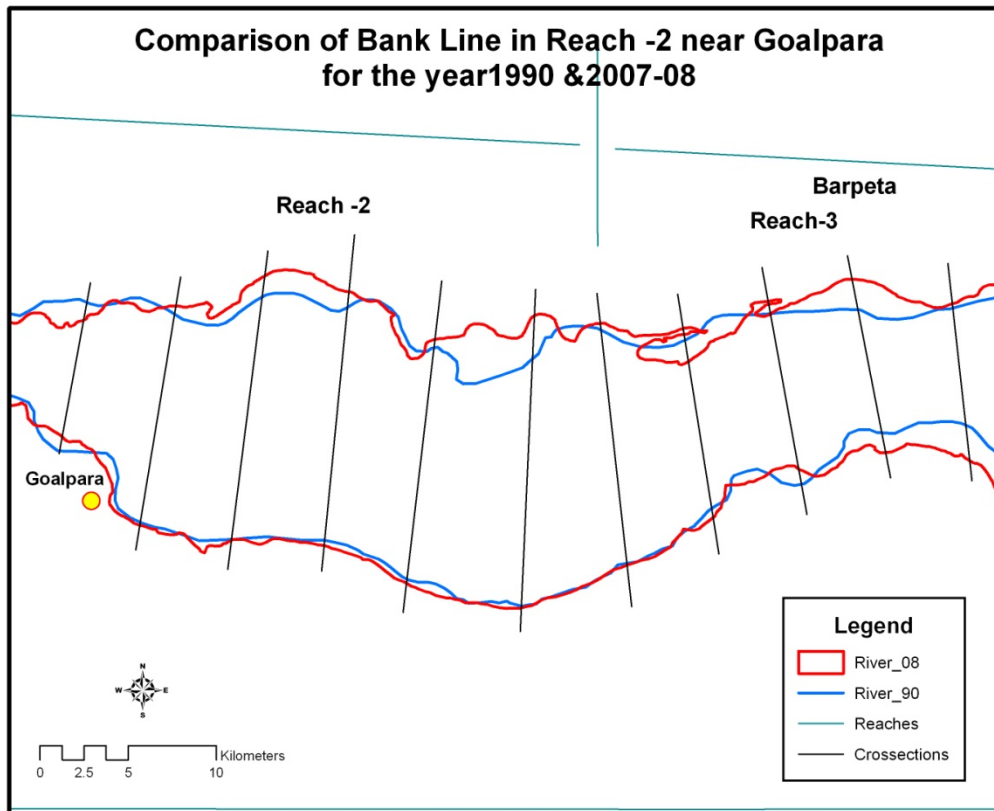


Fig. 44: Comparison of Bank Line Reach -2 near Goalpara for the Year 1990 & 2007-08

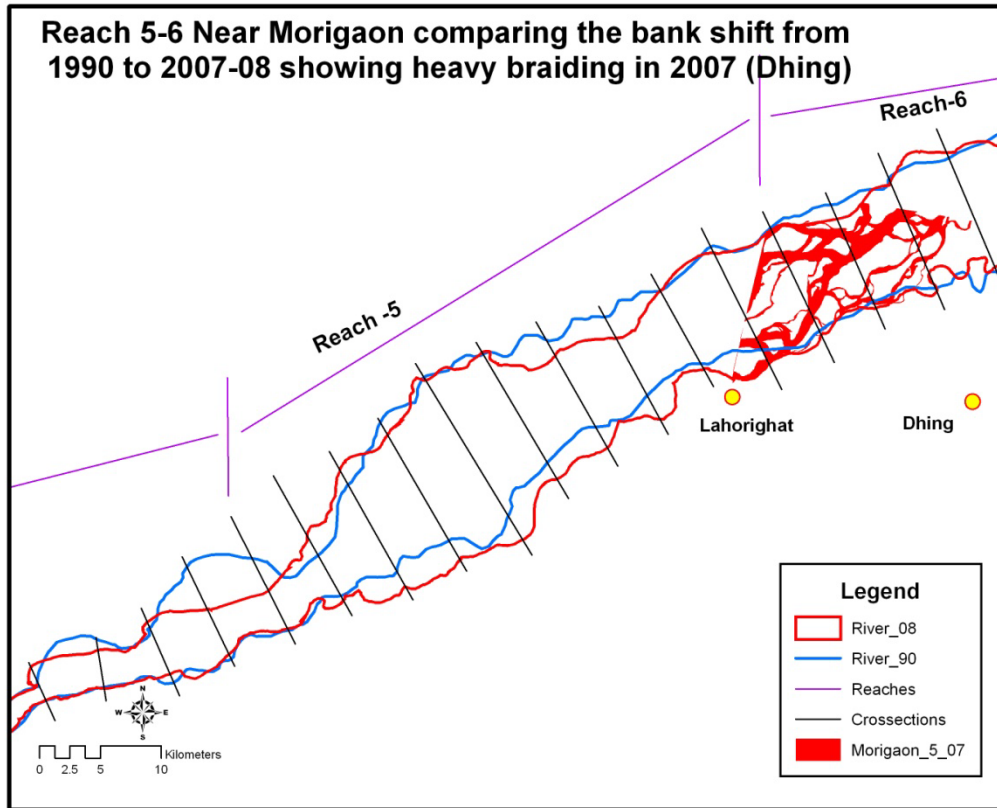


Fig. 45: Reach 5-6 Near Morigaon comparing the bank shift from 1990 to 2007-08 showing heavy braiding in 2007 (Dhing)

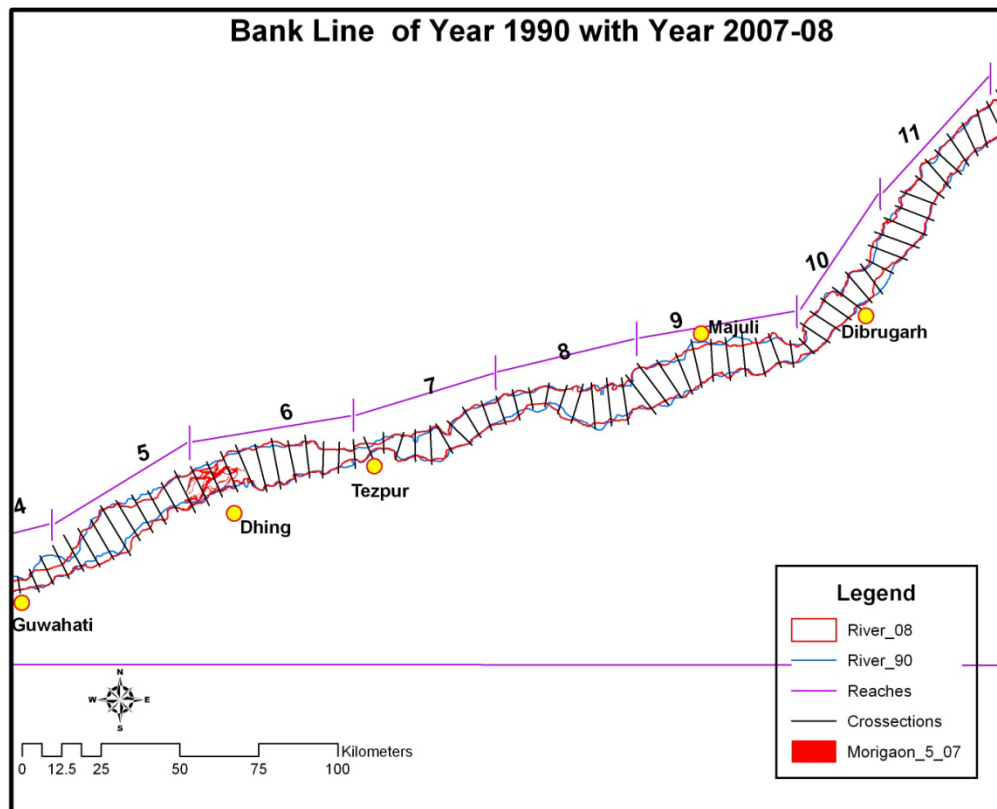


Fig. 46: Bank Line of year 1990 with year 2007-08

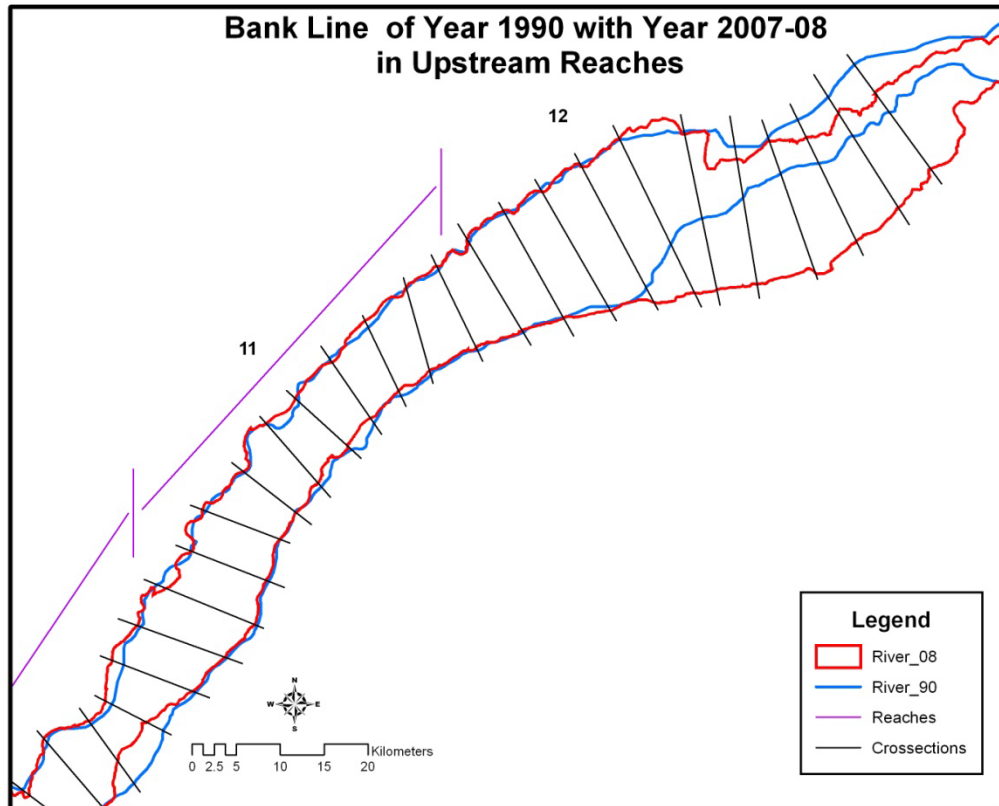


Fig. 47: Bank Line of Year 1990 with Year 2007-08 in Upstream Reaches

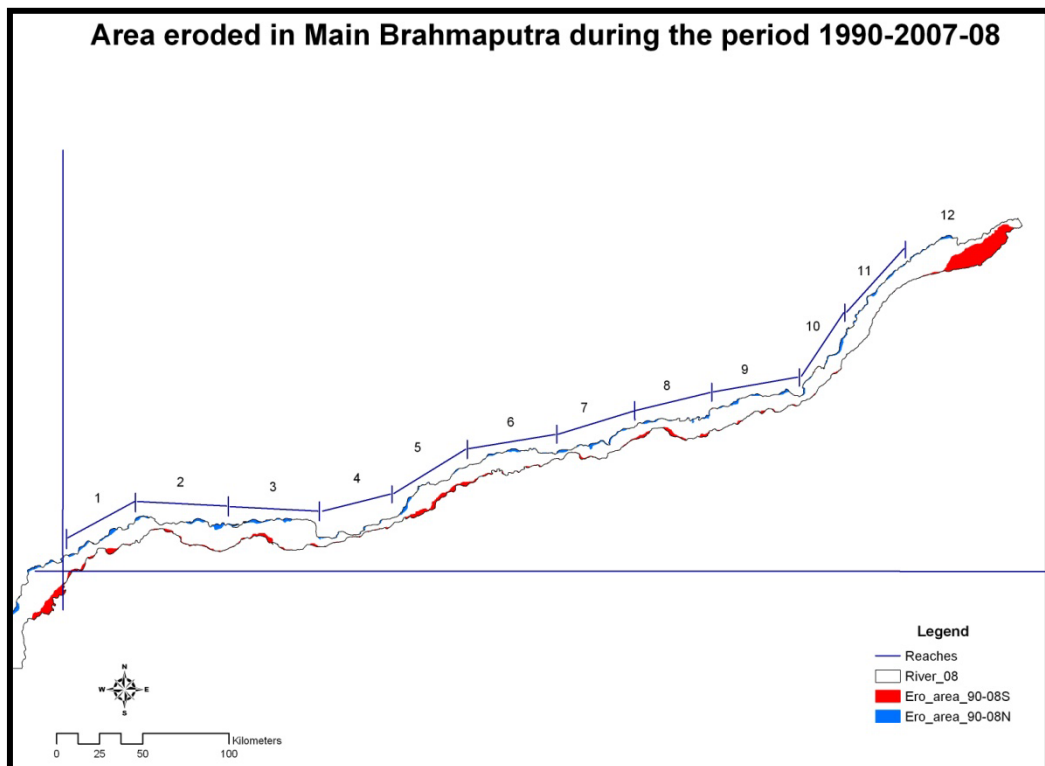


Fig. 48: Area eroded in Main Brahmaputra during the period 1990- 2007-08

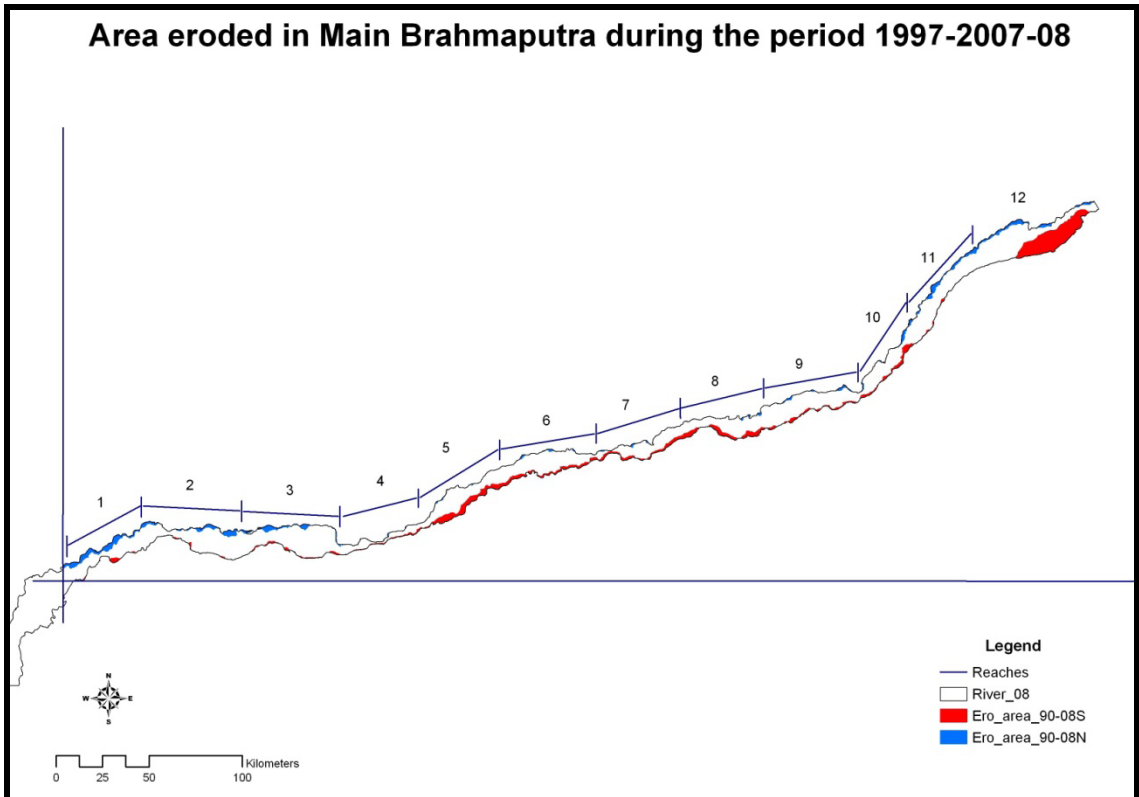


Fig. 49: Area eroded in Main Brahmaputra during the period 1997- 2007-08

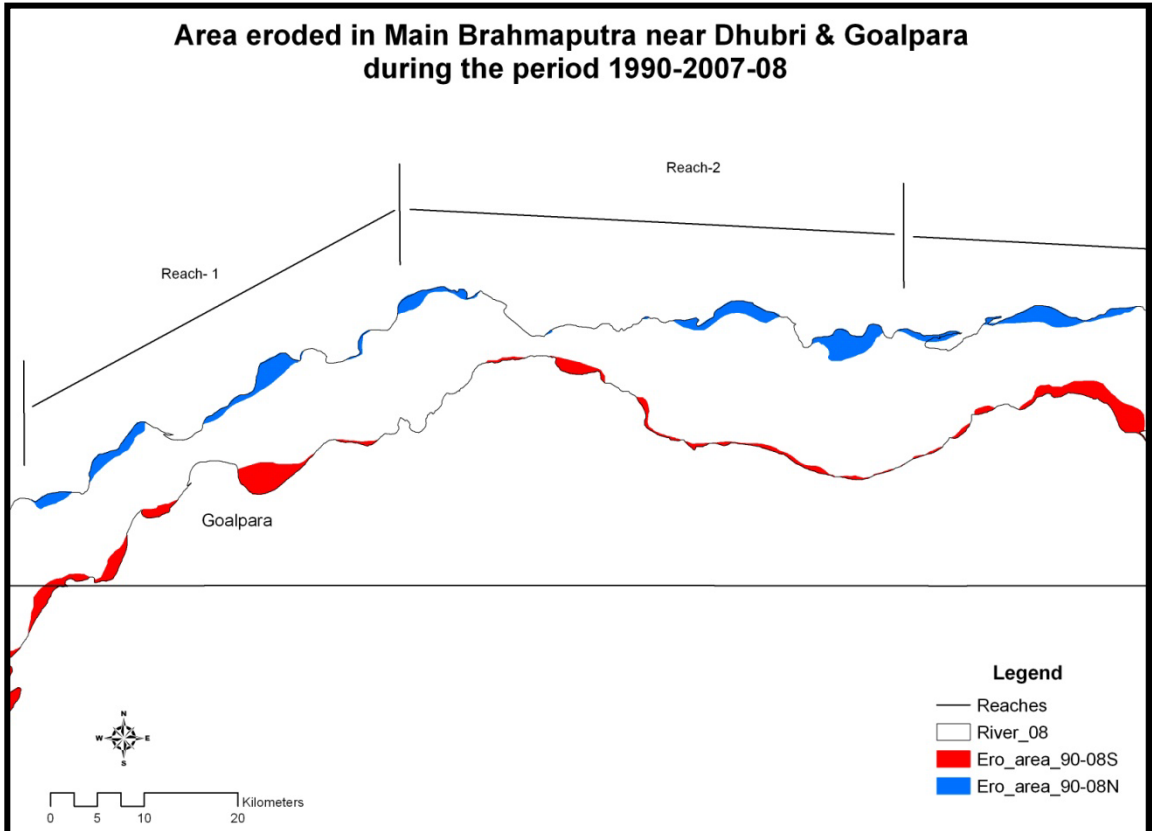


Fig. 50: Area eroded in Main Brahmaputra near Dhubri & Goalpara during the period 1990- 2007-08

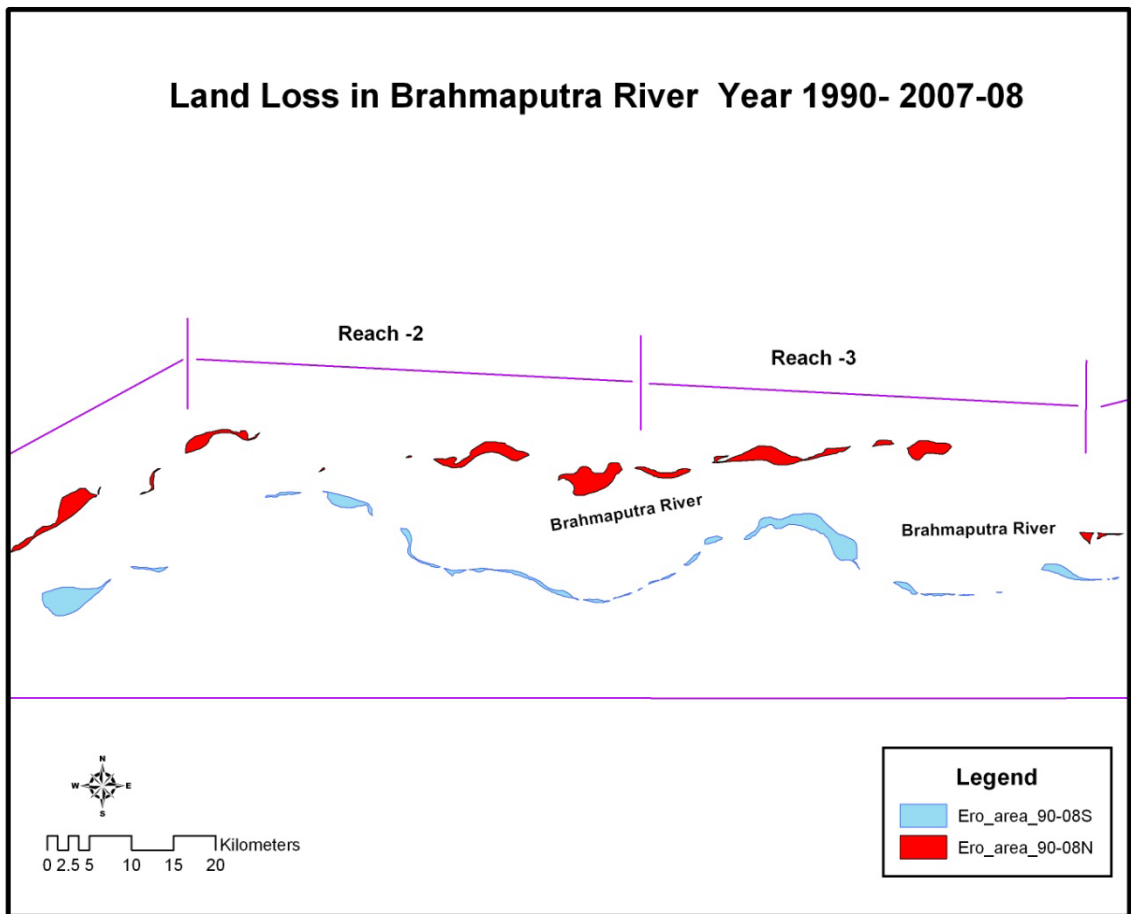


Fig. 51: Land Loss in Brahmaputra River Year 1990- 2007-08

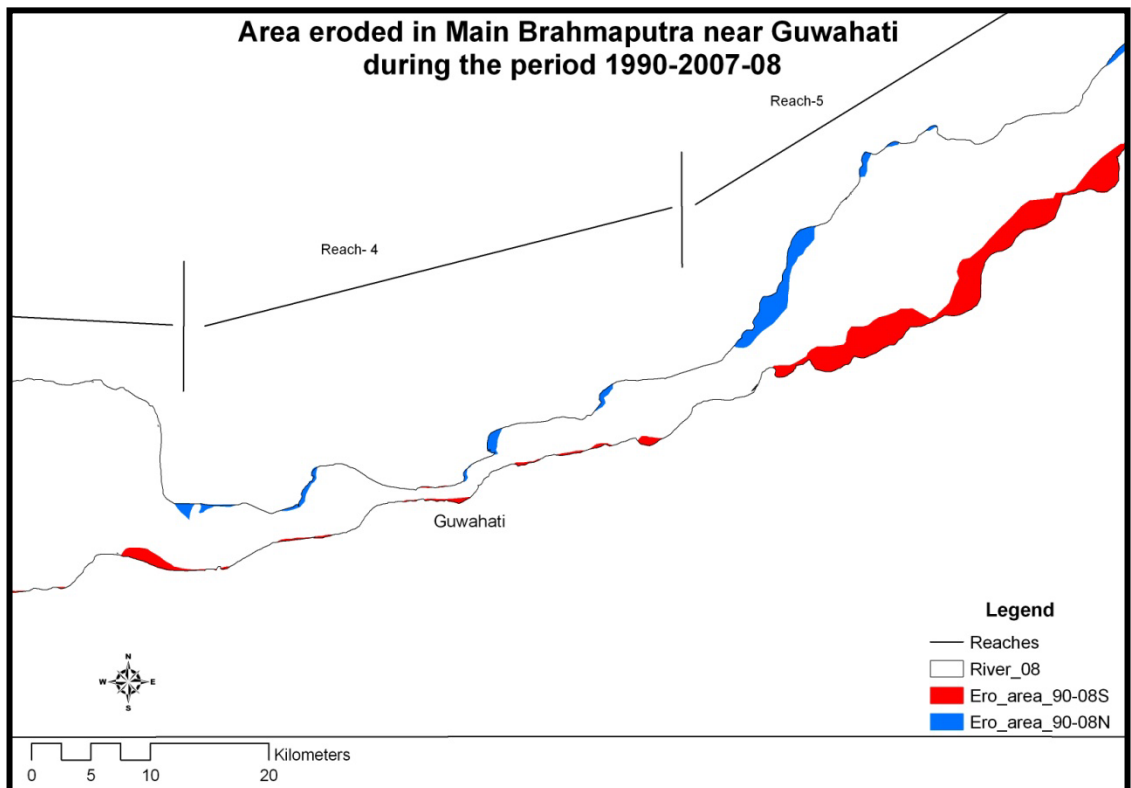


Fig. 52: Area eroded in Main Brahmaputra near Guwahati during the period 1990- 2007-08

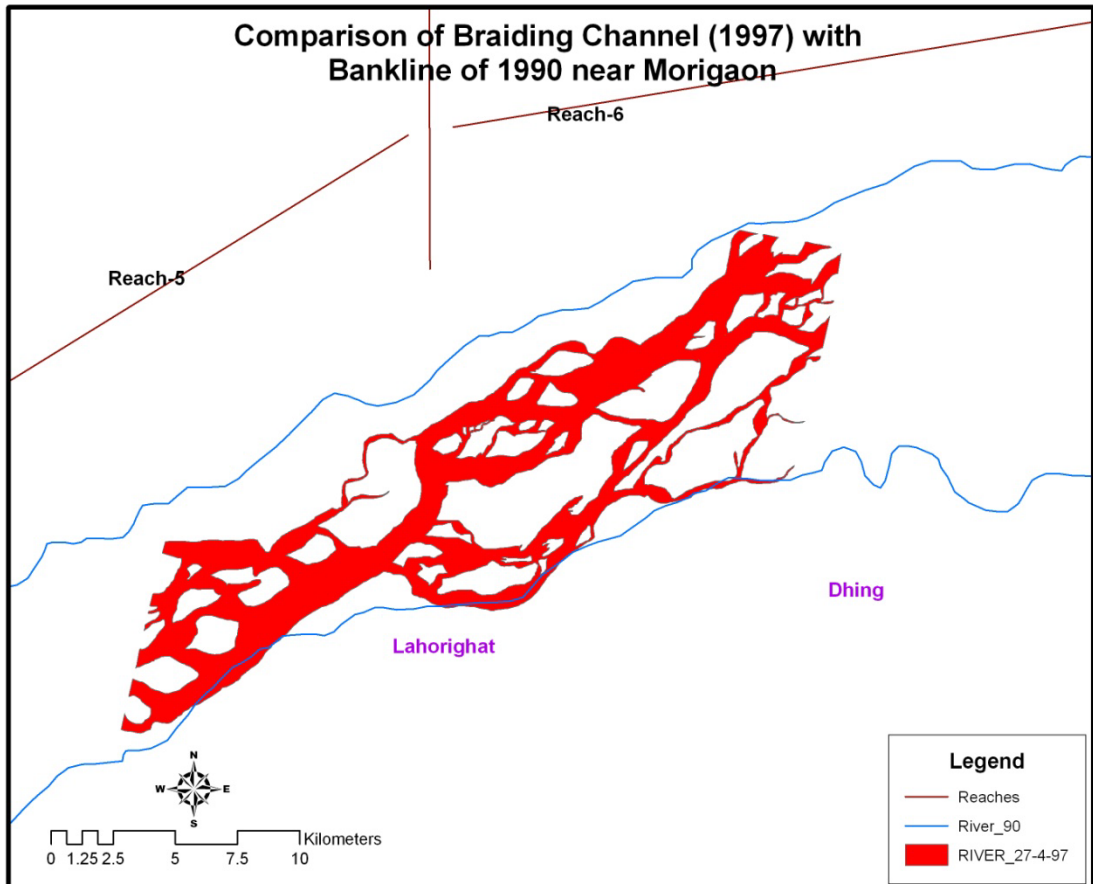


Fig. 53: Comparison of Braiding Channel (1997) with Bankline of 1990 near Morigaon

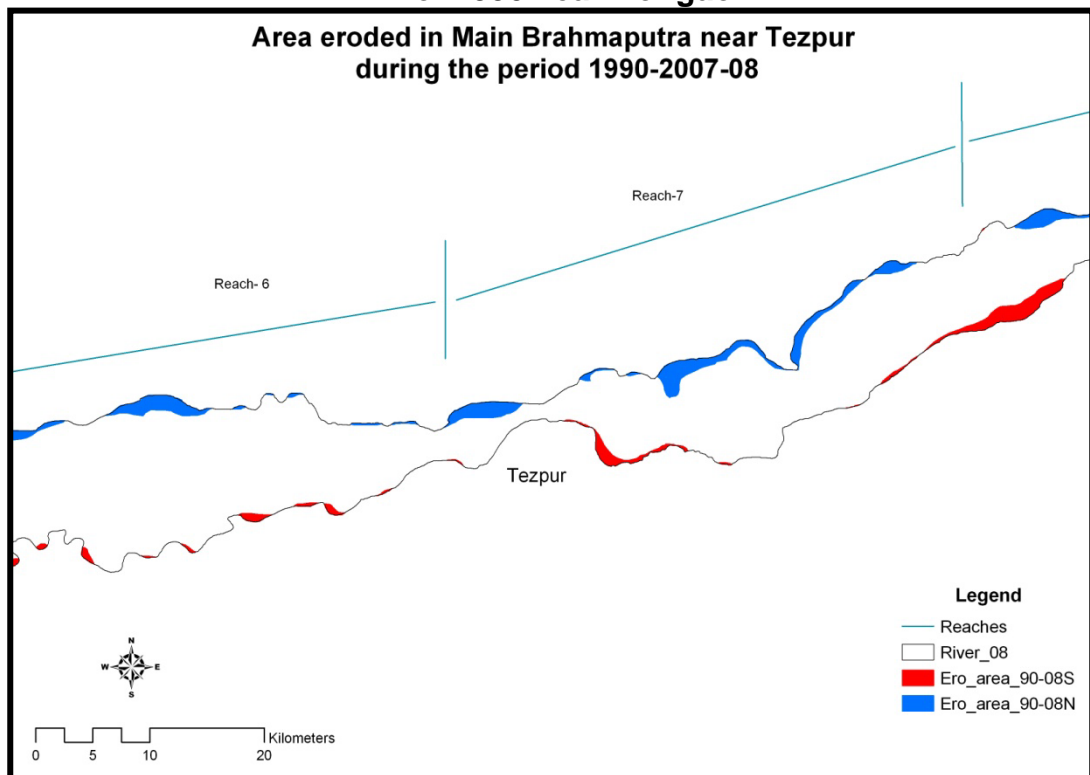


Fig. 54: Area eroded in Main Brahmaputra near Tezpur during the period 1990- 2007-08

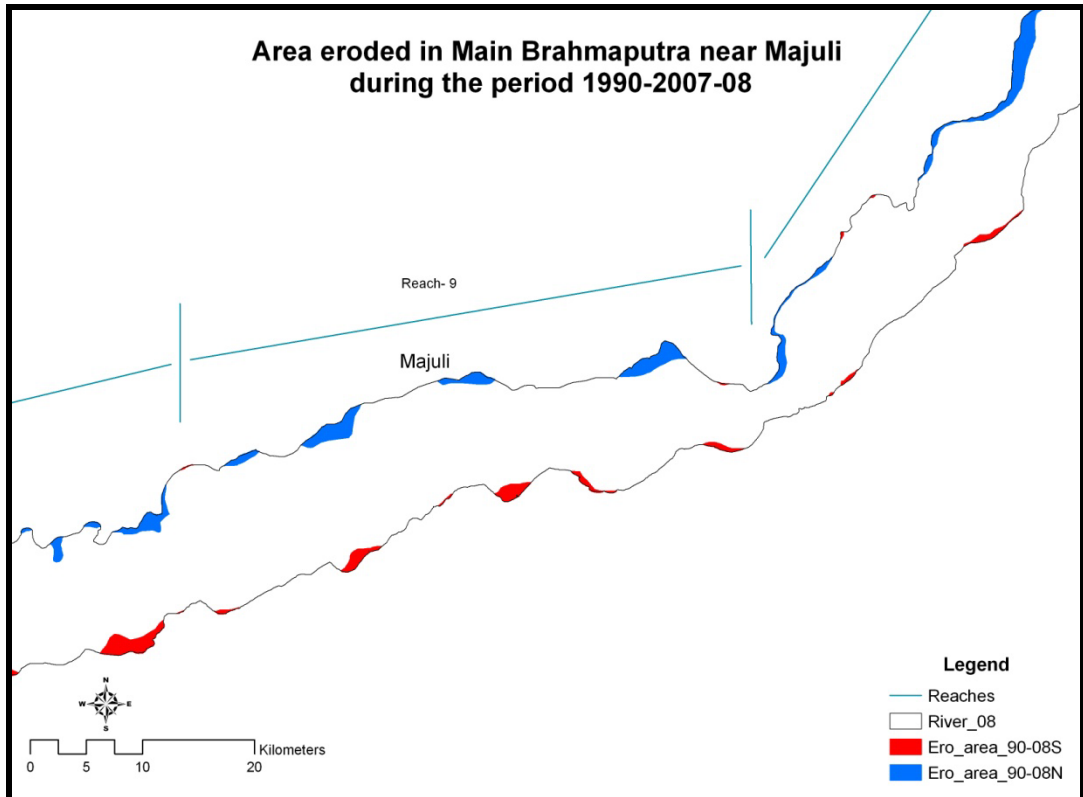


Fig. 55: Area eroded in Main Brahmaputra near Majuli during the period 1990- 2007-08

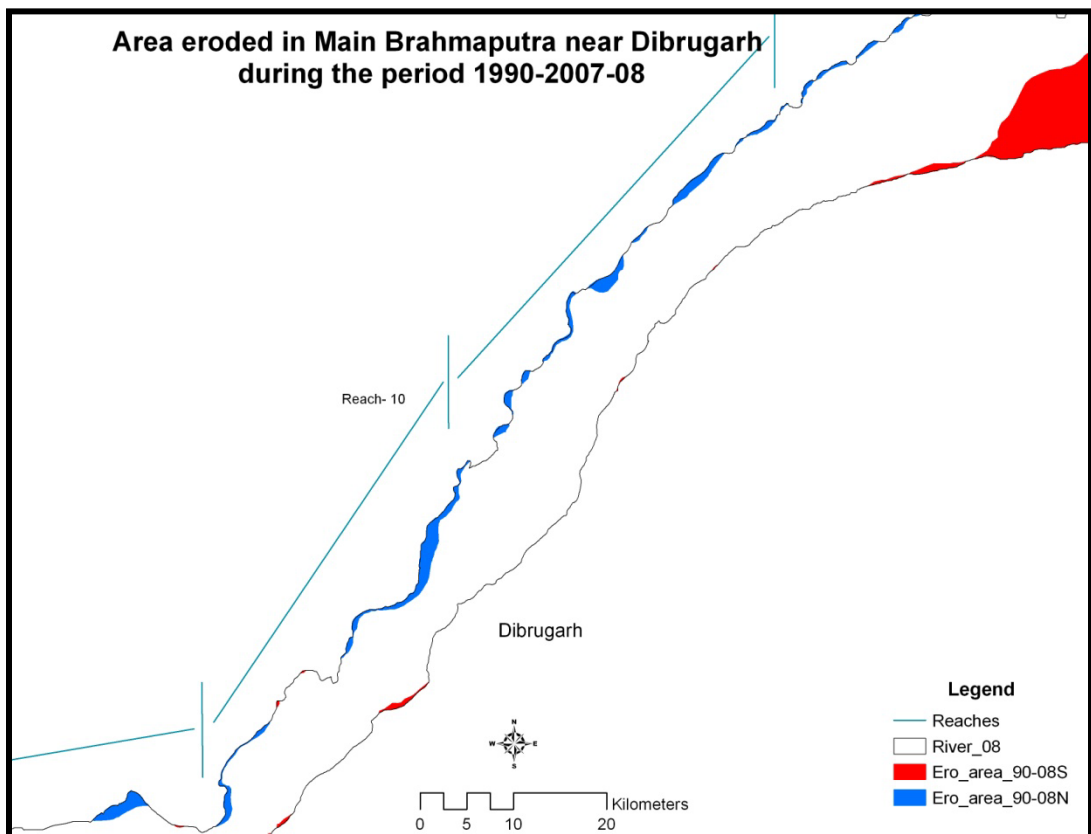


Fig. 56: Area eroded in Main Brahmaputra near Dibrugarh during the period 1990- 2007-08

TABLE 8: PRIORITIZATION WITH RESPECT TO LAND AREA LOST

PRIORITIZATION WITH RESPECT TO LAND AREA LOST						
Satellite based estimation of area eroded in Brahmaputra River for the period 1997 to 2007-08						
Reach No.	South Bank		Reach No.	North Bank		Remarks
	Total Erosion Length Km	Area Eroded Km ²		Total Erosion Length Km	Area Eroded Km ²	
5(Morigaon)	47.91	103.700	1(Dhubri)	40.19	94.129	
8(U/s Tezpur)	44.16	71.227	11(Dibrugarh)	37.86	43.529	
6(Morigaon)	47.8	56.720	3(Palasarbari)	54.87	42.914	
7(Tezpur)	52.95	44.774	2(Goalpara)	39.5	40.902	
10(U/s Majuli)	54.95	42.118	10(U/s Majuli)	16.93	16.878	
9(Majuli)	47.17	28.998	9(Majuli)	24.69	12.327	
3(Palasarbari)	14.02	15.859	6(Morigaon)	24.86	7.275	
4(Guwahati)	24.38	12.079	8(U/s Tezpur)	8.85	5.794	
1(Dhubri)	7.05	10.791	7(Tezpur)	8.58	4.733	
11(Dibrugarh)	43.89	6.066	5(Morigaon)	6	2.138	
2(Goalpara)	4.85	5.052	4(Guwahati)	21.02	1.654	
12(U/s Dibrugarh)	57.54	333.416	12(U/s Dibrugarh)	70.5	55.454	Forest Area excluded in Northern side

TABLE 9: PRIORITIZATION WITH RESPECT TO MAXIMUM BANK SHIFT OF THE LEFT BANK OF BRAHMAPUTRA

S.No.	Reach No.	South Bank	
		Erosion Length (Km)	Maximum erosion in tranverse Direction (Km)
1	5(Morigaon)	47.909	4.125
2	11(Dibrugarh)	28.297	3.716
3	10 (U/s Majuli)	54.95	3.432
4	8(U/s Tezpur)	16.402	2.935
5	8(U/s Tezpur)	9.384	2.709
6	9(Majuli)	9.012	2.653
7	8(U/s Tezpur)	18.372	2.567
8	2(Goalpara)	2.71	2.412
9	7(Tezpur)	30.715	2.237
10	1(Dhubri)	5.423	2.159
11	6(Morigaon)	12.049	1.775
12	9(Majuli)	18.805	1.624
13	6(Morigaon)	4.062	1.601
14	7(Tezpur)	13.073	1.528
15	7(Tezpur)	9.164	1.486
16	11(Dibrugarh)	15.588	1.464
17	6(Morigaon)	31.686	1.392
18	9(Majuli)	3.698	1.226
19	9(Majuli)	5.053	1.216
20	3(Palasbari)	3.518	1.207
21	9(Majuli)	3.996	1.056
22	4(Guwahati)	6.702	0.953
23	4(Guwahati)	17.68	0.847
24	3(Palasbari)	4.89	0.766
25	3(Palasbari)	3.975	0.741
26	9(Majuli)	2.209	0.735
27	9(Majuli)	4.399	0.634
28	1(Dhubri)	1.624	0.553
29	3(Palasbari)	1.634	0.307
30	2(Goalpara)	2.139	0.204

TABLE 10: PRIORITIZATION WITH RESPECT TO MAXIMUM BANK SHIFT OF THE RIGHT BANK OF BRAHMAPUTRA

S. No.	Reach No.	North bank	
		Erosion Length (Km)	Maximum Erosion in Tranverse Direction (Km)
1	1(Dhubri)	33.052	4.251
2	3(Palasbari)	30.605	3.64
3	3(Palasbari)	6.009	3.445
4	2(Goalpara)	35.572	3.354
5	11((Dibrugarh)	20.685	2.655
6	1(Dhubri)	7.141	2.317
7	9((Majuli)	9.135	2.27
8	7(Tezpur)	4.218	1.908
9	8(U/s Tezpur)	1.173	1.677
10	6(Morigaon)	7.982	1.665
11	5(Morigaon)	0.897	1.595
12	10 (U/s Majuli)	5.27	1.501
13	4(Guwahati)	15.439	1.489
14	9(Majuli)	10.949	1.447
15	11(Dibrugarh)	15.636	1.438
16	7(Tezpur)	4.362	1.415
17	10(U/s of Majuli)	9.863	1.393
18	6(Morigaon)	5.05	1.367
19	6(Morigaon)	3.243	1.306
20	8(U/s Tezpur)	1.29	1.237
21	5(Morigaon)	1.669	1.215
22	8(U/s Tezpur)	2.794	1.033
23	9(Majuli)	2.32	0.98
24	3(Palasbari)	3.042	0.935
25	4(Guwahati)	3.101	0.876
26	2(Goalpara)	1.871	0.872
27	5(Morigaon)	3.433	0.746
28	3(Palasbari)	15.217	0.742
29	10(U/s Majuli)	1.801	0.657
30	9(Majuli)	2.287	0.526
31	4(Guwahati)	1.533	0.517
32	4(Guwahati)	0.945	0.484
33	2(Goalpara)	2.055	0.388
34	11(Dibrugarh)	1.538	0.376
35	8(U/s Tezpur)	1.511	0.36
36	8(U/s Tezpur)	2.086	0.331

CHAPTER - I
SATELLITE DATA BASED
ANALYSIS OF CHANNEL MORPHO-
DYNAMIC STUDY FOR EROSION
CONTROL OF BRAHMAPUTRA
RIVER SYSTEM

[B] MAJOR TRIBUTARIES
OF BRAHMAPUTRA RIVER
SYSTEM

Chapter – I (B)

MAJOR TRIBUTARIES OF BRAHMAPUTRA RIVER SYSTEM

There are 13 major north bank tributaries and 10 major south bank tributaries of the Brahmaputra river considered for the present study. The area eroded in a period of 11 years (1997-2008) is given in Table 11 and 12 for north bank and south bank tributaries respectively. The area eroded in a period of 18 years (1990-2008) is given in Table 13 and 14 for north bank and south bank tributaries respectively.

TABLE 11 : SATELLITE BASED ASSESSMENT OF AREA ERODED IN NORTHERN TRIBUTARIES OF BRAHMAPUTRA RIVER FOR THE PERIOD 1997-2008

Sl. No.	Tributary Name (NorthBank)	Tributary Length in Km.	Eroded Area in Right Bank	Eroded Area in Left Bank	Total Eroded Area in Sq.Km.
1	Aiel	131.677	2.501	26.256	28.757
2	Borgang	31.502	7.836	7.882	15.718
3	Bornadi	60.670	0.770	17.554	18.324
4	Borolia	102.048	5.472	61.022	66.494
5	Champamati	101.985	6.335	39.604	45.938
6	Dhansiri North	89.193	0.848	22.443	23.292
7	Gabharu	57.501	3.951	11.724	15.675
8	Jia Bharali	36.206	0.706	7.500	8.206
9	Jiadhol	23.095	18.996	8.856	27.852
10	Manas	48.927	0.403	13.704	14.107
11	Pagladiya	70.233	0.732	17.406	18.137
12	Pahumara	91.432	3.396	20.052	23.448
13	Subansiri	122.906	25.301	24.562	49.863
	TOTAL	967.375	77.247	278.565	355.812

TABLE 12 : SATELLITE BASED ASSESSMENT OF AREA ERODED IN SOUTHERN TRIBUTARIES OF BRAHMAPUTRA RIVER FOR THE PERIOD 1997-2008

Sl. No.	Tributary Name (South Bank)	Tributary Length in Km.	Eroded Area in Right Bank	Eroded Area in Left Bank	Total Eroded Area in Sq.Km.
1	Buri Dihing	120.406	15.386	13.329	28.716
2	Dhansiri South	163.025	29.240	5.291	34.531
3	Dikhow	93.292	14.104	6.726	20.830
4	Disang	197.585	10.113	10.979	21.092
5	Dudhnoi	34.354	8.362	0.091	8.453
6	Jhanji	56.428	7.740	2.806	10.546
7	Jinari	28.790	5.581	0.409	5.991
8	Kolong /Kapili	192.511	21.840	10.346	32.186
9	Krishnai	106.792	12.523	0.610	13.133
10	Kulsi	80.140	8.332	3.308	11.640
	TOTAL	1073.323	133.221	53.897	187.118

Total Eroded Area in Major Tributaries during 1997 to 2008 =
 $355.812 + 187.118 = 542.930$
 Sq.Km

542.930 km²

Eroded Area per year

54.293 Km²/year

TABLE 13 : SATELLITE BASED ESTIMATION OF AREA ERODED IN NORTHERN TRIBUTARIES OF BRAHMAPUTRA RIVER FOR THE PERIOD 1990-2008

Sl. No.	Tributary Name (North Bank)	Tributary Length in Km.	Eroded Area in Right Bank	Eroded Area in Left Bank	Total Eroded Area in Sq.Km.
1	Aiel	131.677	8.549	27.118	35.667
2	Borgang	31.502	9.462	8.300	17.762
3	Bornadi	60.670	2.250	18.814	21.064
4	Borolia	102.048	7.089	66.410	73.499
5	Champamati	101.985	9.194	42.852	52.046
6	Dhansiri North	89.193	1.500	30.509	32.009
7	Gabharu	57.501	7.405	13.671	21.076
8	Jia Bhareli	36.206	1.974	8.956	10.930
9	Jiadhol	23.095	19.554	10.297	29.851
10	Manas	48.927	1.476	15.496	16.972
11	Pagladiya	70.233	1.839	19.717	21.556
12	Pahumara	91.432	4.792	23.204	27.996
13	Subansiri	122.906	29.925	26.144	56.069
	TOTAL	967.375	105.009	311.488	416.497

TABLE 14 : SATELLITE BASED ESTIMATION OF AREA ERODED IN SOUTHERN TRIBUTARIES OF BRAHMAPUTRA RIVER FOR THE PERIOD 1990-2008

Sl. No.	Tributary Name (South Bank)	Tributary Length in Km.	Eroded Area in Right Bank	Eroded Area in Left Bank	Total Eroded Area in Sq.Km.
1	Buri Dihing	120.406	17.711	15.008	32.719
2	Dhansiri South	163.025	31.557	7.899	39.456
3	Dikhow	93.292	15.734	9.201	24.935
4	Disang	197.585	11.581	12.306	23.887
5	Dudhnoi	34.354	9.492	1.306	10.798
6	Jhanji	56.428	9.667	4.085	13.752
7	Jinari	28.790	6.091	1.539	7.630
8	Kolong Kapili	192.511	23.943	12.884	36.827
9	Krishnai	106.792	15.579	1.314	16.893
10	Kulsi	80.140	11.397	4.390	15.787
	TOTAL	1073.323	152.752	69.932	222.684

Total Eroded Area in Major Tributaries during 1990- 2008 = 639.181
416.497+222.684 = 639.181 Sq.Km km²
Eroded Area per year 37.60 Km²/year

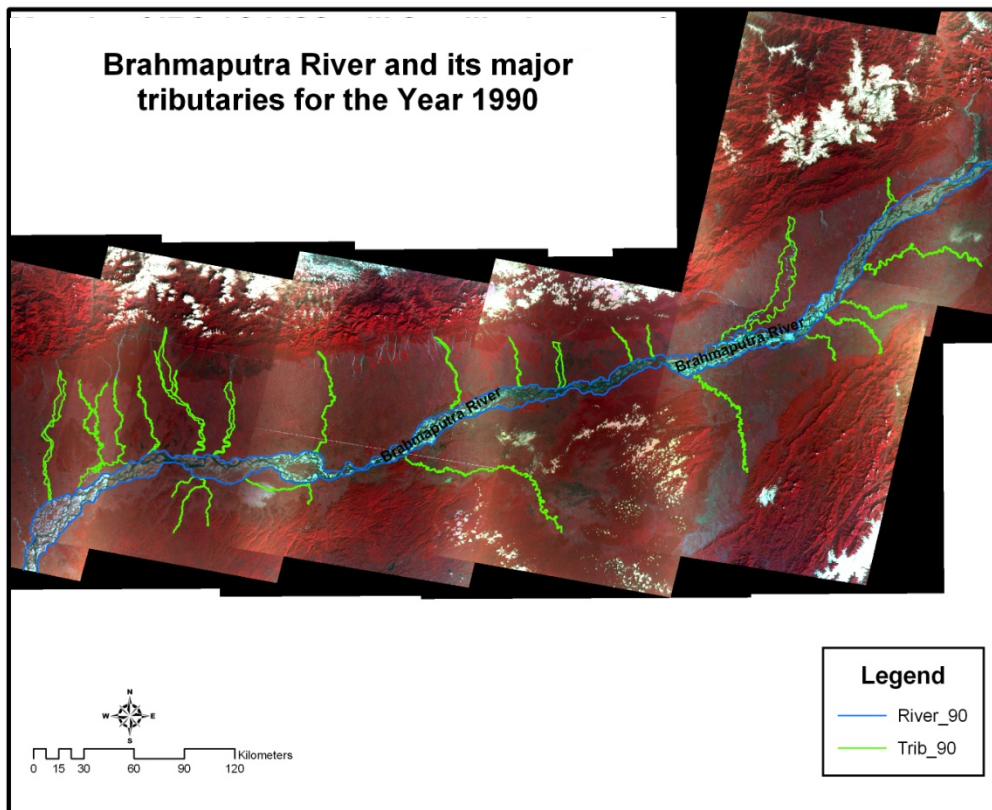


Fig. 57: Brahmaputra River and its major tributaries of the Year 1990

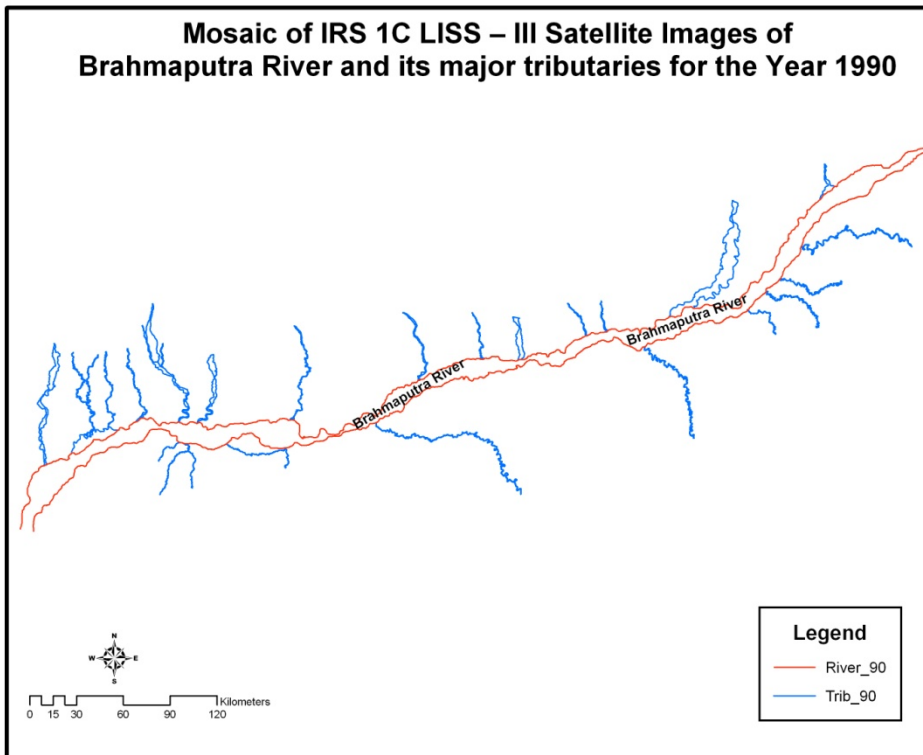


Fig. 58: Brahmaputra River and its major tributaries of the Year 1990

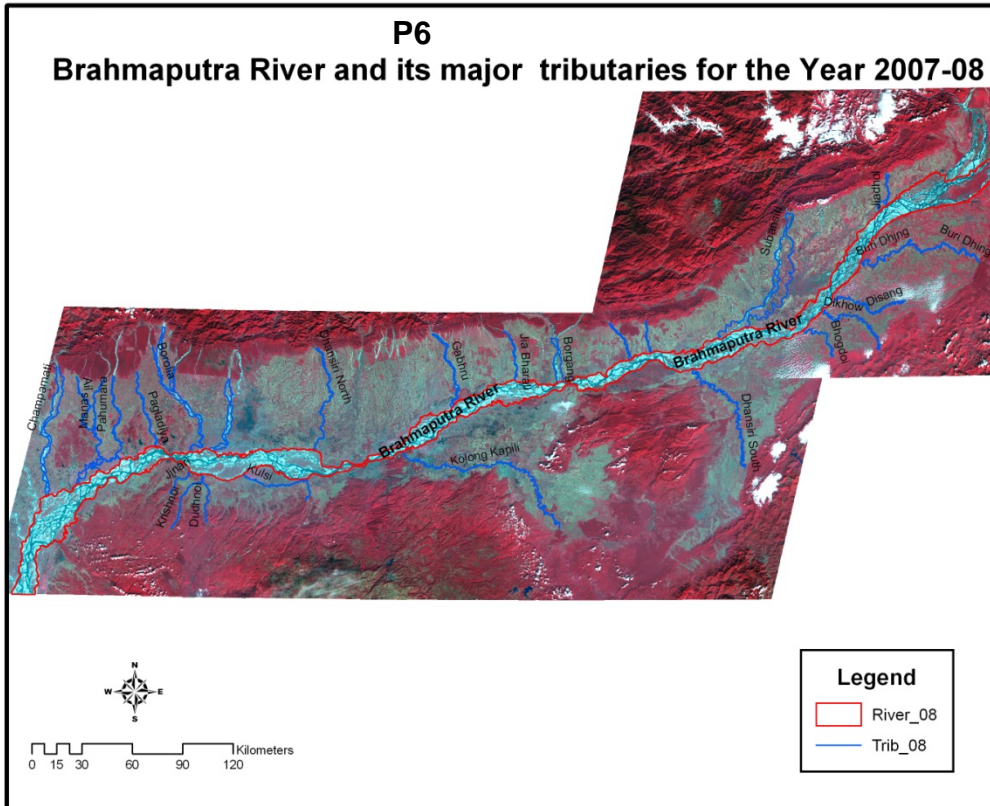


Fig. 59: Mosaic of IRS P6 LISS – III Satellite Images of Brahmaputra River and its major tributaries of the Year 2007-08

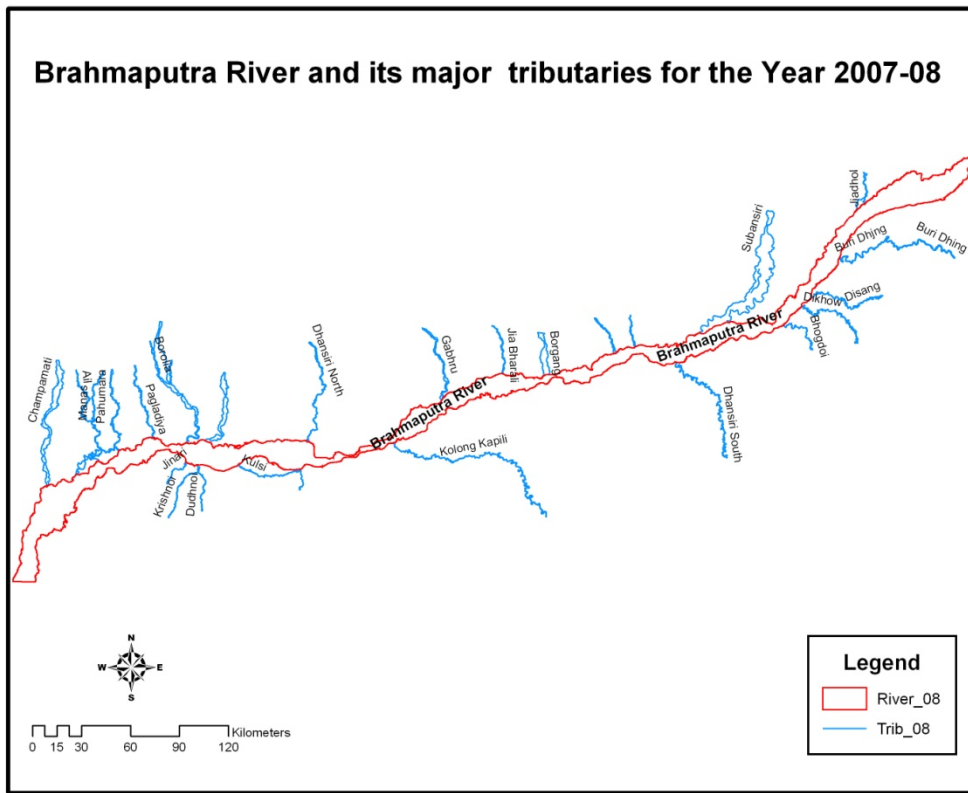


Fig. 60: Brahmaputra River and its major tributaries of the Year 2007-08

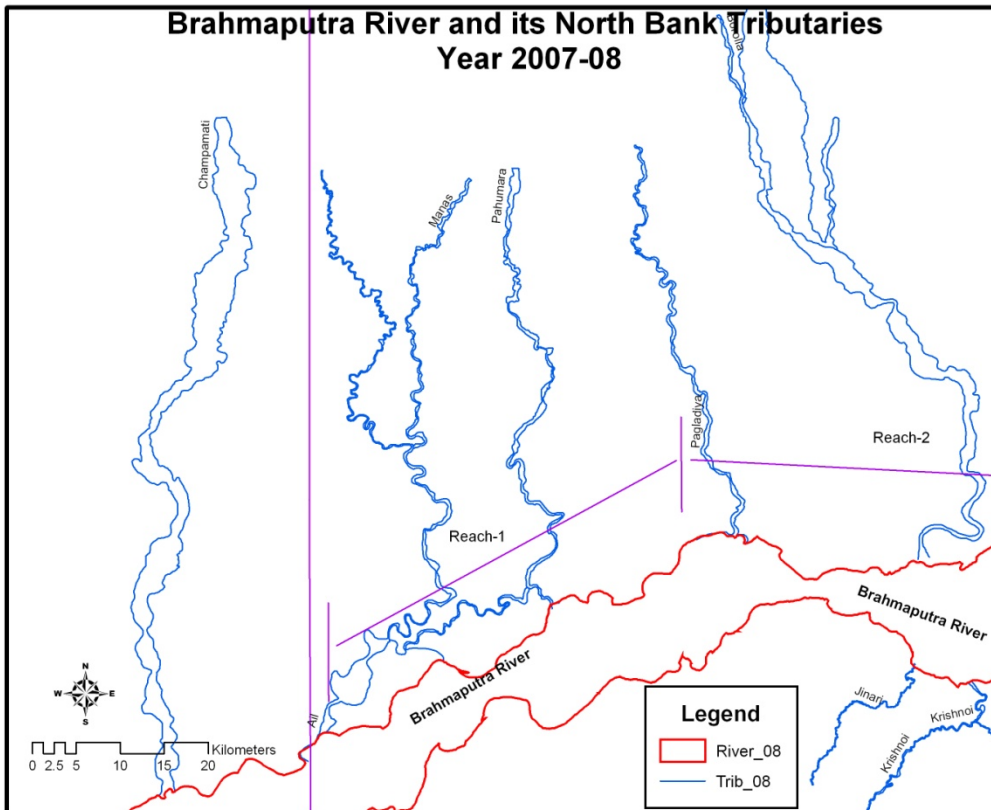


Fig. 61: Brahmaputra River and its North Bank Tributaries Year 2007-08

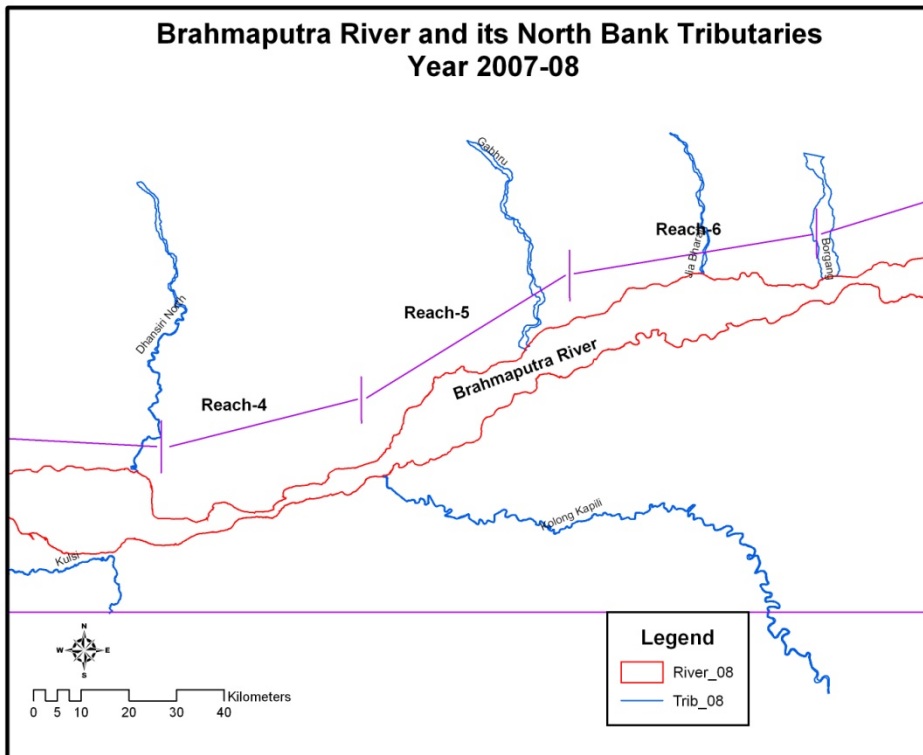


Fig. 62: Brahmaputra River and its North Bank Tributaries Year 2007-08

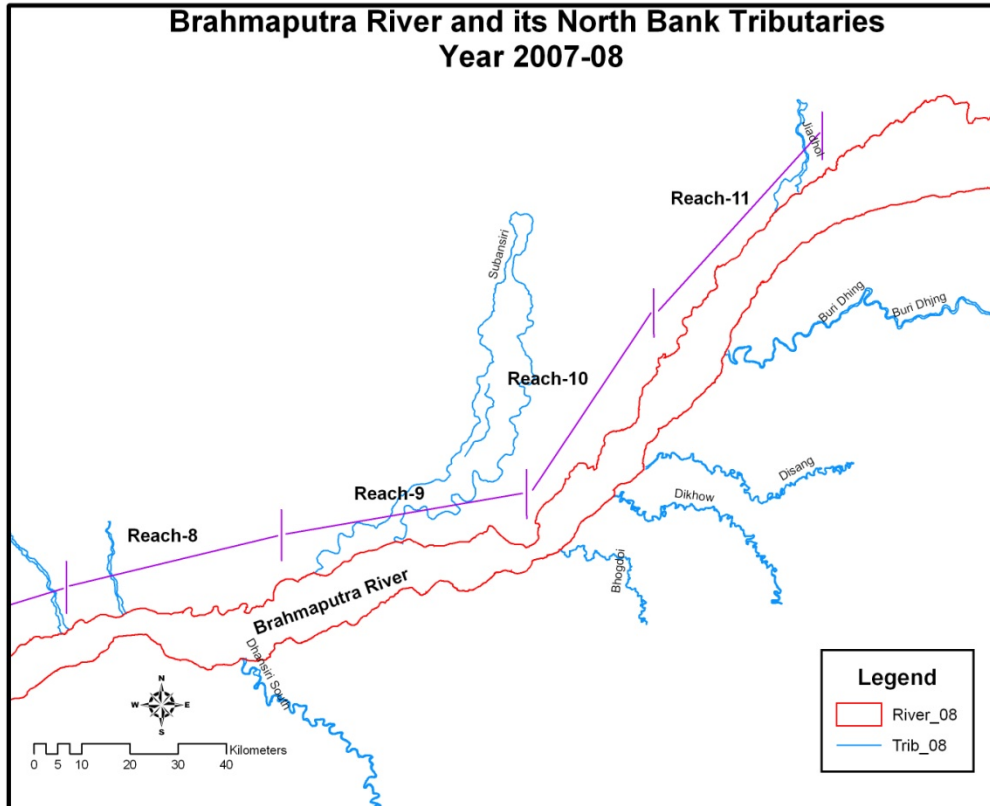


Fig. 63: Brahmaputra River and its North Bank Tributaries Year 2007-08

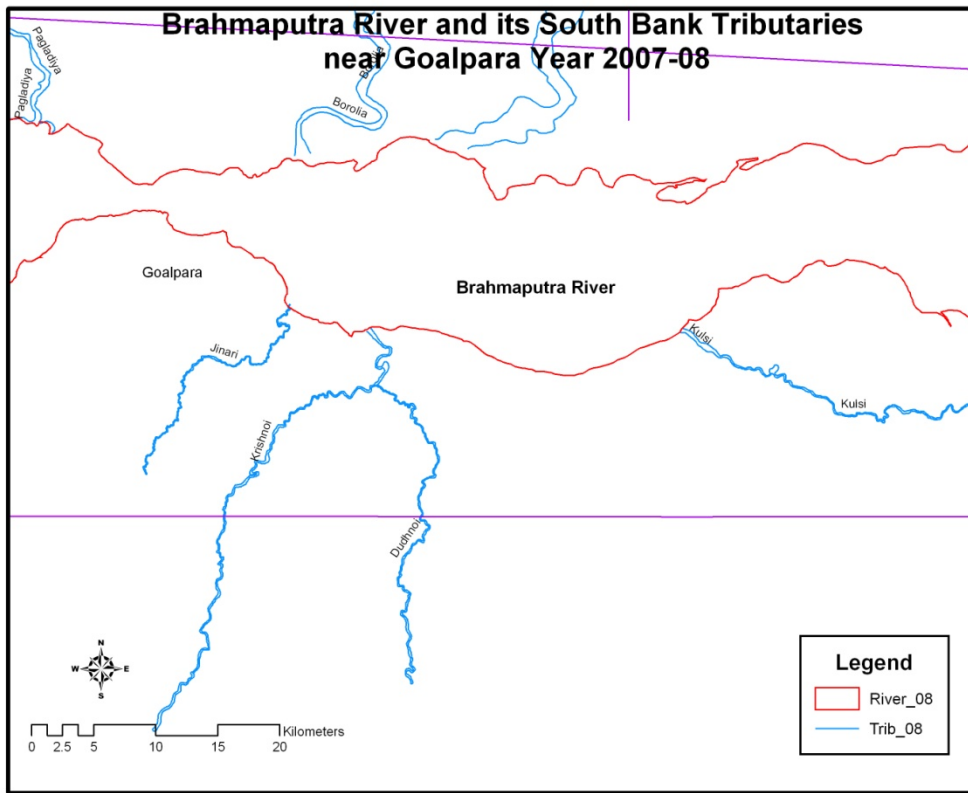


Fig. 64: Brahmaputra River and its South Bank Tributaries Year 2007-08

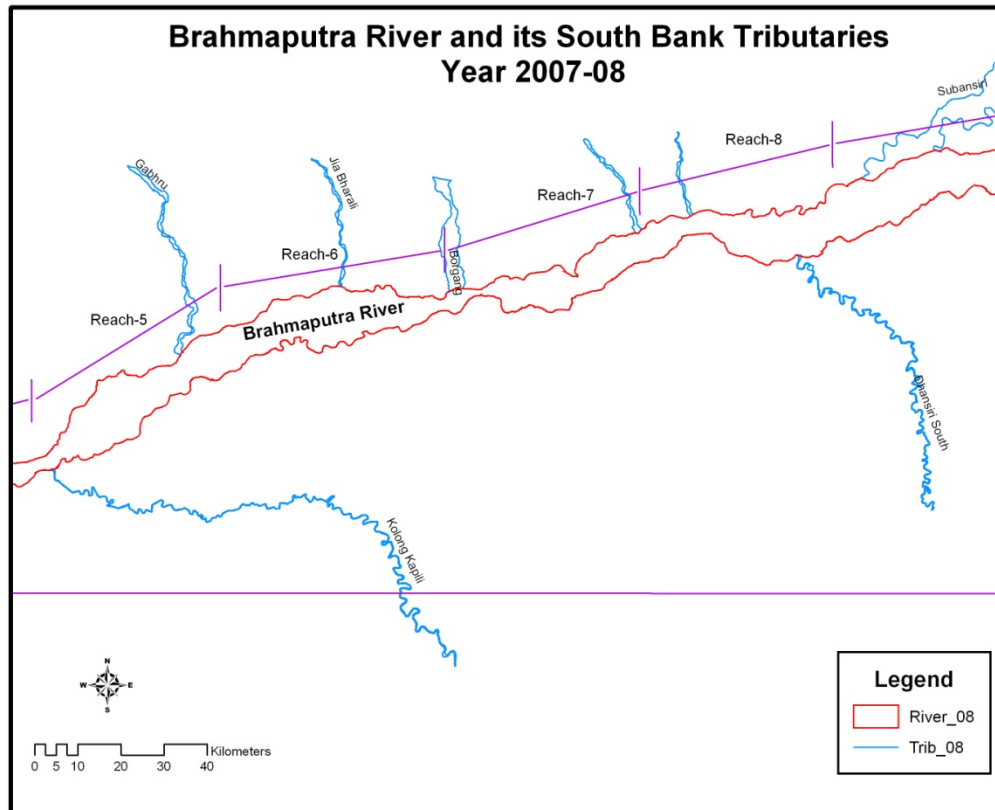


Fig. 65: Brahmaputra River and its South Bank Tributaries Year 2007-08

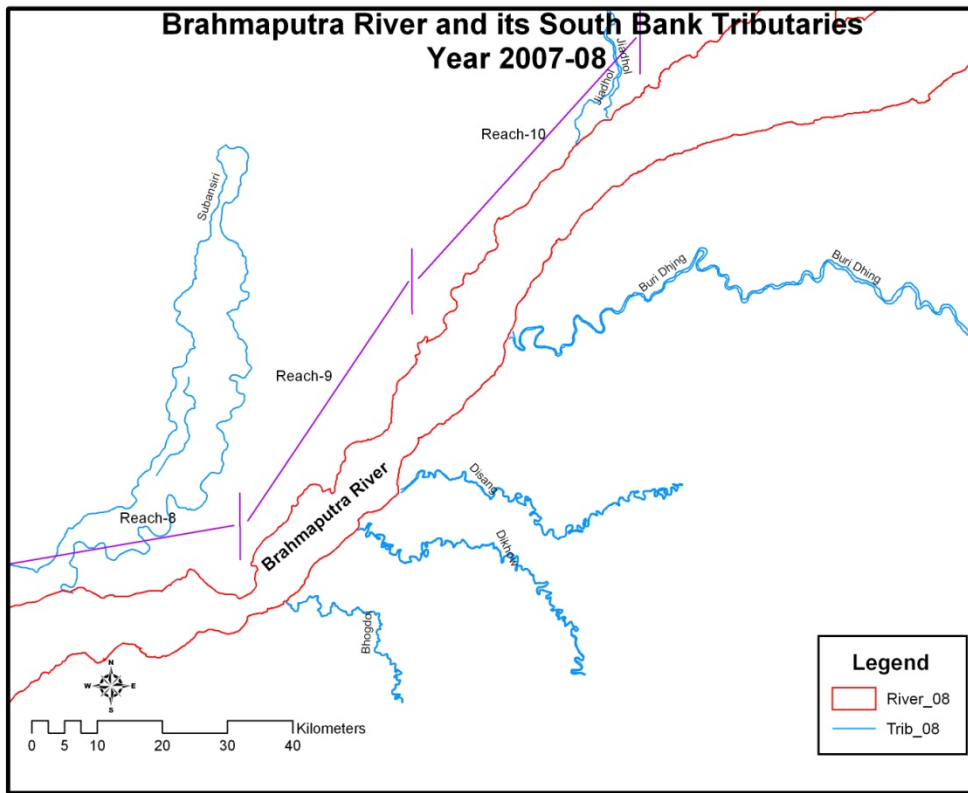


Fig. 66: Brahmaputra River and its South Bank Tributaries Year 2007-08

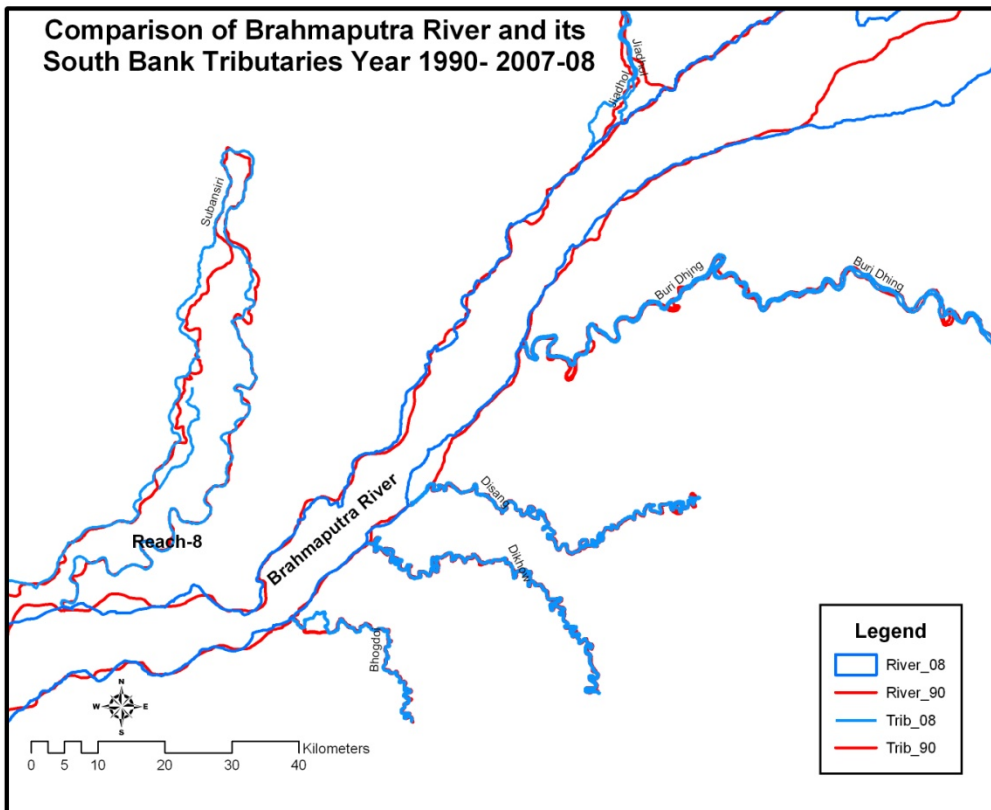


Fig. 67: Comparison of Brahmaputra River and its South Bank Tributaries Year 1990-2007-08

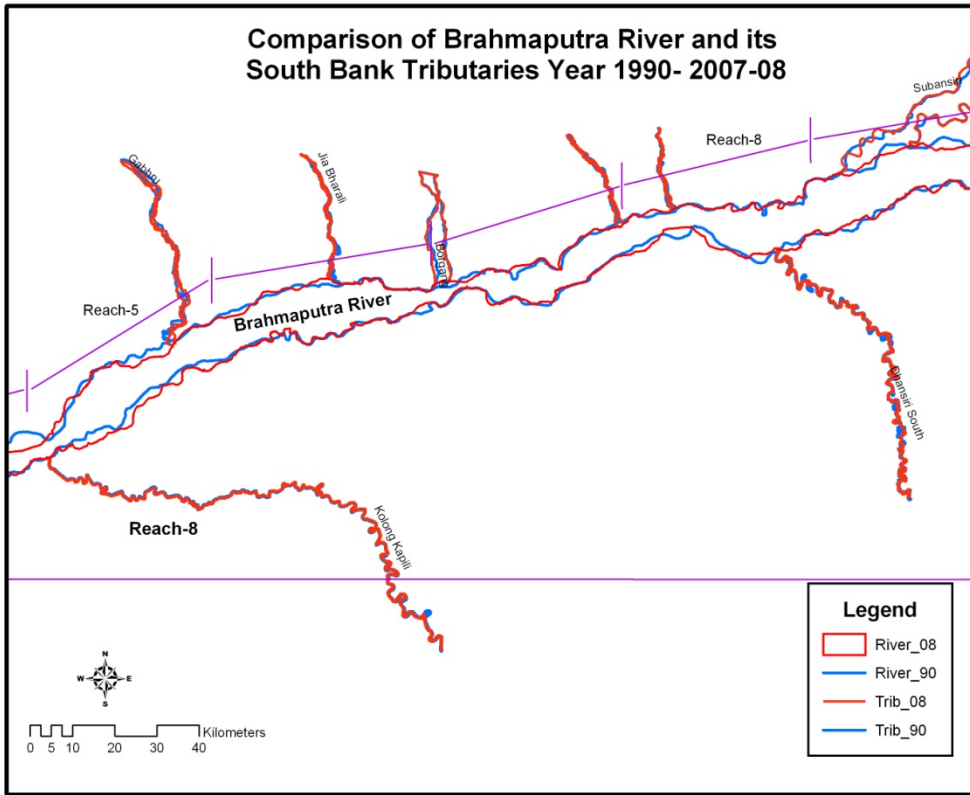


Fig. 68: Comparison of Brahmaputra River and its South Bank Tributaries Year 1990-2007-08

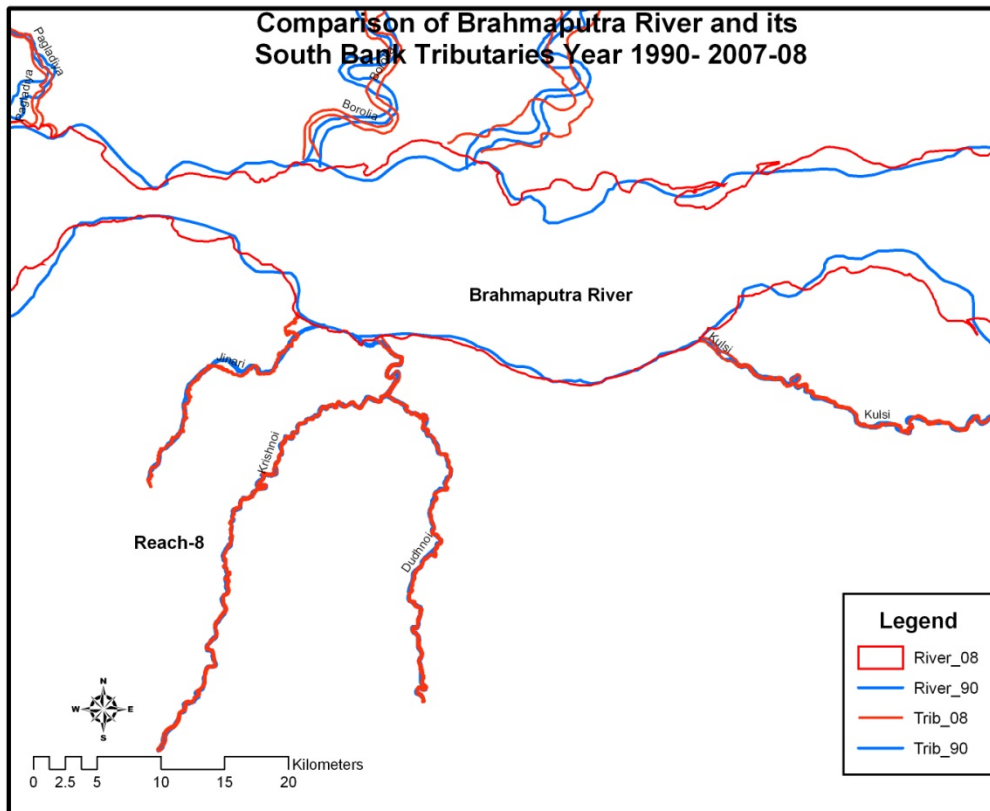


Fig. 69: Comparison of Brahmaputra River and its South Bank Tributaries Year 1990-2007-08

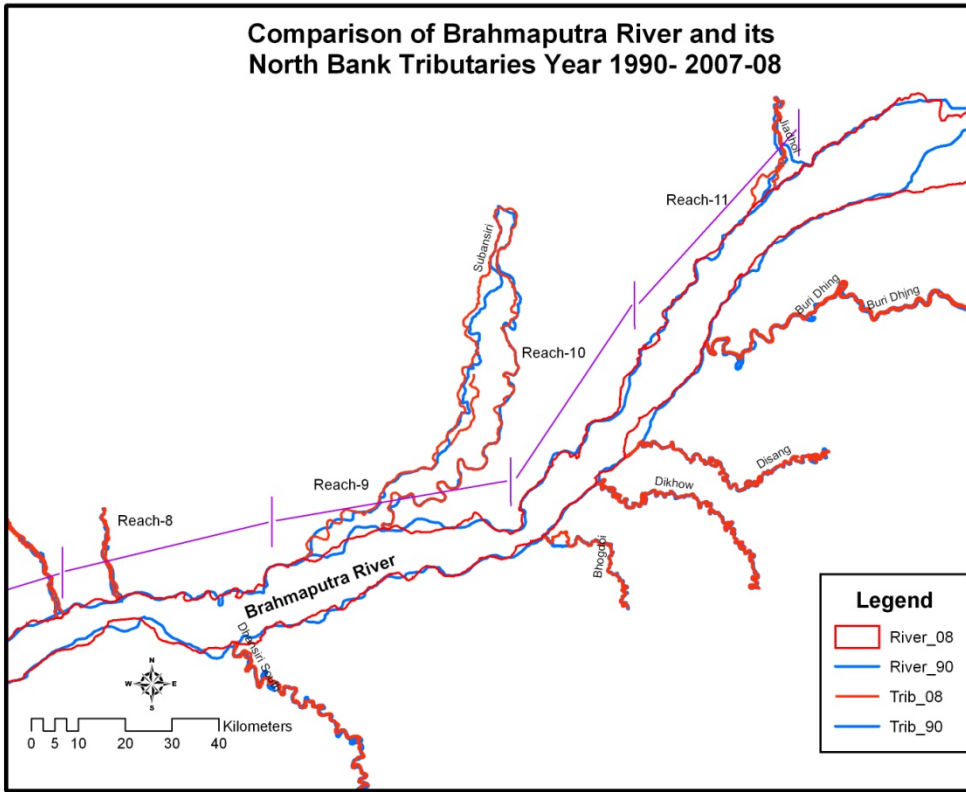


Fig. 70: Comparison of Brahmaputra River and its North Bank Tributaries Year 1990-2007-08

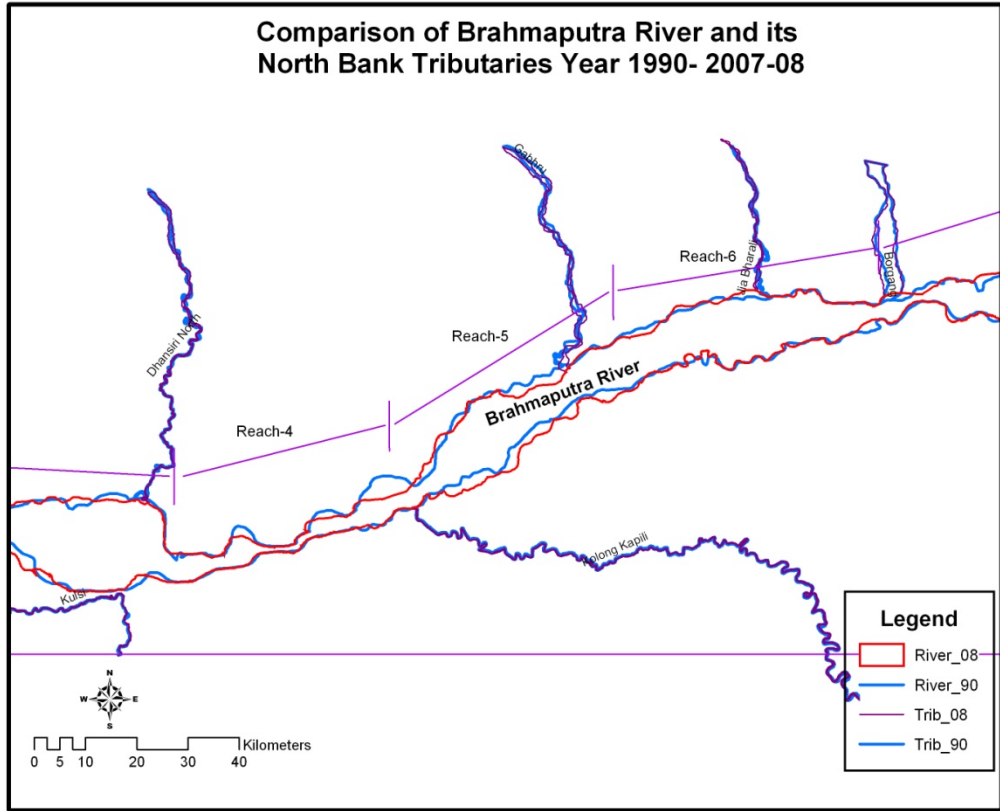


Fig. 71: Comparison of Brahmaputra River and its North Bank Tributaries Year 1990-2007-08

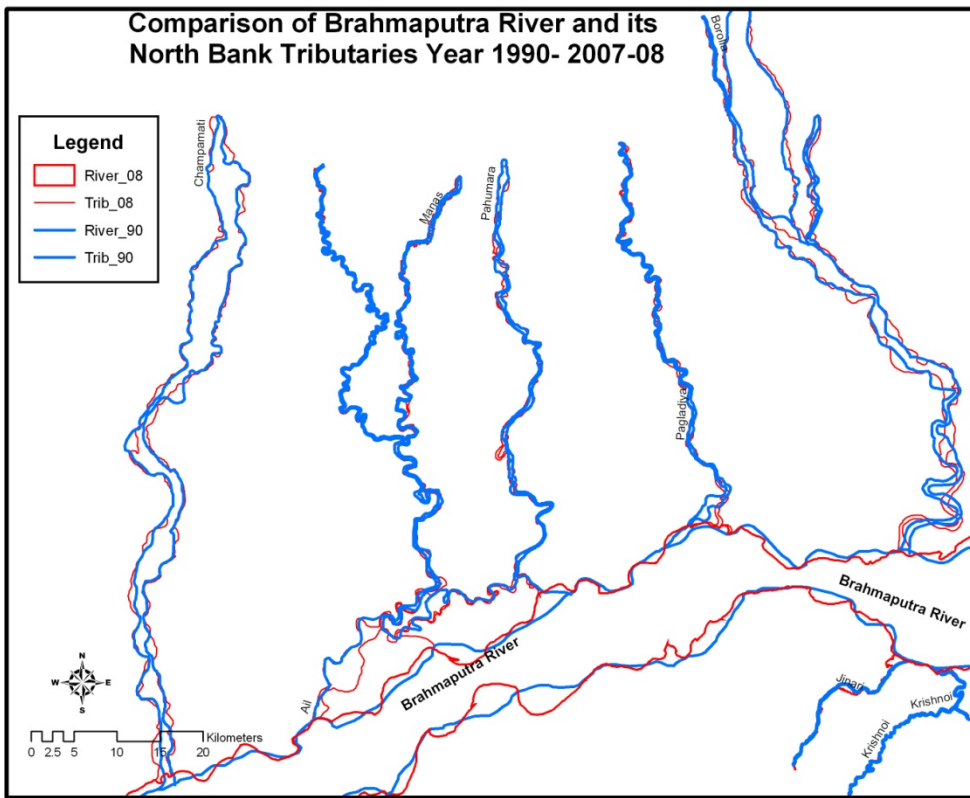


Fig. 72: Comparison of Brahmaputra River and its North Bank Tributaries Year 1990-2007-08

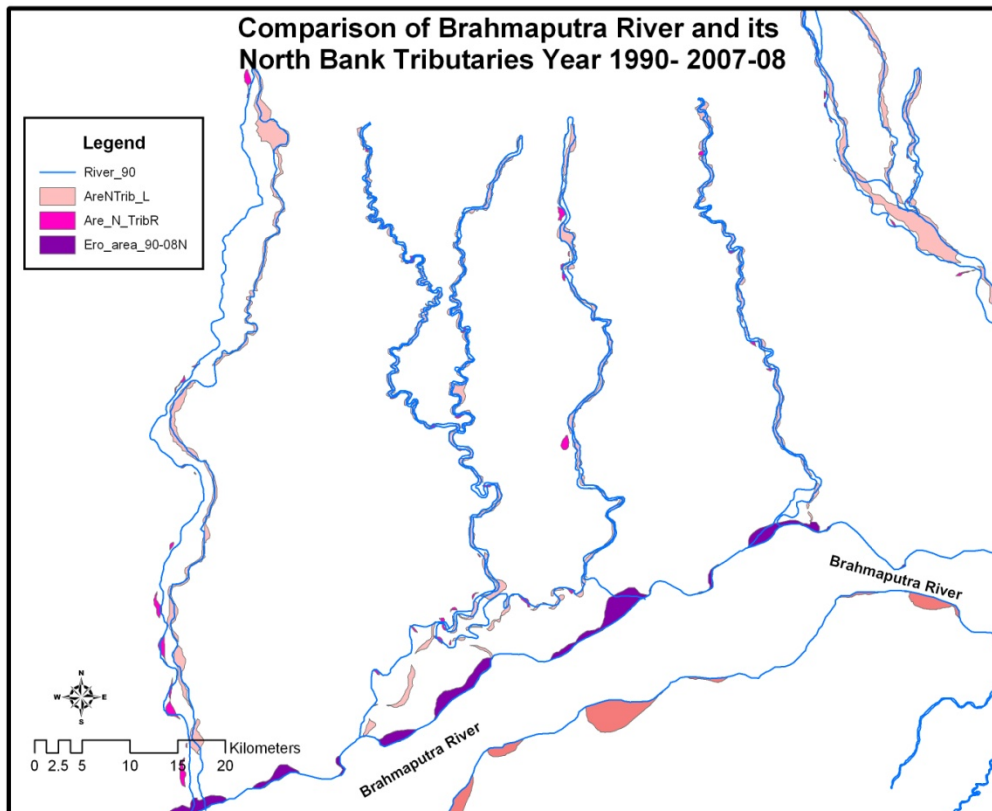


Fig. 73: Comparison of Brahmaputra River and its North Bank Tributaries Year 1990-2007-08

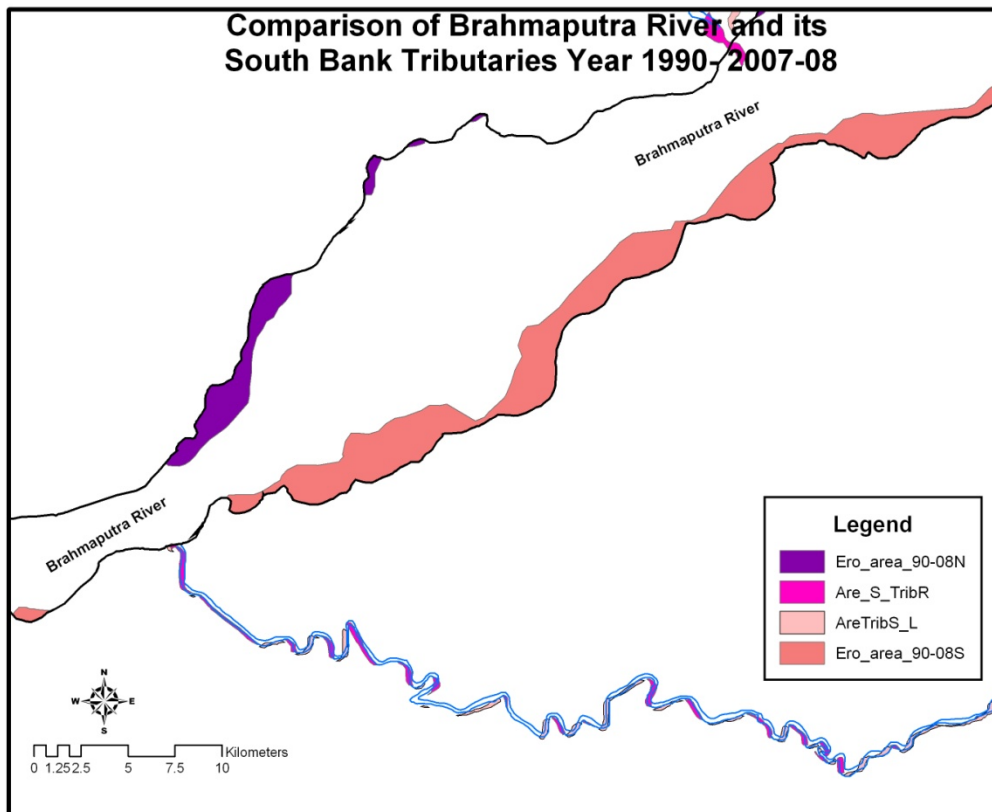


Fig. 74: Comparison of Brahmaputra River and its South Bank Tributaries Year 1990-2007-08

CHAPTER – II
SATELLITE DATA BASED
ANALYSIS FOR MORIGAON SITE
ON BRAHMAPUTRA RIVER

CHAPTER – II

SATELLITE DATA BASED ANALYSIS FOR MORIGAON SITE ON BRAHMAPUTRA RIVER

As decided in the monitoring committee meeting held in the office of Chief Secretary Assam on 17th November 2008, in depth satellite based analysis of the fluvial land-form changes of the Brahmaputra near Morigaon have been conducted and a scheme for pilot study for erosion control has been evolved for this site.

For the above purpose, satellite imageries of IRS 1C/1D for Panchromatic sensor have been processed with the help of ERDAS and Arc-Gis software. The interpretation of these imageries and maps has yielded the quantitative measure of various aspects related to bank erosion. The processed version of these imageries and maps have been placed below.

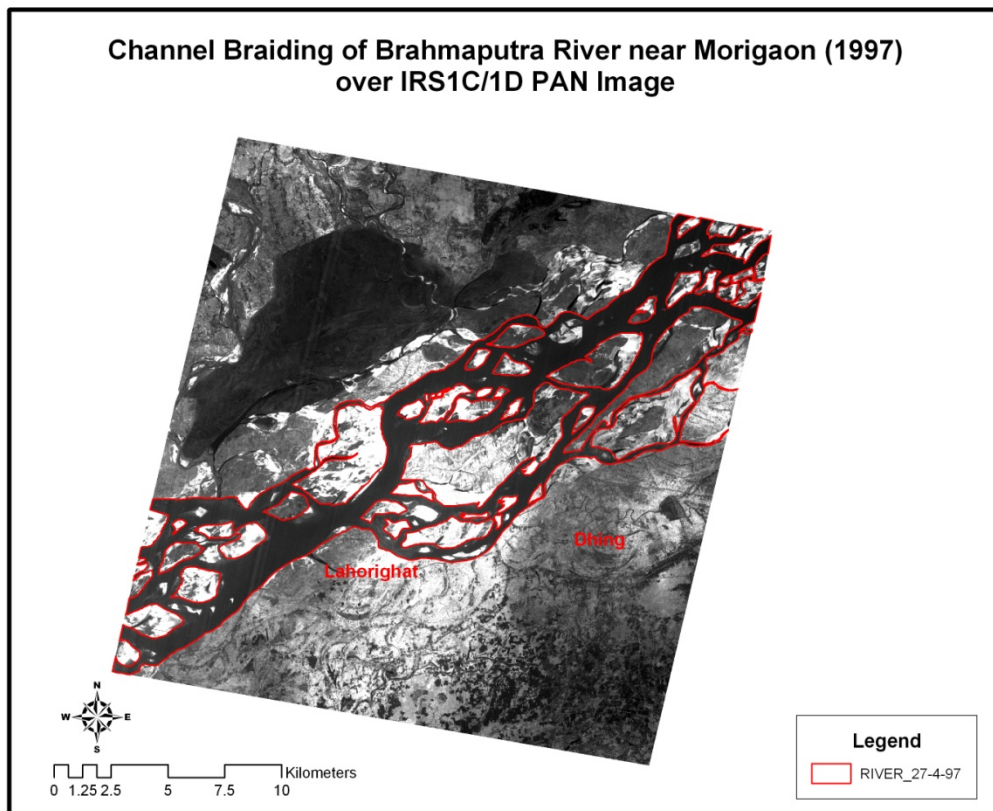


**Fig. 75: Channel Braiding of Brahmaputra River near Morigaon (1997)
over IRS1C/1D PAN Image**

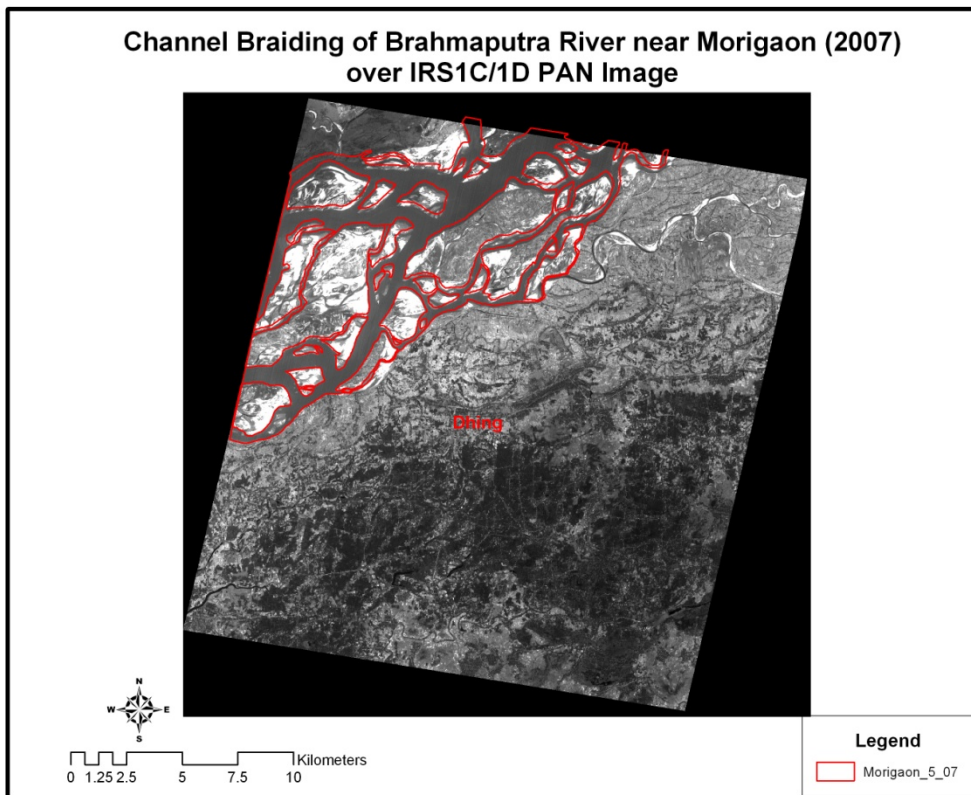


**Fig. 76 Channel Braiding of Brahmaputra River near Morigaon (2007)
over IRS1C/1D PAN Image**

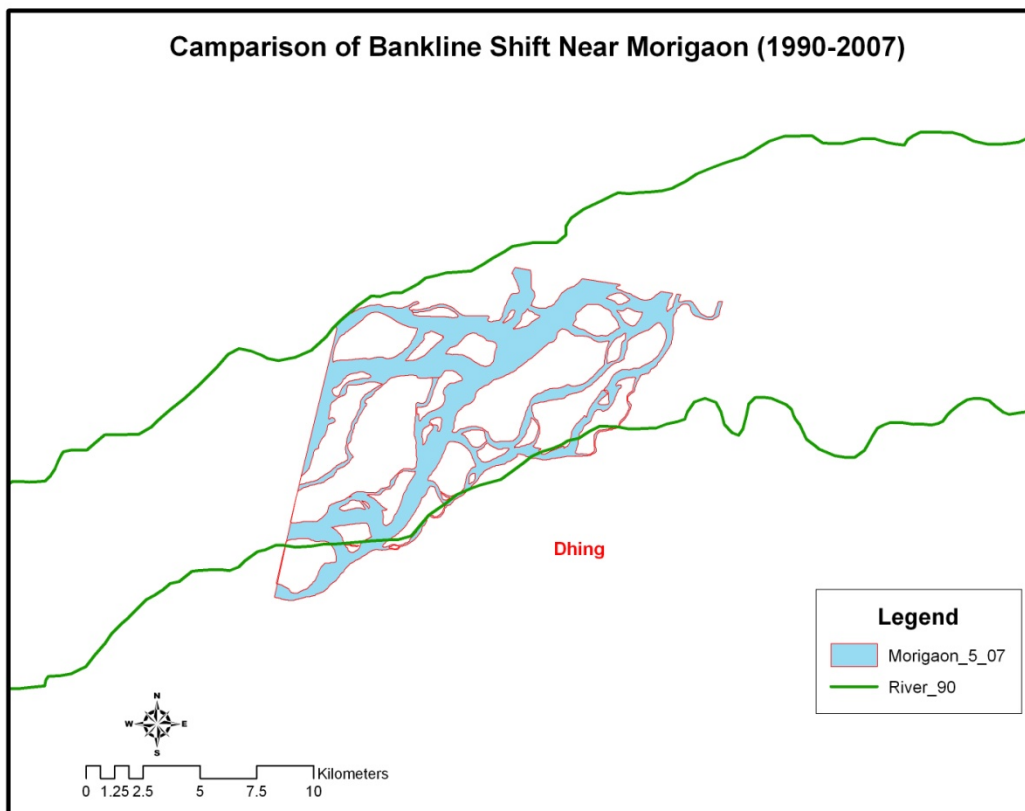


Fig. 77 Comparison of Bankline Shift Near Morigaon (1990-2007)

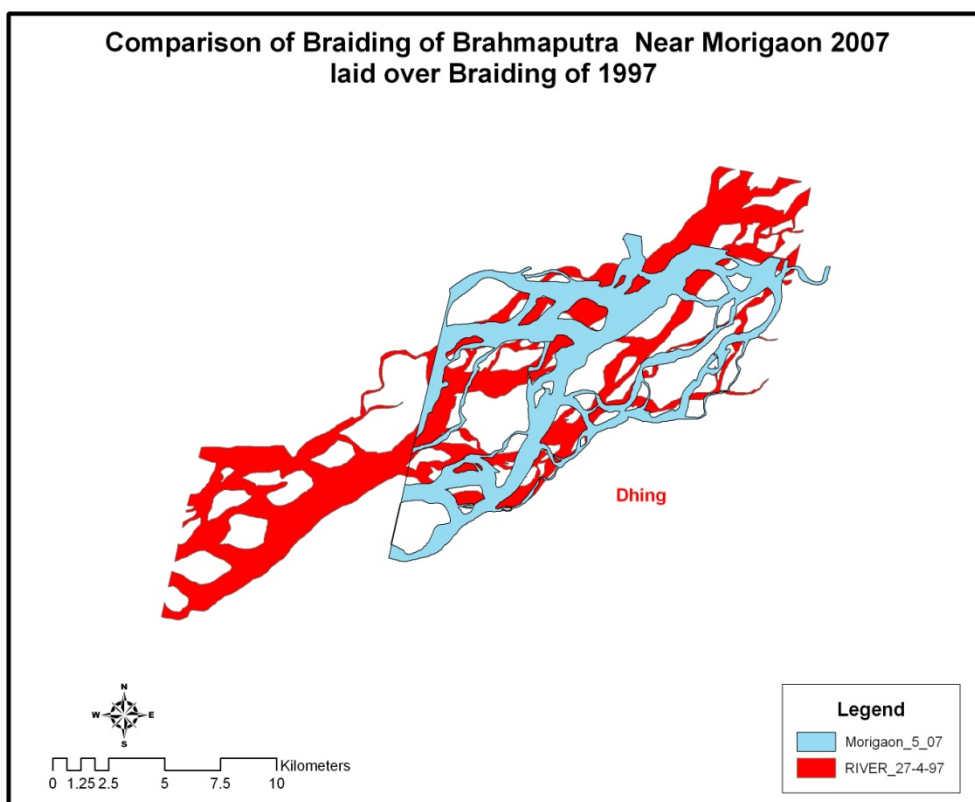


Fig. 78 Comparison of Braiding of Brahmaputra Near Morigaon 2007 laid over Braiding of 1997

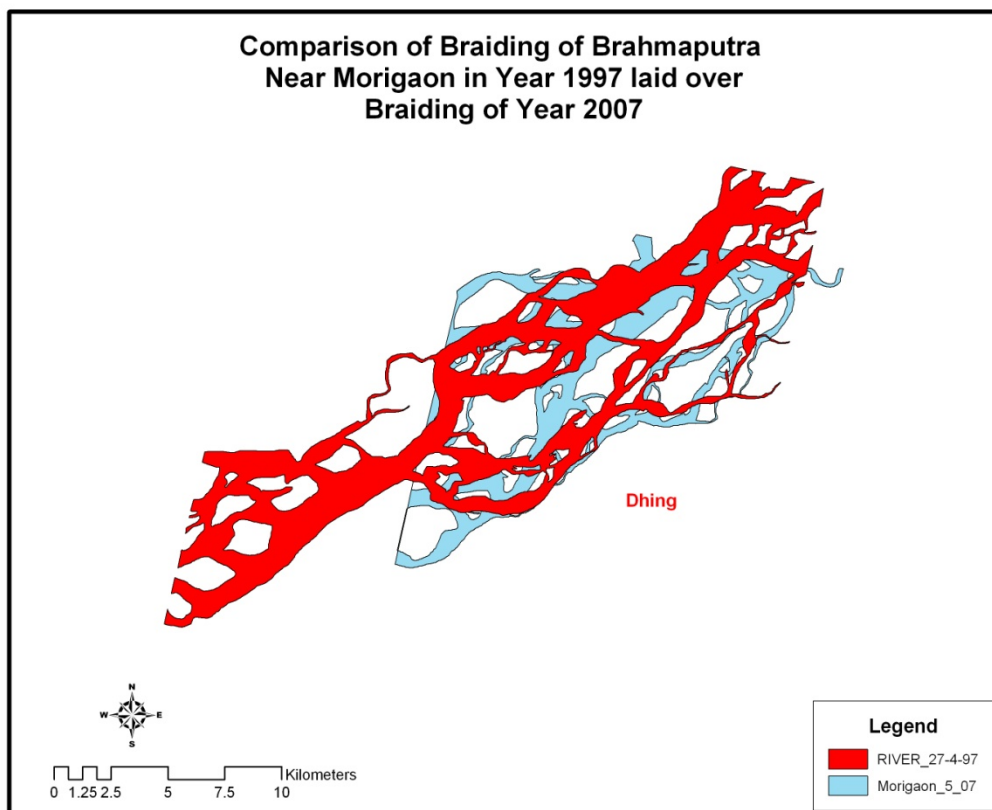


Fig. 79 Comparison of Braiding of Brahmaputra Near Morigaon in Year 1997 laid over Braiding of Year 2007

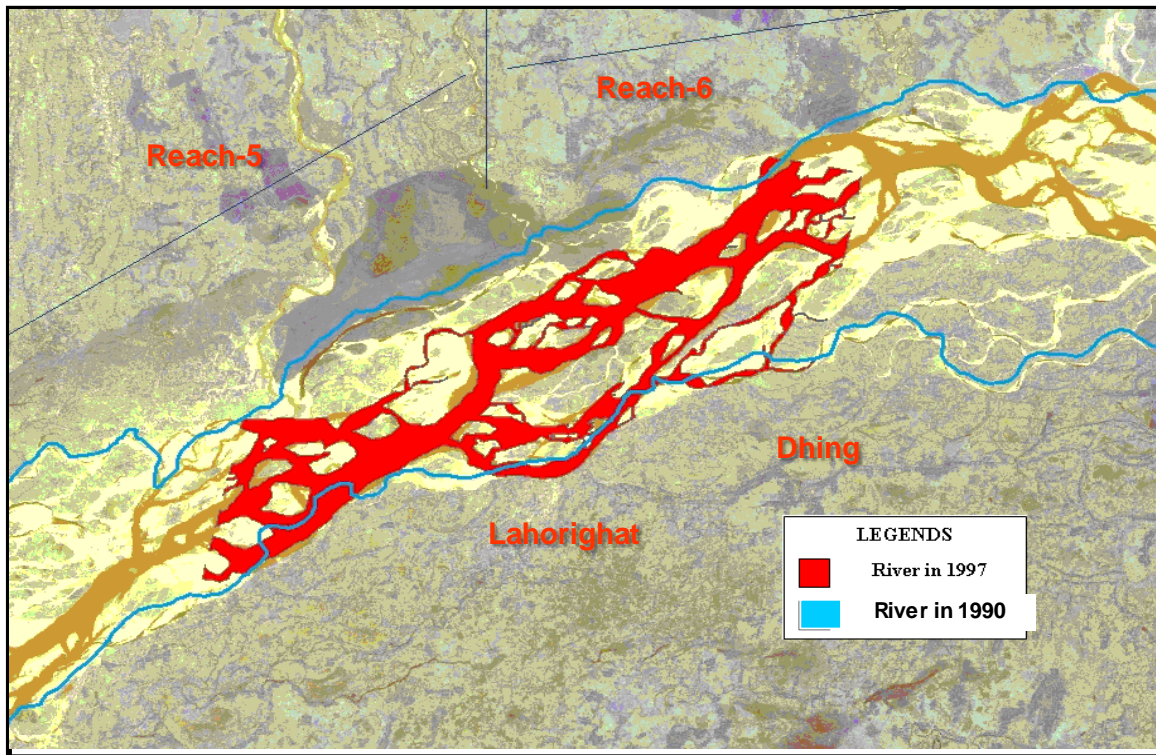


Fig. 80 Superimposed braided channel layer of year 1997 IRS-1D-Pan data at Morigaon site over LISS I image of 1990 (Reach5-6)

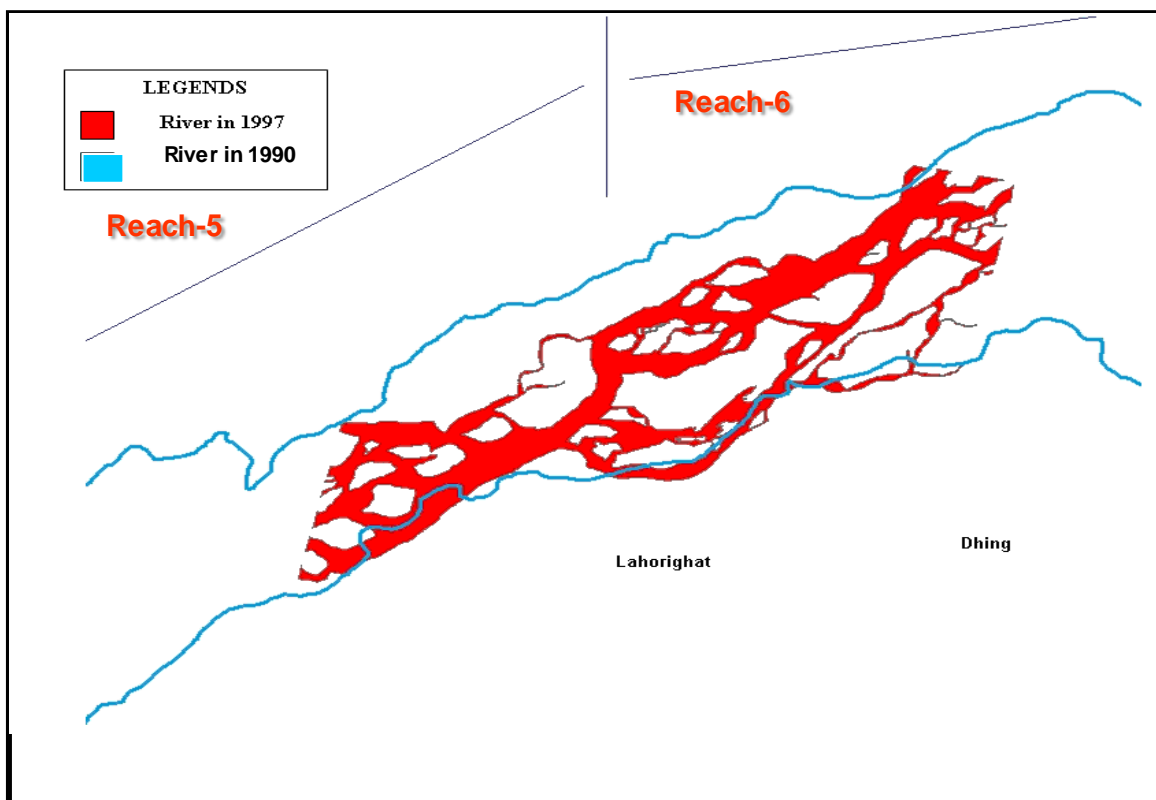


Fig. 81 Superimposed vector layer of PAN Data of Year 1997 near Morigaon site over vector layer of Image Data of the year 1990 at Reach 5-6

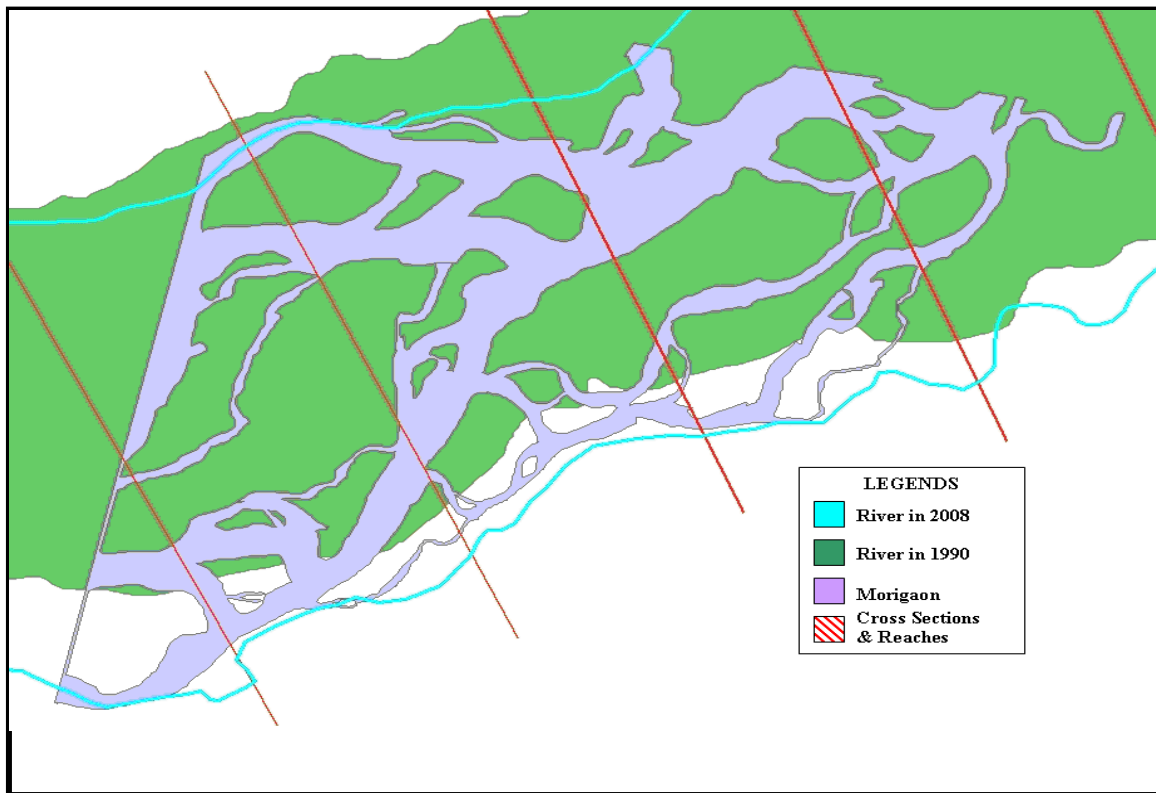


Fig. 82 Comparison of Bank Line Shift near Morigaon site (1990-2007)

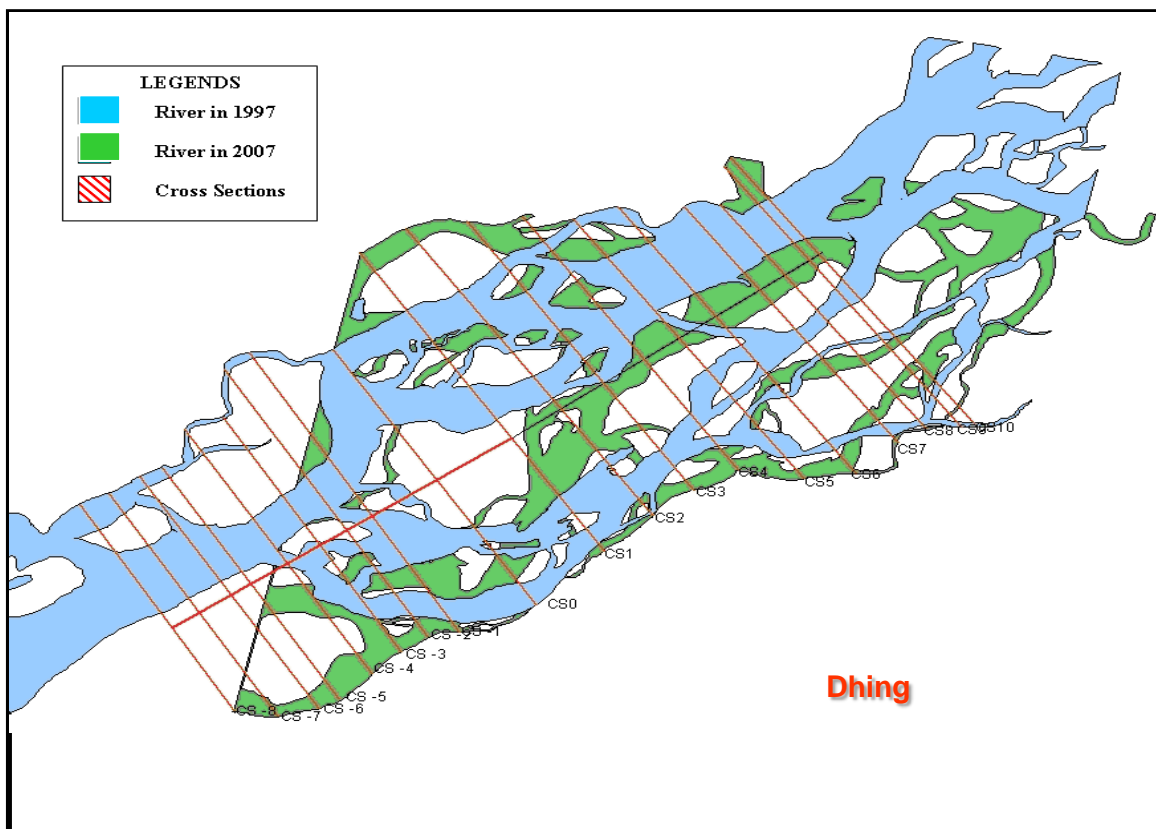


Fig. 83 Comparison of Braiding of Brahmaputra near Morigaon in 1997 with layed over braiding of 2007

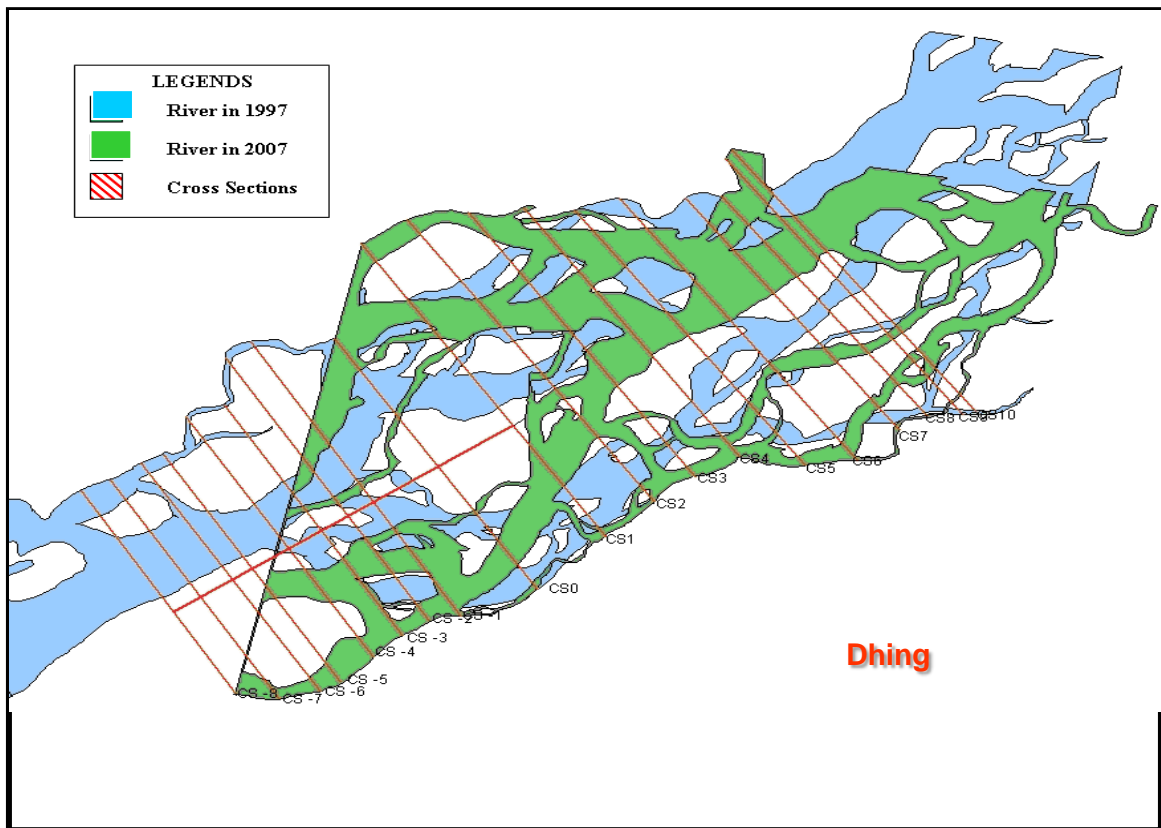


Fig. 84 Comparison of Braiding of Brahmaputra near Morigaon in 2007 with layed over braiding of 1997

TABLE 15: PFI CALCULATION & CHANNEL SHIFT AT MORIGAON SITE AT IDENTIFIED BANK POSITIONS IN YEAR 1997 & 2007

Reference Cross Section	Location North Bank [May,2007] (Lat.- long)		Location South Bank [May,2007] (Lat.- long)		PFI= (T/BN)x 100	PFI= (T/BN) x100	Braiding	Intensity of Braiding	Channel Bank line shifting {Erosion}(m)	
	C/S	Lat.(N)	Long.(E)	Lat.(N)	Long.(E)	1997			2007	South Bank
CS1	26°32'51.66"	92°20'46.95"	26°28'38.39"	92°23'04.33"	9.25	6.02	Increased	Moderately Braided	(+) 208.	(+)1805.
CS2	26°33'12.59"	92°21'20.69"	26°29'9.7"	92°24'35"	7.00	4.31	Increased	Moderately Braided	(+) 44.	(+)1997.
CS3	26°33'19.06"	92°22'10.58"	26°29'32.33"	92°25'06.47"	9.28	7.14	Increased	Moderately Braided	(+)706.	(+)1251.
CS4	26°33'24.24"	92°22'51.47"	26°29'48.47"	92°25'39.66"	8.22	7.65	Increased	Moderately Braided	(+)770.	(+)817.
CS5	26°32'21.29"	92°23'32.4"	26°29'41.42"	92°26'32.37"	9.04	5.75	Increased severly	Moderately Braided	(+)681.	(+)0.00
CS6	26°33'05.38"	92°24'27.95"	26°29'45.33"	92°27'13.24"	6.45	12.20	Decreased severly	Moderately Braided	(+)773.7	(-)1001.
CS7	26°33'11.10"	92°25'15.77"	26°30'12.32"	92°27'44.06"	10.43	7.53	Increased	Moderately Braided	(+)217.	(-)785.
CS8	26°33'33"	92°25'26"	26°30'24.42"	92°28'06.43"	8.13	7.87	Increased	Moderately Braided	(+)164.	0.00
CS9	26°34'06.77"	92°25'28.67"	26°30'36.84"	92°28'25.78"	6.02	7.53	Increased	Moderately Braided	(-)403.	(+)1188.
CS10	26°34'13.67"	92°25'34.87"	26°30'41.25"	92°28'33.38"	6.79	9.04	Decreased	Moderately Braided	(-)645.	(+)1351.

TABLE 16: SOUTH BANK SHIFT OF YEAR 2007 FROM 1997 FOR LOCATED BANK POSITIONS NEAR MORIGAON

Reference Cross section	Location Point of South Bank (2007)		Reach Segment	Reach Length	PFI (1997)	Intensity of Braiding	South Bank line shifting (Erosion) from Year 1997 to 2007 (meter)
	Lat.(N)	Long.(E)					
CS0	26°27'52.44"	92°23'4.33"	0.00	0.00	11.50	Moderately braided	0
CS-1	26°27'29"	92°22'6.26"	2395.07	2395.07	11.67	Moderately braided	311.53
CS-2	26°27'25.21"	92°21'41.34"	691.25	3086.31	7.70	Moderately braided	664.3
CS-3	26°27'13.24"	92°21'20.61"	702.27	3788.58	8.93	Moderately braided	1000.89
CS-4	26°26'53.67"	92°20'57.86"	837.74	4626.32	14.43	Moderately braided	3313.43
CS-5	26°26'33"	92°20'33"	949.94	5576.26	26.67	Low Braiding	3988.99
CS-6	26°26'24.20"	92°20'17.17"	549.93	6126.19	44.12	Low Braiding	3977.71
CS-7	26°26'17.81"	92°19'45.33"	835.51	6961.69	35.14	Low Braiding	3629.91
CS-8	26°26'22"	92°19'9.26"	748.48	7710.18	39.72	Low Braiding	2989.17

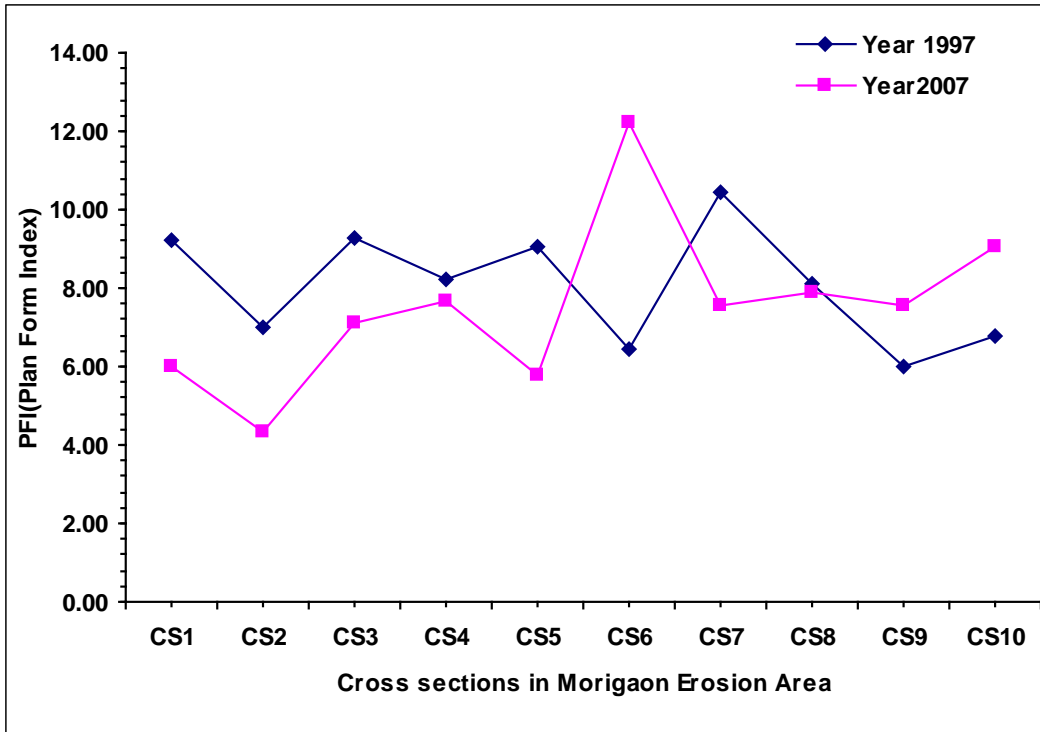


Fig. 85 Plan Form Index Comparison of year 1997 and 2007 for Morigaon Site

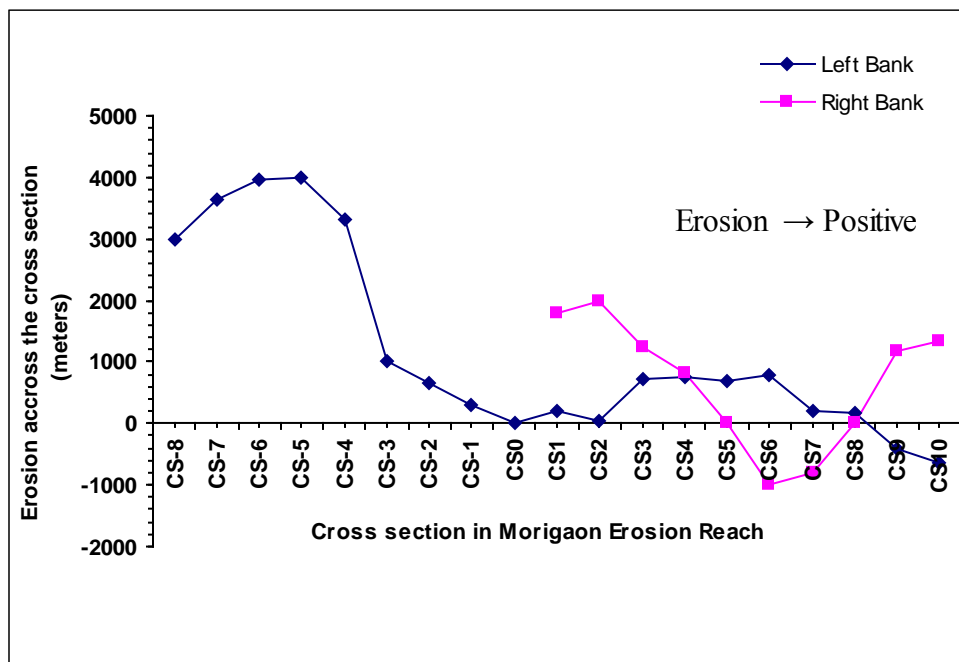


Fig. 86 Bank Line Shift Comparison of Left and Right Bank for 1997 -2007 for Morigaon Site

From the above analysis, the following major findings have emerged

- i) Braiding intensity has registered a significant rise during the course of 1997 – 2007 as evident from the Table No.10 due to unabated stream bank erosion.
- ii) The maximum length of bank retreat due to erosion in the south bank approximately 4 Km.
- iii) The maximum length of bank retreat due to erosion in the North bank approximately 1.99 Km.

Chapter -III

FINDINGS OF PHASE – I STUDY

Chapter – III

FINDING OF PHASE – I STUDY

Table 17: SUMMARY OF LAND LOSS DUE TO EROSION IN MAIN STEM AND MAJOR TRIBUTARIES OF BRAHMAPUTRA RIVER SYSTEM

S. No.	Item	Period of Study				Remarks
		1997 to 2007-08		1990 to 2007-08		
		Annual land loss Sq.km/year	Total Land Lost Sq.km	Annual land loss Sq.km/year	Total Land Lost Sq.km	
1	Main stem	73	725	62	1054	During the shorter period of 1997-2008 Brahmaputra river system has exhibited considerable increase in annual land lost in comparison to prolong period of 1990 to 2007-08
2.	Major Tributaries	54	543	38	639	
	Total	127	1268	100	1693	

From the preceding analyses, the following findings have emerged.

[A] Brahmaputra Main Stem:-

- i) Braiding intensity has registered a sharp rise during the course of 1990 – 2008 as evident from the Table No.5 due to unabated stream bank erosion.
- ii) The total land area lost during 1990 – 2008 in main stem Brahmaputra is assessed through GIS data base of satellite derive maps to be 1054 Sq. Km (without considering the isolation of forest area of Dibru-Saikhowa reserved forest due to avulsion).
- iii) The total land area lost during 1997 – 2008 in main stem Brahmaputra is assessed through GIS data base of satellite derive maps to be 725 Sq. Km (without considering the isolation of forest area of Dibru-Saikhowa reserved forest due to avulsion).
- iv) The total land area lost during 1990 – 2008 is assessed to be 515 Sq. Km in the south bank.
- v) The total land area lost during 1990 – 2008 is assessed to be 539 Sq. Km in the north bank.

- vi) The total land area lost during 1997 – 2008 is assessed to be 397 Sq. Km in the south bank.
- vii) The total land area lost during 1997 – 2008 is assessed to be 328 Sq. Km in the north bank
- viii) Thus, during 1990-2007-08 approximately 1054 Sq. Km. of land area has been lost, giving an annual area loss of 62 Sq.Km/Year.
- ix) During the period of 1997 to 2007-08 the annual rate of erosion has considerably increase to 73 sq.km /year in comparison to 62 sq Km/year for the prolong period of 1990 to 2007-08.
- x) During the recent period of 1997-2007-08, South Bank of Main Brahmaputra stem has exhibited considerably higher erosion in comparison to north Bank in contrast to the prolonged period of 1990-2007-08.
- xi) The maximum length of bank retreat due to erosion in the south bank approximately 4.125 Km at near Morigaon.
- xii) The maximum length of bank retreat due to erosion in the North bank approximately 4.251 Km at near Dhubri.
- xiii) The total length of erosion-affected bank line approximately 743 Km out of which south bank 389 Km and 354 Km in North bank.

[B] Major Tributaries of Brahmaputra River System:-

- i) The total land area lost during 1990 – 2008 in major tributaries of Brahmaputra river system is worked out through GIS data base of satellite derive maps to be 639 Sq. Km .
- ii) The total land area lost during 1997 – 2008 in major tributaries of Brahmaputra river system is assessed through GIS data base of satellite derive maps to be 543 Sq. Km.
- iii) The total land area lost during 1990 – 2008 is assessed to be 223 Sq. Km in the southern tributaries.
- iv) The total land area lost during 1990 – 2008 is assessed to be 416 Sq. Km in the northern tributaries.
- v) The total land area lost during 1997 – 2008 is assessed to be 187 Sq. Km in the southern tributaries.
- vi) The total land area lost during 1997 – 2008 is assessed to be 356 Sq. Km in the northern tributaries.

- vii) Thus, during 1990-2007-08 approximately 639 Sq. Km. of land area has been lost, giving an annual area loss of 38 Sq.Km/Year for major tributaries.
- viii) During the period of 1997 to 2007-08 the annual rate of erosion has considerably increase to 54 sq.km /year in comparison to 38 sq Km/year for the prolong period of 1990 to 2007-08 for major tributaries.
- ix) During the study periods Northern tributaries of Brahmaputra River have exhibited higher erosion in comparison to Southern tributaries.

REFERENCES

REFERENCES

1. Bardhan, M. (1993). Channel stability of Barak river and its tributaries between Manipur-Assam and Assam- Bangladesh borders as seen from satellite imagery, Proc. Nat. Syrup. on Remote Sensing Applications for resource Management with special emphasis on N.E. region, held in Guwahati, Nov. 25-27, 481-485.
2. Bhakal, L., Dubey, B., and Sarma, A.K. 2005. Estimation of bank erosion in the river Brahmaputra near Agyathuri by using geographic information system. Photonirvachak, J. of the Indian Society of Remote Sensing, Vol. 33, No.1, 81-84.
3. Brahmaputra Board (1997). Report on erosion Problem of Majuli Island, Brahmaputra Board, Guwahati.
4. Couper, P.R., 2004, Space and time in river bank erosion research: A review: Area,v.36,no.4,p.387–403.
5. Das, J.D. and Saraf, A.K. 2007. Remote sensing in the mapping of the Brahmaputra/Jamuna River channel patterns and its relation to various landforms and tectonic environment. Intl J of remote sensing, 28, pp3619-3631.
6. Florsheim, J.L., Mount, J.F., and Chin, A., 2008, Bank erosion as a desirable attribute of rivers, BioScience, v. 58, no. 6, p. 519–529.
7. Flosi, G., Downie, S., Hopelain, J., Bird, M., Coey, R., and Collins, B., 1998, California salmonid stream habitat restoration manual: Sacramento, California Department of Fish and Game.
8. Fuller, I.C., Large, A.R.G., Milan, D.J., 2003. Quantifying channel development and sediment transfer following chute-off in a wandering gravel-bed river. Geomorphology 54, 307–323.
9. Goswami, U., Sarma, J.N. and Patgiri, A.D. (1999). River channel changes of Subansiri in Assam. India. *Geomorphology*, 30: 227-244.
10. Johnson, W.C., 1994, Woodland expansion in the Platte River, Nebraska: Patterns and causes: Ecological Monographs, no. 64, p. 45–84.
11. Kotoky P., Bezbaruah D., Baruah J. and J. N. Sarma J. N., “Nature of bank erosion along the Brahmaputra river channel, Assam, India” CURRENT SCIENCE, VOL. 88, NO. 4, 25 FEBRUARY 2005,pp 634-640

12. Kumm, M., Lub, X.X., Rasphonec, A., Sarkkulad, J., and Koponen, J. 2008. *Quaternary International* 186, 100–112.
13. Li, L.Q., Lu, X.X., Chen, Z., 2007. River channel change during the last 50 years in the middle Yangtze River: an example of the Jianli reach. *Geomorphology* 85, 185-196.
14. Mani, P., Kumar, R., and Chatterjee, C. (2003). Erosion Study of a Part of Majuli River-Island Using Remote Sensing Data. *Journal of the Indian Society of Remote Sensing*, Vol. 31, No. 1, pp11-18.
15. Miller, J.R., and Friedman, J.M., 2009, Influence of flow variability on floodplain formation and destruction, Little Missouri River, North Dakota: *Geological Society of America Bulletin*, v. 121, p. 752–759.
16. Moody, J.A., and Meade, R.H., 2008, Terrace aggradation during the 1978 flood on Powder River, Montana, USA: *Geomorphology*, v. 99, p. 387–403.
17. Naik, S.D., Chakravorty, S.K., Bora, T. and Hussain, (1999). Erosion at Kaziranga National Park, Assam, a study based on multitemporal satellite data. Project Report. Space Application Centre (ISRO) Ahmedabad and Brahmaputra Board, Guwahati.
18. NRSA (1980). Brahmaputra flood mapping and river migration studies- airborne scanner survey. National Remote Sensing Agency, Hyderabad, India
19. Rinaldi, M., 2003. Recent channel adjustments in alluvial rivers of Tuscany, central Italy. *Earth Surface Processes and Landforms* 28, 587–608.
20. SAC and Brahmaputra Board (1996). Report on bank erosion on Majuli Island, Assam: a study based on multi temporal satellite data. Space Application Centre, Ahmedabad and Brahmaputra Board, Guwahati.
21. Sarma, J.N. and Basumallick, S. (1980). Bankline migration of Burhi Dihing River, Assam. *Ind. J. Ear. Sci.*, 11(3&4): 199-206.
22. Sarma, J.N., Borah, D., and Goswami, U. 2007 , Change of River Channel and Bank Erosion of the Burhi Dihing River (Assam), Assessed Using Remote Sensing Data and GIS. *Journal of the Indian Society of Remote Sensing*, Vol. 35, No. 1, pp 94-100.

23. Simon, A., and Rinaldi, M., 2000, Channel instability in the loess area of the midwestern United States: *Journal of the American Water Resources Association*, v. 36, no. 1, p. 133–150.
24. Surian, N., 1999. Channel changes due to river regulation: the case of the Piave River, Italy. *Earth Surface Processes and Landforms* 24, 1135–1151.
25. Surian, N., Rinaldi, M., 2003. Morphological response to river engineering and management in alluvial channels in Italy. *Geomorphology* 50, 307–326.
26. U.S. Geological Survey, 2005, Assessing sandhill crane roosting habitat along the Platte River, Nebraska: Fact Sheet 2005–3029, 2 p. [<http://pubs.usgs.gov/fs/2005/3029/>]
27. Yang, X., Damen M.C.J. and Zuidam R.A.van: Satellite remote sensing and GIS for the analysis of channel migration changes in the active Yellow river Delta, China, *Int'l. J. of Applied Earth Observation and Geoinformation*, Vol. 1, Issue 2, pp. 146-157, 1999.

PHASE – II

HYDROLOGICAL DATA PROCESSING & ANALYSIS

TEAM OF INVESTIGATORS

- 1. Prof. Dr. Nayan Sharma**
- 2. Ms. Archana Sarkar**
- 3. Mr. Neeraj Kumar**

TABLE OF MAJOR CONTENTS

Sl. No.	Subject	Page No.
CHAPTER – I	INTRODUCTION	3
CHAPTER – II	BACKGROUND OF ARTIFICIAL NEURAL NETWORKS	11
CHAPTER – III	REVIEW OF LITERATURE	40
CHAPTER – IV	STUDY AREA AND DATA AVAILABILITY	61
CHAPTER – V	METHODOLOGY	77
CHAPTER – VI	RESULTS AND DISCUSSION	98
CHAPTER – VII	SUMMARY	116
CHAPTER – VIII	REFERENCES & BIBLIOGRAPHY	119

Chapter – 1



Introduction

1.1 GENERAL

Management of Water resources requires input from hydrological studies. This is mainly in the form of estimation or forecasting of the magnitude of a hydrological variable like rainfall, runoff and sediment concentrations using past experience. Such forecasts are useful in many ways. They provide a warning of the extreme flood or drought conditions in case of rainfall-runoff modeling and assessment of volume of sediments being transported by a river in case of runoff-sediment modeling. This helps to optimize the design and maintenance of systems like reservoirs and power plants. The contract negotiation and hydropower sales also call for forecasted values of river flows and sediment loads.

1.2 RAINFALL-RUNOFF PROCESS

The rainfall - runoff process is believed to be highly nonlinear, time-varying, spatially distributed, and not easily described by simple models. In addition to rainfall, runoff is dependent on numerous factors such as initial soil moisture, land use, watershed geomorphology, evaporation, infiltration, distribution, duration of the rainfall, and so on. Although many watersheds have been gauged to provide continuous records of stream flow, engineers are often faced with situations where little or no information is available. A number of models have been developed to simulate this process. Depending on the complexities involved, these models are categorized as empirical, black-box, conceptual or physically-based distribution models. In operational hydrology, the system-theoretic black-box and conceptual models are usually employed for rainfall-runoff modeling because the physically-based distributed models are too complex, data intensive and cumbersome to use.

Conceptual rainfall-runoff (CRR) models are designed to approximate with in their structures (in some physically realistic manner) the general internal sub processes and physical mechanics, which govern the hydrologic cycle. CRR models usually incorporate simplified forms of physical laws and are generally nonlinear, time-invariant, and deterministic, with parameters that are representative of watershed characteristic. Until recently, for practical reasons (data availability, calibration problems, etc.) most conceptual

watershed models assumed lumped representations of the parameters. Among the more widely used and reported lumped parameter watershed models are the Sacramento soil moisture accounting (SAC-SMA) model of the U.S. National Weather Service (Burnash et al. 1973. Brazil and Hudlow, 1980) HEC-1 (U.S. Army corps of engineers, 1990) and the Stanford watershed model (SWM) Crawford and Linsley, 1966). While such models ignore the rainfall runoff process, they attempt to incorporate realistic representations of the major nonlinearities inherent in the R-R relationships. Conceptual watershed models are generally reported to be reliable in forecasting the most important features of the hydrograph, such as the beginning of the rising limb, the time and the height of the peak and volume of flow (Kitanidis and Bras, 1980 a;b;Sorooshian, 1983), However, the implementation and calibration of such a model can typically present various difficulties (Duan et al. 1992) requiring sophisticated mathematical tools (Duan et al. 1992.1993.1994; Sorooshain et al., 1993) significant amounts of calibration data (Yapo et al., 1995) and some degree of expertise and experience with the model.

While conceptual models are of importance in the understanding of hydrologic processes, there are many practical situations such as streamflow forecasting where the main concern is with making accurate predictions at specific watershed locations. In such a situation, a hydrologist may prefer not to expend the time and effort required to develop and implement a conceptual model and instead implement a simpler system theoretic model. In the system theoretic approach, difference equation or differential equation models are used to identify a direct mapping between the inputs and outputs without detailed consideration of the internal structure of the physical processes. The linear time series models such as ARMAX (auto regressive moving average with exogenous inputs) models developed by Box and Jenkins (1976) have been most commonly used in such situations because they are relatively easy to develop and implement; they have been found to provide satisfactory predictions in many applications (Bras and Rodriguez-Iturbe, 1985; Salas et al., 1980; wood, 1980) However, such models do not attempt to represent the nonlinear dynamics inherent in the transformation of rainfall to runoff and therefore may not always perform well.

Owing to the difficulties associated with nonlinear model structure identification and parameter estimation, very few truly nonlinear system theoretic watershed models have been reported (Jacoby, 1966; Amorocho and Brandstetter, 1971; Ikeda et al., 1976). In most cases, linearity or piecewise linearity has been assumed (Natale and Todini, 1976a,b). The

model structural errors that arise from such assumptions can, to some extent, be compensated for by allowing the model parameters to vary with time (Young, 1982; Young and Wallis, 1985). For example, real time identification techniques, such as recursive least squares and state space Kalman filtering models have been applied for adaptive estimation of model parameters (Chiu, 1978; Kitanidis and Bras, 1980a,b; Bras and Rodriguez-Iturbe, 1985) with generally acceptable results.

Recently, significant progress in the fields of nonlinear pattern recognition and system control theory have been made possible through advances in a branch of nonlinear system theoretic modeling called artificial neural networks (ANN). An ANN is a nonlinear mathematical structure, which is capable of representing arbitrarily complex nonlinear processes that relate the inputs and outputs of any system. A number of papers have discussed the capability of three-layer feed forward ANNs to approximate any continuous input-output mapping and its derivatives to arbitrary accuracy (Funahashi, 1989; White, 1990; Hornik et al., 1990; Blum and Li, 1991; Ito, 1992; Gallant and White, 1992; Cardaliaguet and Euvrard, 1992; Takahashi, 1993). ANN models have been used successfully to model complex nonlinear input-output time series relationship in a wide variety of fields (Vemuri and Rogers, 1994).

1.3 RUNOFF – SEDIMENT PROCESS

The magnitude of sediment transported by rivers has become a serious concern for the water resources planning and management. The assessment of the volume of sediments being transported by a river is required in a wide spectrum of problems such as the design of reservoirs and dams; hydroelectric power generation and water supply; transport of sediment and pollutants in rivers, lakes and estuaries; determination of the effects of watershed management; and environmental impact assessment. The sediment outflow the watershed is induced by processes of detachment, transportation and deposition of soil materials by rainfall and runoff.

Sediment rating curves are widely used to estimate the sediment load being transported by a river. A sediment-rating curve is a relation between the sediment and river

discharges. Such a relationship is usually established by a regression analysis, and the curves are generally expressed in the form of a power equation.

A number of attempts have been made to relate the amount of sediment transported by river with flow conditions such as discharge, velocity, and shear stress. However, none of these equations have received universal acceptance. Usually, either the weight of the sediments or the sediment concentration is related to the discharge. Many times, these two forms are used interchangeably. McBeab and Al-Nassri (1988) examined this issue and concluded that the practice of using sediment load versus discharge is misleading because the goodness of fit implied by this relation is spurious. They have instead recommended that the regression be established between sediment concentration and discharge. Karim and Kennedy (1990) attempted to establish relations among the velocity, sediment discharge, bed-form geometry, and friction factor of alluvial rivers. Loped and Ffolliott (1993) point out that an additional complexity is introduced to the sediment concentration and streamflow relation due to a hysteresis effect. The sediment concentrations for a given level of streamflow discharge in rising stage of a streamflow hydrograph are greater than on the falling stage. The conventional regression approach is not able to account for this hysteresis effect. A power equation is normally used to represent sediment rating and its transformation. Usually, the power equation is log transformed and linear regression with least squares is applied to estimate the parameters. While applying the equation, the data are transformed to the original domain. The entire process introduces a bias in the estimates. This aspect has been examined by Ferguson (1986) and Jansson (1996). Jansson (1996) proposed a correction factor that is based on the variance of the data and claimed that the use of this factor leads to improvement in the results.

As the sediment-discharge relationship is not linear, conventional statistical tools used in such situations such as regression and curve fitting methods are unable to model the non-linearity in the relationship. On the other hand, the application of physics-based distributed process computer simulation offers another possible method of sediment prediction. But the application of these complex software programs is often problematic, due to the use of idealized sedimentation components, or the need for massive amounts of detailed spatial and temporal environmental data, which are not available. Simpler approaches are therefore required in the form of 'conceptual' solutions or 'black-box' modelling techniques.

Neurocomputing, in the form of artificial neural networks provide one possible answer to the problematic task of sediment transfer prediction.

1.4 POTENTIAL OF ANN TECHNIQUES FOR HYDROLOGICAL MODELING IN BRAHMAPUTRA RIVER BASIN

An Artificial Neural Network (ANN) is a computational method inspired by the studies of the brain and nervous system in biological organisms. ANN represent highly idealized mathematical models of our present understanding of such complex systems. One of the characteristics of the neural networks is their ability to learn. A neural network is not programmed like a conventional computer program, but is presented with examples of the patterns, observations and concepts, or any type of data, which it is supposed to learn. Through the process of learning (also called training) the neural network organizes itself to develop an internal set of features, that it uses to classify information or data. Due to its massively parallel processing architecture the ANN is capable of efficiently handling complex computations, thus making it the most preferred technique today for high speed processing of huge data. ANNs have been in existence since the 1940s, but since current algorithms have overcome the limitations of those early networks great interest in the practical applications of ANNs has arisen in recent decades (Wasserman 1989; Muller and Reinhardt 1990). Various ANN algorithms have an objective to map a set of inputs to a set of outputs. ANNs have been proven to provide better solutions when applied to (1) complex systems that may be poorly described or understood; (2) problems that deal with noise or involve pattern recognition, diagnosis, abstraction, and generalization; and (3) situations where input is incomplete or ambiguous by nature. It has been reported that an ANN has the ability to extract patterns in phenomena, which avoids the selection of a model form such as linear, power, or polynomial. In addition, there are many advantageous characteristics of ANN approach to problem solving viz.: (1) application of a neural network does not require a priori knowledge of the underlying process; (2) one may not recognize all the existing complex relationships between various aspects of the process under investigation; (3) a standard optimization approach or statistical model provides a solution only when allowed to run to completion whereas a neural network always converges to an optimal (sub-optimal) solution condition and; (4) neither constraints nor an a priori solution structure is necessarily assumed or strictly enforced in the ANN development. These characteristics render ANNs to be very suitable tools for handling various hydrological modeling problems.

1.5 OBJECTIVES OF THE STUDY

The assessment of the runoff in a river as well as volume of sediments being transported by a river is required in a wide spectrum of problems such as the design of reservoirs and dams; hydroelectric power generation and water supply; transport of sediment and pollutants in rivers, lakes and estuaries; determination of the effects of watershed management; and environmental impact assessment. The soil erosion and sediment yield is one of the major problems in Himalayan region. The fragile ecosystem of Himalayas has been an increasing cause of concern to environmentalists and water resources planners. Accelerated erosion has occurred in this region due to intensive deforestation, large-scale road construction, mining and cultivation on steep slopes. Keeping this in view, a part of Brahmaputra River, which flows through the eastern Himalayan region of India has been selected for this study.

The main objective of the present study is the application of the emerging technique, namely, artificial neural networks (ANNs) for modeling the rainfall-runoff process as well as the runoff-sediment process for a part of the Brahmaputra River in eastern Himalayan region of India. The principle objective of the study has been achieved through the following milestones:

- i. Development of stage-discharge and runoff-sediment rating curves using artificial neural network (ANN) models and conventional techniques for the important gauging sites in the Brahmaputra River basin.*
- ii. Development of rainfall-runoff and sediment-runoff models using artificial neural network (ANN technique for Subansiri River basin.*
- iii. Validation of the formulated models.*
- iv. Performance evaluation of the formulated models for the Pranhita sub-basin.*

1.6 ORGANIZATION OF THE THESIS

The remainder of the thesis is divided into seven chapters.

CHAPTER TWO gives a brief background on Artificial Neural Networks. This includes the basic definitions of various terminologies used in the applied technique, various

ANN architectures as well as training algorithms. This chapter also addresses various issues of ANN application.

CHAPTER THREE presents the literature review pertaining to some conventional rainfall-runoff-sediment modeling and ANN applications in rainfall-runoff modeling as well as runoff-sediment modeling.

CHAPTER FOUR gives a summary of information on the Brahmaputra river basin and Subansiri River basin, a sub-basin of Brahmaputra river basin, India, which is considered for the present study along with data availability and location of various hydro-meteorological stations in the basin.

CHAPTER FIVE deals with the methodology of ANN model development. It gives the details of selection procedure of input and output variables for various ANN model structures along with some selected performance evaluation criteria for training, testing and validation of the models. It also presents some features of the software, namely, Neural Power used for the model development.

CHAPTER SIX presents the results of the analysis using various developed ANN models.

CHAPTER SEVEN summarises the present work and gives suggestions for future extensions of the work.

At last, attempts were made to compile the useful earlier works in the field of study and are listed at the end in the reference section.

Chapter – 2



Background of Artificial Neural Networks

Artificial Neural Networks provide a unique computing architecture whose potential has only begun to be tapped. Used to address problems that are intractable or cumbersome with traditional methods these new computing architectures are inspired by the structure of the brain and are radically different from the currently dominant architecture of programmed computing.

ANNs are massively parallel systems that rely on dense arrangement of interconnections and surprisingly simple processors and in these learning replaces a priori program development method. Emerging ANN technology is a broad body of often loosely related knowledge and techniques that provide practical alternatives to conventional computing solutions and offers some potential for approaching many currently unsolved problems.

ANN is defined as a structure (network) composed of a number of interconnecting units (artificial neurons). Each unit has an input/output (I/O) and implements a local computation or function. The output of any unit is determined by its I/O characteristics; it's interconnection to other units and possibly external inputs. Although "hand crafting" of the network is possible, the network usually develops an overall functionality through one or more forms of training.

2.1 CHRONOLOGY AND APPLICATION

The development of artificial neural networks began approximately 50 years ago (McCulloch and Pitts 1943), inspired by a desire to understand the human brain and emulate its functioning. Within the last two decades, it has experienced a huge resurgence due to the development of more sophisticated algorithms and the emergence of powerful computation tools. The human brain always stores the information as a pattern. Any capability of the brain may be viewed as a pattern recognition task. The high efficiency and speed with which the human brain processes the patterns inspired the development of ANN and its application in field of pattern recognition. ANN is a computing model that tries to mimic the human brain and the nervous system in a very primitive way to emulate the capabilities of the human being in a very limited sense. ANNs have been developed as a generalization of mathematical models of human cognition or neural biology. Their development is based on the following rules:

1. Information processing occurs at many single elements called nodes, also referred to as units, cells, or neurons.
2. Signals are passed between nodes through connection links.
3. Each connection link has an associated weight that represents its connection strength.
4. Each node typically applies a nonlinear transformation called an activation function to its net input to determine its output signal.

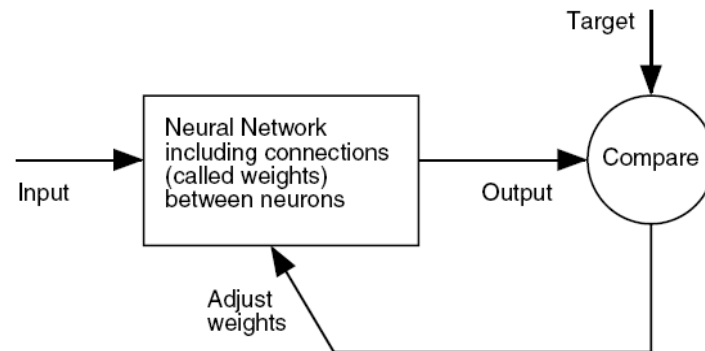


Fig. 2.1 Basic Principle Of Artificial Neural Networks

An ANN is network of parallel, distributed information processing system that relates an input vector to an output vector. It consists of a number of information processing elements called neurons or nodes, which are grouped in layers. The input layer processing elements receive the input vector and transmit the values to the next layer of processing elements across connections where this process is continued. This type of network, where data flow one way (forward), is known as a feed-forward network. A feed-forward ANN has an input layer, an output layer, and one or more hidden layers between the input and output layers. Each of the neurons in a layer is connected to all the neurons of the next layer, and the neurons in one layer are connected only to the neurons of the immediate next layer. The strength of the signal passing from one neuron to the other depends on the weight of the interconnections. The hidden layers enhance the network's ability to model complex functions.

2.2 BIOLOGICAL BASIS OF ANNS

The fundamental unit of a network is neuron, consists of nucleus in its cell body of soma. Neuron or nerve cell is the complex biochemical and electrical signal processing factory. Tree like nerve fibers called dendrites are associated with cell body, which receives

signals from other neurons. Soma is the main body of the nerve cell. The outer boundary is cell membrane and the interior and outside of the cell is filled with intracellular and extra cellular fluid. When some are excited above a certain level, the neuron fires, which it transmits an electrical signal, and that signal passes through the axon. The long fiber, axon extending from the cell body, eventually branches into stands and sub-stands connecting to many other neurons at the synaptic junction, or synapses. The receiving ends of these junctions on other cells can be found both on the dendrites and on the cell bodies. The axon of a typical neuron leads to a new thousand synapses associated with other neurons.

The transmission of a signal from one cell to another at a synapse is a complex chemical process in which specific transmitter substances are released from the sending side of the junction. The effect is to raise or lower the electrical potential inside the body of the receiving cell. If this potential reaches the threshold an electrical activity in the form of short pulses, is generated. When this happens, the cell is said to have fired. These electrical signals of fixed strength and durations are not down the axon. Generally the electrical activity is confined to the interior of a neuron, as the chemical mechanism operates at the synapses.

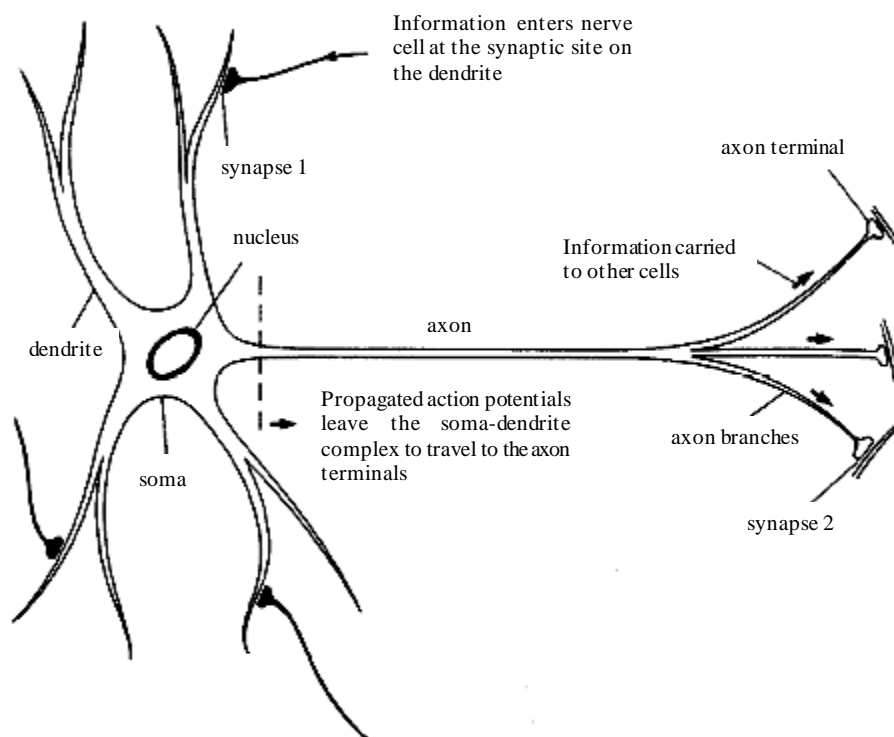


Fig. 2.2 Schematic Diagram Of A Typical Biological Neuron

The dendrites serve as receptors for signals from other neurons, where as the purpose of axon is transmission of the generated activity to other cells (inter-neuron). A third type of neuron, which receives information from muscles or sensory organs such as eye or ear, is called a receptor neuron.

2.3 THE NEURAL NETWORK TOPOLOGY

The topology of a network describes the connection infrastructure of an ANN. Connections link the neurons together and transport the data through the network and different types of connections produce different performance characteristics. Connections between neurons can be classified as being either inhibitory or excitatory. Inhibitory connections tend to prevent a neuron from reacting (negative term in a sum); while excitatory connections cause firing of the neuron (positive sum). At times, ANNs involve inhibitory connections from one neuron to all the others and this is referred to as lateral inhibition.

Other types of connections are delay connections (Fig. 2.3). They introduce a time lag into the data flow, which can be useful for time related phenomena (Day and Davenport, 1993) like the prediction of the flood routing through a sewer system or the control of an overflow weir.

The definition of so called layers and clusters is another frequently applied representation of the topology of an ANN. A layer can be seen as a group of neurons, which share the same input and output connections, but do not interconnect with themselves: Connections occur only between layers and not within a layer (Fig. 2.4). Layers are often classified as being input, output or hidden; whereby an input layer receives data from the outside world, an output layer returns data to the outside world; and hidden layers perform unknown operations between the input and output layers.

As soon as connections exist within a layer, then reference is made to a cluster of neurons. If within a cluster, lateral inhibition is executed for each individual neuron competition is created (Fig. 2.5). Competition occurs, when all the neurons in a cluster are connected to each other through inhibitory connections (Rumelhart and Zipser, 1986). Consequently, neurons in each cluster compete with each other for the right to recognize some feature in the input. The neuron that resembles the input vector the most, wins and yields an output vector, while the other neurons in the cluster are denied any response at all. Eventually, each type of vector presented to the cluster, will cause the response of a different

neuron in the cluster. Hence, each cluster in an ANN could classify a certain feature in the input data.

Another important type of connection, which has a large influence on the general behavior of an ANN, is the feedback connection. A feedback connection directs some or all the data back into the system, thus creating signal loops and cyclic behavior of the corresponding ANN. According to the literature (Oppenheim et al, 1983) a connection is defined as being a feedback connection when the output of a system is used to control or modify the input. Since ANNs consist of numerous I/O neurons, the term feedback will be further clarified in order to avoid confusion.

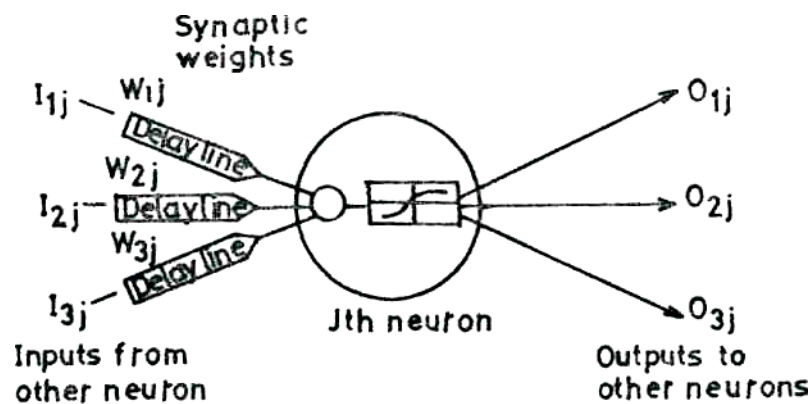


Fig. 2.3 Delay Connections

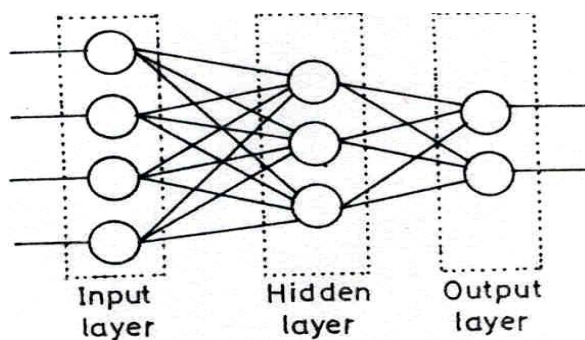


Fig. 2.4 Neuron Layers

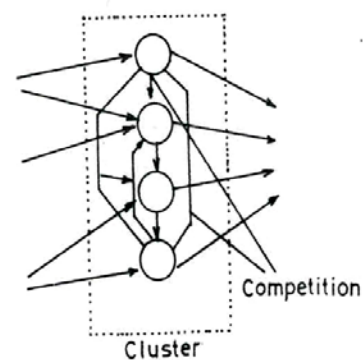


Fig. 2.5 Neuron Clusters

An external feedback connection directs the current output vector to the current input vector of the ANN; whereby the new vector is re-routed through the neurons (Fig. 2.6). This process is repeated until the output vector shows no significant variations anymore. An

internal feedback connection directs the output signal of one neuron to the input of another neuron (Fig. 2.7). Often multiple feedback loops are used between neurons in the same cluster or between different layers.

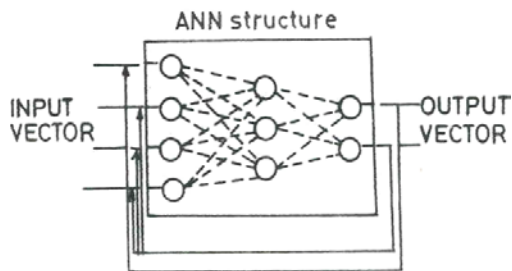


Fig. 2.6 External Feedback Connections

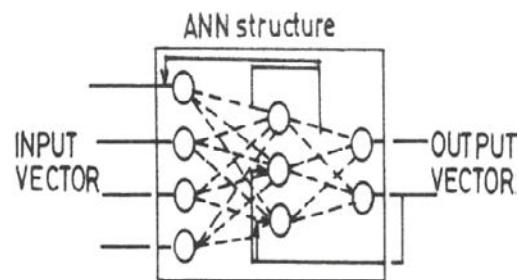


Fig. 2.7 Internal Feedback Connections

In general, Feedback networks (also referred to as recurrent networks) are defined as being systems that settle or relax into an output vector. The data will pass through some or all of the neurons more than once. Because the actual state of a network is dependent on its previous states, the same input vector can produce different output vectors. Stability and convergence characterize the performance of a feedback network. Feedback networks are also referred to as dynamic non-linear systems.

When there is a total lack of feedback connections, one generally speaks of feed-forward networks. This means that a given input vector will always produce one output vector. Once trained (fixed weights), this input vector will always produce the same output vector. Often feed-forward networks are referred to as instantaneous static non-linear mapping systems.

2.4 LEARNING ALGORITHMS

The weight distribution in every ANN is unique and will determine the specific response of the network to any given input vector. In order to perform a required process task, these weights must be determined in advance through a learning process. The learning process for ANNs encompasses the adjustment of weights and this process makes use of a learning algorithm and a training set of examples.

The learning process in an ANN can be seen as teaching the network to yield a particular response to a specific input. This often consists of an iterative process; whereby the network tries to match output vectors to desired ones and uses any deviations to adjust some

or all of its weights. The rules that determine the magnitude of these adjustments are contained in the learning algorithm.

There are three modes through which the learning process can be carried out viz. supervised, unsupervised and batch. In the supervised learning mode, a teacher provides the desired response to the network as soon as an input is applied, thus giving the network an indication how it performs (Fig. 2.8). A child learning the alphabet at school is an example for this type of learning.

In the unsupervised learning mode, the desired response is unknown (Fig. 2.9). Weight adjustments are based on observations of responses to inputs on which there is marginal or no knowledge. Often, this results in self-organization of neurons, trying to recognize patterns, regularities or separating properties in the given input data. For example, a child learning to ride a bicycle will do so with minimal help from outside. The child must figure out independently how to find a balance.

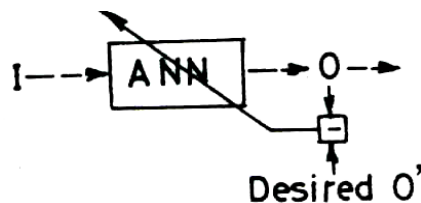


Fig. 2.8 Supervised Learning Mode

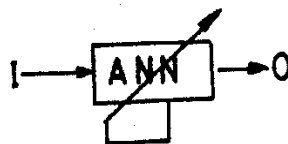


Fig. 2.9 Unsupervised Learning Mode

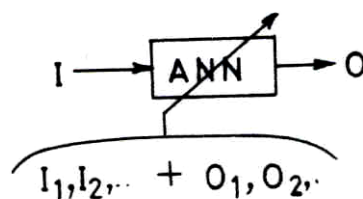


Fig. 2.10 Batch Learning Mode

In batch learning mode, weights are determined in one go, by using a complete set of I/O vectors (Fig. 2.10). All knowledge must be known a priori and is then implemented instantly in the network. There are no normal incremental learning steps. This method of storing input vectors can be seen as putting data records in a database.

Learning algorithms themselves are often based on error minimization. Examples are the least mean square (LMS) learning rule or error gradient descent; but numerous other, more refined routines exist, all of which try to optimize some kind of learning signal (learning rate, maximum likelihood value, cross entropy) and so improve network performance. The resulting modifications made to the weights, are then either based on an award/punishment rule (dot product neuron) or chance (probabilistic neurons).

After numerous training cycles, once the ANN has learned the examples with considerable accuracy, test data is presented to the ANN, which it has never encountered before. The resulting outputs are validated and the network performance is tested using multiple criteria such as generalization ability, robustness, stability, convergence and plasticity. It is only after these results are proven satisfactory, that the ANN is implemented. If test results or performances are unsatisfactory, the network is often retrained using other learning examples, set in a different order, or using more training cycles, etc. Often, for instance, the number of nodes is changed to improve learning; however certain drawbacks to this practice exist.

When enough nodes are available, the ANN can reproduce any desired response because it stores the information instead of learning the mechanics of the cause/effect relationship of the data. This is called over fitting of the data and as a consequence the ANN will have poor generalization ability.

Too few nodes, insufficient data or incorrect data can lead to under fitting of data, again resulting in bad generalization abilities.

Special algorithms exist which not only change the weights during learning, but also change the topology and architecture of the ANN, as done on various levels of interaction. Such an algorithm could, for example, determine weights, network structure and even decide on which training and test examples to use; for instance, a situation could be thought of, where the ANN is confronted with hundreds of rainfall events and the next rain must be predicted.

Finally, some algorithms are not restricted to training use only. Online learning is a powerful characteristic that enables an ANN to adapt temporarily or permanently to changing

conditions. Self organizing maps, for example, can continue learning with each new input vector they receive. An ANN could be created, for example, which simulates flow through a sewer pipe and adapts its parameters when the resistance of a sewer pipe becomes higher; independent of any intervention from an external source.

2.5 STRUCTURE

In order for an ANN to learn a certain response, it must be provided with numerous examples. The data contained in these examples is crucial for the performance to the network. Incorrect input data will certainly result in slow learning, unstable or unreliable networks. Therefore, the training and test examples should be chosen with care and (pre-) processed accordingly.

The term input vector will be used to refer to the input data needed for one training, test or on-line example (Fig. 2.11). Consecutively output vector refers to the final calculated result of the ANN. Each input/output vector has a certain dimension R, representing different features of the data, e.g. 1(1) represents the catchment size, 1(4) is the type of vegetation, etc. When Q different vectors are presented to the ANN randomly or in ordered fashion, we can

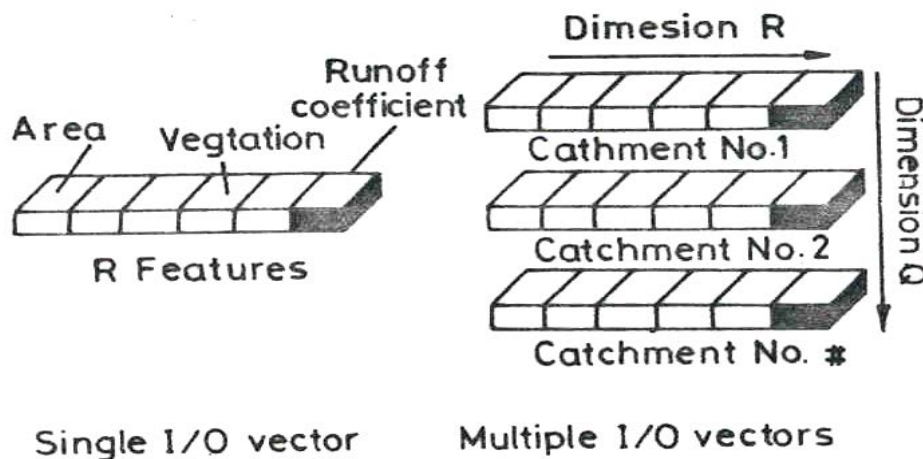


Fig. 2.11 Input Vectors and their Dimensions

define a matrix P, which defines a set of Q I/O vectors of dimension R ($P = Q \times R$). In the training of an ANN, which should, for example, determine the runoff coefficient of an urban catchment area, the input matrix P could consist of 100 catchments ($Q=100$), each representing specified catchment characteristics. The output vectors would then consist of single values, representing the runoff coefficients.

The most important pre-processing actions performed on input data or learning examples, is normalization, filtering and scaling.

Data is normalized, when outliers are present in the data-series. It reduces the influence of these outliers and assumes that while the overall magnitude of each signal may vary, the relation between each feature may not. Data is filtered, when unwanted high or low frequency signals perturb the main signal (e.g., high frequent water level fluctuations due to wind-waves). However, ANNs are known to act as filters themselves, making pre-filtering of data only necessary in extreme cases.

Scaling of data is performed to increase training speed only. It is common practice to scale different data series to a uniform range [0 1]. For example, when the degree of pollution for a surface water sample is determined by using the concentrations of nitrate and benzene; the smaller amounts of benzene will give a better indication of the degree of pollution than the larger nitrate concentrations. If data is not scaled, the learning procedure will initially be dominated by the (in absolute terms) larger nitrate values instead of the smaller benzene values.

2.6 ARCHITECTURE

The architecture of an ANN describes the layout of its structure. It defines the number and size of the implemented clusters and layers, as well as the topology used to connect these groups of neurons with each other. The ANN architecture itself is often changed when learning algorithms and I/O data modifications fail to improve the ANN performance. Simple modification can be made by reducing or increasing the number of nodes or deleting neuron interconnections. Different techniques exist for determining an optimal ANN architecture for a given I/O data problem (Refenes and Vithlani, 1991). In addition to implementation of improved neuron functions, learning algorithms or determination of the optimal number of nodes, modularization can be applied. Modularization is implemented when one specific type of ANNs for different tasks within a system makes best use of the specialized capabilities of each of the independent ANN modules (Nadi, 1991). For example, the vast amount of real time flow data in a complex sewer system, could be compressed to several abstract parameters first (using a self organizing ANN), before it is fed into another ANN which simulates the actual outflow of the sewer system.

2.7 PERFORMANCE INDICATORS

During learning or network optimization, it is often necessary to monitor the effects of a certain intervention or system alteration. Numerous performance indicators exist to quantify progression or drawbacks of certain methods:

- Generalization is the ability of the ANN to formulate an answer to a problem it has never seen before (predict a future flow rate using on-line data).
- Fault tolerance is the ability to keep processing, albeit with reduced accuracy and/or speed, even though data is missing or neurons have been disabled/destroyed (A water level meter fails).
- Convergence speed is the rate at which the network state changes as it moves to a stable state.
- The states of an ANN can be mathematically expressed in a function, representing a 3 dimensional surface of the computational energy of the ANN. Computational energy describes the stable states or solutions of an ANN and the paths leading to them. These stable states are represented as valleys (energy minima) in the 3 dimensional surfaces, also called basins of attraction. By changing the weights, this energy surface is changed and the valleys get larger and deeper, increasing the convergence speed of an ANN.
- Adaptability is the ability of an ANN to modify its response to changing conditions. Four characteristics govern this ability: learning, self organization, generalization and training.
- Reliability is the ability to produce the same result, when the same input vector is repeatedly presented to a network. Reliability is mostly used to describe the performance of feedback networks, since feed-forward networks always produce the same result.
- Robustness is the ability to produce the same result, even though input data is noisy, contains data gaps and contradictory data.
- Sensitivity is closely related to robustness, it shows the extent to which a network response will change, due to variations in the features of the input vector.

❖ **Three other less obvious indicators that can also be used are:**

- Memory requirements: Some ANNs need less (hardware) memory to perform their task, than others. This can be decisive for data base related problems that use pattern storage for instance (Hopfield network).
- Amount of training data needed: for some problems, lack of data poses a constant hindrance to efficient modeling. Thus an ANN requiring less training data to learn a specific response is better suited for these kinds of problems.
- Learning speed: The speed at which new data is learned, can be crucial for on-line applications in fast changing environments. This performance indicator is often used to evaluate new learning algorithms.

With these performance indicators, it is possible to make an evaluation table, showing the different ANN types and their relative performances.

2.8 MODEL OF AN ARTIFICIAL NEURAL NETWORK

The main function of the ANN paradigms is to map a set of inputs to a set of outputs. A single processing unit or neuron is shown in Fig.2.12. The incoming signals are multiplied by respective weights through which they are propagated toward the neurons or node, where they are aggregated (summed up) and the net input is passed through the activation function to produce the output.

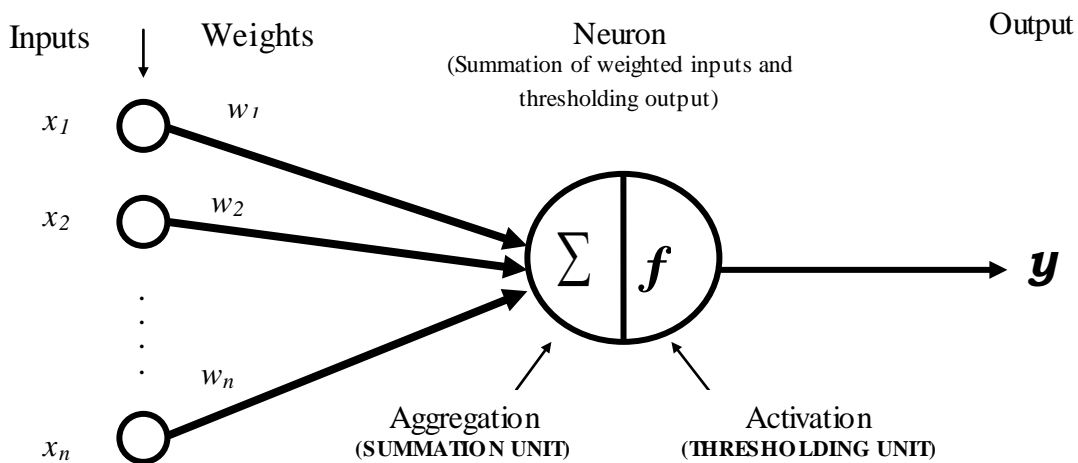


Fig. 2.12 A Single Artificial Neuron (Perceptron)

Let x_i ($i = 1, 2, \dots, n$) are inputs and w_i ($i = 1, 2, \dots, n$) are respective weights. The net input to the node can be expressed as

$$net = \sum_{i=1}^n x_i w_i \quad \dots(2.1)$$

The net input is then passed through an activation function $f(\cdot)$ and the output y of the node is computed as

$$y = f(net) \quad \dots(2.2)$$

To ensure that the neurons response is bounded that is the actual response of the neuron is conditioned, or damped, as a result of large or small activating stimuli and thus is controllable.

Sigmoid function is the most commonly used nonlinear activation function for solving

ANN Problems which is given by $y = f(net) = \frac{1}{1 + e^{-net}}$.

This activation function is shown in Fig. 2.13.

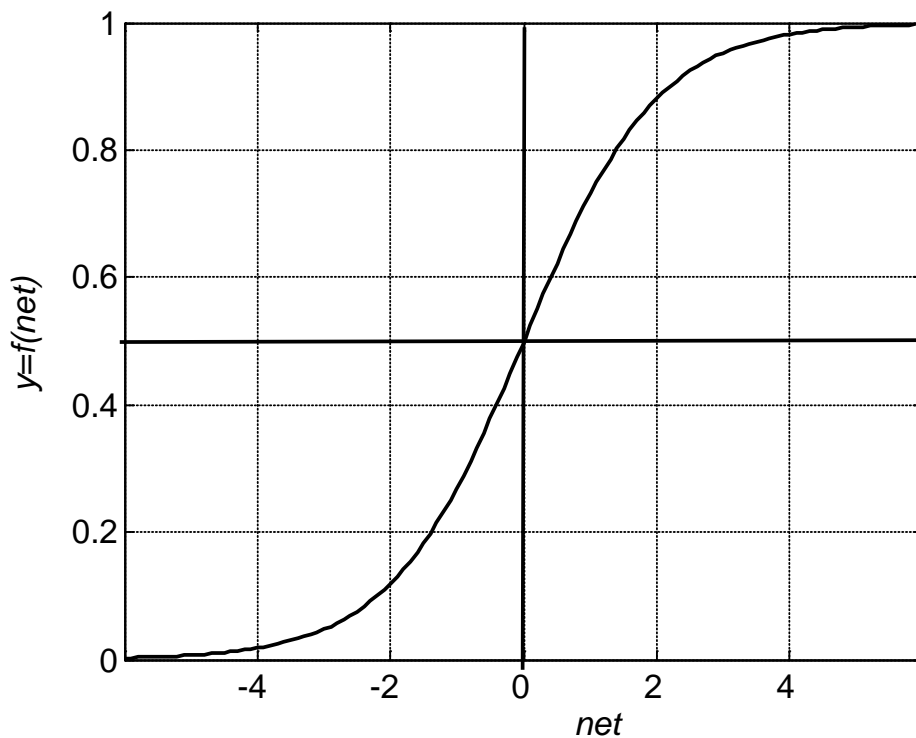


Fig. 2.13 The Sigmoid Function

2.9 MULTILAYER FEED-FORWARD NETWORK

The most important attribute of a multilayer feed-forward network is that it can learn a mapping of any complexity (Zurada. 1992). This network is made up of multiple layers of neurons. In this architecture, besides the input layer and the output layer, the network also has one or more than one intermediate layer(s) called hidden layer(s). Each layer is fully connected to the preceding layer by interconnection strengths or weights. Fig.2.14 illustrates this type of network consisting of a single hidden layer. As can be seen, the generic feed-forward network is characterized by the lack of feedback. Even though this network has no explicit feedback connection when the input is mapped into the output, the output values are often compared with the desired output values, and also an error signal can be employed for adapting the network's weights during the learning process.

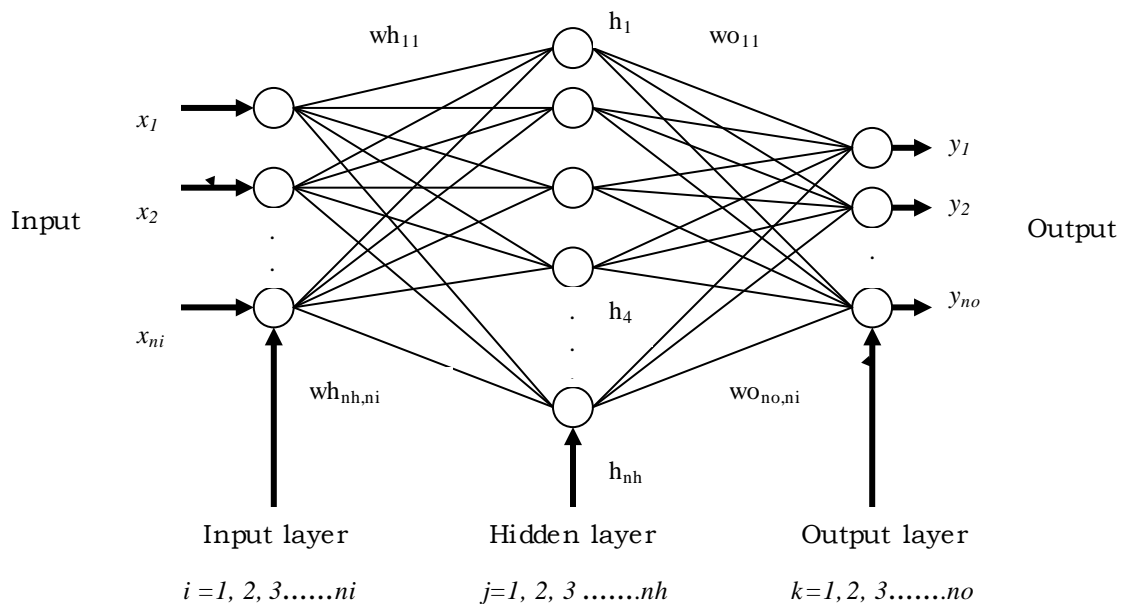


Fig. 2.14 Multilayer Feed – Forward Artificial Neural Network Configuration

2.10 OTHER ANN NETWORKS

Some of the most important networks are explained below:

2.10.1 Back Propagation Network (BP)

Back Propagation network (BP) are the most widely used ANNs. The name comes from the fact that an error term is back propagated through the network during learning and used to change the weights (Fig. 2.15). However, no feedback links are actually incorporated

and there are many other ANNs which also back propagate error terms; so this (historical) name can be confusing.

Normal BP networks have simple supervised feed-forward structures and often consist of an input and an output layer with one or more hidden layers in between. They are fast, relatively simple to train and the most easily to understand. Theoretically any recurrent ANN can be simulated by a back propagation algorithm (Such as a Fourier series approximation). As BP networks suffer from learning deficiencies, like slow learning and convergence to local minima, numerous enhancements have been proposed (Haario and Jokinen, 1991, Sato, 1991, Yu et al., 1993). Nevertheless, BP networks are used in 80% of today's applications and excellent in the areas of prediction and simulation.

2.10.1.1 Back propagation algorithm

Back propagation is systematic method of training multilayer artificial neural networks. It has been used by scientist and engineering community to the modeling and processing of many quantitative phenomena using neural networks. This learning algorithm is applied to multilayer feed forward network consisting of neurons with continuous differentiable activation functions. Such networks associated with the back propagation learning algorithm are called back propagation networks. In the back-propagation algorithm, the network weights are modified by minimizing the error between desired (target) and calculated (predicted) outputs. This algorithm is based on the error-correction learning rule.

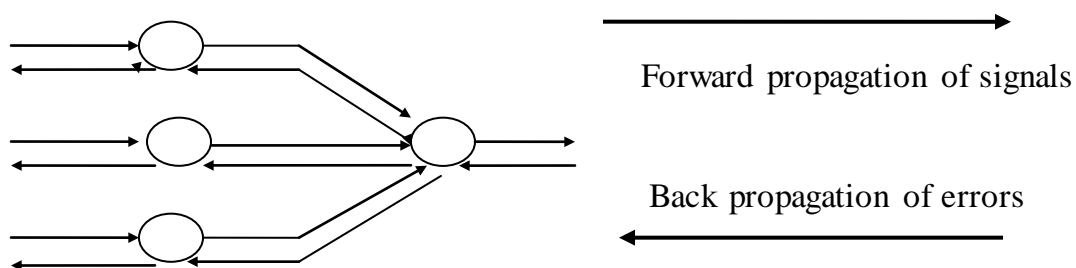


Fig. 2.15 Directions of Signal Flow in a Multilayer ANN

Fig. 2.15 shows the directions of signal flow and error propagation in a multilayer artificial neural network. Back-propagation is an iterative learning process in which all

weight parameters are randomly initialized and then updated (in each iteration) through feed-forward calculations and back-propagation of errors.

2.10.1.2 Learning factors of back propagation

One of the major issues concerning back propagation algorithm is its convergence. The convergence of back propagation is based on some important learning factors such as the initial weights, the learning rate, the nature of training set and the architecture of the network.

(a) Initial weights

The initial weights of a multilayer feed forward network strongly affect the ultimate solution. They are typically initialized by small random values (between -1.0 and 1.0 or -0.5 to +0.5). Equal weights values cannot train the network properly if the solution requires unequal weights to be developed. The initial weights cannot be large, otherwise the sigmoid will saturate, from the beginning and the system will stock at a local minimum. The saturation is avoided by choosing the initial values of the synoptic weights to be uniformly distributed inside a small range of values. The range should not be too small as it can cause the learning to be very small.

(b) Frequency of weight updates

There are two approaches to learning

1. In “per-pattern” learning, used, in the algorithm, weights are changed after every sample presentation.
2. In “per-epoch” (or “batch-mode”) learning, weights are updated only after all samples are presented to the network. An *epoch* consists of such a presentation of the entire set of training samples. Weight changes suggested by different training samples are accumulated together into a single change to occur at the end of each epoch.

(c) Learning rate (η)

A control parameter used by several learning algorithms, which affects the changing of weights. The bigger learning rates cause bigger weight changes during each iteration. Weight vector changes in backpropagation are proportional to the negative gradient of the error; this guideline determines the relative changes that must occur in different weights when a training sample (or a set of samples) is presented, but does not fix the exact

magnitudes of the desired weight changes. The magnitude change depends on the appropriate choice of learning rate, η . A large value of η will lead to rapid learning but the weight may oscillate, while low values imply slow learning. This is typical of all gradient descent methods. The right value of η will depend on the application. Values between 0.1 and 0.9 have been used in many applications in the literature.

(d) Momentum (α)

A simple method of increasing the rate of learning and yet avoiding the danger of instability is to include a momentum term to the normal gradient descent method. To give each weight some inertia or momentum so that it tends to change the direction of average downhill force that it feels. The scheme is implemented by giving a contribution from the previous step to each weight change. The range of momentum is **[0,1]** and a value of 0.9 is generally used for momentum factor.

(e) Data normalization

The variables fall in the range of a 0 to 1, because it smoothens the solution space and averages out some of the noise effects. Such process is called normalization or standardization.

(f) Number of hidden nodes

The size of a hidden layer is usually determined experimentally. In practice, the number of hidden layer is relatively smaller than the number of nodes in the input layer. If the network fails to converge, more neurons are added gradually to the hidden layer till a good performance is achieved.

(g) Data training and generalization

The training data submitted to the network for it to learn and generalized the relation between input and output should be sufficient and proper. There is no rule for choosing the training data. Networks with too many trainable parameters for a given amount of training data learn well but do not generalize well. This phenomena is called over fitting with too few trainable parameter, the network fails to learn the training data.

The available data is divided into two parts one for training another for testing. The purpose of training is to determine the set of connection weights that cause the neural

network to estimate outputs that are sufficiently close to target values. The training data should contain sufficient patterns.

The training set is further divided into two subsets:

- ❖ A subset used for estimation of the model (i.e. training the networks)
- ❖ A subset used for evaluation of the performance of the model. The validation subset is usually 10 to 20 of the training set.

(h) Strength of Feed-forward Neural Network

- ❖ They are able to recognize the relation between the input and output variables without knowing physical consideration.
- ❖ They work well even when the training set contains noise and measurement errors.
- ❖ There is no need to make assumption about the mathematical form the relationship between input and output.

2.10.1.3 Feed-forward calculation

In the feed-forward calculation, the nodes in the input layer receive the input signals which are passed to the hidden layer and then to the output layer. The signals are multiplied by the current values of weights, and then the weighted inputs are added to yield the net input to each neuron of the next layer. The net input of a neuron is passed through an activation or transfer function to produce the output of the neuron. Considering the ANN shown in Fig.2.14, the procedure for feed-forward calculations in different layers is as follows

The net input to j^{th} node of the hidden layer is given by

$$neth_j = \sum_{i=1}^{ni} wh_{ji}x_i \quad \dots(2.3)$$

where ni is the number of neurons in the input layer and wh_{ji} is the connection weight between i^{th} node of the input layer and j^{th} node of the hidden layer. The output of j^{th} node of the hidden layer h_j is

$$h_j=f(neth_j) \quad \dots(2.4)$$

where $f(.)$ is the activation function, e.g. a sigmoid activation function. Thus

$$h_j = \frac{1}{1 + \exp(-neth_j)} \quad \dots(2.5)$$

Similarly, the net input to k^{th} node of the output layer is given by

$$nety_k = \sum_{j=1}^{nh} wo_{kj} \cdot h_j \quad \dots(2.6)$$

where, nh is the number of neurons in the hidden layer and wo_{kj} is the connection weight between j^{th} node of the hidden layer and k^{th} node of the output layer.

The output of k^{th} node of the output layer is

$$y_k = f(nety_k) \quad \dots(2.7)$$

Now operating through the sigmoid activation function

$$y_k = \frac{1}{1 + \exp(-nety_k)} \quad \dots(2.8)$$

After calculation of these outputs the error between desired and calculated output is computed which is propagated in the backward direction, as explained below.

2.10.1.4 Error back-propagation

The error calculated at the output layer is propagated back to the hidden layers and then to the input layer, in order to determine the updates for the weights. This method is derived from the well-known gradient descent method in which the weights updation is performed by moving in the direction of negative gradient along the multidimensional surface of the error function. The sum square error E for a single input-output pair data set is given by

$$E = \frac{1}{2} \sum_{k=1}^{no} (y_k - t_k)^2 \quad \dots(2.9)$$

Where, t_k is the desired output or target at the k^{th} node and y_k is the calculated output at the same node. In order to minimize the above error function, weights are updated by subtracting incremental changes in the weights from their old values.

That is,

$$wo_{kj}^{new} = wo_{kj}^{old} - \Delta wo_{kj} \quad \dots(2.10)$$

(j=1, 2, 3.. . nh, and k=1,2,3.. no)

$$wh_{ji}^{new} = wh_{ji}^{old} - \Delta wh_{ji} \quad \dots (2.11)$$

(i=1, 2, 3.ni, and j=1,2,3.. nh)

Where, Δwo_{kj} and Δwh_{ji} are incremental changes in the weights for output layer and hidden layer respectively.

The incremental changes in the weights for output layer are given by

$$\Delta wo_{kj} = \eta \left(\frac{\partial E}{\partial wo_{kj}} \right) \quad \dots(2.12)$$

where, η is the learning rate.

By using chain rule, $\frac{\partial E}{\partial wo_{kj}}$ can be written as

$$\frac{\partial E}{\partial wo_{kj}} = \frac{\partial E}{\partial y_k} \frac{\partial y_k}{\partial nety_k} \frac{\partial nety_k}{\partial wo_{kj}} \quad \dots(2.13)$$

Now, differentiating Eqn (2.6) with respect to wo_{kj} ,

$$\frac{\partial nety_k}{\partial wo_{kj}} = h_j \quad \dots(2.14)$$

Differentiating Eqn (2.8) with respect to $nety_k$,

$$\frac{\partial y_k}{\partial nety_k} = y_k (1 - y_k) \quad \dots(2.15)$$

Also differentiating Eqn (2.9) with respect to y_k yields

$$\frac{\partial E}{\partial y_k} = (y_k - t_k) = \delta y_k \quad \dots(2.16)$$

where δy_k is the error at the output side of k^{th} output node. Substituting Eqn 2.14 and Eqn. 2.16 in Eqn 2.13, the Eqn 2.12 may be represented as,

$$\Delta wo_{kj} = \eta \delta y_k \cdot y_k (1 - y_k) h_j \quad \dots(2.17)$$

or

$$\Delta wo_{kj} = \eta \Delta y_k h_j \quad \dots(2.18)$$

where, $\Delta y_k = \delta y_k \cdot y_k (1 - y_k) \quad \dots(2.19)$

Δy_k is the error at the input side of the k^{th} output node. Similarly the incremental changes in the weights for the hidden layer are given by

$$\Delta wh_{ji} = \eta \left(\frac{\partial E}{\partial wh_{ji}} \right) \quad \dots(2.20)$$

By using chain rule

$$\frac{\partial E}{\partial wh_{ji}} = \sum_{k=1}^{no} \frac{\partial E}{\partial y_k} \cdot \frac{\partial y_k}{\partial nety_k} \cdot \frac{\partial nety_k}{\partial h_j} \cdot \frac{\partial h_j}{\partial neth_j} \cdot \frac{\partial neth_j}{\partial wh_{ji}} \quad \dots(2.21)$$

Now, differentiating Eq. (2.8) with respect to $\partial nety_k$,

$$\frac{\partial y_k}{\partial nety_k} = y_k (1 - y_k) \quad \dots(2.22)$$

Differentiating Eq. (2.6) with respect to ∂h_j ,

$$\frac{\partial nety_k}{\partial h_j} = wo_{kj} \quad \dots(2.23)$$

Differentiating Eq. (2.5) with respect to $\partial neth_j$,

$$\frac{\partial h_j}{\partial neth_j} = h_j (1 - h_j) \quad \dots(2.24)$$

Also differentiating Eq. (2.3) with respect to ∂wh_{ji} ,

$$\frac{\partial neth_j}{\partial wh_{ji}} = x_i \quad \dots(2.25)$$

Substituting Eqs. (2.16), (2.22) and (2.25) in Eq. (2.21), then the Eq. 2.20 may be represented as,

$$\Delta wh_{ji} = \eta \left(\frac{\partial E}{\partial wh_{ji}} \right) = \eta \sum_{k=1}^{no} \delta y_k y_k (1 - y_k) w o_{kj} h_j (1 - h_j) x_i$$

$$\Delta wh_{ji} = \eta \sum_{k=1}^{no} \delta y_k y_k (1 - y_k) w o_{kj} h_j (1 - h_j) x_i \quad \dots(2.26)$$

Using Eq. (2.19)

$$\Delta wh_{ji} = \eta \sum_{k=1}^{no} \Delta y_k w o_{kj} h_j (1 - h_j) x_i \quad \dots(2.27)$$

where,

$$\delta h_j = \sum_{k=1}^{no} \Delta y_k w o_{kj} \quad \dots(2.28)$$

Here, δh_j is the error at the output side of the j^{th} hidden node.

$$\Delta h_j = \delta h_j h_j (1 - h_j) \quad \dots(2.29)$$

Here, Δh_j is the error at the input side of the j^{th} hidden node.

Substituting Eq. (2.29) in Eq. (2.27)

$$\Delta wh_{ji} = \eta \Delta h_j x_i \quad \dots(2.30)$$

The learning process starts with a random set of weights. During the training process, weights are updated through error back-propagation using Eq. (2.17) or (2.18) and Eq. (2.30) respectively for output and hidden layers. The flowcharts for training of ANN using back-propagation algorithm and that for testing of the trained ANN are shown in Fig. 2.16 and Fig. 2.17 respectively.

2.10.2 Adaline Network

Adaline networks were one of the earliest ANNs. They consist of single neuron elements employing only linear functions and a simple Least Mean Square (LMS) learning. This makes them suited for simple classifications and restricted non-linear system simulation.

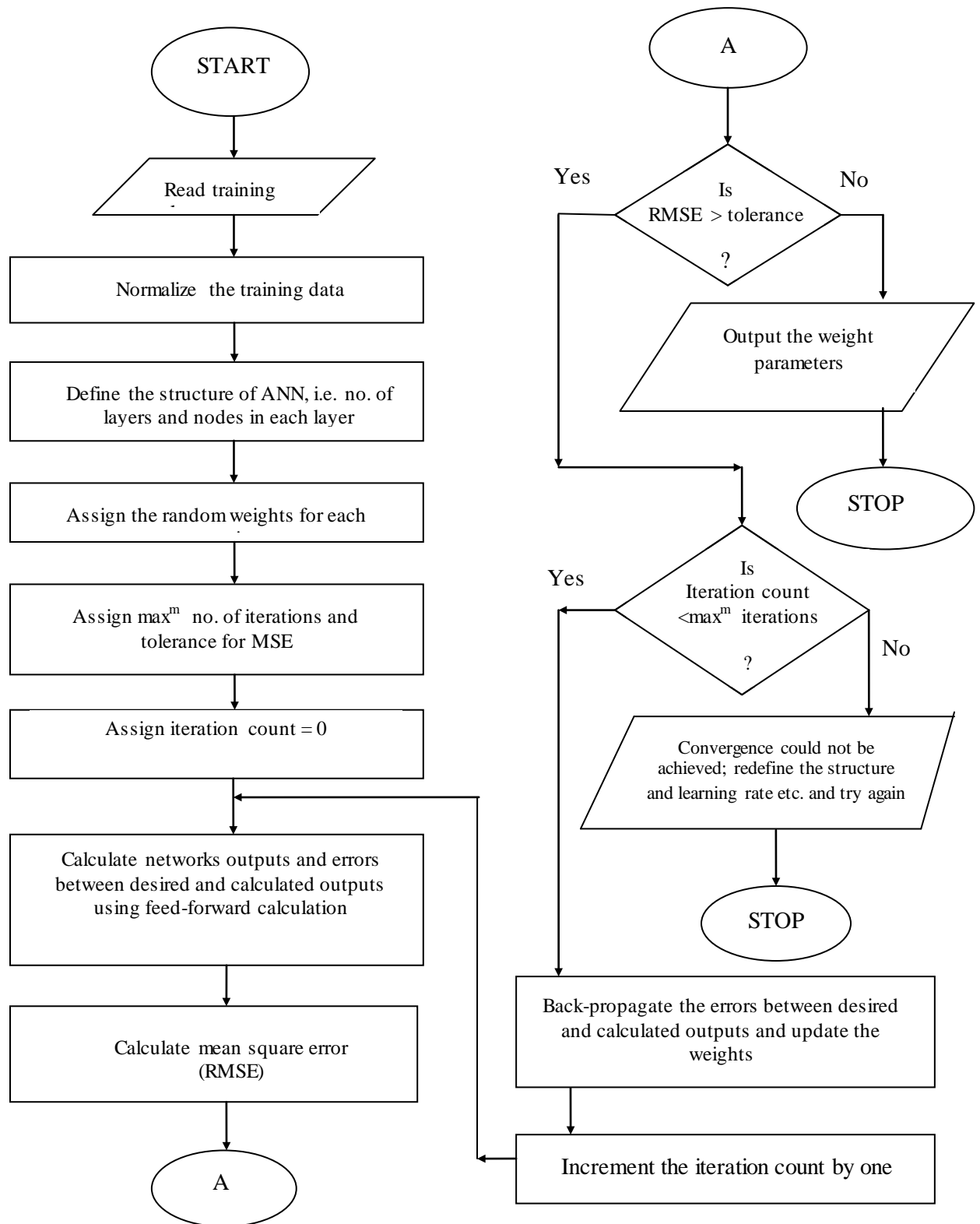


Fig. 2.16 Flowchart for training using back-propagation algorithm

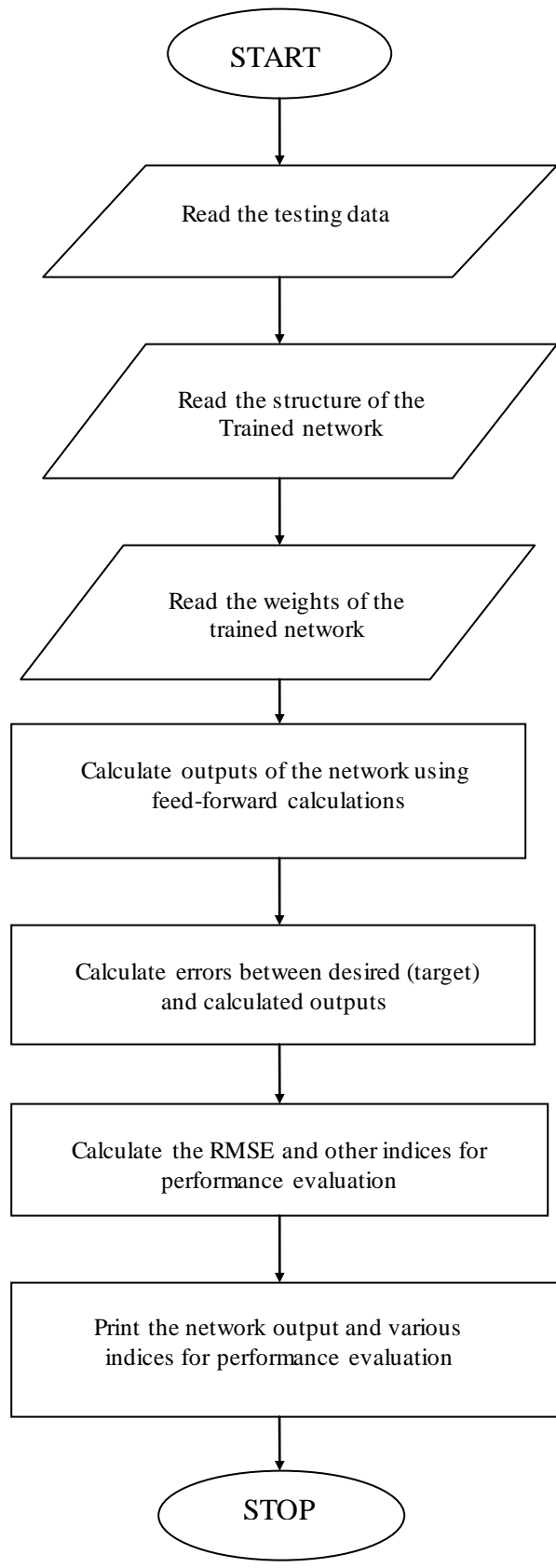


Fig. 2.17 Flowchart for Testing of the Trained ANN

2.10.3 Kohonen Network

The Kohonen network (Kohonen, 1988) was one of the earliest unsupervised feedforward networks; being able to self organize its neuron weights. The network maps input data into a 2 - dimensional grid of neurons with a special distance learning algorithm. The result is a surface area that shows peaks at different areas for different input vectors. This network was originally designed for speech mapping and recognition.

2.10.4 Hopfield Network

The Hopfield network is an example of a batch learning feedback network. A given set of known vectors can be stored in the network by using a special formula to determine the weights. After that, any input vector will slowly converge to the nearest stored pattern (Fig. 2.18). These types of networks are referred to as associative memories; and relate an input to some stored pattern; numerous variations have been invented (BAM, CAM). Hopfield networks are used for database managing, image restoration and other addressable memory problems.

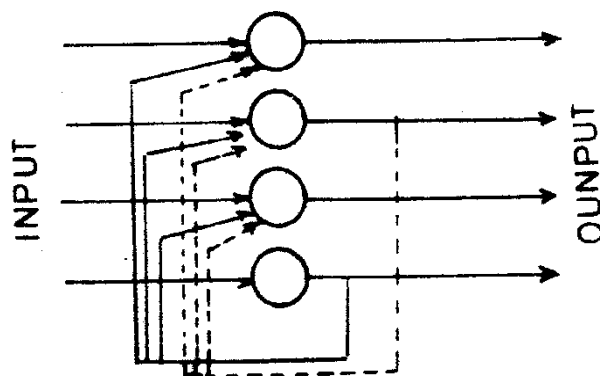


Fig. 2.18 The Hopfield Network

2.10.5 Adaptive Resonance Theory Network (ART)

ART or adaptive resonance theory network is an unsupervised feedback network, which has a complicated, changing structure (Russell, 1991). It uses competitive neurons in self organizing and self stabilizing clusters, which classify input vectors to self defined groups. When an input vector is discriminating enough, the network is able to define a new classification group and thus store a new pattern.

2.10.6 Linear Vector Quantization Network (LVQ)

Linear Vector Quantization (LVQ) network is a supervised feedback network. It is a method whereby supervision and competitive layers are combined. The competitive layer finds subclasses among then input data; and these are then classified into user defined target classes. In contrast to back propagation classification networks, LVQ can also classify non-linearly separable sets of vectors.

2.10.7 Elman Network

It has two hidden layer back propagation network, with the addition of a feedback connection from the output of the first hidden layer to its input. This feedback path allows Elman networks to learn to recognize and generate temporal patterns as well as spatial patterns (Elman, 1990).

2.11 SELECTION OF NETWORK ARCHITECTURE

One of the most important attributes of a layered neural network design is choosing the architecture. The number of input nodes is simply determined by the dimension of the input vector to be generalized or associated with a certain output quality. The dimension of the input vector corresponds to the number of distinct feature of the input pattern. Similarly the number of neurons in the output layer can be made equal to the dimension of vectors to be associated. The size of the hidden layer(s) is the most important consideration when solving the actual problems using multilayer feed-forward neural networks. The most popular and effective strategy for selecting the appropriate number and size(s) of the hidden layer(s) is trial-and-error procedure. A number of networks with one or two hidden- layer(s) are trained with different combination of hidden neurons and a network is selected that yields the minimum root mean square error (MSE). It is also important that the size of the network should be as small as possible. An effective criterion for selecting the best network from these two points of view, i.e. minimum RMSE and smallest size, is Akaike's Information Criterion (AIC). The AIC is an operational way of trading off the size of the network against how well the network fits the data (Akaike, 1974). It is given by

$$AIC = 2k + n \ln \left(\frac{2E}{n} \right) \quad \dots(3.31)$$

Where, E is the sum-square-error; k is the number of parameters; and n is the number of observations. The network with minimum value of AIC is considered to be the best network.

2.12 ISSUES IN ANN APPLICATION

By now, ANNs are firmly established as a viable black–box modeling tool. However, along with numerous advantages, ANNs have some disadvantages too. The first and foremost is the requirement of adequate data of desirable quality and quantity. To be fair to ANNs, this is a crucial requirement with all modeling techniques and ANN cannot be an exception. Presently clear guidelines are not available except that the entire range of likely inputs should be covered. Guidelines to select network architecture for a given type of problems are also badly missing. In this context, ASCE (2000b) has raised the following very pertinent questions, which need to be resolved.

- Can ANNs make to reveal any physics? The application of ANNs can get a boost if some physical explanation of their functioning is available. This will also help in selecting the appropriate type of network and learning algorithm for a given problem. Some neural networks can provide statistical interpretations in terms of conditional probabilities. For instance, a feed forward network can learn the posterior probability of a classification. This problem is receiving attention of many researchers.
- Can an optimal training set be identified? ANNs cannot learn without data –they are data intensive and poor training data will result in poor learning. An optimal data set should fully represent the modeling domain, have minimum required data points and there should not be repetition of data. So far, there are no guidelines about these.
- Can ANNs improve time series analysis? The time series models are based on extracting the correlation and dependence structure of the data. While ANNs have been not given any insight into the process, it would be welcome if ANNs can bring out the relationships among the variables and highlight those features of input data are not revealed by other techniques.
- Can training of ANNs be made adaptive? The most time-consuming part of ANN application is training. As new data become available, the previously trained ANN has to be re-training. Since the catchment properties change with time, it is important to incorporate the new information in the model. The ANN applications will be

immensely benefited if the training can be made adaptive, i.e., the new information is incorporated into the models without the necessity of complete re-training.

- Are ANNs good extrapolators? Many studies have shown that ANNs work well in the range of input data that were used for training and their performance deteriorates if during application, the input data are of this range. This aspect is receiving attention of hydrologists. Imrie *et al.* (2000) have presented a methodology for training ANNs to produce models that generalize well on new data and can extrapolate beyond the range of values included in the calibration range. They claimed good results the data from the catchment of the River Trent and a modified cascade-correlation algorithm.

A think and solution to the above issues will certainly help in better understanding of the artificial neural networks. Of course ANNs cannot be considered as a panacea for all types of problems of water resources or an alternative to other modeling approaches. Gupta *et al.* (2000) have aptly comment: “ We do not advocate that the ANN approach be generally used in place of that the ANN approach does not- in particular, the conceptual approach has potential to be applied to ungauged watersheds or to simulate the potential behavior of a watershed under land use changes... Further, implementation of the ANN approach does not require the considerable amount of expertise and data required to calibrate a conceptual watershed model.” Logically then, ANN should be viewed as alternative to computing techniques.

Chapter – 3



Review of Literature

In recent years ANNs have shown exceptional performance as regression tools, especially when used for pattern recognition and function estimation. They are highly non-linear, and can capture complex interactions among the input variables in a system without any prior knowledge about the nature of these interactions (Hammerstrom, 1993). The main advantage of ANNs is that one does not have to explicitly assume a model form, which is a prerequisite in conventional modelling approaches. Indeed, in ANNs the data points themselves generate a relationship of possibly complicated or orthodox shape. In comparison to the conventional methods, ANNs tolerate imprecise or incomplete data, approximate results, and are less vulnerable to outliers (Haykin, 1994). They are highly parallel, i.e.; their numerous independent operations can be executed simultaneously. Although application of ANN approach in hydrological modeling is recent and limited, it has already produced very encouraging results. A number of researchers have investigated the potential of artificial neural networks in modeling the rainfall runoff process as well as the runoff sediment process. The review is given separately in the following sections.

3.1 ANN APPLICATIONS IN RAINFALL-RUNOFF MODELING

In a preliminary study, Half et al. (1993) designed a three-layer feedforward ANN using the observed rainfall hyetographs as inputs and hydrographs recorded by the U.S. Geological Survey (USGS) at Bellvue, Washington, as outputs. The authors decided to use five nodes in the hidden layer. A total of five storm events were considered. On a rotation basis, data from four storms were used for training, while data from the fifth storm were used for testing network performance. A sequence of 25 normalized 5 min rainfalls was applied as inputs to predict the runoff. This study opened up several possibilities for rainfall-runoff application using neural networks.

In an application using two neural networks, Zhu et al. (1994) predicted upper and lower bounds on the flood hydrograph in Butter Creek, New York. Off-line predictions were made when present flood data were not available and estimates had to be based on rainfall data alone. On-line predictions were based on both rainfall and previous flood data. Data for ANN testing and validation were generated from a nonlinear storage model. Model

performance was strongly influenced by the training data set. The authors found that, while the ANN did well during interpolation, predictions made by ANNs outside the range of the training data set were not encouraging. The process of trying to make ANNs adaptive was computationally very demanding, because the entire training process needed to be repeated with each new data pair. As the lead time for forecasting increased, ANN performance deteriorated. By comparison, ANNs were found to be marginally better than fuzzy inference-based techniques.

In a more detailed study along similar lines, Karunanithi et al. (1994) were interested in estimating streamflows at an ungauged site on the Huron River in Michigan, based on data from USGS stream gauging stations located 30 km upstream and 20 km downstream of the sampling site. They compared ANN performance to an empirical two-station power law relationship that is based on log-transformation of the actual streamflow values. Fig. 3 shows a comparison of observed versus predicted daily flows for a testing period of two years. Daily data were found to exhibit rapid fluctuations, and the authors worked with five-day non-overlapping averages and five-day moving averages to obtain a smoother representation when using regression. However, the raw data were utilized as ANN inputs. They used the cascade-correlation algorithm so that the network architecture could be determined during training. When using empirical regression equations, the largest errors were associated with the highest stream flows. Neural networks were found to better predict these high events, while both methods predicted low streamflows fairly well. These authors stated that ANNs are capable of adapting their complexity to accommodate temporal changes in historical streamflow records. They also found that including another gauging station that supposedly had little or no effect on streamflows at the gauging site caused the performance of the regression technique to deteriorate, while the ANN performance was not affected. The authors claimed that ANNs are likely to be more robust when noisy data is present in the inputs. Karunanithi et al. (1994) found lag time to be important in predicting streamflows. This reflects the longer memory associated with streamflows. The authors did not use any statistical techniques to evaluate the lag time and include it in the network architecture.

Lorrai and Sechi (1995) developed and applied neural networks to rainfall – runoff transformation. The network architecture was developed with two hidden layers and sigmoid response function by using back propagation algorithm. Monthly rainfall, runoff, and temperature were used to develop the model by dividing the data into three ten year period and verified in rest two ten years' block. They found that artificial neural networks provide higher efficiency during model development and were superior to simple

multivariate auto-regressive model. However, the verification of results of the developed models was not so promising.

Smith and Eli (1995) applied a back-propagation neural network model to predict peak discharge and time to peak over a hypothetical watershed. Data sets for training and validation were generated by either a linear or a nonlinear reservoir model. By representing the watershed as a grid of cells, it was possible for the authors to incorporate the spatial and temporal distribution information of rainfall into the ANN model. As an example, the authors chose a synthetic watershed that was composed of 5 X 5 cells. A tree-type drainage pattern was superimposed on the grid to concentrate runoff towards a single watershed outlet. Each cell was treated as a reservoir and water was routed in a cascading fashion. A rainfall depth of one unit was applied instantaneously at several cells on a random basis. Each rainfall pattern in the training set was presented to the network as an input image consisting of Boolean values with 1 representing a wet cell and 0 a dry cell. The peak discharge and the time to peak corresponding to each rainfall pattern were computed using a linear and nonlinear reservoir model and served as target outputs for the ANN model. Many such patterns formed the training set. These cases represented single-storm events for which the number of input units was the same as the number of cells. To simulate the occurrence of several storms in a sequence, three stochastically generated rainfall patterns were imposed consecutively over the synthetic watershed. In this case, the input layer had 75 units, corresponding to three rainfall patterns requiring 25 cells each. The output was either the watershed runoff alone or the runoff and the time to peak. The number of nodes in the hidden layer was determined by trial and error for each case. For single-storm events, the peak discharge and the time to peak were predicted well by the neural network, both during training and testing. The authors were less successful for multiple-storm events. One reason for this may have been insufficient number of nodes in the output layer. In a separate application dealing with multiple storms, Smith and Eli (1995) represented the entire hydrograph by a Fourier series with 21 coefficients, rather than just two attributes as in single-storm events. The ANN output layer now consisted of 21 nodes corresponding to the Fourier coefficients. Using this method, the authors found the prediction of the entire hydrograph to be very accurate for multiple storm events.

The issue of enhancing the training speed using a three-layer network was addressed by Hsu et al. (1995) and Gupta et al. (1997). These studies advocated the linear least squares

simplex (LLSSIM) algorithm, which partitions the weight space to implement a synthesis of two training strategies. The input-hidden layer weights were estimated using a multistart down-hill simplex nonlinear optimization algorithm, while the hidden-output layer weights were estimated using optimal linear least square estimation. The nonlinear portion of the search was thereby confined to a smaller dimension space, resulting in acceleration of the training process. The simplex search involves multiple starts that are initiated randomly in the search space, and the probability of finding local minima is virtually eliminated. The authors applied this technique to daily rainfall-runoff modeling of the Leaf River Basin near Collins, Mississippi. The performance of neural networks was compared with the linear ARMAX time series model and the conceptual SAC-SMA model. Even though all the models seemed to underestimate low flows in general, the ANN performance was found to be superior to the other models. Gupta et al. (1997) concluded that the LLSSIM is likely to be a better training algorithm than back-propagation or conjugate gradient techniques, especially in the absence of a good initial guess of weights.

In another related study over the Leaf River Basin, Hsu et al. (1997) used a three-layer feedforward ANN and a recurrent ANN to model daily rainfall-runoff. They concluded that the feedforward ANN needed a trial-and-error procedure to find the appropriate number of time-delayed input variables to the model and also was not suitable to distributed watershed modeling. On the other hand, the recurrent ANN was able to provide a representation of the dynamic internal feedback loops in the system, eliminating the need for lagged inputs and resulting in a compact weight space. However, both ANNs performed equally well at runoff prediction.

In a study by Minns and Hall (1996), data for network training consisted of model results from one storm sequence, and two such sequences were generated for testing. Each storm sequence was generated using a Monte Carlo procedure that preserved predetermined storm characteristics. For each such storm sequence, the corresponding runoff sequence was constructed using a simple nonlinear model for flood estimation (called RORB) that allowed for different levels of nonlinearity in the response. A three-layer network with back-propagation was used. Network inputs consisted of concurrent and 14 antecedent rainfall depths and 3 antecedent runoff values, and the network output was current runoff. It was found that ANN performance was hardly influenced by level of nonlinearity, with performance deteriorating only slightly for high levels of nonlinearity. Using 2 hidden layers

1 and the associated extra cost on network training could rectify this. Minns and Hall (1996) point out the importance of standardization based on maximum and minimum values of inputs and outputs. Whenever the network was required to predict, 'out of range', of the standardized values, the performance dropped significantly, suggesting that ANNs are not very good extrapolators.

Jayawardena and Fernando (1995, 1996) and Fernando and Jayawardena (1998) also used RBF methods for flood forecasting. They illustrated the application of (REF) artificial neural networks using an orthogonal least squares algorithm (OLS) to model the rainfall-runoff process. Hourly rainfall and runoff data from a 3.12 km² watershed were collected and used in developing the ANN. The autocorrelation of runoff, and the cross correlation between rainfall and runoff indicated that the discharges at a certain time were influenced by antecedent rainfall from up to three previous hours. Therefore, the input nodes contained three antecedent discharges and two rainfall values—that is, $Q(t-1)$, $Q(t-2)$, $Q(t-3)$, $R(t-2)$, and $R(t-3)$. The output was the discharge at the current hour, $Q(t)$. Both a multiple layer perceptron (MLP) neural network and a REF network were developed and compared with the statistical ARMAX model. Even though both the REF and MLP networks performed well, it was found that RBF networks could be trained much faster than MLP networks using back propagation. Both networks performed better than the ARMAX model.

Shamseldin (1997) compared ANNs with a simple linear model, a season-based linear perturbation model, and a nearest neighbor linear perturbation model. Daily average values of rainfall and runoff from six different watersheds around the world were collected for this study. Three different types of input information were compiled from this data. These were weighted averages of recent rainfall measurements, seasonal information on <I>-index and average discharges, and nearest neighbor information. Four different scenarios based on combinations of some or all of these types of input information were examined. The author adopted a three-layer neural network, and the conjugate gradient method was used for training. A two-parameter gamma function representation was chosen as the impulse response of the rainfall series. The parameters were also estimated as part of the training procedure. The network output consisted of the runoff time series. The results suggested that the neural networks generally performed better than the other models during training and testing.

Yang *et al.* (1997) described the development of an ANN model to simulate fluctuations in midspan water-table depths and drain outflows as influenced by daily rainfall and potential evapotranspiration rates. The model was developed using field observations of water-table depths from 1991 to 1993 and drain outflows from 1991 to 1994 made at an agricultural field in Ottawa, Canada. The root mean squared error and standard deviation of errors of simulated results were found to range from 46.5 to 161.1 mm and 46.6 to 139.2 mm, respectively, thus showing potential applications of ANNs in land drainage engineering.

Dawson and Wilby (1998) used a three-layer back-propagation network to determine runoff over the catchments of the Rivers Amber and Mole. The two catchments are about 140 km² in size, and are prone to floods. ANN inputs were past flows and averages of past rainfall and flow values. The ANN output consisted of predicting future flows at 15 min intervals up to a lead time of six hours. Their results show that ANNs performed about as well as an existing forecasting system that required more information. When compared with actual flows, the ANNs appeared to overestimate low flows for the Mole River.

Thirumalaiah and Deo (1998) highlighted the use of neural networks in real-time forecasting of water levels at given site (Jagdapur on river Indravathi, a major tributary of the river Godavari) with a lead time of 1 and 2 day of daily stream levels continuously throughout the year based on the same levels at some upstream gauging station and/or using the stage time history recorded at the same site. The network was trained by using three algorithms, namely, error back propagation, cascade correlation, and conjugate gradient. The training results were compared with each other. The network was verified with untrained data.

Tokar and Johnson (1999) reported that ANN models provided higher training and testing accuracy when compared with regression and simple conceptual models. Their goal was to forecast daily runoff for the Little Patuxent River, Maryland, with daily precipitation, temperature, and snowmelt equivalent serving as inputs. It was found that the selection of training data has a large impact on accuracy of prediction. The authors trained and tested the ANN with wet, dry, and average-year data, respectively, as well as combinations of these, in order to illustrate the impact of the training series on network performance. The ANN that was trained on wet and dry data had the highest prediction accuracy. The length of training record had a much smaller impact on network performance than the types of training data.

Jain and Srivastava (1999) studied the application of ANNs for reservoir inflow forecasting and further development of reservoir operation policy. An auto-regressive integrated moving average time series model and an ANN based model were fitted to the monthly inflow data series and their performances were compared. The ANN was found to model the high flow better, whereas, the low flows were better predicted through the auto-regressive integrated moving average model. Reservoir operation policies were formulated through dynamic programming.

Zealand *et al.* (1999) investigated the utility of artificial neural networks approach for short term forecasting of stream flows to a portion of the Winnipeg River system in North-West Ontario, Canada. Forecasting was conducted on a catchment area of approximately 20,000 km² using quarter monthly time intervals. A very close fit was obtained during the calibration phase and the ANNs developed consistently outperformed a conventional model during the verification phase for all four forecasts lead-time.

Thirumalaiah and Deo (2000) demonstrated the application of neural networks to real-time forecasting of hourly flood runoff with a warning time of a few hours (i.e with a lead time of 1, 2, and 3 hour) and daily river stage with a warning time of a few days (with a lead time of 1day and 2 day) at given sites in Godavari river basin, as well as to the prediction of rainfall sufficiency for India. The study showed the capability of neural networks in all of these applications and they performed better than the statistical models.

ASCE Task Committee (2000 a) investigated the preliminary application and role of artificial neural networks (ANNs) in hydrology. The study offers a brief comparison of the nature ANNs and other modeling philosophies in hydrology. A discussion on the strengths and limitations of ANNs brought out the similarities they had with other modeling approaches, such as the physical model.

ASCE Task Committee (2000 b) examined the hydrologic applications and role of ANNs in various branches of hydrology. It was found that ANNs are robust tools for modeling many of the nonlinear hydrologic processes such as rainfall- runoff, stream flow, ground-water management, water quality simulation and precipitation. A good physical understanding of the hydrologic process being modeled can help in selecting the input vector and designing a more efficient network. However, artificial neural networks tend to be very data intensive, and there appears to be no established methodology for design and successful implementation. The merits and limitations of ANNs were discussed and potential research avenues were explored briefly.

Anmala *et al.* (2000) used ANNs for predicting runoff over three medium-sized watersheds in Kansas. The performance of ANNs possessing different architectures and recurrent neural networks were evaluated by comparisons with other empirical approaches. Monthly precipitation and temperature formed the inputs and monthly average runoff was chosen as the output. The issues of overtraining and influence of derived inputs were addressed and it appeared that a direct use of feed-forward neural networks without time-delayed input may not provide a significant improvement over other regression techniques.

Thandaveswara and Sajikumar (2000) investigated rational procedure for clustering or grouping of river basins based on the hydrological homogeneity by applying artificial neural network. First, an attempt was carried out to check whether the classifications in the data hyperspace have any physical meaning or not. Subsequently, it was attempted to check whether the clustering with factors that affect runoff has any effect in runoff values of each cluster. The statistics presented indicates that there was congregation about the cluster center. Finally, they investigated the use of clustering of basins based on homogeneity in data hyperspace.

In another study Tokar and Markus (2000) have compared the ANN models with traditional conceptual models in predicting watershed runoff as a function of rainfall, snow water equivalent, and temperature. The ANN technique was applied to model watershed runoff in three basins with different climatic and physiographic characteristics – the Fraser River in Colorado, Raccoon Creek in Iowa, and Little Patuxent River in Maryland. In the Fraser River watershed, the ANN technique was applied to model monthly streamflow and was compared with a conceptual water balance (watbal) model. In the Raccoon River watershed, the ANN technique was applied to model the daily rainfall-runoff process and was compared to the Sacramento soil moisture accounting (SAC-SMA) model. The daily rainfall-runoff process was also modeled using the ANN technique in the Little Patuxent River basin and the training and testing results were compared to those of a simple conceptual rainfall-runoff (SCRR) model. In all cases, the ANN models provided higher accuracy, a more systematic approach, and shortened the time spent in training of the models.

Coulibaly *et al.* (2001) also agree that various ANN-based models tend to outperform the conventional models on forecasting peak hydrologic events. In their study, the authors have addressed the issue of selection of appropriate model input using a peak and low flow criteria (PLC). The optimal artificial neural network (ANN) models selected using the PLC significantly outperform those identified with the classical root-mean-square error (RMSE) or

the conventional Nash-Sutcliffe coefficient (NSC) statistics. The comparative forecast results indicate that the PLC can help to design an appropriate ANN model to improve extreme hydrologic events (peak and low flow) forecast accuracy.

Birkundavyi et. al. (2002) investigated the performance of ANNs as potential models capable of forecasting daily streamflows in the Mistassibi River basin, located in the northeastern Quebec. The results based on mean square errors and Nash coefficients show that ANNs outperform the deterministic model PREVIS for up to 5-day-ahead forecasts. Moreover, the results obtained with the ANN are also superior to the ones obtained with a classic autoregressive model coupled with a Kalman filter.

Chibanga et al (2003) have modeled the derived flow series(by simple reservoir routing) and the time series of historic flow measured at the Kafue Hook Bridge (KHB), Kafue River basin in Vietnam, separately using artificial neural networks (ANNs). For each of these two series, relevant inputs were given to a host of three layer feedforward back propagation (FF-BP), ANNs to predict the current, derived flow or KHB flow. A couple of ANN models selected on the basis of defined criteria were then used to forecast the flows at in time steps ahead. To evaluate the forecasting performance of the best ANN models, comparison with best autoregressive moving average models with exogenous inputs ARMAX were made. In both cases the ANNs gave more robust forecasts over long terms than ARMAX models thereby making ANNs a viable alternative in flow forecasting

Chiang et al (2004) have presented a system comparison of two basic types of neural networks, static and dynamic, their study. Two back-propagation learning algorithms, the standard BP and conjugate gradient (CG) method, were used for the static network and the real- time recurrent learning (RTRL) algorithm was used for the dynamic-feedback network. In comparison of searching algorithms for a static network, the results show that CG method was superior to the standard BP method in terms of the efficiency and effectiveness of the constructed network's performance. For a comparison of the static neural network using the CG algorithm with the dynamic neural network using RTRL, the authors concluded that: (i) the static-feedforward neural network could produce satisfactory results only when there were a sufficient and adequate training data set, (ii) the dynamic neural network generally could produce better and more stable flow forecasting than the static network, and (iii) the RTRL algorithm helps to continually update the dynamic network for learning- this feature is

especially important for the extraordinary time-varying characteristics of rainfall-runoff process.

Sarkar (2005) has presented the application of artificial neural network (ANN) methodology for real time flood forecasting in a medium size catchment of the Ajay River in Jharkhand state of India. The author has designed and developed back propagation ANN models for 1-hour ahead to 6-h ahead runoff predictions at the Sarath gauging site of the Ajay River basin. Various combinations of the flood events have been used for the training of ANN models. The performance of each model structure has been evaluated using common performance criteria, i.e., root mean square error (RMSE), coefficient of correlation (r), and coefficient of determination (R^2). The criteria selected by the author to avoid over training was generalization of ANN through cross validation. Fairly accurate hourly runoff predictions have been obtained using the data of six flood events suggesting that the ANN models are particularly suited for flood forecasting purposes. The two important parameters, when predicting a flood hydrograph, are the magnitude of peak discharge and the time to peak discharge. The author has found that the ANN flood forecasting models have been able to predict this information with great accuracy. However, the forecasting efficiency goes down with increasing lead time.

Jy S. Wu *et al.* (2005) demonstrated the application of ANNs for watershed-runoff and stream-flow forecasts. A watershed runoff prediction model was developed to predict stormwater runoff at a gauged location near the watershed outlet. Another stream flow forecasting model was formulated to forecast river flow at downstream locations along the same channel. Input data for both models include the current and preceding records of rainfall and stream flow gathered at the watershed outlet and downstream locations. Computational algorithms for both models were based on commercially available software. A case study was conducted on a small urban watershed in Greensboro, North Carolina. These two ANN - hydrologic forecasting models were successfully applied to provide near-real-time and near-term -flow predictions with lead times starting from the present time and advancing to a few hours late on 15-min increments. An important aspect of this research was the development of methodology for input data organization, model performance evaluation, and ANN processing techniques. Encouraging results obtained indicate that ANN - hydrologic forecasting models can be considered an alternate and practical tool for stream-flow forecast, which is particularly useful for assisting small urban watersheds to issue timely and early flood warnings.

Sarkar *et al.* (2006) developed back propagation ANN runoff models to simulate and forecast daily runoff for a part of the Satluj river basin of India and observed that only rainfall and temperature considered as input are not adequate to develop a model for the simulation as well as forecasting of the catchment runoff, resulting from rainfall and snowmelt contribution. In order to improve upon the performance of the models, it was suggested that to consider the runoff of the upstream site as an additional input to the model.

Thomas *et al.* (2006) developed ANN model and trained using the daily rainfall and stream flow for the Sindh river up to Madhikhera dam site for a period of seven years from 1992 to 1999 and then tested for 2000 and 2001 and the results were compared with the observed daily discharges of the corresponding period. The efficiency of the ANN model varied between 70.36% and 94.57% during calibration and between 63.02% and 92.76% during validation. The results suggested that a three layer feed forward ANN having a single hidden layer with five neurons in the hidden layer can effectively be used to relate the Rainfall-Runoff process.

Kumar and Viswanadh (2006) established relationship between rainfall and runoff using feed forward multi layer neural networks and investigated the performance of neural networks as potential models capable of forecasting annual runoff. The study was taken up for Osmansagar catchment, Hyderabad, Andhra Pradesh, India. The best fit model (1-10-1) was trained using data for 38 years (1941 – 1979) and validated on 14 years (1980 – 1993). Based on the evaluation of the performance criteria such as root mean square error and the correlation coefficient, the study revealed that ANNs perform well in estimating the runoff.

Kisi (2007) presented a comparison of different artificial neural network algorithms for short term daily streamflow forecasting. Four different ANN algorithms, namely, backpropagation, conjugate gradient, cascade correlation, and Levenberg – Marquardt were applied to continuous flow data of the North Platte river in the United States. The models were verified with untrained data. The results from the different algorithms were compared with each other. The correlation analysis was used in the study and found to be useful for determining appropriate input vectors to the ANNs.

Kumar (2007) developed an ANN model for the prediction of runoff from Nagwan watershed of Damoder Valley Corporation (DVC), Hazaribagh, Jharkhand, India. He used the back propagation algorithm in the training of feed-forward multilayer neural networks with fixed iteration 15000 and 17000 for single and two hidden layer(s) respectively. The daily rainfall and runoff data of active monsoon period i.e. 1st June to 30th September were

used in the development of the model. The data of the years 1993 – 1999 were used for the training; years 2000 – 2002 were used for testing of the trained ANN. Six selected performance evaluation criterion, viz. correlation coefficient, coefficient of efficiency, root mean square error, integral square error, coefficient of variation and volumetric error were employed for the performance evaluation of model. He found that network architecture with five number of inputs (rainfall of current day, rainfall of two previous days and runoff of two previous days), six neurons in the single hidden layer, and one neuron in output layer yielded the good results for the runoff prediction.

Kalteh (2008) developed a rainfall-runoff model using an ANN approach in a watershed in northern Iran, and described different approaches including Neural Interpretation Diagram, Garson's algorithm, and randomization approach to understand the relationship learned by the ANN model. The results indicated that ANNs are promising tools not only in accurate modelling of complex processes but also in providing insight from the learned relationship, which would assist the modeller in understanding of the process under investigation as well as in evaluation of the model.

Modarres (2009) developed an effective ANN model for studying the rainfall-runoff relationship in the main upstream basin of the Zayandehrud watershed in the western region of Isfahan Province in the center of Iran and verified the models by the global statistics such as root mean square error (RMSE), coefficient of correlation and coefficient of efficiency. In the second step, the non-parametric test for the equality of the mean, variance and probability distribution of the observed and simulated runoff were used to validate rainfall-runoff models and to compare them with global statistics. The study illustrated that the modelers should select appropriate and relevant evaluation measures from the set of existing metrics based on the particular requirements of each individual applications.

3.2 ANN APPLICATIONS IN RUNOFF-SEDIMENT MODELING

There are numerous studies related to the application of ANN's to rainfall-runoff modeling (ASCE Task Committee, 2000). But the application of ANN approach for modeling runoff-sediment process is very recent and few, but has already produced very encouraging results.

In a research project by Rosenbaum (2000), ANN technique has been used to predict sediment distribution in Swedish harbors. The authors have chosen factored wave energy, sedimentation potential and discharge as input to three layer back propagation ANN models

for the prediction of sediment quantity. Seven years data has been used for training and two years for verification. The authors found that though the ANN model had substantial error in prediction, particularly for the high peaks still the general trend of sedimentation could be predicted. Considering the uncertainties associated with the assessment of sedimentation, the predictive accuracy of the ANN was reasonable.

Baruah et. al. (2001) developed neural network models of Lake surface chlorophyll and sediment content from LandsatTM imagery in order to assess the water quality of the lake Kasumigaura in Japan. In this study, back propagation neural network has been used to model the transfer function between chlorophyll concentration and suspended solid, and sensor received radiances at the first four bands of LandsatTM. The authors found that back propagation neural network with only one hidden layer could model both the parameters better than conventional regression techniques.

Jain (2001) used the ANN approach to establish an integrated stage-discharge-sediment concentration relation for two sites on the Mississippi River. Based on the comparison of results for two gauging sites, the author has shown that the results are much closer to the observed values than the conventional technique and that a network whose inputs are the current and previous stage, discharge, and sediment concentration of two previous periods can adequately map the current discharge and sediment concentration.

In a study by Nagy et al. (2002), an ANN is used to estimate the natural sediment discharge in rivers in terms of sediment concentration. The selection of water and sediment variables used in the model is based on the prior knowledge of the conventional analysis, based on the dynamic laws of flow and sediment. The model parameters as well as fluvial variables are extensively investigated in order to get the most accurate results. In verification the estimated sediment concentration values agree well with the measured ones. The model is evaluated by applying it to other groups of data from different rivers. The authors have addressed the importance of choosing an appropriate neural network structure and providing field data to that network for training purpose. It is found in general that the ANN approach gives better results compared to several commonly used formulas of sediment discharge.

Tayfur (2002) used ANNs for sheet sediment transport modeling. A three-layer feed-forward artificial neural network structure was constructed and a back propagation algorithm was used for the training of ANNs. Even based runoff driven experiment sediment data were used for the training and testing of the ANNs. In training, data on slope and rainfall intensity

were fed into the network as inputs and data on sediment discharge were used as target outputs. The performance of the ANNs was tested against that of the most commonly used physically based models, whose transport capacity was based on one of the dominant variables- flow velocity, shear stress, stream power and unit stream power. The comparison results revealed that the ANNs performed as well as the physically-based models for simulating nonsteady-state sediment loads from different slopes.

Cigizoglu (2002) made a comparison between ANNs and sediment rating curves for two rivers with very similar catchment areas and characteristics in the north of England. Data from one river are used to estimate sediment concentrations and flux in the other for both estimation techniques. The author has highlighted the potential advantages of ANNs in sediment concentration and flux estimation. In particular, an ANN approach can give information about the structure of events (hysteresis) which is impossible to achieve with sediment rating curves.

Agarwal (2002) studied the simulation and forecasting of runoff and sediment yield for Vamsadhara river catchment for different time units (viz. daily, weekly, ten-daily, and monthly) using a new improved ANN modeling technique and the results so obtained were compared with the single - input linear transfer function and multi-input linear transfer function models. Two computer algorithms in FORTRAN language (viz. ANN.FOR and LTF.FOR) were developed respectively for ANN, linear transfer function simulation and forecasting models. The multi-input linear transfer function runoff simulation models for different time base were found superior to respective single-input linear transfer function models in model development but not in model verification. However, the pattern learned ANN runoff simulation models for different time units were found superior to both single-input and multi-input linear transfer function models only in model development. The ANN sediment yield simulation models were superior to single-input and multi-input linear transfer function models both in calibration and verification.

Yitian and Gu (2003) developed a model for prediction flow and sediment transport in a river system by incorporating flow and sediment mass conservation equations into an artificial neural network (ANN), using actual river network to design the ANN architecture, and expanding hydrological applications of the ANN modeling technique to sediment yield predictions. The ANN river system model is applied to modeling daily discharges and annual sediment discharges in the Jingjiang reach of the Yangtze River and Dongting Lake, China.

By the comparison of calculated and observed data, it was demonstrated that the ANN technique is a powerful tool for real-time prediction of flow and sediment transport in a complex network of rivers. A significant advantage of applying the ANN technique to model flow and sediment phenomena was the minimum data requirements for topographical and morphometric information without significant loss of model accuracy. The methodology and results presented show that it is possible to integrate fundamental physical principles into a data-driven modeling technique and to use a natural system for ANN construction. This approach may increase model performance and interpretability while at the same time making the model more understandable to the engineering community.

In a study by Sarkar et al (2004), ANN technique has been applied to model the sediment-discharge relationship of an Indian river. Daily data of sediment load and discharge of Kosi River of Bihar in India have been used. The authors have made a comparison between the results obtained using ANNs and sediment rating curves. The sediment load estimations in the river obtained by ANNs have been found to be significantly superior to the corresponding classical sediment rating curve ones. A significant advantage of using the ANN approach is that it can successfully model the hysteresis effect that is associated with unsteady flow in open channels.

Singh (2004) has done a case study for the Satluj basin to demonstrate the applicability of ANN in model development. Rainfall-runoff and runoff-sediment models have been developed for the Sutluj River basin upto Kasol gauge site. The results of ANN modeling have been compared with those of the conventional techniques, viz. linear multiple regression approach for rainfall-runoff modeling and sediment rating curve analysis for runoff-sediment modeling. A back propagation ANN with the generalized delta rule as the training algorithm has been employed in this study. The structure of all ANN models was three layered back propagation ANN with non-linear sigmoid as activation function uniformly applied between the layers with constant 0.15 and 0.5 learning rate and momentum respectively. The statistical and hydrological evaluation criteria used were root mean square error (RMSE), correlation coefficient (r), coefficient of efficiency (CE) and volumetric error (EV).

Kisi (2005) investigated the abilities of neuro-fuzzy (NF) and neural network (NN) approaches to model the streamflow-suspended sediment relationship by using the daily streamflow and suspended sediment data for two stations - Quebrada Blanca station and Rio Valenciano station - operated by the US Geological Survey as case studies. The NF and NN

models were established for estimating current suspended sediment values using the streamflow and antecedent sediment data. The sediment rating curve and multi-linear regression were also applied to the same data. Statistic measures were used to evaluate the performance of the models. Based on comparison of the results, it was found that the NF model gives better estimates than the other techniques.

Schnabel and Maneta (2005) tested the performance of a feed-forward back propagation artificial neural network (ANN) and a multiple quadratic regression (MQR) model using data from the Parapunus Catchment, a wooded rangeland located in SW Spain. Both models were calibrated using rainfall and discharge time series and derived variables such as rainfall intensity, runoff coefficient and rate of change of discharge. The final set of variables used in the analysis was done based on sensitivity analysis for the ANN model and based on an analysis of statistical significance of parameters in the MQR model. The performance of ANN and MQR were similar but better than rating curves of a single variable. In addition, ANN and MQR were similar but better than rating curves of a single variable. In addition, ANN and MQR can reproduce the hysteretic loop of sediment-discharge relationship.

Sinha (2005) used a multilayered feed forward neural network to establish an integrated stage-discharge-sediment concentration relation for Thebes site for the Mississippi river and found excellent reproducing ability of ANNs for the observed values and also found that a network whose inputs are the current and previous stage, discharge and sediment concentration of two previous periods, can adequately map the current discharge and sediment concentration. The performance of input training set based on only stage data was observed very poor.

Agarwal *et al.* (2006) simulated the daily, weekly, ten-daily, and monthly monsoon runoff and sediment yield from an Indian catchment using back propagation artificial neural network (BPANN) technique, and the results compared with the observed and with those due to single and multi-input linear transfer function models. Normalizing the input by its maximum for the pattern and batch learning algorithms in BPANN, the model parsimony was achieved through network pruning utilizing error sensitivity to weight a criterion, and it was generalized through cross validation. The performance based on correlation coefficient and coefficient of efficiency suggested the pattern-learned artificial neural network (ANN) based on runoff simulation to be superior to both single- and multi-input models in calibration. The single input models were however superior in verification. The ANN based sediment-yield

models performed better than both single- and multi-input models in calibration as well as cross-validation/verification.

Kerem *et al.* (2006) estimated the river suspended sediment using another ANN algorithm, generalized regression neural network, GRNN, as the majority of the ANN applications in water resources involve the employment of feed forward back propagation (FFBP) method. They opted the present methodology, because the Generalized regression neural network does not require an iterative training procedure as in back propagation method and the GRNN simulations do not face the frequently encountered local minima problem in FFBP applications, as GRNN does not generate estimates physically not plausible. The neural networks were trained using daily river flow and suspended sediment data belonging to Juniata Catchment in USA. The suspended sediment estimations provided by two ANN algorithms are compared with conventional sediment rating curve and multi linear regression method results. The mean squared error and the determination coefficient were used as comparison criteria. Also the estimated and observed sediment sums are examined in addition to two previously mentioned performance criteria. The ANN estimations were found significantly superior to conventional method results.

Raghuvanshi *et al.* (2006) developed five ANN models to predict daily and weekly runoff and sediment yield for Nagwan watershed, Damodar Valley Corporation (DVC), Hazaribagh, Jharkhand, India. All five models were developed both with one and two hidden layers. Each model was developed with five different network architectures by selecting a different number of hidden neurons. The models were trained using monsoon season (June to October) data of five years (1991– 1995) for different sizes of architecture, and then tested with respective rainfall and temperature data of monsoon season (June to October) of two years (1996 – 1997). Training was conducted using the Levenberg – Marquardt backpropagation where the input and output were presented to the neural network as a series of learning sets. Simulated surface runoff and sediment yield were compared with observed values and the minimum root-mean-square error and Nash Sutcliff efficiency (coefficient of efficiency) criteria were used for selecting the best performing model. Regression models for predicting daily and weekly runoff and sediment yield were also developed using the above training datasets, whereas these models were tested using the testing datasets. In all cases, the ANN models performed better than the linear regression based models. The ANN models with a double hidden layer were observed to be better than those with single hidden layer. Further, the ANN model prediction performance improved with increased number of hidden neurons and input variables. As a result, models considering both rainfall and temperature as

input performed better than those considering rainfall alone as input. Training and testing results revealed that the models were predicting the daily and weekly runoff and sediment yield satisfactorily. Therefore, these ANN models based on simple input can be used for estimation of runoff and sediment yield, missing data, and testing the accuracy of other models.

Tayfur and Guldal (2006) developed an artificial neural network (ANN) model to predict daily total suspended sediment (TSS) in rivers. The model is constructed as a three-layer feedforward network using the back-propagation algorithm as training tool. The model predicts TSS rates using precipitation (P) data as input. For network training and testing 240 sets of data sets were used. The model successfully predicted daily TSS loads using the present and past 4 days precipitation data in the input vector with $R^2 = 0.91$ and MAE = 34.22 mg/L. The performance of the model was also tested against the most recently developed non-linear black box model based upon two-dimensional unit sediment graph theory (2D-USGT). The comparison of results revealed that the ANN model requires a period of more than 75d of measured P-TSS data for training the model for satisfactory TSS estimation. The statistical parameter range ($x_{\min} - x_{\max}$) plays a major role for optimal partitioning of data into training and testing sets. Both sets had comparable values for the range parameter.

Kisi (2007) investigated the abilities of range-dependent neural networks (RDNN) to improve the accuracy of streamflow-suspended sediment rating curve in daily suspended sediment estimation. A comparison was made between the estimates provided by the RDNN and those of the following models: Artificial neural networks (ANN), linear regression (LR), range-dependent linear regression (RDLR), sediment rating curve (SRC) and range-dependent sediment rating curve (RDSRC). The daily streamflow and suspended sediment data belonging to two stations – Calleguas Station and Santa Clara Station – operated by the US Geological Survey were used as case studies. Based on comparison of the results, it was found that the RDNN model gives better estimates than the other techniques. RDLR technique was also found to perform better than the single ANN model.

Lohani *et al.* (2007) applied a fuzzy logic technique to model the stage-discharge-sediment concentration relationship. The technique has been applied to two gauging sites in the Narmada basin in India. Performance of the conventional sediment rating curves, neural networks and fuzzy rule-based models was evaluated using the coefficient of correlation, root mean square error and pooled average relative (underestimation and overestimation) errors (PARE) of sediment concentration. Comparison

of results showed that the fuzzy rule-based model could be successfully applied for sediment concentration prediction as it significantly improves the magnitude of prediction accuracy.

Jain (2008) investigated the abilities of compound neural networks (CNNs) to model integrated stage-discharge-suspended sediment rating relationship. Using the data of two stations on the Mississippi River and one station on Conococheague Creek, CNNs were trained. A comparison of the results of applying a single ANN and a CNN shows that the estimates of CNN are closer to the observed values than those of single ANN.

Rai and Mathur (2008) developed a back propagation feed-forward artificial neural network (ANN) model for the computation of event-based temporal variation of sediment yield from the watersheds. The training of the network was performed by using the gradient descent algorithm with automated Bayesian regularization, and different ANN structures were tried with different input patterns. The model was developed from the storm event data (i.e. rainfall intensity, runoff and sediment flow) registered over the two small watersheds and the responses were computed in terms of runoff hydrographs and sedimentographs. Selection of input variables was made by using the autocorrelation and cross-correlation analysis of the data as well as by using the concept of travel time of the watershed. Finally, the best fit ANN model with suitable combination of input variables was selected using the statistical criteria such as root mean square error (RMSE), correlation coefficient (CC) and Nash efficiency (CE), and used for the computation of runoff hydrographs and sedimentographs. Further, the relative performance of the ANN model was also evaluated by comparing the results obtained from the linear transfer function model. The error criteria viz. Nash efficiency (CE), error in peak sediment flow rate (EPS), error in time to peak (ETP) and error in total sediment yield (ESY) for the storm events were estimated for the performance evaluation of the models. Based on these criteria, ANN based model results better agreement than the linear transfer function model for the computation of runoff hydrographs and sedimentographs for both the watersheds.

In a study by Rajaei et al. (2009), artificial neural networks (ANNs), neuro-fuzzy (NF), multi linear regression (MLR) and conventional sediment rating curve (SRC) models were considered for time series modeling of suspended sediment concentration (SSC) in rivers. As for the artificial intelligence systems, feed forward back propagation (FFBP) method and Sugeno inference system were used for ANNs and NF models, respectively. The models were trained using daily river discharge and SSC data belonging to Little Black River and Salt River gauging stations in the USA. Obtained results demonstrated that ANN and NF

models were in good agreement with the observed SSC values; while they depicted better results than MLR and SRC methods. The values of cumulative suspended sediment load estimated by ANN and NF models were closer to the observed data than the other models.

Based on the above review it seems that more work on ANN based studies is required to be done on different river basins of India using the latest software to get better prediction accuracy. The ANN studies available in the field of hydrology provide enough evidence that the ANNs are highly capable in learning and extracting the behavior of a system, when sufficient data is available for the training of the ANN model. ANNs have proven application efficiency especially in the hydrological processes like rainfall, runoff, sediment yield etc. The performance of the developed ANN model has frequently been compared with other empirical, conceptual and statistical models. The comparison is normally input dependent and the ANNs have been resulted with the superior performance. The use of artificial neural networks for runoff and sediment yield simulation and forecasting is an advancing area of research that is yet to be fully explored.

Chapter – 4



Study Area And Data Availability

4.1 THE BRAHMAPUTRA RIVER

The Brahmaputra is a major international river covering a drainage basin of 580,000 km², extending from 82°E to 97° 50' E longitudes and 25° 10' to 31° 30' N latitudes. The basin spans over an area of 293,000 km² (50.51%) in Tibet (China), 45,000 km² (7.75%) in Bhutan, 194,413 km² (33.52%) in India and 47,000 km² (8.1%) in Bangladesh. Its basin in India is shared by Arunachal Pradesh (41.88%), Assam (36.33%), Nagaland (5.57%), Meghalaya (6.10%), Sikkim (3.75%) and West Bengal (6.47%) (59). Originating in a great glacier mass at an altitude of 5,300 m just south of the lake Konggyu Tso in the Kailas range, about 63 km southeast of Mansarovar lake in southern Tibet at an elevation of 5300m, the Brahmaputra flows through China (Tibet), India and Bangladesh for a total distance of 2880 km, before emptying itself into the Bay of Bengal through a joint channel with the Ganga. It is known as the Tsangpo in Tibet (China), the Siang or Dihang in Arunachal Pradesh (India), the Brahmaputra in Assam (India) and the Jamuna, Padma, and Meghana in Bangladesh.

Before entering India, the river flows in a series of big cascades as it rounds the Namcha-Barwa peak. The river forms almost trough receiving the flows of its tributaries both from North and South. The river, with its Tibetan name Tsangpo in the uppermost reach, flows through southern Tibet for about 1,625 km eastward and parallel to tributaries, viz., the Nau Chhu, the Tsa Chhu, the Men Chhu, the Charta Tsangpo, the Raga Tsangpo, the Tong Chhu, the Shang Chhu, the Gya Chhu, the Giamda Chhu, the Po Tsangpo and the Chindru Chhu and the right bank tributaries, viz. the Kubi, the Kyang, the Sakya Trom Chhu, the Rhe Chhu, the Rang Chhu, the Nyang Chhu, the Yarlang Chhu, and the Trulung Chhu join the river along its uppermost reach. At the extreme eastern end of its course in Tibet the Tsangpo suddenly enters a deep narrow gorge at Pe, where in the gorge section the river has a gradient ranging from about 4.3 to 16.8 m/km (Fig. 3.1).

The river enters in India near Tuning in Arunachal Pradesh. After travelling for a distance of 278 km up to Kobo, it meets with two rivers the Dibang and the Lohit in Assam near Kobo. Below this confluence point, the river is known by the name of the Brahmaputra. It passes through Assam into Bangladesh and at last it meets with the Ganga near Goalundo

in Bangladesh before joining the Bay of Bengal. Its total length is 2,880 km comprising of 1,625 km in Tibet, 918 km in India and 337 km in Bangladesh. It is also one of the most braided rivers in the world with width variation from 1.2 km at Pandu near Guwahati to about 18.13 km near Gumi few km distances downstream to this point.

Traversing through deep narrow gorges of the Himalayan terrain the Tsangpo takes a southward turn and enters Indian territory at an elevation of 660 m. The river then enters the State of Assam (India) taking two important tributaries the Dibang and the Lohit. At the exit of the gorge the slope of the river is only 0.27 m/km. At the head of the valley near Dibrugarh the river has a gradient of 0.09-0.17 m/km, which is further reduced to about 0.1 m/km near Pandu (Fig. 3.1). The mighty Brahmaputra rolls down the Assam valley from east to west for a distance of 640 km up to Bangladesh border (Table 4.1).

Table 4.1 The Brahmaputra river: Country and Indian state-wise break-up of basin area and channel length

Country	Basin area (Km²)	Channel Length (Km)
I. Tibet (China)	293,000	1,625
2. Bhutan	45,000	-
3. India	194,413	918
(a) Arunachal Pradesh	81,424	278
(b) Assam	70,634	640
(c) Nagaland	10,803	-
(d) Meghalaya	11,667	-
(e) Sikkim	7,300	-
(f) West Bengal	12,585	-
4. Bangladesh	47,000	337

4.2 LONGITUDINAL SECTION OF THE BRAHMAPUTRA RIVER

The longitudinal section of the Brahmaputra river from its origin to the outfall point is depicted in Fig. 4.1.

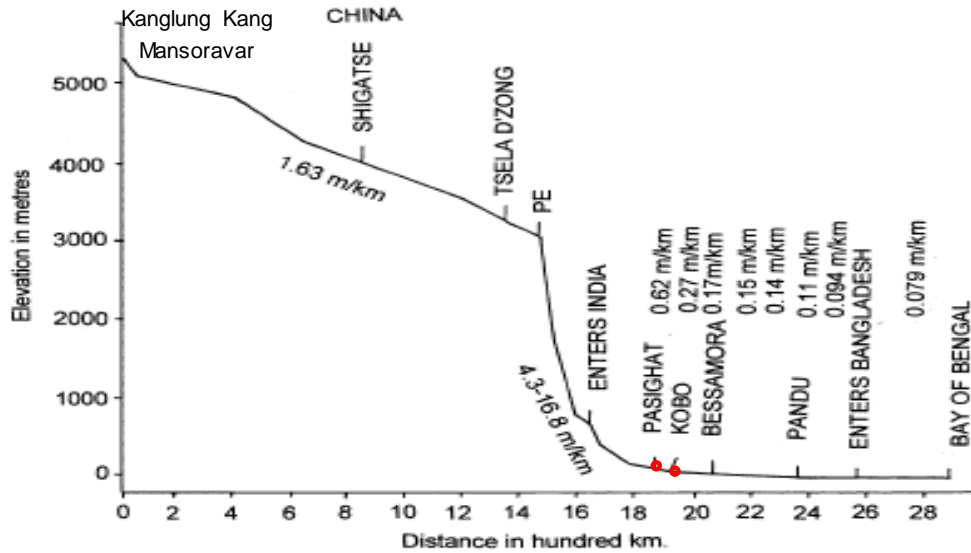


Fig. 4.1 Longitudinal Profile of the Brahmaputra River (Modified After WAPCOS, 1993)

4.3 THE BRAHMAPUTRA BASIN

The Brahmaputra basin is confined by the great Himalayan ranges in the North and Northeast, Naga-Patkai hills in the East, and Mikir hills and Shillong plateau in the South. The Assam valley is the eastern continuation of the Indo-Gangetic plains of the Indian subcontinent valley. It is very narrow in the east and gradually expands to the west to nearly 80 km width, covering an area of about 5,62,704 km². In this valley, the river itself occupies a width of 6 to 12 km in most places. The basin of the river extends from parts of Tibet, Nepal, Bangladesh, Northeast India and Bhutan. The state wise distribution within India and the country wise distribution of the basin are presented in Table 4.2.

The Indian part of the basin has a maximum east-west length of about 1,540 km and a maximum north-south width of about 682 km along 93° east longitude. The basin is characterized by large variations in relief slope, landforms, climate, vegetation and land use. The upper basin lying in Tibet (China) and in the eastern Himalayas of Arunachal Pradesh, Sikkim and Nagaland comprise mostly mountain ranges and narrow valleys and the channels are restricted within steep and narrow valleys in the mountains. In Assam and Meghalaya, the basin consists of hills, plateaus and plains covered by forests, tea gardens, agricultural lands and built-up areas. In West Bengal also, the basin covers hills and valleys dominated by forests, tea gardens, agricultural lands and built-up areas. The lower portion of the basin in Bangladesh consists largely of fertile plains and delta regions.

The Brahmaputra basin in India is most generously gifted with a fabulous water wealth that accounts for nearly 30% of the total water resources and about 40% of the total hydropower potential of the country. However, so far the utilisation of this enormous water resources potential of the region is limited. For example, less than 5% of the existing hydropower potential, 10% of the irrigation potential and about 4% of the ground water potential have so far been harnessed.

The Brahmaputra river is characterized by high intensity flood which flows during the monsoon season, June through September, with an average annual flood discharge of 48,160 m³/sec (August, 1998 at Pancharatna). The highest flood discharge recorded in the Brahmaputra at Pandu (Assam) was of the order of 72,148 m³/sec (in year 1962), which had a recurrence interval of 100 years (173). The daily hydrograph of the river at Pandu exhibits drastic fluctuations in discharge during the monsoon season, whereas the time series of annual maximum flood events for the period 1955-2000 do not indicate any perceptible trend (59).

Analysis of 100-year rainfall records at Guwahati also does not show any distinct long term trend (59). However, there is a considerable variation in the spatio-temporal distribution of rainfall with marked seasonality. For example, precipitation varies from as low as 120 cm in parts of Nagaland to above 600 cm in the southern slopes of the Himalayas. A gradual increase in rainfall from the valley bottom towards the lower ranges of the Himalayas, followed by a decrease towards the higher ranges is evident from the observed records at Dibrugarh (285 cm) in the eastern part of the valley through Pasighat (507 cm) in the foothills to Tuting (274 cm) further up in the Himalayas. Monsoon rains from June to September accounts for 60-70% of the annual rainfall. These rains that contribute a large portion of the runoff in the Brahmaputra and its tributaries are primarily controlled by the position of a belt of depressions, called the monsoon trough, extending from northwest India to the head of the Bay of Bengal. In the course of the north-south oscillations in summer, when this axis moves closer to the foothills of the Himalayas, heavy precipitation occurs in Assam and adjoining highlands. The severity of rainstorms occasionally reaches as high as 40 cm per day. The years 1998 and 2004 which saw extremely high floods in the region also recorded excessively high rainfall, especially in the upper basin areas. Rainfall recorded at Guwahati during the monsoon months in 1998, June through September, is 922 mm, while at Dibrugarh it is 2002 mm and Pasighat in Arunachal Pradesh 4,573 mm accounting for 60%, 67% and 75% of the annual rainfall respectively (59). During the flood season, all the districts in Arunachal

Pradesh receive rainfall much above the normal rainfall. The intensity of rainfall recorded at Dibrugarh on June 28, 1998 is of the order of 17 mm/hr.

The Brahmaputra basin, especially its monsoon dominated wetter parts, is enormously rich in biotic resources with a great diversity of flora and fauna types marked by significant variations, both in vertical and horizontal distributions. The forest cover of the basin in India, as indicated by recent satellite surveys, is 144,922 km², which accounts for 59% of the total geographical area (Myint and Hofer, 1997). In contrast to this, the total basin forest cover including the portion outside India accounts for only 14.07% of the total geographical area of the basin. The distribution of forest cover in different states lying within the basin in India is estimated as: Arunachal Pradesh (82.8%), Nagaland (68.9%), Meghalaya (63.53%), Sikkim (39.52%), West Bengal (21.4%) and Assam (20.56%) (Myint and Hofer, 1997). In fact, Arunachal Pradesh accounts for about 60% of the forest cover in the Indian part of the basin.

The vegetation changes from tropical evergreen and mixed deciduous forest in the Assam valley and the foothills, through temperate coniferous belts in the middle Himalayas to alpine meadows and steppes in the still higher ranges. There has been considerable decline in the forest cover due to deforestation, land use conversion and land degradation in the basin. Shifting cultivation, involving traditional slash and burn technique of agriculture which is widely being practiced in the hills of northeast India, is a major cause of environmental degradation leading to deterioration of forest cover, loss of biodiversity, soil erosion, loss of soil fertility and crop yield, reduction in ground water recharge, increase in surface runoff, lowering of water table and acceleration in the rates of sedimentation in rivers and reservoirs downstream.

The Brahmaputra basin in northeast India provides a unique habitat for an exquisite variety of fauna, some of which belong to the most rare and endangered species. The floodplain of the Brahmaputra river in Assam is dotted with a large number of wetlands, numbering more than 3,500, which have great significance as unique habitats for exquisite varieties of flora and fauna and also as natural flood water retention basins. Degradation and destruction of these wetlands have considerable impact on the deteriorating flood hazard scenario in the state.

4.4 THE BRAHMAPUTRA RIVER SYSTEM

The Brahmaputra river, termed as a moving ocean (173), is an antecedent snow-fed large Trans-Himalayan river which flows across the rising young Himalayan range.

Considerable variations in width, gradient, discharge and channel pattern occur throughout its course. Geologically, the Brahmaputra is the youngest of the major rivers of the world and unique in many respects. It happens to be a major river for three countries, viz., China, India and Bangladesh. The river basin of the Brahmaputra is bounded on the north by the Kailas and Nyen- Chen-Tanghla ranges of mountains; on the east by the Salween river basin and the Patkai range running along the Indo-Myanmar border; on the south by the Nepal Himalayas, the Naga and Barail ranges and the Meghalaya Plateau; and on the west by the Ganga river basin.

The maximum meridional extent of the basin is 1,540 km along 29°30' N latitude and maximum latitudinal extent is 780 km along 90° E longitude. The total length of the river is 2,880 km (Table 3.1). Several tributaries join the river all along its length. The average annual runoff of the Brahmaputra at Pasighat, Pandu and Bahadurabad in Bangladesh is 186,290,494,357 and 589,000 million cubic metre respectively. The monsoon flow of the Brahmaputra at Tesla Dzong in Tibet is 36.27% of the flow at Pasighat (173).

Throughout its course within India, the Brahmaputra is braided with some well defined nodal points where the river width is narrow and restricted within stable banks. All along its course in the valley, abandoned wetlands and back swamps are common. The river carries about 735 million metric tons of suspended sediment loads annually.

The Indian section of the Brahmaputra river receives innumerable tributaries flowing down the northern, north-eastern and southern hill ranges. The mighty Brahmaputra along with the well-knit network of its tributaries controls the geomorphic regime of the entire region, especially the Brahmaputra valley. In the north, the principal tributaries are the Subansiri, the Jia Bhareli, the Dhansiri, the Puthimari, the Pagladiya, the Manas and the Champamati. Amongst these, the Subansiri, the Jia Bhareli and the Manas are the Trans-Himalayan rivers. The principal south bank tributaries are the Burhi Dehing, the Disang, the Dikhow, the Dhansiri (south), the Kopili and the Krishnai. Hydrological characteristics of 18 important north bank tributaries and 10 important south bank tributaries are presented in Table 4.2.

It is observed that three Trans-Himalayan tributaries, the Subansiri, the Jia Bhareli and the Manas on the north have a basin more than 10,000 km², i.e., only two south bank tributaries namely the Dhansiri and the Kopili form a basin area more than 10,000 km². The Manas river combined with the Aie and the Beki rivers drains biggest area of 41, 350 km².

The 442 km long Subansiri river and the 360 km long Burhi Dehing river are considered longest, respectively, among the north-bank and south bank tributaries (Water Year book, CWC, 2002). In terms of the average annual discharge, the Subansiri carries a discharge of 755,771 m³/sec, which ranks first among all the important tributaries. The Jia Bhareli and the Manas in the north carrying an average annual suspended sediment load of 2,013 ha.m and 2,166 ha.m, respectively, are the leading rivers in the case of sediment discharge (59). Of all the north and south bank tributaries, as many as fourteen have sediment yields in excess of 500 tons/ km²/year, the highest being 4,721 tons/km² /year.

4.5 THE TRIBUTARIES OF THE BRAHMAPUTRA RIVER

In the past, the Dibang and the Lohit, two major rivers joined the Dihang a short distance upstream of Kobo to form the Brahmaputra. Now, the situation has undergone a radical change. Dibang and Lohit joined Dihang through another channel Dibru, developed through phenomenon river avulsion. Dibru is receiving major part of the discharge of Lohit for the last few years. The river receives numerous tributaries from both sides all along its course, thereby progressively growing in its size. Some of the tributaries are trans-Himalayan rivers with considerable discharges. In the north, the principal tributaries are the Subansiri, the Jia Bhareli, the Dhansiri (north), the Puthimari, the Pagladiya, the Manas, the Champamati. On the south bank the main tributaries are the Burhi Dehing, the Disang, the Dikhow, the Dhansiri (south) and the Kopili. The Brahmaputra also has some important tributaries, like the Teesta, the Jaldhaka, the Torsa, the Kaljani and the Raidak flowing through North Bengal.

The important tributaries on both the north and the south bank of Brahmaputra are listed in Table 4.3 along with chainage in km of their present outfalls from Indo Bangladesh border. The position of the outfall changes whenever bank erosion takes place there. Besides these tributaries, there are many other small streams which drain directly into the river.

Certain fluvio-geomorphic features which are found in the Brahmaputra basin have a significant bearing on the characteristics of the north and south bank tributaries. The variations in environmental settings, including geology, geomorphology, physiography, relief, precipitation and soils of the two regions belonging to the north bank and south bank river basins bring about notable differences between these two groups of rivers. On the north, the rainfall is heavier and the hills are less stable and more liable to soil erosion and landslides. In consequence, the north bank tributaries carry larger silt charge. The

characteristics of north bank and south bank tributaries (173) reveal the following points of differences -

4.5.1 The North Bank Tributaries

- (i) The north bank tributaries have higher rainfall and pass through the Himalayan reaches with steep channel gradient.
- (ii) In case of northern tributaries, the long section of river course is in the hilly terrain while the small section is in the plains.
- (iii) The northern tributaries carry an enormous sediment load as compared to the southern tributaries. On an average, the sediment yield of the north-bank tributaries is three times higher than that of the south bank tributaries coming out of the Naga, Mikir hills and the Meghalaya plateau (173).
- (iv) Due to steep slope and heavy sediment load, these streams are braided over major portion of their travel. These have shallow braided channels for a considerable distance from the foot of the hill and in some cases right up to the outfall.
- (v) The northern tributaries have generally coarse sandy beds with occasional gravel beds up to some distance from the foothills.
- (vi) These tributaries generally have flashy floods.
- (vii) The basins of all the north bank tributaries have hypsometric curves with a plateau indicating a relatively youthful stage in their development.
- (viii) The north bank tributaries show a general parallel drainage pattern.
- (ix) The northern tributaries have shallow braided channels.
- (x) The northern tributaries are characterized by frequent shifting of their channels during floods. As revealed by the study, the northern tributaries have peculiar channel shifting patterns. The Subansiri and all other eastern rivers shift their channels westward, while the rivers between the Pagladiya and Subansiri shift eastwards. Again from the Manas up to the river Sonkosh in the west, all the rivers migrate westward.

4.5.2 The South Bank Tributaries

- (i) These tributaries have comparatively flatter gradient and deep meandering channels almost from the foot hills.
- (ii) The southern tributaries have beds & banks composed of fine alluvial soils.
- (iii) The southern tributaries have their long courses over the plains.
- (iv) These tributaries have comparatively less silt charge with finer fractions.

- (v) In contrary to the north bank basins, the basins of the tributaries from the south bank indicate much mature stage with hypsometric curves showing a continuously decreasing profile.
- (vi) The south bank tributaries while keeping the parallel drainage pattern, show signs of dendritic configuration.
- (vii) The southern tributaries change their courses less frequently.
- (viii) The southern ones have their meandering channels over the plains.

4.6 HYDROLOGICAL CHARACTERISTICS OF SOME MAJOR TRIBUTARIES

The hydrological characteristics such as basin area, length, average annual discharge, average annual suspended load and the sediment yield of some major tributaries are outlined in Table 3.2 (173).

Table 4.2 Hydrological characteristics of some major tributaries

Tributaries	Basin Area (Km²)	Length (Km)	Average annual discharge (m³/sec)	Average annual suspended load (ha. m)	Sediment yield (ton/ Km² /year)
Northern Tributaries					
1. Subansiri	28,000	442	755,771	992	959
2. Ranganadi	2,941	150	74,309	186	1,598
3. Burai	791	64	20,800	16	529
4. Bargang	550	42	16,000	27	1,749
5. Jia Bhareli	11,716	247	349,487	2013	4721
6. Gabhru	577	61	8450	11	520
7. Belsiri	751	110	9300	9	477
8. Dhansiri (North)	1,657	123	26,577	29	463
9. Noa Nadi	907	75	4450	6	166
10. Nanoi	860	105	10,281	5	228
11. Bamadi	739	112	5756	9	323
12. Puthimari	1,787	190	26,324	195	2,887

13. Pagladiya	1674	197	15201	27	1,883
14. Manas-Aie-Beki	41,350	215	307,947	2,166	1,581
15. Champamati	1,038	135	32,548	13	386
16. Gaurang	1379	98	22,263	26	506
17. Tipkai	1,364	108	61,786	31	598
18. Gadadhar	610	50	7,000	0.21	272
Southern Tributaries					
I. Burhi Dehing	8,730	360	1411,539	210	1,129
2. Disang	3,950	230	55,101	93	622
3. Dikhow	3,610	200	41,892	34	252
4. Jhanzi	1,130	108	8,797	16	366
5. Bhogdoi	920	160.	6072	15	639
6. Dhansiri (South)	10,242	352	68,746	147	379
7. Kopili	13,556	297	90,046	118	230
8. Kulsi	400	93	11,643	0.6	135
9. Krishnai	1,615	81	22,452	10	131
10. Jinari	594	60	7,783	3	96

**Table 4.3 Tributary distances measured from Indo-Bangladesh border
(Along the upstream) (WAPCOS, 1993)**

Sl. No	North Bank Tributaries	Chainage in km.
1.	Simen	580
2.	Jiyadhol	540
3.	Subansiri	430
4.	Burai	392
5.	Bargang	382
6.	Jia Bhareli	338
7.	Gabhru	300
8.	Belsiri	280
9.	Dhansiri	270
10.	Noa Nadi	230
11.	Nanai Nadi	215

12.	Bar Nadi	205
13.	Puthimari	172
14.	Pagladiya	170
15.	Beki	115
16.	Manas	85
17.	Champamati	63
18.	Gaurang	43
19.	Tipkai	40
20.	Sankosh	0
Sl. No	South Bank Tributaries	Change in km
1.	Dibru	592
2.	Burhi Dehing	540
3.	Disang	515
4.	Dikhow	505
5.	Jhanzi	495
6.	Dhansiri (south)	420
7.	Kopili	220
8.	Kulsi	140
9.	Deosila	130
10.	Dudhnai	108
11.	Krishai	107
12.	Jinari	100
13.	Jinjiram	0

4.7 HYDROLOGIC AND PHYSIOGRAPHIC CHARACTERISTICS OF THE BRAHMAPUTRA RIVER

The hydraulic characteristics describing the average annual runoff of the Brahmaputra and its major tributaries are represented in Fig. 3.2 a schematic diagram. The statistical details of the river are described below:

- (a) Total basin area from its source to its confluence with Ganga at Goalundo
in Bangladesh 580,000 km²

(i)	Basin area within Tibet	293,000 km ²
(ii)	Basin area in Bhutan and India	240,000 km ²
(iii)	Basin area in Bangladesh	47,000 km ²
(b)	Length from its source to outfall in Bay of Bengal	2,880 km
	(i) Length within Tibet	1,625 km
	(ii) Length within India	918 km
	(iii) Length within Bangladesh	337 km
(c)	Gradient	
	(i) Reach within Tibet	1 in 385
	(ii) Reach between Indo-China border and Kobo in India	1 in 515
	(iii) Reach between Kobo and Dhubri	1 in 6,990
	(iv) Reach within Bangladesh First 60 km from Indian Border	
	1 in 11,340	
	Next 100 km stretch	1 in 12,360
	Next 90 km stretch	1 in 37,700
(d)	Observed discharge	
	(i) Maximum observed discharge at Pandu (on 23.8.1962)	72,727 m ³ /sec
	(ii) Minimum observed discharge at Pandu (on 20.2.1968)	1,757 m ³ /sec
	Average dry season discharge at Pandu	4,420 m ³ /sec
(e)	Normal annual rainfall within basin ranges between 2,125 mm in Kamrup district of Assam and 4,142 mm in Tirap district of Arunachal Pradesh.	

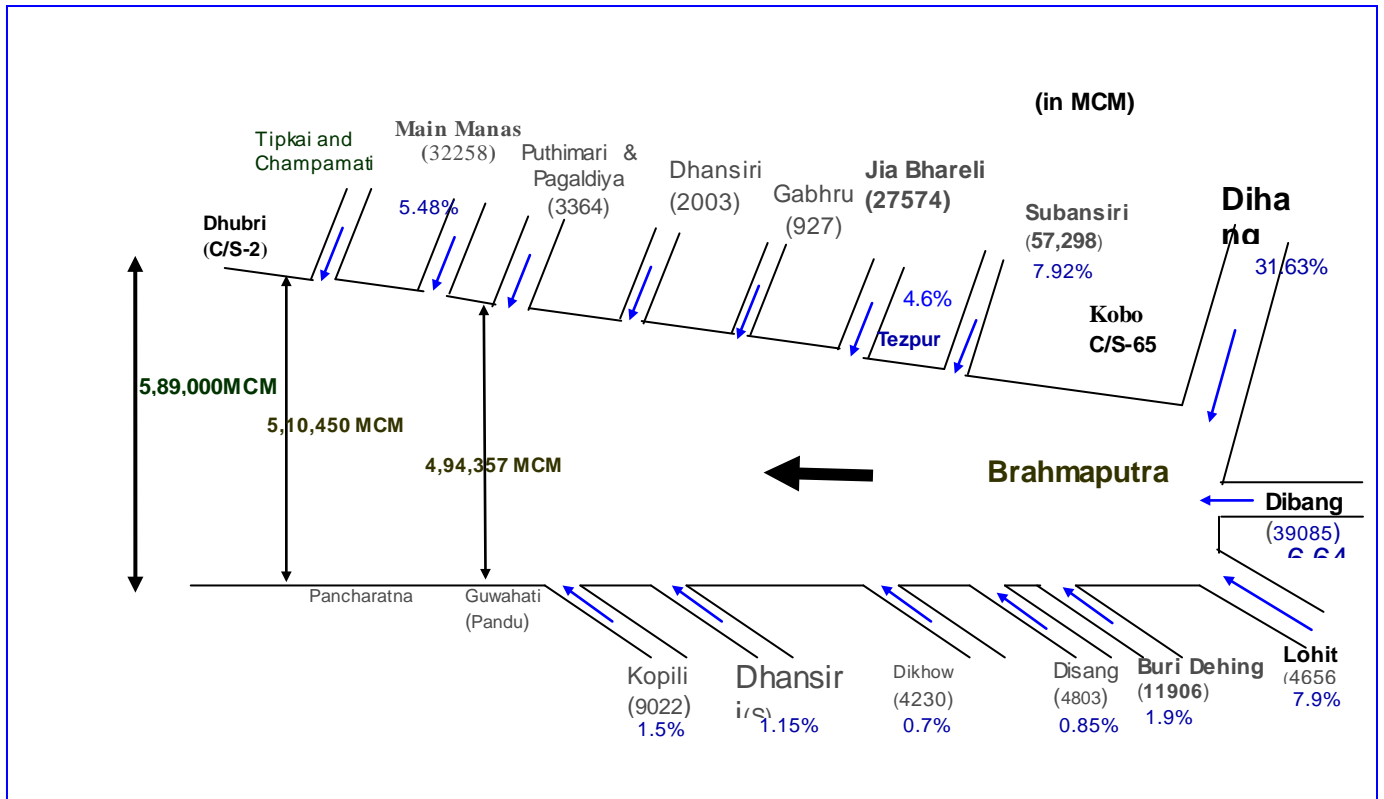


Fig. 4.2 Average Annual Runoff of the Brahmaputra and its Tributaries

High variability in discharge of the river is mainly caused by seasonal rhythm of the monsoon and the freeze-thaw cycle of the Himalayan snow. As regards the pattern of sediment transport, the river has the record of carrying excessive sediment load which is believed to be one of the important factors responsible for braiding.

4.8 THE STUDY AREA

In the present study, For the rating curve modelling, three gauging sites, two on the main stem of the brahmaputra River, namely Pandu and Panchratna and one at the outlet of the biggest northern tributary (Subansiri River), namely, Choulduaghat have been considered. For rainfall-runoff and sediment runoff modelling in a sub basin, the Subansiri River basin has been taken up a the study area (Fig. 4.3).

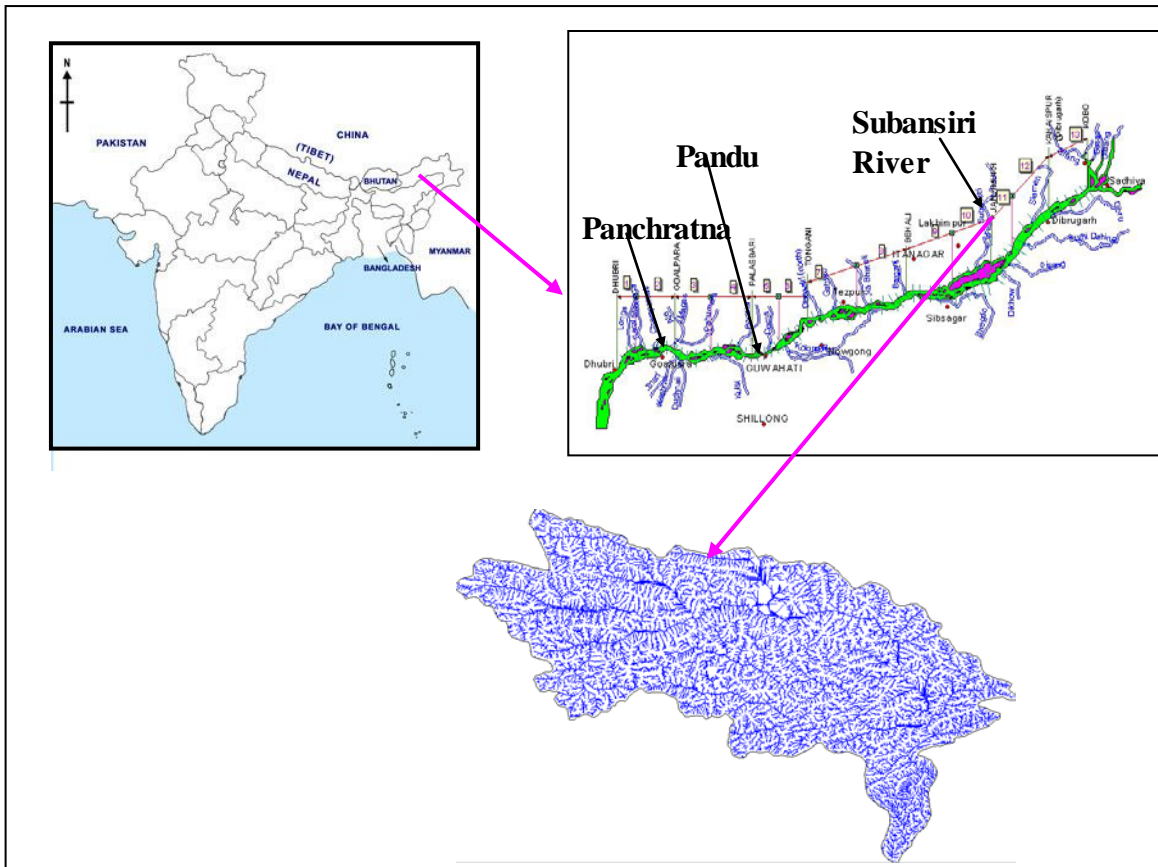


Fig. 4.3: Study Area

4.8.1 Rainfall in Subansiri River

Major portion of rainfall in Arunachal Pradesh occurs in monsoon season of June to September and heavy precipitation is generally limited to South-Western parts. The southern part receives a seasonal rainfall of 50mm to 3000mm. The average annual rainfall of subansiri basin is 2150 mm.

4.8.2 Stream-flow and River Gauges on Subansiri

River gauges have been established since 1956 on Subansiri River system. There are at present four gauge stations. Daily flow at Choulduaghat and at lower Subansiri dam site are available from 1956 and 1977 respectively. The data of Choulduaghat are pertinent to this study.

4.8.3 Sediment Load in Subansiri Basin

The sub-Himalayan range of Subansiri generally consists of soft sandstones and weathered rocks. Land formation of the catchment having steep slope and shallow braided channels, therefore, carries heavy charge of coarse sediment particles of sizes 0.2 mm dia upto 2 mm dia in suspension.

Due to granulometric characteristics of the soils present in this river basin, their density of deposition and coverage is guided by the energy potentialities of the flood volume based on the runoff. As the precipitation is intensive during the period May to October and the grade of flowing surface being a steep one, sediment deposits at areas nearer to and along the foot hills are heavier materials and debris such as boulders and shingles and towards the lower portions of the catchment they are of porous detritus materials such as fine sands and silt.

Daily suspended sediment load data at Choulduaghat site is available from 1974 onwards.

4.9 DATA USED

- **Hydrological data:** Daily stage, discharge and sediment concentration at Pandu, Panchratna and Choulduaghat for 10 years from 1997 to 2006
- **Meteorological data:** Daily rainfall at Daporizo, Ziro, Bomdilla, Bhalukpong, Choulduaghat, Badatighat, North Lakhimpur for three years from 2003-2005. Daily average temperature at one grid point within the Subaasiri basin for three years from 2003-2005.

Chapter – 5



Methodology

In recent years ANNs have shown exceptional performance as regression tools, especially when used for pattern recognition and function estimation. They are highly non-linear, and can capture complex interactions among the input variables in a system without any prior knowledge about the nature of these interactions (Hammerstrom, 1993). The main advantage of ANNs is that one does not have to explicitly assume a model form, which is a prerequisite in conventional modeling approaches. Indeed, in ANNs the data points themselves generate a relationship of possibly complicated or orthodox shape. In comparison to the conventional methods, ANNs tolerate imprecise or incomplete data, approximate results, and are less vulnerable to outliers (Haykin, 1994). They are highly parallel i.e. their numerous independent operations can be executed simultaneously. Although application of ANN approach in water resources is recent and limited, it has already produced very encouraging results.

In the present study, various ANN models have been developed for simulating the sediment concentration of the Pranhita sub-basin at six gauging sites. In this chapter, the methodology of ANN models development has been described. First various aspects of ANN modeling are discussed. Then some salient features of the software used are described and then the steps followed for the implementation of the ANN sediment concentration models using the software are given.

5.1. VARIOUS ASPECTS OF ANN MODELING

There are no fixed rules for developing an ANN, even though a general framework can be followed based on previous successful applications in engineering.

Some issues that typically arise while developing an ANN are briefly described in this section.

5.1.1. Selection of Input and Output Variables

The goal of an ANN is to generalize a relationship of the form

$$Y^m = f(X^n) \quad \dots(5.1)$$

Where X^n is an n -dimensional input vector consisting of variables $x_1, \dots, x_i, \dots, x_n$; and Y^m is an m -dimensional output vector consisting of resulting variables of interest $y_1, \dots, y_i, \dots, y_m$. We use the term “generalize” to imply that the functional form of $f(\cdot)$ in Eq. 6.1 to Eq.6.6 will not be revealed explicitly, but will be represented by the network parameters. In hydrology, the values of x_i can be causal variables such as rainfall, temperature, previous flows, water levels, spatial locations, evaporation, basin area, elevation, slopes, pump operating status, contaminant loads, meteorological data, and so on. The values of y_i can be hydrological responses such as runoff, streamflow, ordinates of a hydrograph, optimal pumping patterns, rain fields, hydraulic conductivities, contaminant concentrations, and others.

The selection of an appropriate input vector that will allow an ANN to successfully map to the desired output vector is not a trivial task. Unlike physically based models, the sets of variables that influence the system are not known a priori. In this sense of nonlinear process identification, an ANN should not be considered as a mere black box. A firm understanding of the hydrologic system under consideration is an important prerequisite for successful application of ANNs. For instance physical insight into the problem being studied can lead to better choice of input variables for proper mapping. This will help in avoid loss of information that may result if key input variables are omitted, and also prevent inclusion of spurious inputs that tend to confuse the training process. A sensitivity analysis can be used to determine the relative importance of a variable (Maier and Dandy 1996) when sufficient data is available. The input variables that do not have a significant effect on the performance of an ANN can be trimmed from the input vector, resulting in a more compact network.

5.1.2. Collecting and Preprocessing Data

Most hydrologic data are obtained from gauges that are placed on site or through remote sensing instruments. Also, either an existing or laboratory experiments can be used to generate the data patterns for specific applications (French *et al.* 1992; Ranjithan *et al.* 1993; Rogers and Dowla 1994; Smith and Eli 1995; Minns and Hall 1996). Again, there appears to be no fixed method for determining the number of input-output data pairs that will be required. To ensure a good approximation, Carpenter and Barthelemy (1994) stated that the number of data pairs used for training should be equal to or greater than the number of data parameters (weights) in the network. An optimal data set should be representative of the probable occurrence of an input vector and should facilitate the mapping of the underlying

nonlinear process. Inclusion of unnecessary patterns could slow network learning. In contrast, an insufficient data set could lead to poor learning. This makes it useful to analyze and preprocess the data before it is used for ANN application. Routine procedures such as plotting and examining the statistics are sometimes effective in judging the reliability of the data and possibly to remove outliers. In many cases, the data needs to be encoded, normalized, or transformed before being applied to an ANN.

5.1.3. Designing the ANN

This is important step, involves the determination of the ANN architecture and selection of a training algorithm. An optimal architecture may be considered the one, yielding the best performance in terms of error minimization, while retaining a simple and compact structure. No unified theory exists for determination of such an optimal ANN architecture. Often, more than one ANN can generate similar results. The numbers of input and output nodes are problems dependent. They are equal to n and m in Eq. 5.1, the flexibility lies in selecting the number of hidden layers and in assigning the number of nodes to each of these layers. A trail-and-error procedure is generally applied to decide on the optimal architecture. As discussed earlier, the cascade-correlation-training algorithm is an efficient method to find the optimal architecture.

The potential of feed-forward neural networks can be attributed to three main factors (Kothari and Agyepong 1996): (1) multilayered feedforward neural networks do not need an explicit mathematical equation relating inputs and outputs; (2) a feedforward network with a single hidden layer with an arbitrary number of sigmoidal hidden nodes can approximate any continuous function; and (3) a feedforward network with a single hidden layer of 'm' sigmoidal nodes achieves an integrated squared error of $O(1/m)$ while a linear combination of a set of 'm' fixed basis functions achieves an integrated squared error of $O(1/m^{2/d})$, where 'd' is the dimension of the input (Barron 1993). Points 1 and 3 above refer to computational superiority of feedforward ANN, while 2 hints to an existence theorem that establishes the capabilities of a feedforward ANN. It does not, however, allow for a systematic determination of the number of hidden nodes to use in a given situation. The number of hidden layer neurons significantly influences the performance of a network; with too few nodes the network will approximate poorly, while with too many nodes it will overfit the training data.

The influence of the size of a neural network on its generalization performance is well known (Baum and Haussler 1989; Kothari and 1997 Agyepong). Bishop (1995) provides

an excellent review of proposed approaches that allow the determination of network architecture with acceptable performance on the training and generalization data. Some of the popular techniques include network growing (e.g., Gallant 1986; Nadal 1989; Fahlman and Lebiere 1991; Bose and Garga 1993; Kwok and Yeung 1995) and network pruning (e.g., Mozer and Smolensky 1989; Karnin 1990; LeCun *et al.* 1990; Hassibi and Stork 1993; Reed 1993). These algorithms treat the network structure as an optimization parameter along with the weights. Pruning algorithms generally start with a large network and proceed by removing weights to which sensitivity of the error is minimal. Growing methods, on the other hand, typically start with a small network and add nodes with full connectivity to nodes in the existing network when a suitably chosen measure (e.g., entropy, covariance, etc.) stops decreasing. An alternative to these methods is called soft weight sharing (Nowlan and Hinton, 1992), where groups of weights are encouraged to have equal values, allowing for a reduction in the effective number of free parameters in the network. Soft weight sharing can train a large network with a small amount of training data (Agyepong and Kothari 1997); however, to ensure convergence to good solutions, proper initialization of the weights is necessary.

5.1.4. Training and Cross Training

This is similar to the idea of calibration that is an integral part of most hydrologic modeling studies. The available data set is generally partitioned into three parts for training, cross training, and validation. The purpose of training is to determine the set of connection weights and nodal thresholds that cause the ANN to estimate outputs that are sufficiently close to target values. The dataset reserved for training is used to achieve this goal. This fraction of the complete data to be employed for training should contain sufficient patterns so that the network can mimic the underlying relationship between input and output variables adequately. The weights and threshold values are assigned small random values initially (usually, $-0.3 \sim 0.3$). During training, these are adjusted based on the error, or the difference between ANN output and the target responses. This adjustment can be continued recursively until a weight pace is found, which results in the smallest overall prediction error. However, there is the danger of overtraining a network in this fashion, also referred as over fitting. This happens when the network parameters are too fine-tuned to the training data set.

It is as if the network, in the process of trying to “learn” the underlying rule, has started trying to fit the noise component of the data as well. In other words, overtraining results in a network that memorizes the individual examples, rather than trends in the data set

as a whole. When this happens, the network performs very well over the data set used for training, but shows poor predictive capabilities when supplied with data other than the training patterns. To prevent this kind of over fitting, a cross training procedure is usually recommended. The goal of this procedure is to stop training when the network begins to overtrain. The second portion of the data is reserved for this purpose. After the adjustment of network parameters with each epoch, the network is used to find the error for this data set. Initially, errors for both the training and cross training data sets go down. After an optimal amount of training has been achieved, the errors for training set continue to decrease, but those associated with the cross training data set begin to rise. This is indication that furthers training will likely result in the network over fitting the training data. The process of training is stopped at this time, and the current set of weights and thresholds are assumed to be the optimal values. The network is ready for use as a predictive tool. If the available data set is too small for partitioning, the simplest way to prevent overtraining is to stop training when the mean square error ceases to decrease significantly.

5.1.5. Model Validation

Similar to other modeling approaches in hydrology, the performance of a trained ANN can be fairly evaluated by subjecting it to new patterns that it has not seen during training. The performance of the network can be determined by computing the percentage error between predicted and desired values. In addition, plotting the model output versus desired response could also be used to assess ANN performance. Since finding optimal network parameters is essentially a minimization process, it is advisable to repeat the training and validation processes several times to ensure that satisfactory results have been obtained.

5.2. FEATURES OF ANN SOFTWARE - NEURAL POWER

The ANN software used in this study is Neural Power. Neural Power is an easy-to-use powerful Artificial Neural Network (ANN) program. With its user friendly interface, simple operation and highly efficient performance, most of general ANN problems can be handled with great results. Neural Power can be applied in following fields: multi-nonlinear regression, forecasting, curve fitting, pattern recognition, classification, decision making, problem optimization and time series analysis.

5.2.1. Neural Power is Suitable for:

- ◆ People who have to work or analyze data in any form.
- ◆ People working on problems that are complex, laborious, 'fuzzy' or simply unresolvable using present methods.
- ◆ People who simply want to improve on their current techniques and gain competitive advantage.

5.2.2. Features of Neural Power

- ◆ Multi-learning data files supported: almost all other similar software only one data file for the learning process. Sometimes, this is not enough for a real problem.
- ◆ Normal and grid data types supported: no other software supports "grid" data type learning.
- ◆ Visual and real time monitoring of learning process. Almost all aspects of network can be controlled in graphical mode, i.e. use any connection weight, and variations of RMSE.
- ◆ Visual design of network structures.
- ◆ Step-by-step learning.
- ◆ Support interrupting/suspending and resuming of learning process. Learning can start from a set of random weights specified by a user.
- ◆ Genetic Algorithms can be used as one of the learning algorithms.
- ◆ No limitation on hidden layer numbers and node number for each layer. Each layer can have different transfer functions.
- ◆ Includes six types of the most-often used transfer functions, in addition, customers can define functions of their own.
- ◆ Fast convergence of learning.
- ◆ Easy settlement for time series analysis.
- ◆ Abilities for optimal study and 2D-3D graphical analysis.
- ◆ Excel-like, multi-window data file editor enhanced by VB, Java and Delphi/Pascal script languages.
- ◆ Many very useful data analysis tools beyond neural network: create data chart, 2-D, 3-D function chart, curve fit with over 30 pre-defined functions, function/equation fit and equation solve.

5.2.3. System Requirements

Running the 32-bit version of Neural Power requires a minimum 486 processor and Window 95/98/2000/ME/XP or NT 4.0. A complete installation requires about 10 MB of hard disk space. 64 MB or high RAM is recommended.

There are three main procedures: “Data Files”, “Learning/Training” and “Applications” for being selected. The Data file editor provides a spreadsheet-like tool for easy pre-and post-processing of data. In addition, many extra jobs can be performed here also, i.e. charting, regression.

The Excel-style data file editor is mainly used for creating new or viewing/editing existed data files. Such data files will be used for either the learning/training process or for applications later. “InputSheet” is especially for input data entry of learning data; while “OutputSheet” is for output data corresponded. “ChartStore” is for chart store, view and edit. The chart can be created with the data either from input data or output data, or copy from result charts of Learning or Application procedures.

5.2.4. File Format

- ◆ Neural Power data file (.ogy): any numerical data or strings may be contained. However, if this file to be used for learning later, be sure no string data is contained within the file except for the column title. For string data, represent them by real values, for example, “1” for “True” and “0” for “False”.
- ◆ Excel file (.xls): Read/save MS Excel data file directly, without OLE linker. Data values only, all other information will be ignored. If there are more than two worksheets in “xls” file, only first two will be inputted.
- ◆ Lotus 1-2-3 file (.wks, .wk1) and Quattro Pro file (.wq1): Direct read without OLE.
- ◆ Comma-delimited text file (.csv, .txt): Save and load most general data file format. Reading data with separate of tab space, space, “.”, and “;” automatically; while saving data with separate of “;”.
- ◆ Dbase file (.dbf): Save and load popular desktop database directly.
- ◆ MS Access file (.mdb): Save and load another popular desktop database files through DAO.
- ◆ Neural Power network file (.par): Load Neural Power network file for viewing connection weight.

5.2.5. Learning/Training

The learning/training process shows that the free parameters of a neural network are adapted through observed data (data file). The objective is to obtain “Network Weights File” which will be used for “Application” later.

To start “learning”, one needs to load one or more data files (.ogy) initially. Multi-files are allowed in the meantime, if they are all for the same problem and have similar data structures. The files with “checked” will be used for learning; while, “Not checked” files are for testing/verification.

Data types are classified into two catalogs: “Normal Type” and “Grid Type”:

- ◆ Normal type: one pattern consists of the data placed in any row of the output sheet that correspond to the data in some row of input sheet. Within a data file, the pattern number is the same as the row number, and the row number in the output sheet must be identical with that in input sheet. If using a different data file and the same question, however, the row number can be various.
- ◆ Grid Type: all input data and output data in one file are considered as one pattern. Row numbers are not necessary identical between input and output. However the row and column number should be matched for different data file correspondence within the same problem, e.g. in input and output, respectively.

5.2.6. Learning Algorithm

There are five learning algorithm supported in Neural Power currently:

1. Incremental Back Propagation (IBP): the network weights are updated after presenting each pattern from the learning data set, rather than once per iteration. This is referred to as Standard Back Propagation, and is the most preferred algorithm for large data sets.
2. Batch Back Propagation (BBP): the network weights update takes place once per iteration, while all learning data pattern are processed through the network.
3. Quick Propagation (QP): Quick propagation is a heuristic modification of the back propagation algorithm. It's proved to be much faster than standard back-propagation for many problems.
4. Genetic Algorithm (GA): Genetic algorithm is employed to find optimal connections weights.
5. Levenberg-Marquardt Algorithm.

5.2.7. Connection Types

Two kinds of connections are in existence:

Multilayer normal feed-forward: A Multilayer Feed forward network consists of one or more layers. Each layer receives an input vector, which is either the external input vector or the output vector of the prior layer. The layers are placed in a linear order, so that the input to the first layer is the external input, the input to the second layer, if it exists, is the output of the first layer, and so on, with layers 2,3,..., receiving their inputs from the previous layer. The last layer in the sequence is the output layer; its output vector represents the network output. Every other layer besides the output layer is referred to as a “hidden” layer, because their activation is not externally visible. This is most commonly used and is generally recommended for most of the applications.

Multilayer full feed-forward: The Multilayer Full Feed Forward architecture is similar to Multilayer Normal Feed forward, expect for two differences. First, each layer is provided with the external input. Second, each layer receives input from every layer below it in the linear ordering. For example, if the network has 3 layers, the first one receives the input vector, as usual. The second one receives an input vector that is the concatenation of the input vector and the output of the first layer. The third layer receives inputs from the input vector, and the output vectors of both prior layers.

5.2.8. Transfer Functions

The transfer function denoted by $\xi(\mu_k)$, defines the output of a neuron in terms of the activity level at its input. Six commonly used functions are predefined as below:

- ◆ The Sigmoid function, ranged from 0 to 1, is defined as:

$$\xi(\mu_k) = 1/[1+\exp(-a\mu_k)]$$

- ◆ The Hyperbolic Tanh function, ranged from -1 to 1, is defined by:

$$\xi(\mu_k) = [1-\exp(-a\mu_k)]/[1+\exp(-a\mu_k)]$$

- ◆ The Gaussian function, ranged from 0 to 1, defined as:

$$\xi(\mu_k) = e^{(-a.\mu_k^2)}$$

- ◆ The Linear function: ranged from $-\alpha$ to $+\alpha$:

$$\xi(\mu_k) = a.\mu_k$$

- ◆ The Threshold Linear function: ranged from 0 to +1:

$$\xi(\mu_k) = 0 \text{ if } \mu_k < 0$$

$$\xi(\mu_k) = 1 \text{ if } \mu_k > 1$$

$$\xi(\mu_k) = \alpha\mu_k \text{ if } 0 \leq \mu_k \leq 1$$

- ◆ The Bipolar Linear function: ranged from -1 to +1:

$$\xi(\mu_k) = -1 \text{ if } \mu_k < -1$$

$$\xi(\mu_k) = 1 \text{ if } \mu_k > 1$$

$$\xi(\mu_k) = \alpha'\mu_k \text{ if } -1 \leq \mu_k \leq 1$$

where, α' is a parameter called “slope” of transfer functions.

5.2.9. Weight Editor

Default, connection weights will be started from random values. However, may be started learning with specified weight values by utilizing the weights editor.

5.2.10. Learning Parameters

In the “settlements” section, one can set parameters such as learning rate, momentum, screen update rate and stop criteria. All of those parameters may be modified at any time during learning.

5.2.11. Applications

In the application module, the network file (.par) obtained through the learning progress will be used for further analysis:

- ◆ Query/Forecasting
- ◆ Optimize analysis
- ◆ 2-D and 3-D analysis
- ◆ Error surface analysis
- ◆ Importance analysis

Before carrying out above analysis, a network file (.par) must be loaded firstly. Forecasting or verification can easily be done here. The data values can be either inputted directly or loaded from a data file. In the situation where the time series items are included in the output data series (recorded in Network file), and if you have input data values directly, the initial data must be inputted corresponding to the output items that contain the time series.

During the learning process, will be seen the observed data (red line) vs. calculated data (green line) for all output variables as the learning progresses.

5.3. DEVELOPMENT OF REGRESSION AND ANN MODELS FOR STAGE-DISCHARGE AND SEDIMENT-DISCHARGE CURVES IN BRAHMAPUTRA BASIN

5.3.1. Input Variables

The selection of training data that represents the characteristics of a catchment and meteorological patterns is extremely important in modeling. The training data should be large enough to contain the characteristics of the watershed and to accommodate the requirements of the ANN architecture. If the information included in the training data set is insufficient, an increase in the complexity of a network (i.e., an increase in the number of neurons or layers in a network) will not enable the network to generalize the patterns in the physical phenomena. To the contrary, an increase in the complexity of the models might mislead the modeler to overfit the training data and lead to poor forecasts (Tokar and Johnson, 1999).

The error back propagation ANN models used in the present study are basically static-feedforward ANNs, the most widely used ANN structures, but they lack feedback connections to effectively remember and handle the previous states of information. One way that information can be introduced in static-feedforward ANNs is to input a time delay pattern that constitutes the tapped delay line information. Therefore, this network must determine the input variables, output variables and the lag time of the basin before constructing rainfall-runoff-sediment processes in order to increase its accuracy. In general, the selection of input variables and output variables is problem dependent. The appropriate input variables will allow the network to successfully map to the desired output and avoid loss of important information. In the present study, the input dimensions are determined by the input variables and the lag time.

5.3.1.1 *Input variables for stage-discharge regression and ANN models*

The daily data of stage and discharge were available at the sites, namely Pandu (main Brahmaputra River), Panchratna (main Brahmaputra River) and Choulduaghat (Subansiri River) for ten years from January 1997 to December 2006. Out of this, six years data were used for training, two years data for testing and two years data for validation.

The output from the model is the discharge at time step t , Q_t . It has been shown by many authors that the current discharge can be mapped better by considering, in addition to the current value of stage, the discharge and stage at the previous times. Therefore, in addition to H_t , i.e., stage at time step t , other variables such as H_t , H_{t-1} , H_{t-2} , Q_{t-1} , Q_{t-2} were

also considered in the input. Various combinations of input data considered for training of ANN in the present study are given in Table 5.1. However, the input-output variables of ANNH-1 have been used for the conventional sediment rating curve analysis.

Table 5.1 Various ANN stage-discharge Models

ANN Model	Input Variables	Output Variables
ANNH-1	H_t	Q_t
ANNH-2	H_t, H_{t-1}, Q_{t-1}	Q_t
ANNH-3	$H_t, H_{t-1}, H_{t-2}, Q_{t-1}, Q_{t-2}$	Q_t
ANNH-4	$H_t, H_{t-1}, H_{t-2}, H_{t-3}, Q_{t-1}, Q_{t-2}, Q_{t-3}$	Q_t
ANNH-5	$H_t, H_{t-1}, H_{t-2}, H_{t-3}, H_{t-4}, Q_{t-1}, Q_{t-2}, Q_{t-3}, Q_{t-4}$	Q_t

Where Q=Discharge, H=Stage

5.3.1.2 Input variables for runoff-sediment regression and ANN models

The daily data of discharge and sediment concentration were available at the sites namely, Pandu (main Brahmaputra River), Panchratna (main Brahmaputra River) and Choulduaghat (Subansiri River) for ten years from January 1997 to December 2006. Out of this, six years data were used for training, two years data for testing and two years data for validation.

The output from the model is the sediment concentration at time step t , S_t . It has been shown by many authors that the current sediment concentration can be mapped better by considering, in addition to the current value of discharge, the sediment and discharge at the previous times. Therefore, in addition to Q_t , i.e., discharge at time step t , other variables such as Q_{t-1} , Q_{t-2} , and S_{t-1} , S_{t-2} , were also considered in the input. Various combinations of input data considered for training of ANN in the present study are given in Table 5.2. However, the input-output variables of ANNS-1 have been used for the conventional sediment rating curve analysis.

Table 5.2 Various ANN Runoff-Sediment Models

ANN Model	Input Variables	Output Variables
ANNS-1	Q_t	S_t
ANNS-2	Q_t, Q_{t-1}, S_{t-1}	S_t
ANNS-3	$Q_t, Q_{t-1}, Q_{t-2}, S_{t-1}, S_{t-2}$	S_t
ANNS-4	$Q_t, Q_{t-1}, Q_{t-2}, Q_{t-3}, S_{t-1}, S_{t-2}, S_{t-3}$	S_t
ANNS-5	$Q_t, Q_{t-1}, Q_{t-2}, Q_{t-3}, Q_{t-4}, S_{t-1}, S_{t-2}, S_{t-3}, S_{t-4}$	S_t

Where Q=Discharge, S=Sediment Concentration

5.3.2. Regression Models Using Conventional Techniques

Regression models have been developed for runoff-sediment modeling. Sediment rating curve analysis has been carried out for the six sites. These models have been calibrated, using six years data and then validated with two year data and again cross validated with remaining two+86 year data.

5.3.2.1 Rating curves for stage-discharge and runoff-sediment modeling

Rating curves are widely used to estimate the discharge vis-à-vis sediment load being transported by a river. A rating curve is a relation between the sediment and river discharge. Rating curves may be plotted showing average discharge/sediment concentration or load as a function of stage/discharge averaged over daily, monthly, or other time periods. Rating curves are developed on the premise that a stable relationship between discharge/sediment concentration and stage/discharge can be developed which, although exhibiting scatter, will allow the mean discharge/sediment yield to be determined on the basis of the stage/discharge history. A problem inherent in the rating curve technique is the high degree of scatter, which may be reduced but not eliminated. Discharge/Sediment Concentration does not necessarily increase as a function of stage/discharge.

Mathematically, a rating curve may be constructed by log-transforming all data and using a linear least square regression to determine the line of best fit. The log-log relationship

between Discharge(Q)/Sediment load (S) and Stage(H)/Discharge(Q) is of the form:

$$Q = a H^b \quad \dots(5.2)$$

$$S = c Q^d \quad \dots (5.3)$$

where , 'a', 'b', 'c' and 'd' are constants

5.4 DEVELOPMENT OF RAINFALL-RUNOFF AND SEDIMENT-RUNOFF ANN MODELS FOR SUBANSIRI RIVER BASIN

5.4.1 Input data and ANN model development for Rainfall-Runoff models

The daily data of discharge for ten years (1997-2006) were available at the Choulduaghat site which has been considered as the outlet of the basin for the present study. Daily rainfall data were available for three years (2003-2005) at Daporizo, Ziro, Bomdilla, Bhalukpong, Choulduaghat, Badatighat and North Lakhimpur. Daily average temperature at one grid point within the Subansiri basin for three years from 2003-2005 has been used. Similarly, three years of daily discharge data has also been used for ANN models development.

The output from the model is the runoff at time step t , Q_t . It has been shown by many authors that the current runoff can be mapped better by considering, in addition to the current value of rainfall and temperature, the rainfall, temperature and runoff at the previous times. Therefore, in addition to R_t , and T_t i.e., rainfall and temperature at time step t , other variables such as R_{t-1} , R_{t-2} , T_{t-1} , T_{t-2} , and Q_{t-1} were also considered in the input. Various combinations of input data were considered based upon a cross correlation of the data at various stations with varying lag time as given in Table 5.3. Based on the cross correlation, various ANN models considered for ANN training are given in Table 5.4.

5.4.2 Input data and ANN model development for Runoff-sediment models

The daily data of discharge and suspended sediment concentration for ten years (1997-2006) were available at the Choulduaghat site which has been considered as the outlet of the basin for the present study. Daily rainfall data were available for three years (2003-2005) at Daporizo, Ziro, Bomdilla, Bhalukpong, Choulduaghat, Badatighat and North

Lakhimpur. Daily average temperature at one grid point within the Subansiri basin for three years from 2003-2005 has been used. Similarly, three years of daily discharge and suspended sediment concentration data has also been used for ANN models development.

The output from the model is the sediment concentration at time step t , S_t . It has been shown by many authors that the current sediment concentration can be mapped better by considering, in addition to the current value of rainfall, temperature, runoff and the rainfall, temperature, runoff and sediment concentration at the previous times. Therefore, in addition to R_t , T_t and Q_t , i.e., rainfall, temperature and runoff at time step t , other variables such as R_{t-1} , R_{t-2} , T_{t-1} , T_{t-2} , Q_{t-1} , Q_{t-2} , and S_{t-1} were also considered in the input. Various combinations of input data were considered based upon a cross correlation of the data at various stations with varying lag time as given in Table 5.3. Based on the cross correlation, various ANN models considered for ANN training are given in Table 5.5.

Table 5.3: Cross Correlation of Data

	1	2	3	4	5	6	7	8	9	10	11	12	13	14	15	16	17
ZIRO	1																
ZIRO(t-1)	0.2838	1.0000															
ZIRO(t-2)	0.1156	0.2832	1.0000														
DAPORIJO	0.2864	0.1763	0.0618	1.0000													
DAPORIJO(t-1)	0.1729	0.2861	0.1762	0.2517	1.0000												
DAPORIJO(t-2)	0.0825	0.1724	0.2861	0.0847	0.2516	1.0000											
Bhalukpong(t-1)	0.3518	0.2053	0.1695	0.2969	0.2489	0.2089	1.0000										
Bhalukpong(t-1)	0.2199	0.3513	0.2052	0.1975	0.2967	0.2488	0.4183	1.0000									
BOMDILA	0.4551	0.3347	0.1498	0.2297	0.1804	0.1392	0.3946	0.2662	1.0000								
BOMDILA(t-1)	0.2566	0.4549	0.3346	0.1610	0.2295	0.1802	0.2226	0.3945	0.4069	1.0000							
BADATIGHAT	0.2834	0.2182	0.0839	0.1906	0.1470	0.1429	0.3313	0.2171	0.2534	0.1736	1.0000						
Choulduaghat	0.2788	0.2135	0.1061	0.3523	0.2252	0.1996	0.4444	0.2960	0.2371	0.2133	0.3809	1.0000					
N-LAKHIMPUR	0.2854	0.2228	0.1212	0.3279	0.2068	0.1340	0.4297	0.2908	0.2510	0.2060	0.4220	0.7039	1.0000				
Temp G1	0.2106	0.2070	0.1995	0.2385	0.2369	0.2365	0.3656	0.3688	0.2897	0.2984	0.2666	0.3694	0.3285	1.0000			
Temp G1(t-1)	0.2090	0.2087	0.2069	0.2357	0.2379	0.2368	0.3668	0.3656	0.2865	0.2891	0.2674	0.3725	0.3309	0.9838	1.0000		
Temp G1(t-1)	0.2050	0.2069	0.2086	0.2327	0.2351	0.2379	0.3703	0.3667	0.2816	0.2859	0.2618	0.3658	0.3298	0.9663	0.9837	1.0000	
Dis (Choudght)	0.2594	0.2666	0.2433	0.3425	0.3266	0.3094	0.4823	0.4764	0.3922	0.3772	0.2906	0.5395	0.4491	0.7191	0.7223	0.7255	1.0000

Table 5.4: Various ANN rainfall-runoff models

ANN Model	Input Variables	Output Variables
ANNR-1	R_t (Ziro, Daporizo, Bhalukpong, Bomdilla, Badatighat, Choulduaght)	Q_t
ANNR-2	R_t (Ziro, Daporizo, Bhalukpong, Bomdilla, Badatighat, Choulduaght), $T_t(G1)$	Q_t
ANNR-3	R_t (Ziro, Daporizo, Bhalukpong, Bomdilla, Badatighat, Choulduaght), R_{t-1} (Ziro), $T_t(G1)$	Q_t
ANNR-4	R_t (Ziro, Daporizo, Bhalukpong, Bomdilla, Badatighat, Choulduaght), R_{t-1} (Ziro), $T_t(G1)$, $T_{t-1}(G1)$	Q_t
ANNR-5	R_t (Ziro, Daporizo, Bhalukpong, Bomdilla, Badatighat, Choulduaght), R_{t-1} (Ziro), $T_t(G1)$, $T_{t-1}(G1)$, $T_{t-2}(G1)$	Q_t
ANNR-6	R_t (Ziro, Daporizo, Bhalukpong, Bomdilla, Badatighat, Choulduaght), R_{t-1} (Ziro), $T_t(G1)$, Q_{t-1} (choulduaghat)	Q_t

Table 5.5: Various ANN sediment-runoff models

ANN Model	Input Variables	Output Variables
ANNS-1	R_t (Ziro, Daporizo, Bhalukpong, Bomdilla, Badatighat, Choulduaght), Q_t (Choulduaghat)	S_t
ANNS-2	R_t (Ziro, Daporizo, Bhalukpong, Bomdilla, Badatighat, Choulduaght), $T_t(G1)$, Q_t (Choulduaghat)	S_t
ANNS-3	R_t (Ziro, Daporizo, Bhalukpong, Bomdilla, Badatighat, Choulduaght), R_{t-1} (Ziro), $T_t(G1)$, Q_t (Choulduaghat)	S_t
ANNS-4	R_t (Ziro, Daporizo, Bhalukpong, Bomdilla, Badatighat, Choulduaght), R_{t-1} (Ziro), $T_t(G1)$, Q_t (Choulduaghat), S_{t-1} (Choulduaghat)	S_t

5.5 ANN MODELS

5.5.1 TRAINING OF ANN MODELS

The training of various ANN models has been accomplished through the ANN software, namely, Neural Power (NPP 2.5, 2004). A back-propagation ANN with the generalized delta rule as the training algorithm has been employed in this study. The structure of the ANN models were three and four layer BPANN developed with non-linear sigmoid as activation function uniformly between the layers. Nodes in the input layer were equal to number of input variables, nodes in hidden layer were varied from the number of input nodes to approximately double of input nodes (Hipel, et al., 1994) and the nodes in the output layer was one as the models provide single output. Therefore, various ANN models were trained considering different hidden node numbers on a trial and error fashion and the best performing model has been reported in the results.

The learning of ANN initiates with the normalization (re-scaling) of all data with the maximum value of respective variable thus reducing the data domain in the range 0 to 1. This was accomplished through the software. All interconnecting links between nodes of successive layers were assigned random values called weight between +0.5 to -0.5 and a constant value of 0.15 and 0.8 was considered for learning rate ' η ' and momentum term ' α ' respectively. The quick propagation (QP) learning algorithm has been adopted for the training of all the ANN models. QP is a heuristic modification of the standard back propagation and is very fast (Neural Power, 2003). The network weights were updated after presenting each pattern from the learning data set, rather than once per iteration.

The criteria selected to avoid over training was generalization of ANN through cross-validation (Haykin, 1994). For this purpose, the data were divided into training, testing and validation sets. Training data (730/731 patterns) were used for estimation of weights of the ANN model and testing data (365/366 patterns) for evaluation of the performance of ANN model during training. Training was stopped when the error for the testing dataset started increasing. In this way, the training and testing datasets have been used to assess the performance of various candidate model structures, and thereby choose the best one. The particular ANN model with the best performing parameter values was chosen and the generalized performance of the resulting network has been measured on the validation data set (two years data) to which it has never before been exposed. The performance of the model was tested through the statistical criterion discussed in the following section.

5.5.2 Performance Evaluation Criteria

The statistical and hydrological evaluation criteria used in the present study are root mean square error (RMSE), correlation coefficient (R) and coefficient of efficiency (CE) or coefficient of determination (DC or R^2).

5.5.2.1 Root mean square error (RMSE)

It yields the residual error in terms of the mean square error expressed as (Yu, 1994)

$$\text{RMSE} = \sqrt{\frac{\text{residual variance}}{n}} = \left(\sum_{j=1}^n (Y_j - \hat{Y}_j)^2 / n \right)^{1/2} \quad \dots(5.4)$$

where, Y and \hat{Y} are the observed and estimated values respectively and n is the number of observations.

5.5.2.2 Correlation coefficient (R)

It is expressed as

$$R = \frac{\sum_{j=1}^n \left\{ (Y_j - \bar{Y}) (\hat{Y}_j - \bar{\hat{Y}}) \right\}}{\left\{ \sum_{j=1}^n (Y_j - \bar{Y})^2 \sum_{j=1}^n (\hat{Y}_j - \bar{\hat{Y}})^2 \right\}^{1/2}} \times 100 \quad \dots(5.5)$$

where, \bar{Y} and $\bar{\hat{Y}}$ are mean of observed and estimated values.

5.5.2.3 Coefficient of determination (DC)

Based on the standardization of residual variance with initial variance, the coefficient of determination can be used to compare the relative performance of the two approaches effectively (Nash and Sutcliffe, 1970). It is expressed as:

$$\begin{aligned} \text{DC} &= \left\{ 1 - \frac{\text{residual variance}}{\text{initial variance}} \right\} \times 100 \\ &= \left\{ 1 - \frac{\sum_{j=1}^n (Y_j - \hat{Y}_j)^2}{\sum_{j=1}^n (Y_j - \bar{Y})^2} \right\} \times 100 \quad \dots(5.6) \end{aligned}$$

The coefficient of determination is also commonly known as the coefficient of efficiency which may be written in a number of ways and represents the fraction of variance that is explained by regression. The closer this ratio is to unity, the better is the regression relation.

Chapter – 6



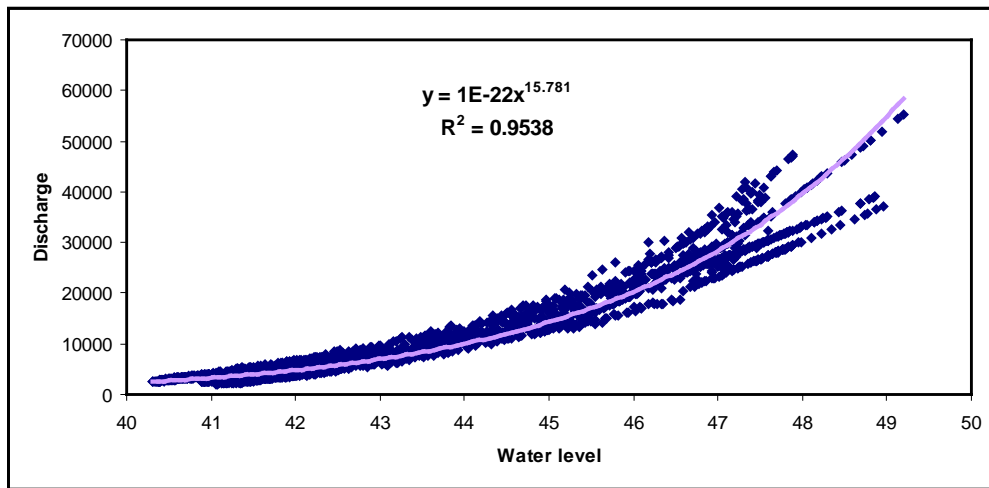
Results and Discussion

6.1 RUNOFF AND SEDIMENT MODELING BASED ON RATING CURVE TECHNIQUE

Based on the rating curve technique (Eq. 5.2) the equations for the three sites are given below:

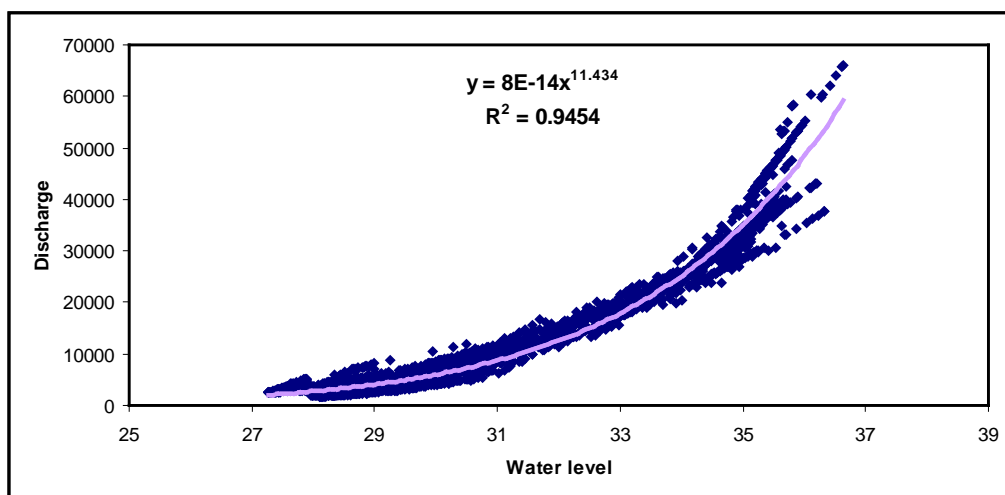
1. Stage discharge Rating Curve for Pandu site on Brahmaputra River

$$C=1.0 E-22Q^{16.781} \quad \dots(6.1)$$



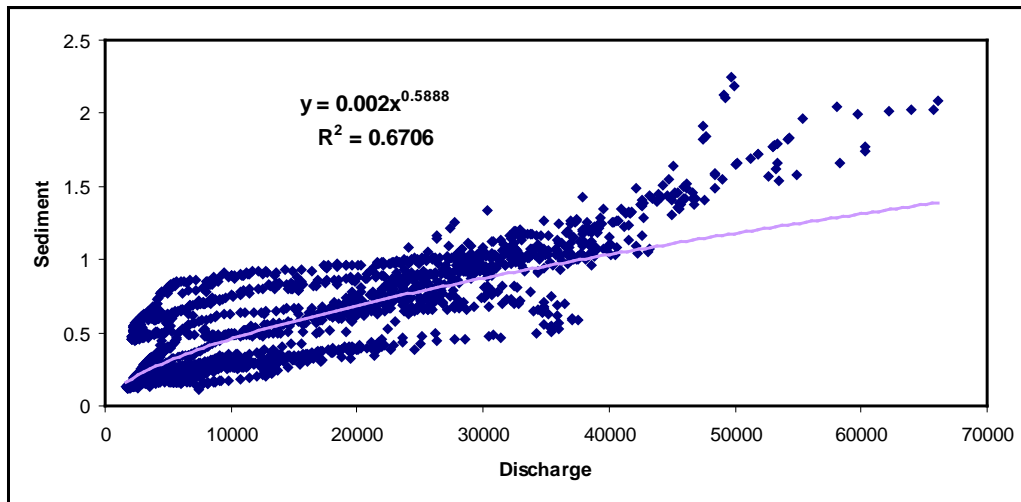
2. Stage discharge Rating Curve for Panchratna site on Brahmaputra River

$$C=8.0 E-14Q^{11.484} \quad \dots(6.2)$$



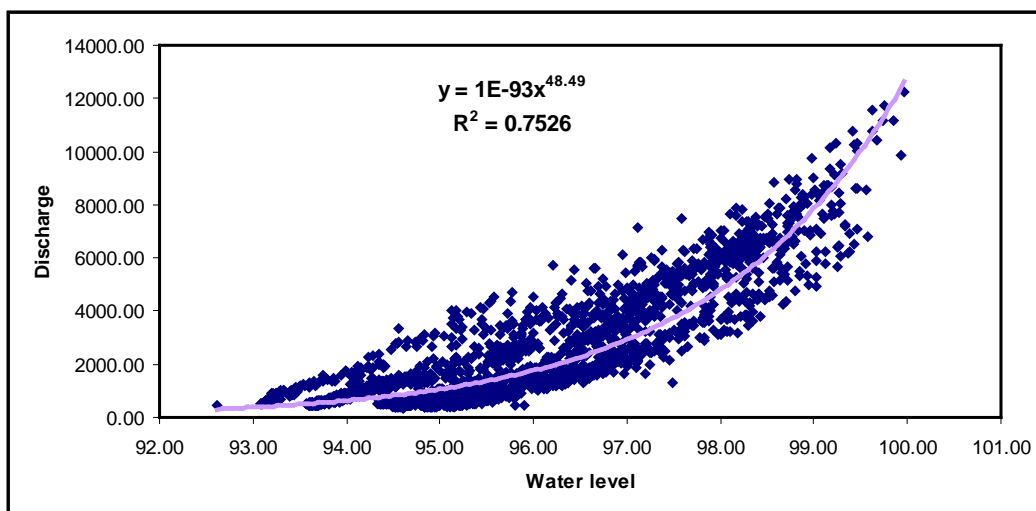
3. Sediment discharge Rating Curve for Panchratna site on Brahmaputra River

$$C=0.002Q^{0.6888} \quad \dots(6.3)$$



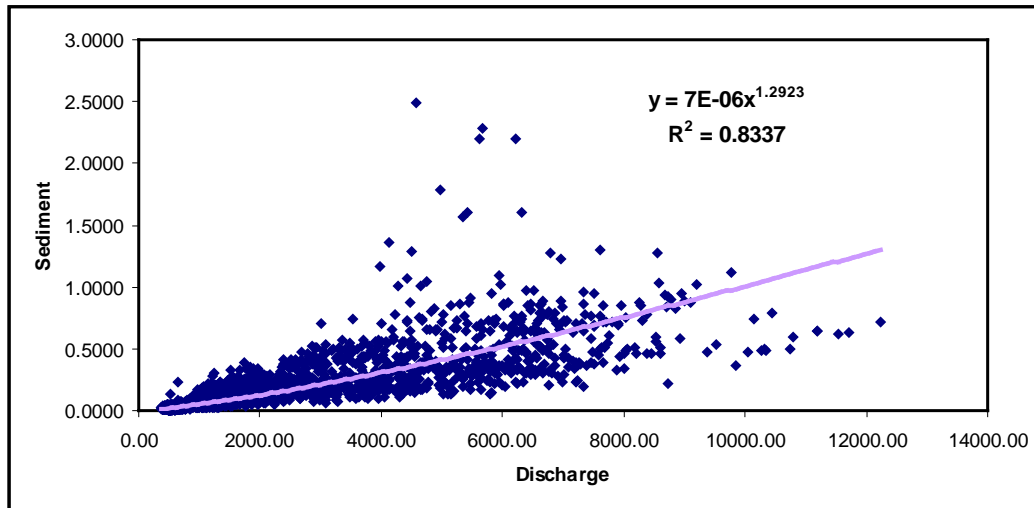
4. Stage discharge Rating Curve for Chouldhuaghat site on Subansiri River

$$C=1.0 E-93Q^{48.48} \quad \dots(6.4)$$



5. Sediment discharge Rating Curve for Chouldhuaghat site on Subansiri River

$$C=1.0 E-06Q^{1.2823} \quad \dots(6.5)$$



where, H = River stage in m.

S = Sediment Concentration in g/l

Q = Discharge in the river in Cumec

6.2 RATING CURVE MODELING BASED ON ANN TECHNIQUE

The statistical performances of various ANN models for all the three study gauging sites are summarized in Table 6.1 to Table 6.5. The tables show the comparative performance of all the models during training, testing and validation.

6.2.1 Stage discharge ANN Modeling for Pandu site on Brahmaputra River

The results are summarized in Table 6.1.

Table 6.1 Comparative performance of various stage discharge ANN models for Pandu site (Brahmaputra River)

ANN model	Training			Testing		Validation	
	RMSE	R	DC	R	DC	R	DC
ANNPH-1 (1-2-1)	2468.6	0.974	0.949	0.998	0.974	0.987	0.749
ANNPH-2 (3-2-1)	745.2	0.995	0.995	0.999	0.999	0.998	0.995
ANNPH-3	710.46	0.998	0.996	0.999	0.999	0.998	0.994

(5-4-1)							
ANNPH-4 (7-6-1)	676.85	0.998	0.996	0.999	0.999	0.997	0.995
ANNPH-5 (9-7-1)	654.29	0.998	0.996	0.999	0.999	0.997	0.995

It is observed from Table 6.1 that the RMSE values are generally low for all the ANN models. There are two candidate models in RMSE criteria, ANNPH2, i.e., ANN model with two hidden nodes and ANNPH4 model with three hidden nodes. In ANNPH2 model, the RMSE value is 745.2 during training. In ANN3 model, the RMSE value is 710.46 during training.

It can be seen from Table 6.1 that the correlation coefficient (R) values are very high (more than 0.90, i.e., 90%) for all the ANN models, during all the three phases, i.e., training, testing as well as validation. It is also observed that there is not much decrease in the R values during validation as compared to the training phase. The performance of ANNPH3 model is the best in R statistic. The R values for ANN are 0.998, 0.999 and 0.998 during training, testing and validation respectively. The increase in R values of ANNPH3 during validation indicates good generalization capability of the ANN model.

In the determination coefficient (DC) statistic, all the ANN models perform well. The DC values are fairly high (more than 0.90) for all models during all the three phases. In DC statistic also, ANNPH2 model performs the best. The DC values for ANN2 are 0.995, 0.999, and 0.995 during training, testing and validation respectively. There is not much decrease in the DC values during validation which indicate good generalization capability of the ANN models.

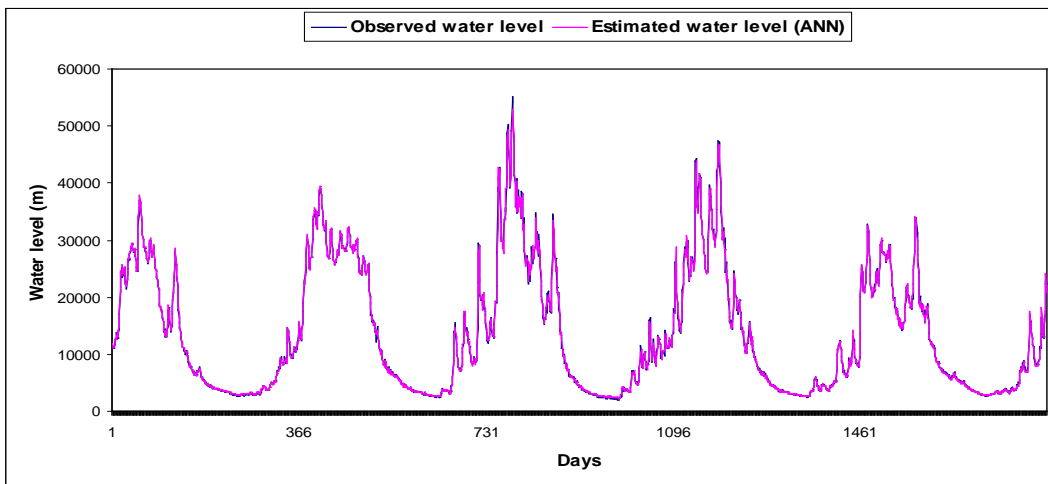
Therefore, ANN2 is the best performing model in all the three statistical and hydrological criteria. Fig. 6.1 presents the plots of observed and estimated discharge for ANN2 model during training (a), testing (b) and validation (c). It is observed from Fig 6.1 that there is very little mismatch between the observed and estimated discharge series for ANN2 model during all the three phases.

6.2.2 Stage Discharge Modeling for Panchratna site on Brahmaputra River

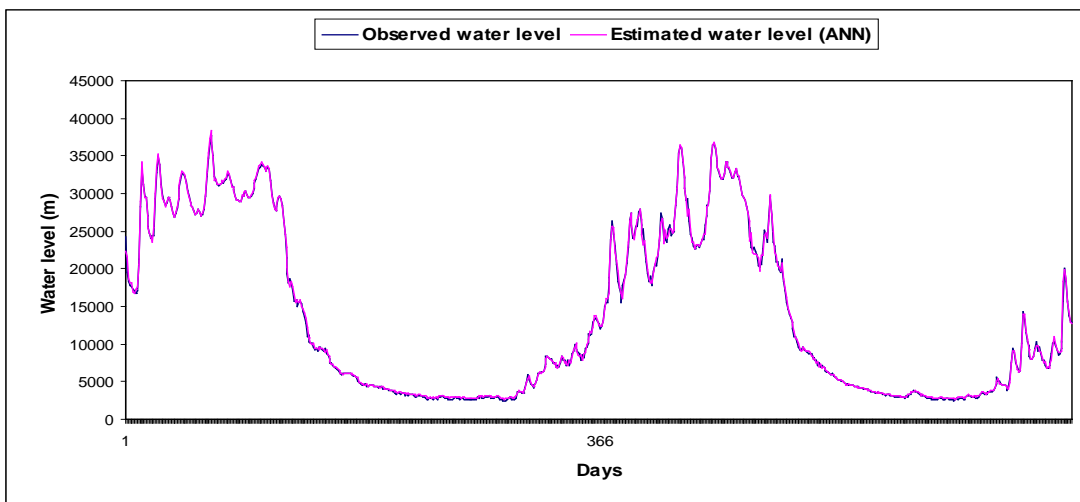
The results are summarized in Table 6.2.

Table 6.2 Comparative performance of various stage discharge ANN models for Panchratna site (Brahmaputra River)

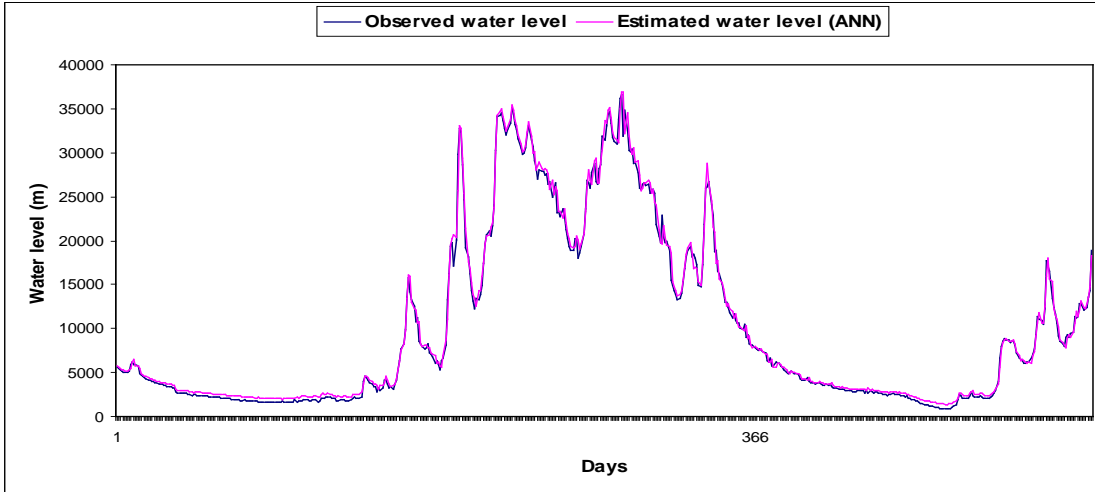
ANN model	Training			Testing		Validation	
	RMSE	R	DC	R	DC	R	DC
ANNPRH-1 (1-2-1)	2285.6	0.984	0.968	0.975	0.893	0.991	0.977
ANNPRH-2 (3-5-1)	1189.7	0.999	0.999	0.993	0.986	0.991	0.982
ANNPRH-3 (5-4-1)	853.71	0.998	0.998	0.997	0.992	0.996	0.991
ANNPRH-4 (7-6-1)	856.66	0.998	0.996	0.997	0.992	0.996	0.991
ANNPRH-5 (9-7-1)	857.52	0.998	0.996	0.997	0.991	0.996	0.991



(a) Training



(b) Testing



(c) Validation

Fig. 6.1 Comparative Performance of Observed Discharge with Estimated Discharge using ANNPH-2 at Pandu

It is observed from Table 6.2 that the RMSE values are generally low for all the ANN models. There are two candidate models in RMSE criteria, ANNPRH3, i.e., ANN model with four hidden nodes and ANNPRH4 model with six hidden nodes. In ANN3 model, the RMSE value is 853.71 during training. In ANN4 model, the RMSE value is 856.66 during training.

It can be seen from Table 6.1 that the correlation coefficient (R) values are very high (more than 0.90, i.e., 90%) for all the ANN models, during all the three phases, i.e., training, testing as well as validation. It is also observed that there is not much decrease in the R values during validation as compared to the training phase. The performance of ANNPRH3 model is the best in R statistic, the R values are 0.998, 0.997 and 0.996 during training, testing and validation respectively.

In the determination coefficient (DC) statistic, all the ANN models perform well. The DC values are fairly high (more than 0.90) for all models during all the three phases. In DC statistic also, ANNPRH3 model performs the best. The DC values for ANN2 are 0.998, 0.992, and 0.991 during training, testing and validation respectively. There is not much decrease in the DC values during validation which indicate good generalization capability of the ANN models.

Therefore, ANNPRH3 is the best performing model in all the three statistical and hydrological criteria. Fig. 6.2 presents the plots of observed and estimated discharge for ANN3 model during training (a), testing (b) and validation (c). It is observed from Fig 6.2

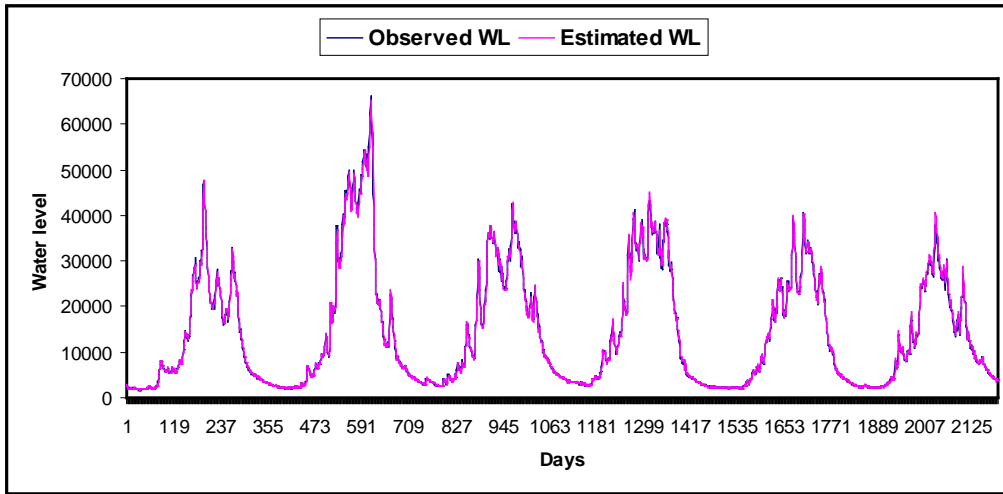
that there is very little mismatch between the observed and estimated discharge series for ANNPRH3 model during all the three phases.

6.2.3 Sediment discharge Modeling for Panchratna site on Brahmaputra River

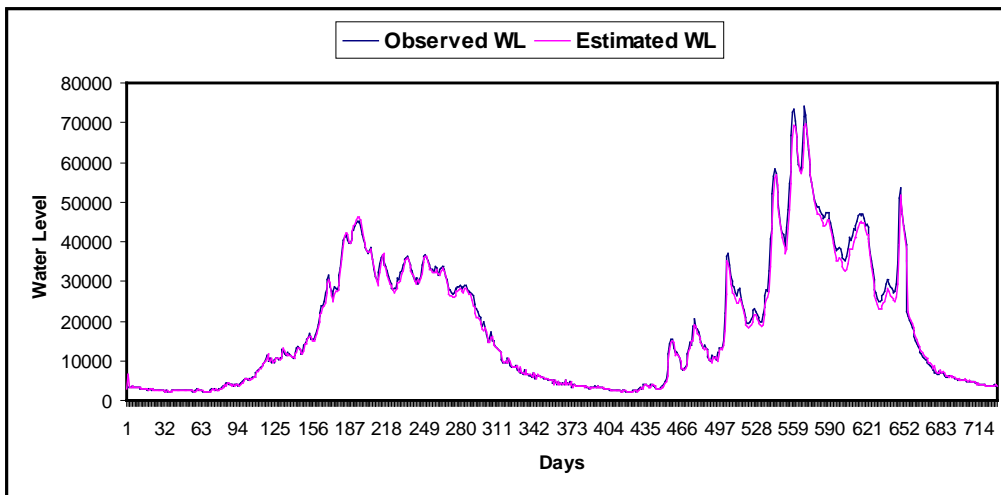
The results are summarized in Table 6.3.

Table 6.3 Comparative performance of various sediment-discharge ANN models for Panchratna site (Brahmaputra River)

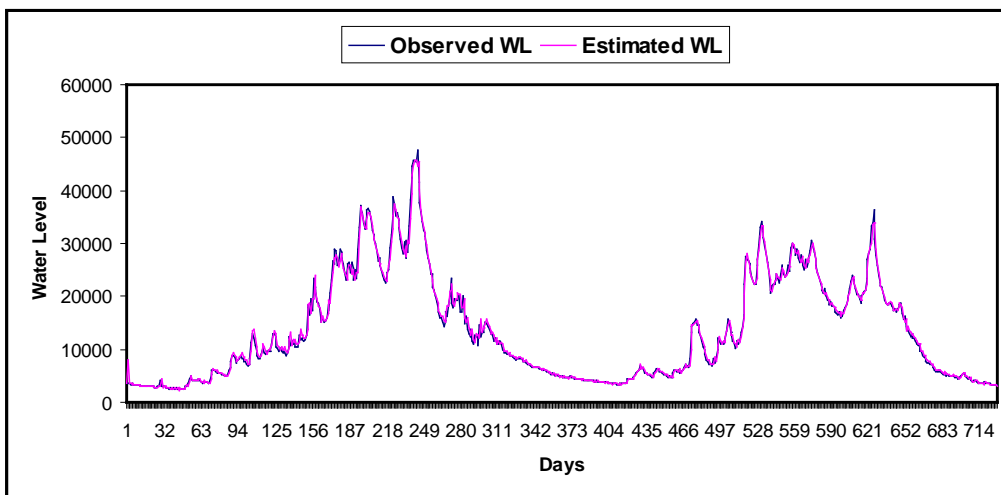
ANN model	Training			Testing		Validation	
	RMSE	R	DC	R	DC	R	DC
ANNPRS-1 (1-2-1)	0.1788	0.878	0.771	0.417	0.468	0.996	0.628
ANNPRS-2 (3-3-1)	0.0378	0.995	0.989	0.996	0.991	0.770	0.990
ANNPRS-3 (5-4-1)	0.0348	0.996	0.991	0.995	0.990	0.996	0.993
ANNPRS-4 (7-10-1)	0.0379	0.995	0.989	0.994	0.988	0.996	0.990
ANNPRS-5 (9-12-1)	0.0347	0.996	0.991	0.992	0.983	0.995	0.989



(a) Training



(b) Testing



(c) Validation

Fig. 6.2 Comparative performance of observed discharge with estimated discharge using ANNPRH-3 at Panchratna

It is observed from Table 6.3 that the RMSE values are generally low for all the ANN models. There are two candidate models in RMSE criteria, ANNPRS3, i.e., ANN model with four hidden nodes and ANNPRS5 model with six hidden nodes. In ANNPRS3 model, the RMSE value is 0.0348 during training. In ANNPRS5 model, the RMSE value is 0.0347 during training.

It can be seen from Table 6.3 that the correlation coefficient (R) values are very high (more than 0.90, i.e., 90%) for all the ANN models, during all the three phases, i.e., training, testing as well as validation. It is also observed that there is not much decrease in the R values during validation as compared to the training phase. The performance of ANNPRS3 model is the best in R statistic. The R values for ANN are 0.996, 0.995 and 0.996 during training, testing and validation respectively.

In the determination coefficient (DC) statistic, all the ANN models perform well. The DC values are fairly high (more than 0.90) for all models during all the three phases. In DC statistic also, ANNPRS3 model performs the best. The DC values for ANNPRS3 are 0.991, 0.990, and 0.993 during training, testing and validation respectively. There is increase in the DC values during validation which indicate good generalization capability of the ANN models.

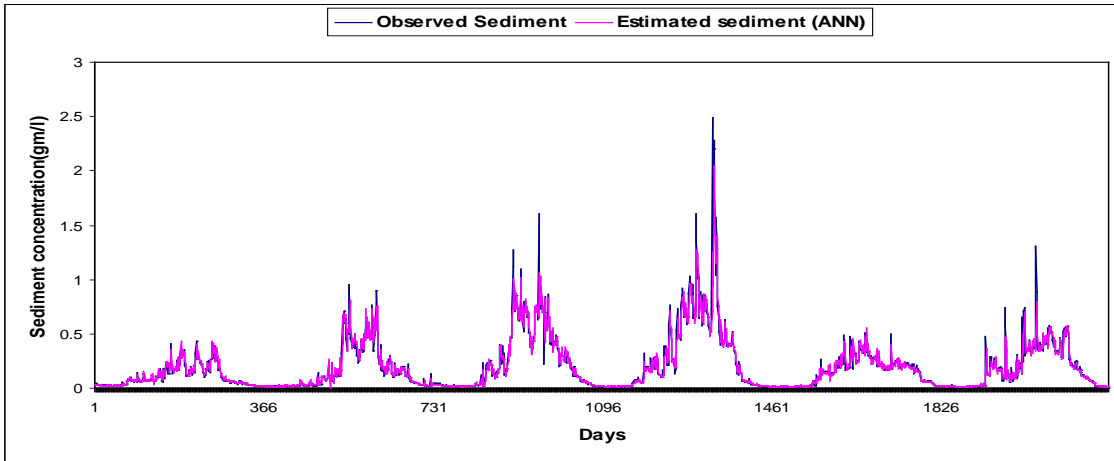
Therefore, ANNPRS3 is the best performing model in all the three statistical and hydrological criteria. Fig. 6.3 presents the plots of observed and estimated discharge for ANN3 model during training (a), testing (b) and validation (c). It is observed from Fig. 6.3 that there is very little mismatch between the observed and estimated discharge series for ANN2 model during all the three phases.

6.2.4 Stage discharge Modeling for Chouldhuaghat site on Subansiri River

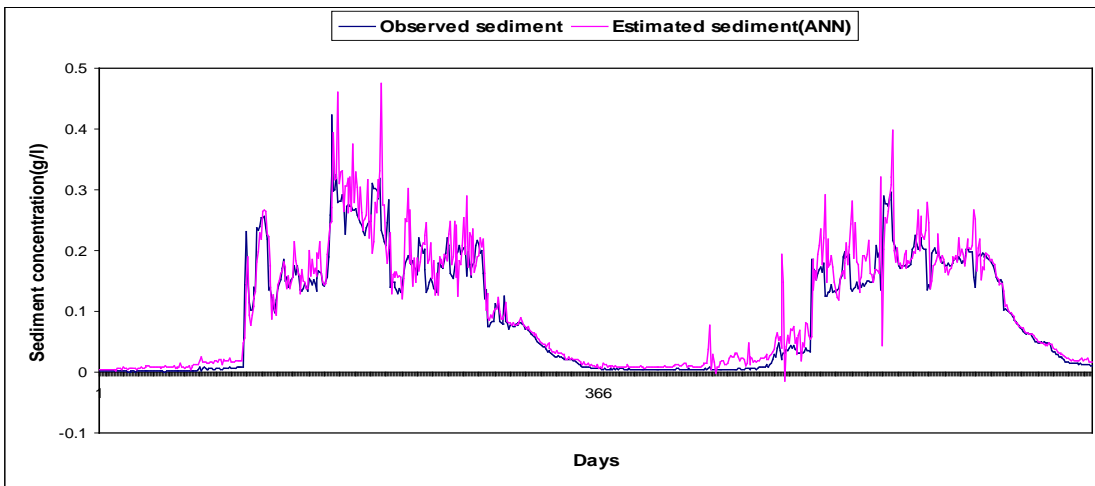
The results are summarized in Table 6.4.

Table 6.4 Comparative performance of various stage-discharge ANN models for Choudhuaghat site (Subansiri River)

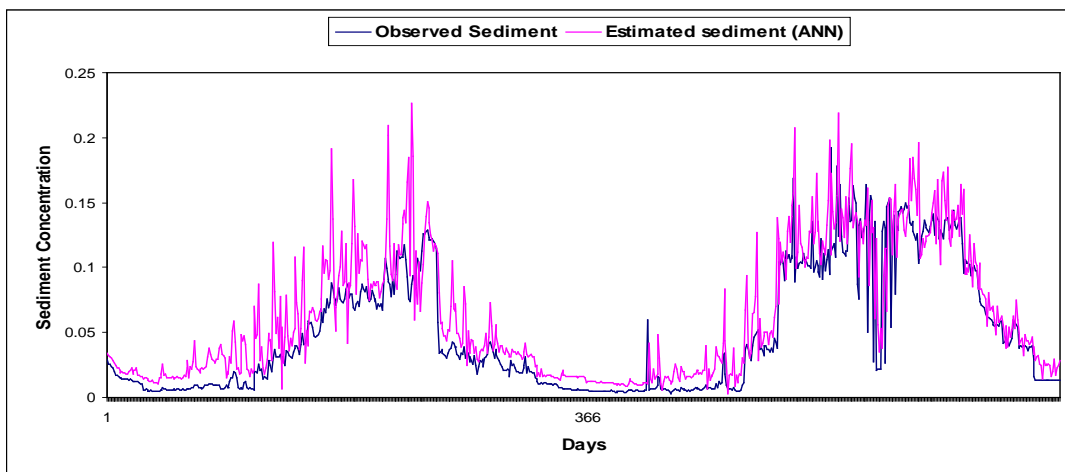
ANN model	Training			Testing		Validation	
	RMSE	R	DC	R	DC	R	DC
ANNCH-1 (1-2-1)	957.89	0.903	0.813	0.955	0.097	0.969	0.047
ANNCH-2 (3-5-1)	384.71	0.985	0.970	0.986	0.966	0.983	0.948
ANNCH-3 (5-4-1)	363.78	0.986	0.973	0.986	0.969	0.986	0.961
ANNCH-4 (7-6-1)	356.01	0.987	0.974	0.986	0.971	0.986	0.968
ANNCH-5 (9-7-1)	340.63	0.988	0.976	0.987	0.970	0.988	0.971



(a) Training



(b) Testing



(c) Validation

Fig. 6.3 Comparative Performance of Observed Sediment Concentration with Estimated Sediment Concentration using ANNPRS-3 at Panchratna

It is observed from Table 6.4 that the RMSE values are generally low for all the ANN models. The performance of ANNCH5 model is the best in RMSE statistic.. In ANNCH5 model, the RMSE value is 340.63 during training.

It can be seen from Table 6.4 that the correlation coefficient (R) values are very high (more than 0.90, i.e., 90%) for all the ANN models, during all the three phases, i.e., training, testing as well as validation. It is also observed that there is not much decrease in the R values during validation as compared to the training phase. The performance of ANNCH5 model is the best in R statistic. The R values for ANN are 0.988, 0.987 and 0.988 during training, testing and validation respectively.

In the determination coefficient (DC) statistic, all the ANN models perform well. The DC values are fairly high (more than 0.90) for all models during all the three phases. In DC statistic also, ANNCH5 model performs the best. The DC values for ANNCH5 are 0.976, 0.970, and 0.971 during training, testing and validation respectively. There is increase in the DC values during validation which indicate good generalization capability of the ANN models.

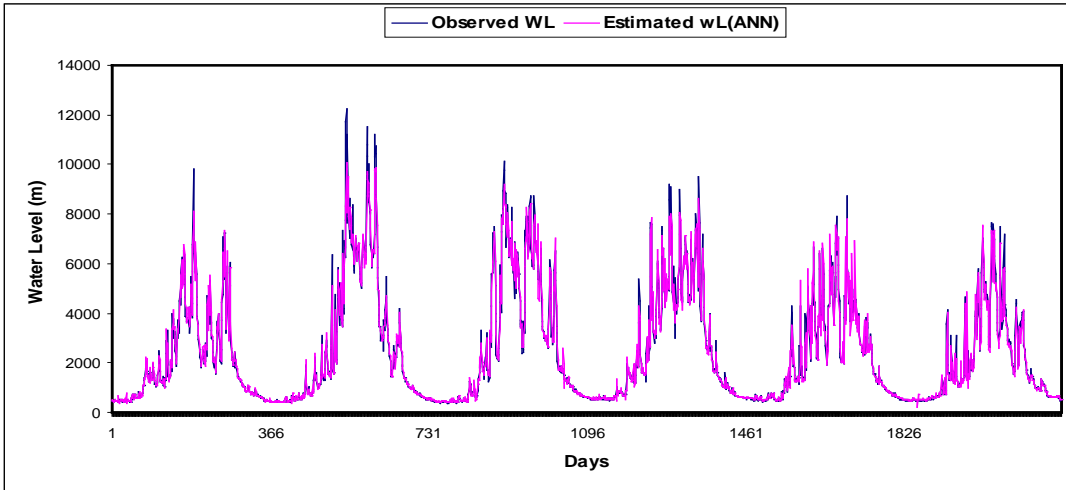
Therefore, ANNCH5 is the best performing model in all the three statistical and hydrological criteria. Fig. 6.4 presents the plots of observed and estimated discharge for ANN3 model during training (a), testing (b) and validation (c). It is observed from Fig. 6.4 that there is very little mismatch between the observed and estimated discharge series for ANN2 model during all the three phases.

6.2.5 Sediment discharge Modeling for Chouldhuaghat site on Subansiri River

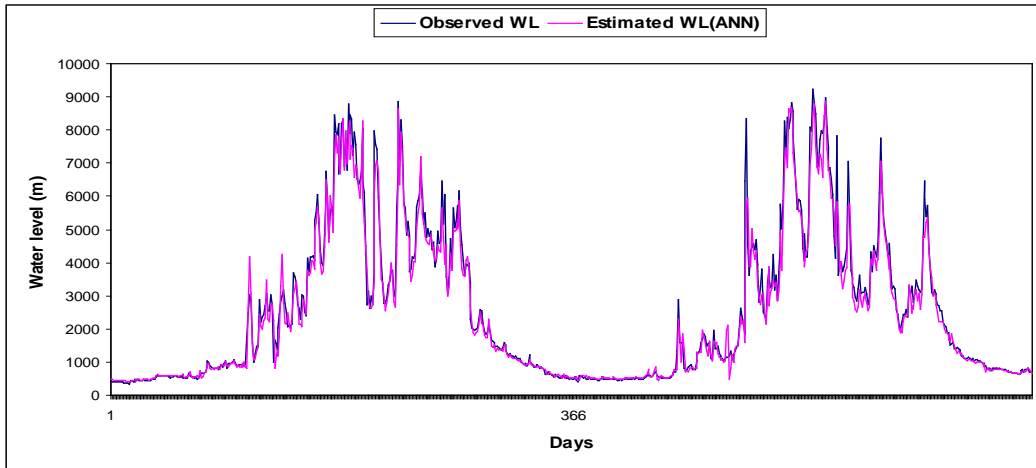
The results are summarized in Table 6.5.

Table. 6.5. Comparative performance of various runoff-sediment ANN models for Chouldhuaghat site on Subansiri River

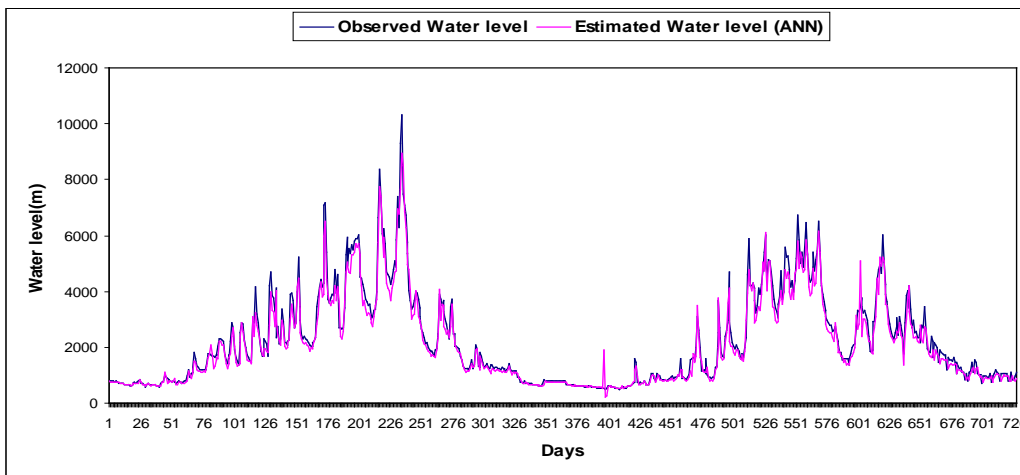
ANN model	Training			Testing		Validation	
	RMSE	R	DC	R	DC	R	DC
ANNCS-1 (1-2-1)	0.154	0.780	0.606	0.787	0.025	0.708	0.089
ANNCS-2 (3-3-1)	0.0822	0.942	0.888	0.940	0.845	0.879	0.587
ANNCS-3 (5-4-1)	0.084	0.939	0.881	0.940	0.836	0.887	0.583
ANNCS-4 (7-10-1)	0.077	0.950	0.902	0.948	0.861	0.900	0.627
ANNCS-5 (9-12-1)	0.076	0.950	0.904	0.942	0.860	0.889	0.672



(a) Training



(b) Testing



(c) Validation

Fig. 6.4 Comparative Performance of Observed Sediment Concentration with Estimated Sediment Concentration Using ANNCH-5 at Choulduaghat

It is observed from Table 6.5 that the RMSE values are generally low for all the ANN models. The performance of ANNCH5 model is the best in RMSE statistic.. In ANNCS5 model, the RMSE value is 0.076 during training.

It can be seen from Table 6.4 that the correlation coefficient (R) values are very high (more than 0.90, i.e., 90%) for all the ANN models, during all the three phases, i.e., training, testing as well as validation. It is also observed that there is not much decrease in the R values during validation as compared to the training phase. The performance of ANNCS5 model is the best in R statistic. The R values are 0.995, 0.942 and 0.889 during training, testing and validation respectively.

In the determination coefficient (DC) statistic, all the ANN models perform well. The DC values are fairly high (more than 0.90) for all models during all the three phases. In DC statistic also, ANNCS5 model performs the best. The DC values for ANNCS5 are 0.904, 0.860, and 0.672 during training, testing and validation respectively. There is not much decrease in the DC values during validation which indicate good generalization capability of the ANN models.

Therefore, ANNCS5 is the best performing model in all the three statistical and hydrological criteria. Fig. 6.5 presents the plots of observed and estimated discharge for ANNCS5 model during training (a), testing (b) and validation (c). It is observed from Fig. 6.5 that there is very little mismatch between the observed and estimated discharge series for ANN2 model during all the three phases.

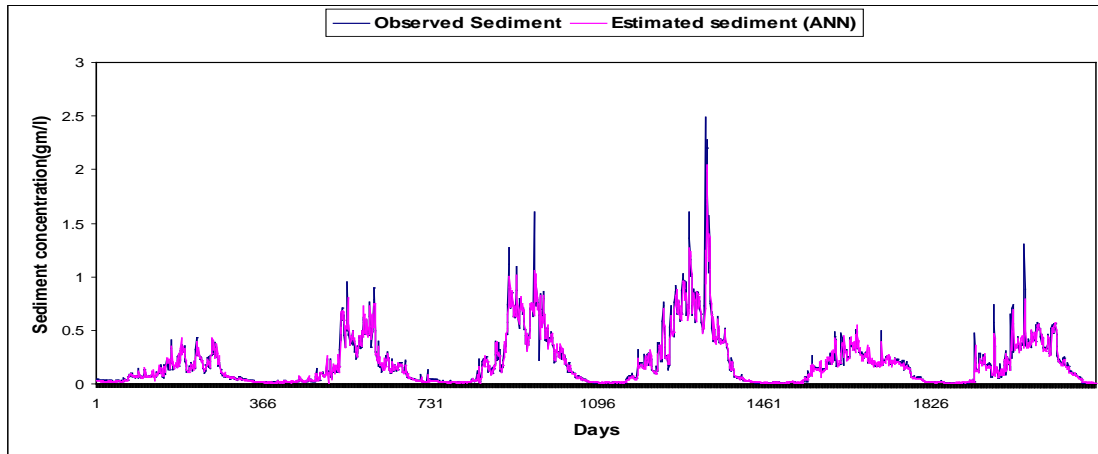
6.3 ANN BASED RAINFALL RUNOFF MODELLING

6.3.1 Rainfall- Runoff in Subansiri Basin using ANN

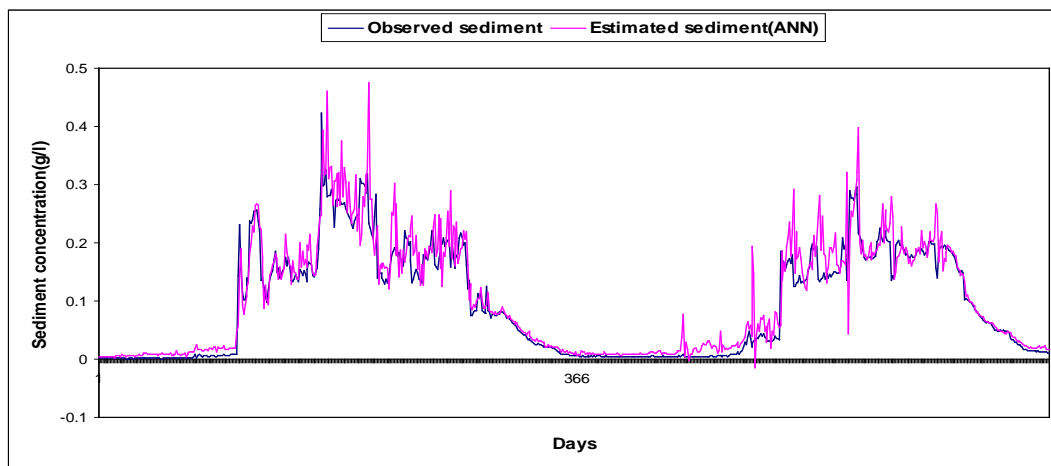
The results are summarized in Table 6.6.

Table 6.6 Comparative performance of various rainfall-runoff ANN models for Subansiri Basin

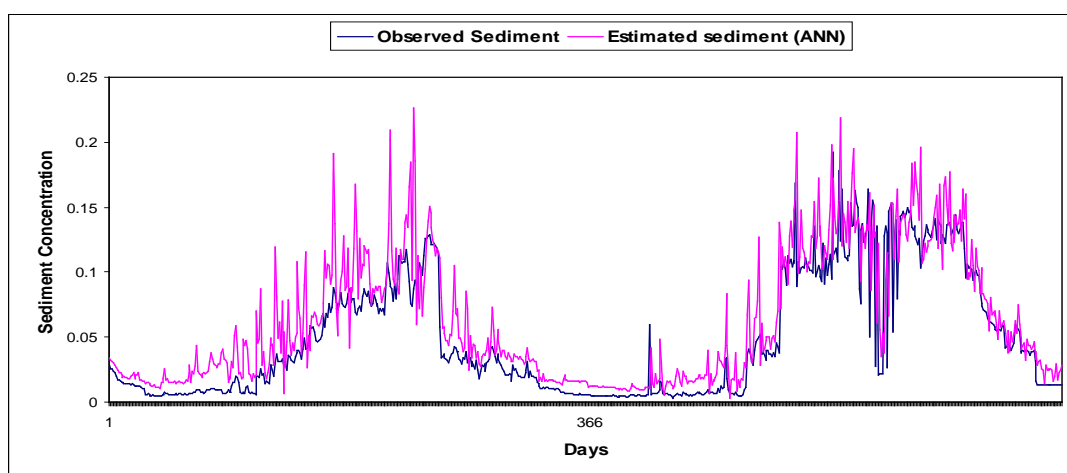
ANN model	Training			Testing	
	RMSE	R	DC	R	DC
ANNR-1 (6-6-1)	1345.0	0.74	0.55	0.61	0.37
ANNR-2 (7-7-1)	1062.5	0.85	0.72	0.80	0.62
ANNR-3 (8-8-1)	1044.9	0.86	0.73	0.81	0.64
ANNR-4 (9-9-1)	1049.6	0.87	0.76	0.78	0.60
ANNR-5 (10-10-1)	1053.8	0.85	0.72	0.81	0.64
ANNR-6 (9-9-1)	450.26	0.9748	0.9502	0.9721	0.9448



(a) Training



(b) Testing

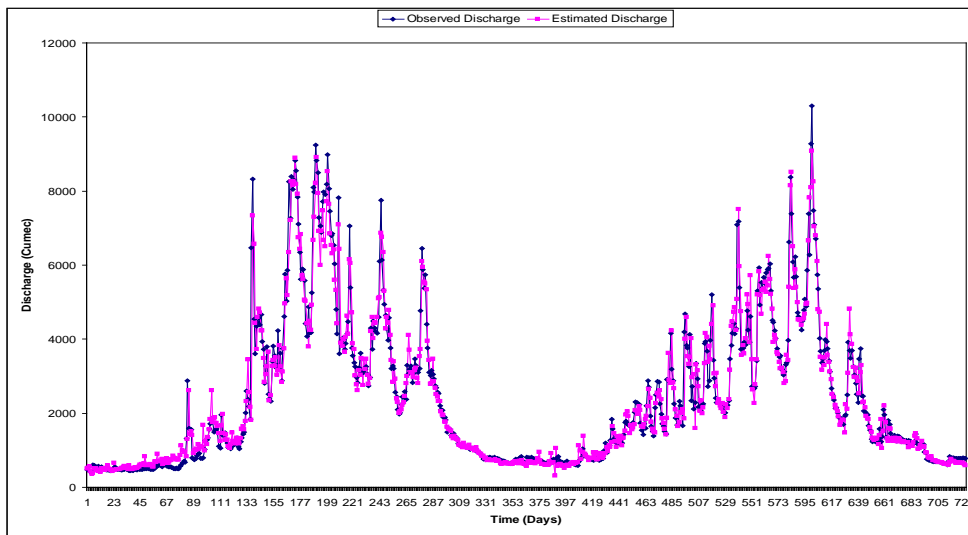


(c) Validation

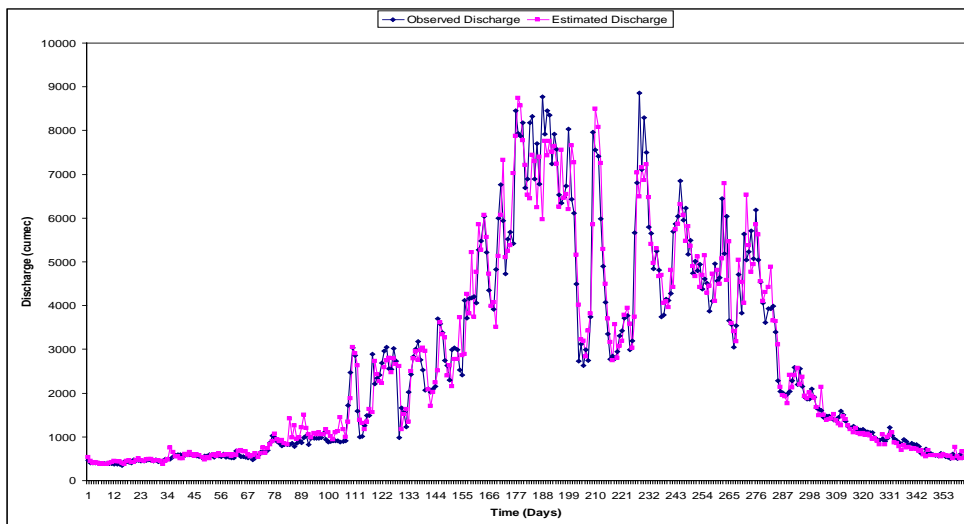
Fig. 6.5 Comparative performance of observed sediment concentration with estimated sediment concentration using ANNCS-5 at Chouldhuaghat

It is observed from Table 6.6 that the performance of ANNR-3 model without previous discharge as input and ANNR-6 model with previous discharge as input are the best among the two types of ANN models developed for rainfall-runoff modeling. However, the performance of ANNR-6 is much higher than the ANNR-3 model in all the three statistical criterion and in both the phases, i.e., training as well as testing/validation. The RMSE value is 450.26 for ANNR-6 compared to the RMSE value of 1044.9 for ANNR-6 which is less than 50%. Similarly, the R and DC values for ANNR-3 are much higher than those of ANNR-3.

Therefore, ANNR-6 is the best performing model in all the three statistical and hydrological criteria. Fig. 6.6 presents the plots of observed and estimated discharge for ANNR-6 model during training (a), and validation (b).



(a) Training



(b) Testing

Fig. 6.6 Comparative Performance of Observed Discharge with Estimated Discharge using ANNR-6 for Subansiri Basin

6.3.2 Sediment-Runoff Modeling for Subansiri Basin using ANN

The results are summarized in Table 6.7.

Table 6.7 Comparative performance of various sediment-runoff ANN models for Subansiri Basin

ANN model	Training			Testing	
	RMSE	R	DC	R	DC
ANNS-1 (7-7-1)	0.0537	0.804	0.6458	0.7766	-5.5621
ANNS-2 (8-8-1)	0.0454	0.8640	0.7465	0.7558	-5.3152
ANNS-3 (9-9-1)	0.0469	0.854	0.729	0.777	-5.3152
ANNS-4 (10-10-1)	0.01738	0.9812	0.9629	0.9821	0.9474

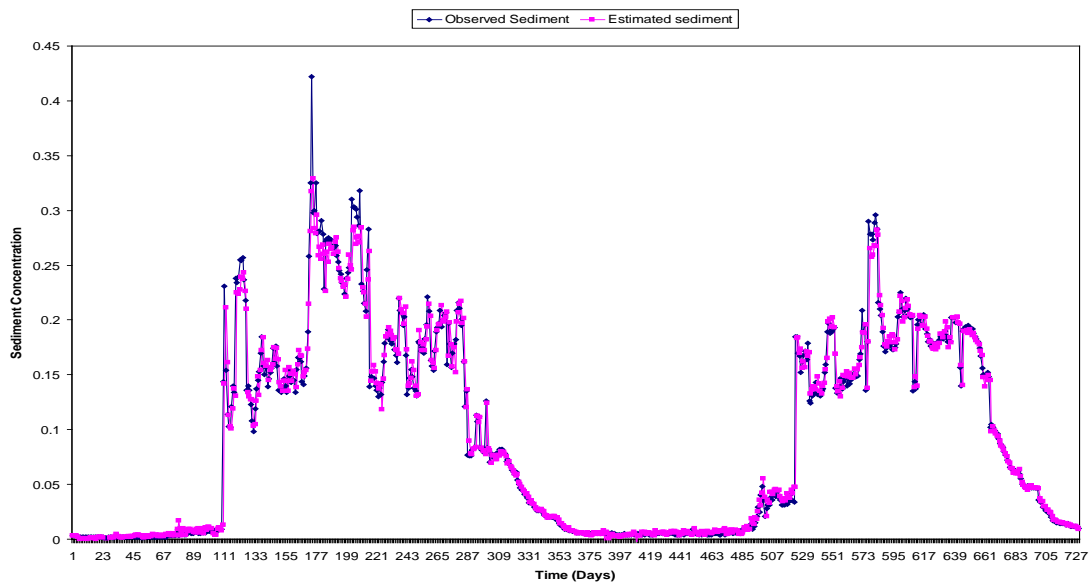
The results of sediment-runoff modeling using ANN have been found to be very close to the observed values as indicated through the statistical performance.

It is observed from Table 6.7 that the RMSE values are generally low for all the ANN models. The performance of ANNS4 model is the best in RMSE statistic. In ANNS4 model, the RMSE value is 0.01738 during training.

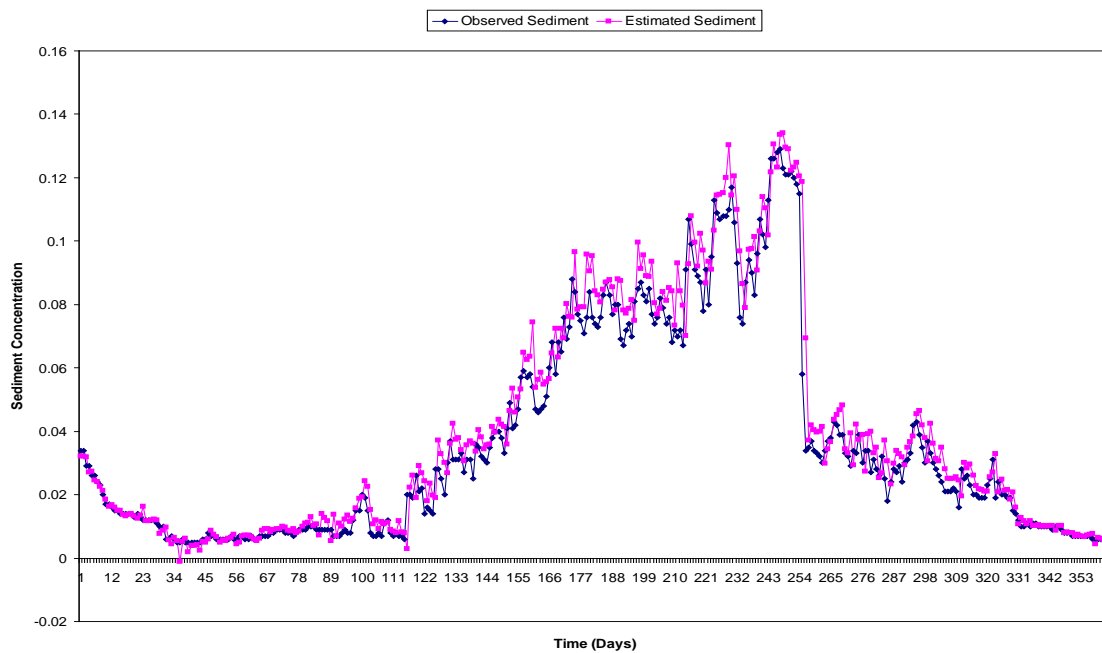
It can be seen from Table 6.4 that the correlation coefficient (R) values are very high (more than 0.90, i.e., 90%) for ANNS4 model, during the two phases, i.e., training as well as testing. It is also observed that there is not much decrease in the R values during validation as compared to the training phase. The R values for ANNS4 are 0.9812 and 0.921 during training and testing respectively.

In the determination coefficient (DC) statistic also, ANNS4 model performs the best. The DC values for ANNS4 are 0.9629 and 0.9474 during training and testing respectively. There is increase in the DC values during validation which indicate good generalization capability of the ANN models.

Therefore, ANNS4 is the best performing model in all the three statistical and hydrological criteria. Fig. 6.7 presents the plots of observed and estimated discharge for ANNS4 model during training (a) and testing (b).



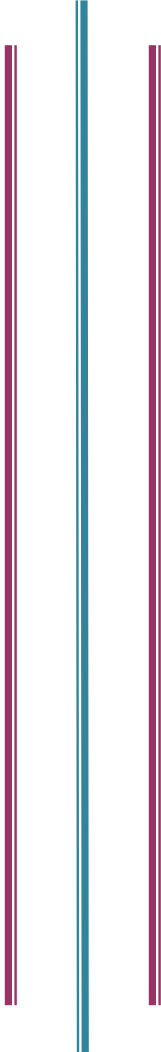
(a) Training



(b) Testing

Fig. 6.7 Comparative Performance of Observed Sediment Concentration with Estimated Sediment Concentration using ANNS-4 for Subansiri Basin

Chapter – 7



Summary

In this study, the modeling of two hydrological processes, namely, rainfall-runoff process and runoff sediment process by ANNs has been accomplished for Subansiri River basin, the biggest sub-basin of Brahmaputra within India. The data of daily rainfall, daily average temperature, daily stage, daily sediment concentration/load and daily discharge for the period 1996-2005 at various hydrometeorological stations in the study basin have been considered for stage-discharge and runoff-sediment rating curves using artificial neural network (ANN) models & conventional techniques for the important gauging sites in the Brahmaputra River basin and development of rainfall-runoff & sediment-runoff models using artificial neural network (ANN technique for Subansiri River basin).

A back-propagation ANN with the generalized delta rule as the training algorithm has been employed in this study. The structure of all the ANN models were three layer BPANN developed with non-linear sigmoid as activation function uniformly between the layers. Nodes in the input layer were equal to number of input variables, nodes in hidden layer were varied from the number of input nodes to approximately double of input nodes (Hupal, 1994) and the nodes in the output layer was one as the models provide single output. All interconnecting links between nodes of successive layers were initially assigned random weights and a constant value of 0.15 and 0.5 was considered for learning rate η and momentum term α respectively. The quick propagation (QP) learning algorithm has been adopted for the training of all the ANN models. The network weights were updated after presenting each pattern from the learning data set, rather than once per iteration. The criteria selected to avoid over training was generalization of ANN through cross-validation (Haykin, 1994). The statistical and hydrological evaluation criteria used are root mean square error (RMSE), correlation coefficient (R) and determination coefficient (DC).

From the preceding analysis, the following findings have emerged:

[A] Brahmaputra Main Stem

(i) Pandu Site

Daily Mean value of stage = 44.2 m

Daily Mean value of Discharge = 12561.95 cumec

(ii) Panchratna

Daily Mean value of stage = 31.51m

Daily Mean value of Discharge = 15492.42 cumec

Daily Mean value of sediment conc = 0.4911 g/l
= 491.1 ppm

[B] Subansiri Basin

Basin area (upto Chouldughat site) = 28,000 Sq. Km

River Length = 442 Km

Av annual rainfall = 2150 mm

Daily Mean value of stage = 94.38m

Daily Mean value of Discharge = 2410.27 cumec

Daily Mean value of sediment conc = 0.1137 g/l
= 113.7 ppm

The results of modeling using ANN approach obtained in this study indicate the capability of back propagation ANN models in simulation of daily river flows using daily discharge, rainfall and temperature data (correlation more than 90%). Because the ANN approach presented here does not provide models that have physically realistic components and parameters, it is by no means a substitute for conceptual modeling. However, the results suggest that the ANN approach may provide a superior alternative to the regression approach for developing input-output simulation and forecasting models in situations that do not require modeling of the internal structure of the basin.

The results of sediment-runoff modeling using ANN have been found to be much closer to the observed values (correlation more than 99%) than the conventional sediment rating curve technique. The study shows that the ANN technique can be successfully applied for the development of reliable relationships between sediment and discharge in a river when other approaches cannot succeed due to the uncertainty and the stochastic nature of the sediment movement.

Moreover, the ANN technique has preference over the conventional methods as ANNs can accept any number of effective variables as input parameters without omission or simplification as commonly done in the conventional methods. The presented ANN models were constructed by using only field river data, and it has no boundary conditions in application. The only restriction is that the model cannot estimate accurately the discharge or sediment load for data out of the range of the training pattern data. Such a problem can easily be overcome by feeding the training patterns with wide range data.



References and Bibliography

References and Bibliography

- Agarwal, A., Mishra, S. K., and Ram, S., and Singh, J. K. 2006.** Simulation of runoff and sediment yield using artificial neural networks. *Biosystems Engineering*, **94(4)**: 597 – 613.
- Akaike, H. 1974.** A new look at the statistical model identification. *IEEE Trans. Autom. Control*. AC – 19, 716 – 723.
- Anmala, J., Zhang, B., and Govindaraju, R. S. 2000** Comparison of ANNs and empirical approaches for predicting watershed runoff. *Journal of Water Resources Planning and Management, ASCE*, **126 (3)**: 156 – 166.
- ASCE Task Committee. on Application of Artificial Neural Networks in hydrology (2000 a).** Artificial neural networks in hydrology. I: Preliminary concepts. *Journal of Hydrologic Engineering, ASCE*, **5(2)**: 115 – 123.
- ASCE, Task committee on Application of Artificial Neural Networks in Hydrology (2000 b).** Artificial neural networks in hydrology. II: Hydrologic applications. *Journal of Hydrologic Engineering, ASCE*, **5(2)**: 124 – 137.
- Barron, A. R. 1993.** Universal approximation bounds for superposition of a sigmoid function. *IEEE Trans. Information Theory*, 39, 930 – 945.
- Baum, E., and Haussler, D. 1989.** What sized net gives valid generalization. *Neural Information Processing Sys.* 1, 81 – 90.
- Bishop, C. M. 1995.** *Neural Networks for pattern recognition.* Oxford University Press, New York.
- Bose, N. K., and Garga, A. K. 1993.** Neural Network design using Voronoi diagrams. *IEEE Transactions on Neural Networks*, **45(5)**: 778-787.
- Caamaño, D., Goodwin, P., and Milos, M. 2006.** Derivation of a bedload sediment transport formula using artificial neural networks, *7th International Conference on Hydroinformatics HIC 2006, Nice, FRANCE.*
- Christopher S. H., Ran, Q., Joel E. V., and Keith, L. 2006.** Adding sediment transport to the integrated hydrology model (InHM) : Development and testing. *Advances in Water Resources* Vol. **29(6)**: 930 – 943.

- Cigizoglu, H. K. 2002.** Suspended sediment estimation and forecasting using artificial neural networks. *Turkish J. Eng. Env. Sci.* **26(2002)**, 15 – 25.
- Corpenner, W. C., and Barhelemy, J. 1994.** Common misconcepts about neural networks as approximators. *Journal of Computing in Civil Engineering, ASCE.* 8(3): 345 – 358.
- CWC 2002 .** Water and Related studies. Central Water Commission, New Delhi.
- David, W. P., and Beer, C. E. 1975a.** Simulation of soil erosion. I: Development of a mathematical erosion model. *Transactions of the American Society of Agricultural Engineers*, **18(1)**: 126–129.
- David, W. P., and Beer, C. E. 1975b.** Simulation of soil erosion. II: Stream flow and suspended sediment simulation results. *Transactions of the American Society Agricultural Engineers*, **18(1)**: 130–133.
- Day, S. P., and Davenport, M. R. 1993.** Continuous time temporal back-propagation with adaptable time delays. *IEEE Transactions on Neural Networks.* **4(2)**: 348 – 354.
- Elman, J. L. 1990.** Finding structure in time. *Cognitive Science*, Vol. 4, No.2, pp 348 – 354.
- Elwell, H. A. 1978.** Modelling of soil losses in southern Africa. *Journal of Agricultural Engineering Research*, 23: 117-127.
- Fahlman, S. E., and Lebiere, C. 1991.** The cascade-correlation learning architecture. CMU Tech. Rep. CMU-CS-90-100. Carnegie Mellon University, Pittsburgh, Pa.
- Ferguson, R. I. 1986.** River loads underestimated by rating curves. *Water Resources Research*, **22(1)**: 74 – 76.
- Foster, G. R., and Meyer, L. D. 1972a.** A closed form soil erosion equation for upland areas. *Sedimentation (Einstein)*, H. W. Shen, ed., Colorado State University Press, Fort Collins, Colorado.
- Foster, G. R., and Meyer, L. D. 1972b.** Transport of soil particles by shallow flow. *Transactions of the American Society of Agricultural Engineers*, **15(1)**: 99 -102.
- Foster, G. R. 1982.** “Modelling the erosion processes.” *Hydrological modelling of small watersheds*, ASAE Monograph No. 5, C. T. Haan, H. Johnson, and D. L. Brakensiek, eds., *American Society of Agricultural Engineers*, St. Joseph, Mich., 297–380.
- French, M. N., Krajewski, W. F., and Cuykendal, R. R. 1992.** Rainfall forecasting in space and time using a neural network. *Journal of Hydrology, Amsterdam*, **137**: 1-31.
- Gallant, S. I. 1986.** Three constructive algorithms for network learning. *Proc. 8th ANN Conf. of the Cognitive Sci. Soc., Cognitive Science Society*, ANN Arbor, 652-660.

- Govindaraju, R. S., and Kavvas, M. L. 1991.** Modeling the erosion process over steep slopes: Approximate analytical solutions. *Journal of Hydrology*, **127(1-4)**: 279–305.
- Gupta, H. V., Ksu, K., and Sorooshian, S. 1997.** Superior training of artificial neural networks using weight-space partitioning. Proc. IEEE Int. Con. on Neural Networks, *Institute of Electrical and Electronics Engineers*, New York.
- Hammerstrom, D. 1993.** Neural Networks at Work. *IEEE spectrum*, 30, 46 -53.
- Hario, H., and Jokinen, P., 1991.** Increasing the learning speed of back-propagation algorithm by linearization. *Artificial Neural Networks*, T. Kohonen et al., pp 629 – 634.
- Hassibi, B., and Stork, D. G. 1993.** Second order derivatives for networks pruning; optimal brain surgeon. *Proc., Neural Information Processing Sys. 4*, MIT Press, Cambridge, Mass., 164 – 171.
- Haykin, S., 1994.** Neural Networks - A Comprehensive Foundation *McMillan*, New York.
- Hipel, K. W., Ian, A., Panu, U. S., and Singh, V. P. 1994.** Stochastic and Statistical Methods in Hydrology and Environmental Engineering, Vol. 3. The series analysis in Hydrology and Environmental Engineering, Kluwer Academic Publishers, The Netherlands.
- Hsu, Kuo-lin., Gupta, H. V. and Soroosh, Sorooshian. 1995.** Artificial Neural Network modeling of the rainfall-runoff process. *Water Resources Research*, **31 (10)**: 2517 – 2530.
- Imrie, C. E., Durucan, S., and Korre, A. 2000.** River flow prediction using Artificial Neural Networks. Generalization Beyond the calibration Range. *Journal of Hydrology*, Vol. 233, 138 – 153.
- Jain, S. K. and Srivastava, D. K. 1999.** Application of ANN for reservoir inflow prediction and operation. *Journal of Water Resources Planning and Management, ASCE*, **125 (5)**: 263 – 271.
- Jain, S. K. 2001.** Development of integrated sediment rating curves using ANNs. *Journal of Hydraulic Engineering, ASCE*, **127(1)**: 30 -37.
- Jain, S. K. 2008.** Development of integrated discharge and sediment rating relation using a compound neural network. *Journal of Hydrologic Engineering, ASCE*, **13(3)**: 124 – 131.

- Jansson, M. B. 1996.** Estimating a sediment rating curve of the Reventazon river at Palomo using mean loads within discharge classes. *Journal of Hydrology*, Amsterdam, **183(3-4)**: 227 – 241.
- Jy. S. Wu, P. E., Han, J., Annambhotla, S., and Bryant, S. 2005.** Artificial neural networks for forecasting watershed runoff and stream flows. *Journal of Hydrologic Engineering*, ASCE. **10(3)**: 216 – 222.
- Kalin, L., Govidaraju, R. S., and Hantush, M. M. 2003.** Effect of geomorphologic resolution on modeling of runoff hydrograph and sedimentograph over small watersheds. *Journal of Hydrology*, **276(1-4)**: 89–111.
- Kalin, L., Govidaraju, R. S., and Hantush, M. M. 2004.** Development and application of a methodology for sediment source identification. I: Modified unit sedimentograph approach.” *Journal of Hydrologic Engineering*, ASCE, **9(3)**:184–193.
- Karim, M. F., and Kennedy, J. F. 1990.** Menu of coupled velocity and sediment-discharge relations for rivers. *Journal of Hydrologic Engineering*, ASCE, **116(8)**: 978 – 996.
- Karnin, E. D. 1990.** A simple procedure for pruning back propagation trained neural networks. *IEEE Tran. Neural Networks*, 1, 239 -242.
- Karunanithi, N., Grenney, W. J., Whitley, D., and Bovee, K. 1994.** Neural networks for river flow prediction. *Journal of Computing in Civil Engineering*, ASCE. **8(2)**: 201 - 220.
- Kerem, H., Cigizoglu, and Alp, M. 2006.** Generalized regression neural network in modelling river sediment yield. *Advances in Engineering Software archive*, **37(2)**: 63 - 68.
- Kisi, O. 2005.** Suspended sediment estimation using neuro-fuzzy and neural network approaches. *Hydrological Sciences Journal*, **50(4)**: 683 – 689.
- Kisi, O. 2007.** Streamflow forecasting using different artificial neural network algorithms. *Journal of Hydrologic Engineering*, ASCE., **12(5)**: 532 – 539.
- Kisi, O. 2007.** Development of streamflow-suspended sediment rating curve using a range dependent neural network. *International Journal of Science & Technology*, **2(1)**: 49 – 61.
- Kohonen, T. 1998.** Self organization and associative memory. 2nd Ed., Springer Verlag, New York.
- Kothari, R., and Agyepong, K. 1996.** On lateral connections in feedforward neural networks. Proc., *IEEE Int. Conf. on Neural Networks*, Institute of Electrical and Electronics Engineers, New York, 13 – 18.

- Kothari, R., and Agyepong, K. 1997.** Induction specialization of context units for temporal pattern recognition and reproduction. *Proc. IEEE Neural Networks for signal processing* V11, J. Principe, L. Giles, N. Morgan, and E. Wilson, Eds., *Institute of Electrical and Electronics Engineers*, New York, 131 -140.
- Kothiyari, U. C., Tiwari, A. K., and Singh, R. 1997.** Estimation of temporal variation of sediment yield from small catchment through the kinematic method. *Journal of Hydrology*, **203(1-4)**: 39-57.
- Kumar, A. 1993.** Dynamic models of daily rainfall-runoff-sediment yield for sub-catchment of *Ramganga* river. Ph.D. Thesis, Department of Soil and Water Conservation Engineering, G. B. Pant University of Agriculture and Technology, Pantnagar – 263 145, Uttarakhand, India.
- Kumar, D. 2007.** Hydrological response prediction of a watershed using artificial neural networks. M. Tech. Thesis, Department of Soil and Water Conservation Engineering, G. B. Pant University of Agriculture and Technology, Pantnagar – 263 145, Uttarakhand, India.
- Kumar, C. S. V. S. and Viswanadh, G. K. 2006.** Performance of artificial neural networks in rainfall-runoff modeling. *Proc. 2nd International Conference on Hydrology and Watershed Management*, Centre for Water Resources, Jawaharlal Nehru Technological University, Hyderabad – 500 072, Andhra Pradesh, India.
- Kwkwk, T., and Yeung, D. 1995.** Constructive feedforward neural networks for regression problems, A survey Tech. Rep., Hong Kong University of Science and Technology, Hong Kong.
- Laguna, A., and Giraldez, J. V. 1993.** The description of soil erosion through a kinematic wave model. *Journal of Hydrology*, **145(1-2)**: 65-82.
- LeCun, Y., Denkar, J. S., and Solla, S. A. 1990.** Optimal brain damage. *Proc., Neural Information Processing Sys. 2*, MIT Press, Cambridge, Mass., 598 – 605.
- Lohani, A. K., Goel, N. K., and Bhatia, K. K. S. 2007.** Deriving stage-discharge-sediment concentration relationships using fuzzy logic. *Hydrological Sciences Journal*, **52(4)**: 793 – 807.
- Lopes, V. L., and Ffolliott, P. F. 1993.** Sediment rating curves for a clearcut Ponderosa Pine watershed in Northern Arizona. *Water Resour. Bull.*, **29(3)**: 369 – 382.
- Lorrai, M. and Sechi, G. M. 1995.** Neural nets for modeling rainfall-runoff transformations. *Water Resources Management*, **9**: 299 – 313.
- Maier, H. R., and Dandy, G. C. 1996.** Use of artificial neural networks for prediction of water quality parameters. *Water Resources Research*, Vol. 32, No. 4, pp. 1013 – 1022.

- Maier, H. R., and Dandy, G. C. 2000.** Neural network for the prediction and forecasting of water resources variables: a review of modeling issues and applications. *Environ. Modelling and Software*, 15, 101 – 124.
- McBean, E. A., and Al-Nassri, S. 1998.** Uncertainty in suspended sediment transport curves. *Journal of Hydrologic Engineering, ASCE*, **114(1)**: 63 – 74.
- McCulloch, W. S., and Pitts, W. 1943** A logic Calculus of the ideas immanent in nervous activity. *Bull. of Math. Biophys.*, 5, 115 – 133.
- Mingguo, Z., Qiangguo, C., and Qinjuan, C. 2008.** Modelling the runoff-sediment yield relationship using a proportional function in hilly areas of the Loess Plateau, North China. *Geomorphology*, **93(3 – 4)**: 288 – 301.
- Minns, A.W., and Hall, M.J. 1996.** Artificial neural networks as rainfall-runoff models. *Hydrological Sciences Journal*, **41(3)**: 399-417.
- Mishra, S. K., Tyagi, J. V., Singh, V. P., and Singh, R. 2006.** SCS-CN-based modeling of sediment yield. *Journal of Hydrology*, Vol. **324(1 – 4)**: 301 – 322.
- Mozer, M. C., and Smolensky, P. 1989.** Skeletonization: A technique for trimming the fat from a network via relevance assessment. *Advances in neural information processing systems 1*, D. Touretzky, ed., Morgan Kaufmann, San Monteo, Calif., 107 -115.
- Nadal, J. P. 1989.** Study of a growth algorithm for neural networks. *Int. J. Neural Sys.*, 55 - 59
- Nadi, F. 1991.** Topological design of modular neural networks. *Artificial Neural Networks*, T. Kohonen et al., pp 213 – 217.
- Nagy, H. M., Watanabe, K., and Hirano, M. 2003.** Prediction of sediment load concentration in rivers using artificial neural network model. *Journal of Hydraulic Engineering, ASCE*, **128(6)**: 588 – 595.
- Narayana, D. V. V. and Babu, R. 1983.** Estimation of soil erosion in India. *Journal of Irrigation and Drainage Engineering, ASCE*, **109(4)**: 419 – 434.
- Nash, J. E., and Sutcliffe, J. V. 1970.** River flow forecasting through conceptual models, Part 1 – A: Discussion principles. *Journal of Hydrology*, Vol. 10, 282 – 290.
- Nearing, M. A., Foster, G. R., Lane, L. J., and Finkner, S. C. 1989.** A process-based soil erosion model for USDA-Water erosion prediction project technology. *Transactions of the American Society of Agricultural Engineers*, **32(5)**: 1587–1593.

- Neural Power. 2003.** Neural Networks Professional Version 2.5, CPC - X Software, Copyright: 1997-2003, Demoverion, http://www.geocities.com/neural_power.
- Nowlan, S. J., and Hinton, G. E. 1992.** Simplifying neural networks by soft weight sharing. *Neural Computation*, 4, 473 – 493.
- Onstad, C. A. and Foster, G. R. 1975.** Erosion modeling simulation for the process of soil erosion by water. *Transaction of the ASCE*, **18(2)**: 288 – 292.
- Oppenheim Alan, V.** “Signals and systems”. Prentice-Hall Editions, p 685.
- Ozturk, F., Yurekli, K., and Apaydin, H. (2008).** Stochastic Modeling of Suspended Sediment from Yesilirmak Basin, Turkey, *International Journal of Natural and Engineering Sciences* **2 (1)**: 21-27. (ISSN: 1307 – 1149)
- Pyasi, S. K. 1997.** Memory based input – output runoff and sediment yield models for the upper *Ramganga* Himalayan Catchment, Ph.D. Thesis, Department of Soil and Water Conservation Engineering, G. B. Pant University of Agriculture and Technology, Pantnagar – 263 145, Uttarakhand, India.
- Raghuvanshi, N. S., Singh, R. and Reddy, L. S. 2006.** Runoff and sediment yield modeling using artificial neural networks: Upper Siwane River, India. *Journal of Hydrologic Engineering, ASCE*, **11(1)**: 71 – 79.
- Rai, R. K., and Mathur, B. S. 2008.** Event - based sediment yield modeling using artificial neural network. *Water Resources Management*, **22(4)**: 423 – 441.
- Ramchandrarao, P. 2003** Godavari daily discharge report, Godavari Circle Hyderabad, Central Water Commission, Govt. of India.
- Ranjithan, S., Eheart, J. W., and Rarret, jr., J. H. 1993.** Neural network - screening for groundwater reclamation under certainty. *Water Resources Research*, 29(30): 563 – 574.
- Reed, R. 1993.** Pruning algorithm - A survey. *IEEE Trans. Neural Networks* 4, 740 – 744.
- Refenes, A. N., and Vithlani, S. 1991.** Constructive learning by specialization. *Artificial Neural Networks*, T. Kohonen et al., pp 923 – 929.
- Rogers, L. L., and Dowla, F. U. 1994.** Optimization of groundwater remediation using artificial neural networks with parallel solute transport modeling. *Water Resources Research*, 30920, 457 – 481.
- Rumelhart, D. E., Hinton, G. E. and Williams, R. J. 1986.** Learning internal representations by error propagation. *Parallel Distributed Processing*, Vol. I MIT Press, Cambridge, Mass: 318 – 362.

- Rumelhart, D. E., and Zipser 1986.** Feature discovery by competitive learning. Parallel distribution processing, Explorations in the microstructure of cognition, Vol. 1, pp 318 – 364.
- Rusell, I. F. 1991.** Self organizing competitive learning and adaptive resonance networks. *Int. Jour. of Neural Networks*, Vol. 2, No. 2/3/4.
- Sadeghi, S. H., Mizuyama, T., and Vangah, B. G. 2007.** Conformity of MUSLE estimates and erosion plot data for storm-wise sediment yield estimation. *Terr. Atmos. Ocean. Sci.*, Vol. 18 (1): 117-128.
- Sarkar, A., Kumar, R., Singh, R. D., Thakur, G., and Jain, S. K. (2004).** Sediment-discharge modeling in a river using artificial neural networks. *Proc. International Conference ICON – HERP*, Oct 26 – 28, 2004, IIT Roorkee, India.
- Sarkar, A. 2005.** Real time flood forecasting using artificial neural networks in an Indian river. *Proc. International Conference on Monitoring, Prediction and Mitigation of Water Related Disasters (MPMD-2005)*, January 12-15, 2005, Kyoto, Japan.
- Sarkar, A., Agarwal, A. and Singh, R. D. 2006.** Artificial Neural Network models for rainfall-runoff forecasting in a hilly catchment. *Journal of Indian Water Resources Society*, 26(3-4): 1 – 4.
- Sato, A., 1991.** An analytical study of the momentum term in a back-propagation algorithm. *Artificial Neural Networks*, T. Kohonen et al, pp 617 – 622.
- Schnabel, S., and Maneta, M. 2005.** Comparison of a neural network and a regression model to estimate suspended sediment in a semiarid basin. *Geomorphological Process and Human Impacts in River Basins*, Proceedings of the International Conference held at Solsona, Catalonia, Spain, May 2004, Publ. 299, 2005, 91 – 100.
- Shamseldin, A. Y., O ‘ Connor, K. M. and Liang, G. C. 1997.** Methods for combining the outputs of different rainfall-runoff models. *Journal of Hydrology*, 197: 203 – 229.
- Sharma, T. C. and Dickinson, W. T. 1980.** System model for daily sediment yield. *Water Resources Research*, 16(3): 501 – 506.
- Shieh, C. L., and Lee, S. Y. 2005.** Sediment yield model for a watershed: a case study of Choushui River, Taiwan. *Geophysical Research Abstracts*, Vol. (7): 05931, 2005, European Geosciences Union.
- Singh, P. V. 1999.** Linear time invariant rainfall-runoff and storage-runoff forecasting models using transfer function approach for Himalayan Watershed. M.Tech. Thesis, Department of Soil and Water Conservation Engineering, G. B. Pant University of Agriculture and Technology, Pantnagar – 263 145, Uttarakhand, India.
- Singh, R. P. 2000.** Genetic Algorithm approach in development and optimization of memory based transfer function models for runoff and sediment prediction – A case study. M. Tech. Thesis, Department of Soil and Water Conservation Engineering, G. B. Pant University of Agriculture and Technology, Pantnagar – 263 145, Uttarakhand, India.

- Singh, U. P. 2004.** Hydrology modeling using artificial neural networks. M. Tech (Water Resources Engineering) dissertation, Department of Civil Engineering, Malaviya National Institute of Technology, Jaipur – 302 017 (Rajasthan), India.
- Sinha, A. 2005.** Stage-Discharge-Sediment analysis using Artificial Neural Networks. M. Tech (Water Resources Engineering) dissertation, Department of Civil Engineering, Indian Institute of Technology, Delhi, India.
- Smith, J. and Eli, R. N. 1995.** Neural Network models of rainfall-runoff process. *Journal of Water Resources Planning and Management, ASCE*, **121(6)**: 499 – 508.
- Srivastava, P. K., Rastogi, R. A. and Chauhan, H. S. 1984.** Prediction of storm sediment yield from a small watershed. *Journal of Agricultural Engineering, ISAE*, **21(1 - 2)**: 121 – 126.
- Tayfur, G. 2001.** Modeling two-dimensional erosion process over infiltrating surfaces. *Journal of Hydrologic Engineering, ASCE*, **6(3)**: 259–262.
- Tayfur, G. 2002.** Applicability of sediment transport capacity models for nonsteady state erosion from steep slopes. *Journal of Hydrologic Engineering, ASCE*, **7(3)**: 252–259.
- Tayfur, G., and Sing, V. P. 2004.** Numerical model for sediment transport over nonplanar, nonhomogeneous surfaces. *Journal of Hydrologic Engineering, ASCE*, Vol. **9(1)**: 35 – 41.
- Tayfur, G., and Guldal, V. 2005.** Artificial neural networks for estimating daily total suspended sediment in natural streams. *Nordic Hydrology*, **37(1)**: 69 – 79.
- Thandaveswara, B. S. and Sajikumar, N. 2000.** Classification of river basins using artificial neural networks. *Journal of Hydrologic Engineering, ASCE*, **5(3)**: 290 – 298.
- Thirumalaiah, K. and Deo, M. C. 1998.** River stage forecasting using artificial neural networks. *Journal of Hydrologic Engineering, ASCE*, **3(1)**: 26 – 32.
- Thirumalaiah, K. and Deo, M. C. 2000.** Hydrological forecasting using neural networks. *Journal of Hydrologic Engineering, ASCE*, **5(2)**: 180 - 189.
- Thomas, T., Jaiswal, R. K. and Singh, S. 2006.** Hydrological modeling of streamflows using artificial neural networks. *Proc. 2nd International Conference on Hydrology and Watershed Management*, Centre for Water Resources, Jawaharlal Nehru Technological University, Hyderabad – 500 072, Andhra Pradesh, India.
- Tokar, A. S. and Johnson, P. A. 1999.** Rainfall – Runoff modeling using artificial neural networks. *Journal of Hydrologic Engineering, ASCE*, **4(3)**: 232 – 239.

- Tokar, A. S. and Markus, M. 2000.** Precipitation – Runoff modeling using artificial neural networks and conceptual models. *Journal of Hydrologic Engineering, ASCE*, **5(2)**: 156 – 161.
- Wasserman, P. D. 1989.** Neural computing: theory and practice. Van Nostrand Reinhold, New York.
- Webros, P. J. 1974.** Beyond Regression: new tools for prediction and analysis in behavior sciences. Ph.D Thesis, Harvard University, Cambridge, Mass.
- Wischmeir, W. H. and Smith, D. D. 1958.** Rainfall energy and its relationship to soil loss. *Transactions of American Geophysics Union*, **39**: 285 – 291.
- Woolhiser, D. A., Smith, R. E., and Goodrich, D. C. 1990.** *KINEROS: A kinematic runoff and erosion model: Documentation and user's manual*, USDA Agriculture Research Service ARS-77, Washington, D.C. United States.
- Wu, T. H., Hall, J. A. and Bonta, J. V. 1993.** Evaluation of runoff and erosion models. *Journal of Irrigation and Drainage Engineering, ASCE*, **119(4)**: 364 – 382.
- Yang, C. C., Prasher, S. O., Lacroix, R., Sreekanth, S., Patni, N. K. and Masse, L. 1997.** Artificial neural network model for subsurface drained farm lands. *Journal of Irrigation and Drainage Engineering, ASCE*, **123(4)**: 285 – 292.
- Yitian, L., and Gu RR. 2003.** Modeling flow and sediment transport in a river system using an artificial neural network. *Environmental Management*, **31(1)**: 122 – 134.
- Yu, X., Loh, N. K. and Miller, W.C., 1993.** A new acceleration method for the back-propagation algorithm. *IEEE Transactions on Neural Networks.*, pp 1157 -1161.
- Yu, P.S., Liu, C. L., and Lee T. Y. 1994.** Application of a transfer function model to a storage runoff process. *Stochastic and statistical methods in Hydrology and Environmental Engineering*, Vol. 3, 87 – 97.
- Zealand, C. M., Burn, D. H. and Simonovic, S. P. 1999.** Short term steam flow forecasting using Artificial Neural Networks. *Journal of Hydrology*, **214**: 32 – 48.
- Zurada, M. Zacek. 1992.** Introduction to artificial neural system, St. Paul, New York: West publishing company.

PHASE – III

RUNOFF AND SEDIMENT MODELLING IN A SUB-BASIN OF BRAHMAPUTRA RIVER

TEAM OF INVESTIGATORS

- 1. Prof. Dr. Nayan Sharma**
- 2. Mr. Belay Zeleke**
- 3. Ms Anupama Nayak**
- 4. Md. Parwez Akhtar**
- 5. Mr. Neeraj Kumar**

TABLE OF MAJOR CONTENTS

Sl. No.	Subject	Page No.
CHAPTER-1	INTRODUCTION	3
CHAPTER-2	LITERATURE REVIEW	9
CHAPTER-3	DESCRIPTION OF STUDY AREA	44
CHAPTER-4	FORMULATION AND DEVELOPMENT OF FLOW SIMULATION MODEL	59
CHAPTER-5	RESULTS AND DISCUSSIONS	79
CHAPTER-6	PILOT STUDY SCHEMES FOR EROSION CONTROL ON THE BRAHMAPUTRA RIVER FOR MORIGAON SITE; AND NEAR GUWAHATI AIRPORT OF BRAHMAPUTRA RIVER	94
CHAPTER-7	SUMMARY	116
CHAPTER-8	REFERENCES	118

CHAPTER -1

INTRODUCTION

INTRODUCTION

1.1 INTRODUCTION

The flow resistance characteristics of an alluvial stream are highly complex which warrant considerable research efforts. Due to this reason water surface level, velocity and discharge computations in alluvial streams have great deal of uncertainties. The art of modelling an alluvial river is still in developing stage and lot of ground yet remain to be uncovered. The dynamics of flow is further complicated in a natural stream due to wide differences in hydraulic properties and resistances of flow in the main channel and the subsidiary channels.

The position of the free surface is likely to change with respect to time and space and also by the fact that the depth of flow, the discharge and the slopes of the channel bottom and of the free surface are interdependent. To add to the intensity of parameters, a more profound problem defines the flow behavior and attributes i.e., the fact that rivers and other watercourses, in most cases, run through loose material and the water carries/transport some of this material along with it. Generally the loose non-cohesive material through which a river flows is generally termed as “sediment”.

An integrated study in Fluvial Hydraulics and Sediments Transport involves the analysis of the capacity of the river or channel to carry water and sediment, and the corresponding morphological changes in both the main channel and floodplain. Sediment transport in concise, replicates the various aspects of the dynamics of solid particle movement, properties of the transported materials, and characteristics of the transporting medium, which in turn, may be affected by the solids transported.

The morphological changes of rivers are deeply interrelated with bed deformation and bank erosion because of the mutual relationship between water flow and sediment transport. A better understanding of these processes is very important in river engineering to prevent disasters due to flooding, to design and manage hydraulic structures, like bridges and water intake towers, and to maintain river ecosystems and the landscape for environmental Engineering purposes.

Reliable and quantitative estimate of the bed aggradation or degradation are very important in river engineering and management projects as well as accurately predicting the water surface elevations during floods in estimating flood related damage. Thus, engineers are greatly

interested in accurately predicting the behavior of river under various flows and sediment loads so that better information can be obtained for the planning and design of river control structures, flood protection measures and other water diversion structures.

In the present study, it will be endeavor to investigate the flow propagation behavior at different flow stages with varying sediment transport capacity and sediment concentration and thereby predicting time variant bed profile using recently launched flow simulation model HEC-RAS for **622.73 km** reach of Brahmaputra.

1.2 EARLIER RESEARCH

To date, there are many empirical formulas for the calculation of sediment discharge in alluvial channels, but few have gained general applications to estuaries and coastal waters. For sediment transport in rivers, Yang and Wan (1991) provided a good summary of the well-cited equations, such as those proposed by Einstein (1950), Meyer-Peter and Muller (1948), Bagnold (1966), Yalin (1977), Engelund and Hansen (1972), and Ackers and White(1973) transport and local flow characteristics to numerical modelers.

A number of sediment transport studies have been conducted in channels and flumes to develop analytical solutions for simplifying the governing equations describing complex phenomenon of the aggradation and degradation processes (Sinnakaudan, 2006). Researchers have separately treated the suspended load and the bed load calculation. However recent literature shows that total sediment load (or bed material load) equations are much preferred and researchers are now moving toward employing more complex analytical methods. Good appraisals of available total sediment load equations and their performance were given by Acker and White (1973), Garde and Raju(2000), Yang and Wan (1991), Chen (1973), Chang(1984). Some of the available total bed material load equations are developed by Graf (1971), Ackers and White (1973), Rijn (1996), and Yang (1973). The existing equations are mostly developed based on flume data in western countries including America and Western Europe. However not all of these equations are widely used or evaluated in other parts of the world (Karamisheva, 2006). Several equations such as Ackers–White (1973) have been incorporated into current loose boundary models such as *HEC-6* (USACE 1993) and the Graf (1971) equation is available in *Fluvial-12* (Chang 1993) to simulate the sediment transporting capability of rivers.

The prediction of open channel flows using numerical models is of great interest to hydraulic researchers and engineers. Most open channel flows are well described by the Saint Venant equations. Although the Saint Venant equations are derived based on the shallow water hypothesis, many studies have revealed that the equations are also applicable to the rapidly varied flows such as dam-break flows. So far, many numerical schemes for the Saint Venant equations have been developed. However, most conventional schemes are incapable of encompassing the diverse and complex open channel flows. For example, the four-point implicit scheme was found to have numerical stability problems with Tran critical flow (Cao and Carling 2002).

One-dimensional (1-D) modelling of sediment transport in streams has seen extensive development over the past decades. Chen (1973), for the first time formulated a model that included sediment transport for generalized use. Dass (1975) developed multi-stream flow and compound stream flow models by adopting the uncoupled solution procedure to route water and sediment in non uniform channels. Steady and step wise quasi-unsteady 1-D models, such as HEC-6 (HEC 1990a) model, Chang's(1984) model, and others, have been widely tested and applied to sedimentation studies in reservoirs and rivers in which the long wave assumption is valid and the long-term results are mainly considered. Many unsteady flow models (Cunge et al. 1980) have been developed and applied to river estuaries and other situations where the unsteadiness of flow prevails. With a lot of enhancement and refinement, 1-D models continue to have their place in engineering applications. The majority of the early 1-D sediment transport models decoupled the flow and sediment calculations, which resulted in simpler computer codes. This strategy was justified because of the different time scales of flow and sediment transport and the inherent inaccuracies introduced by the use of empirical formulas for bed roughness and sediment transport capacity. Recently, much effort has been made toward relaxing the limit in time and space steps and extending the applicability of the fully decoupled model. One effective approach is to couple the equations of flow and sediment movement, which was done by Cao et al. (2002), who compared the numerical stability of coupled and decoupled models and found out that the coupled model is more stable. However, the implementation of a coupled model for non uniform sediment transport is rather complicated, which is one of the reasons the decoupled models are still used by many scientists. Another approach, which has substantially improved sediment transport modeling, is the non equilibrium (also referred as non saturated) sediment transport model (Cao and Carling, 2002). In the traditional equilibrium (or saturated) transport model, the

actual sediment transport rate is assumed equal to the sediment transport capacity at every cross section (i.e., locally at equilibrium state, and the bed change is calculated by the sediment continuity equation (Cao and Carling, 2002). However, in many cases, such as sediment strongly overloading or under loading, the inflow sediment discharge imposed at the inlet is significantly different from the transport capacity, which might lead to difficulties in the calculation of bed changes near the inlet, thus requiring a small time step. The non equilibrium transport model adopts the mass transport equation to determine the actual sediment transport rate, which should be more suitable for the simulation of sediment transport in natural rivers that are mostly in non equilibrium state.

1.3 OBJECTIVE

The study is aimed to:

- Application of flow simulation model HEC-RAS to investigate flow characteristics and behavior at different flow stages with varying sediment inflows and prediction of longitudinal bed profile.
- Investigation of the suitability of available sediment predictor for assessing the sediment transport capacity for the study reach.
- Estimation of stream power for justifying aggradation and degradation in the study reach.

1.4 STUDY AREA

The area under the consideration for the present study encloses a **622.73 km** river stretch of Brahmaputra encompassing 65 no. of different cross-sections, 7 reaches with Kobo on the northern most (65 no.) to Dhubri on the south (2 no.). The prime data, the study utilizes is the survey data of the cross sections taken in the years 1993 and 1997. The other hydrologic data of the river at different locations (Pandu, Jogighopa etc.) for the years 1993 to 2002 sourced from Central Water Commission and Brahmaputra Board). Photographic images derived from different digital satellites imageries processing in the earlier works are incorporated to draw the idea of the area at a glance.

1.5 THE METHODOLOGY

The methodology for this work is to first assess Manning's n in all segments(all 7 reaches) of the whole study area (**622.73 K.M.**) through simulating the flow and comparing the computed water surface profiles at down stream with observed water surface profiles using 1-D hydraulic model namely HEC-RAS 4.0. Secondly, the sediment transport module in HEC-RAS 4.0 proposed to be performed for the study reach to estimate long term aggradation and degradation to predict the longitudinal bed profile through appropriately feeding inflowing sediment concentration, sediment inflow from tributaries, bed material sampling and selection of appropriate sediment transport function along with flow data and calibrated resistance parameter. For the model constituted in this work, several available sediment discharge predictors will be experimented and to adopt the method which yield best possible results.

CHAPTER -2

LITERATURE REVIEW

LITERATURE REVIEW

2.1 INTRODUCTION

Sediment transport problems related to the identification and mitigation of flood hazard on alluvial fans in arid and semiarid environments is a current and critical concern of the engineering profession. In particular, estimating the length and maximum depth of deposition or erosion that occurs during a flow event when there is a change in the longitudinal slope of the channel is an important problem. Deposition occurs when the slope changes from steep to mild and erosion occurs when the slope changes from mild to steep. Once, a flood is over, or in a gradual time span, large changes on the river bed are observed with banks or piers eroded, while other locations get covered or aggraded. It might be impacted that when extremely large floods with limited sediment supplies and high sediment carrying capacities occur in rivers with erodible bed and bank materials, scour will continue to take place within the erosive capacity of the stream till it approaches the minimum/optimum value required to transport the available material.

Traditional approaches have investigated the ways in which stream flows, sediment loads and channel forms vary along a river from headwaters to mouth and with time over periods ranging from hours to years. Represented in their most simple form, rivers have been viewed a unidirectional systems that change progressively from headwaters to mouth. The river continuum concept takes the physical structure of a stream, coupled with the hydrological regime and energy inputs to produce a series of responses (in form as stream flow hydrographs, etc.)

2.2 HISTORY

An exemplary representation of history of river channel evolution may be envisioned through Fig: 2.1 (Schumm 2000).

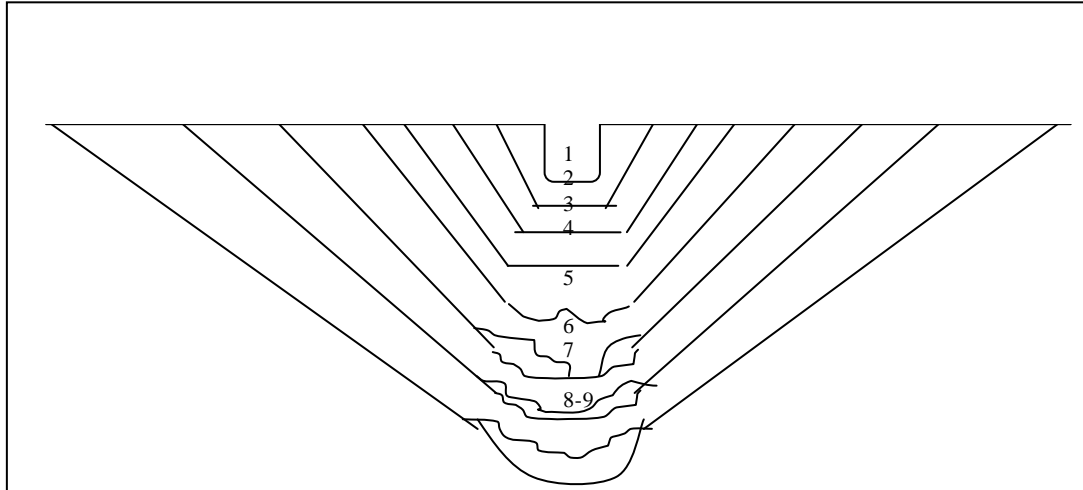


Fig: 2.1 Cross Section of Valley and Incising Stream at time

The historical background of a river is based on how the channel evolved through the passage of time. In the Fig: 2.1, the evolutionary transient phases of a channel in the vertical plane are presented. From 1-4 the channel is confined by the bed rock valley walls. During stages 5-7 the channel is constrained by bedrock valley wall and terraces of older alluvium. Finally, at the stage of 8-9 the channel has reached to regime (Schumm; 2000).

High floods are usually accompanied by high sediment charge, it could be speculated that the oldest streams were wide, shallow, steep, braided bed-load channel (Fig: 2.2a) The decrease in the sediment load perhaps were more rapid than the discharge a meander-braided transition pattern developed with a well defined single thalweg (Fig: 2.2b). The thalweg, in turn, became the channel as a new floodplain formed and the channel further narrowed with further reduction of sediment load (Fig: 2.2c). Finally, as bed load became a fraction of its former volume, a meandering mixed load channel with large meanders formed (Fig: 2.2 d).

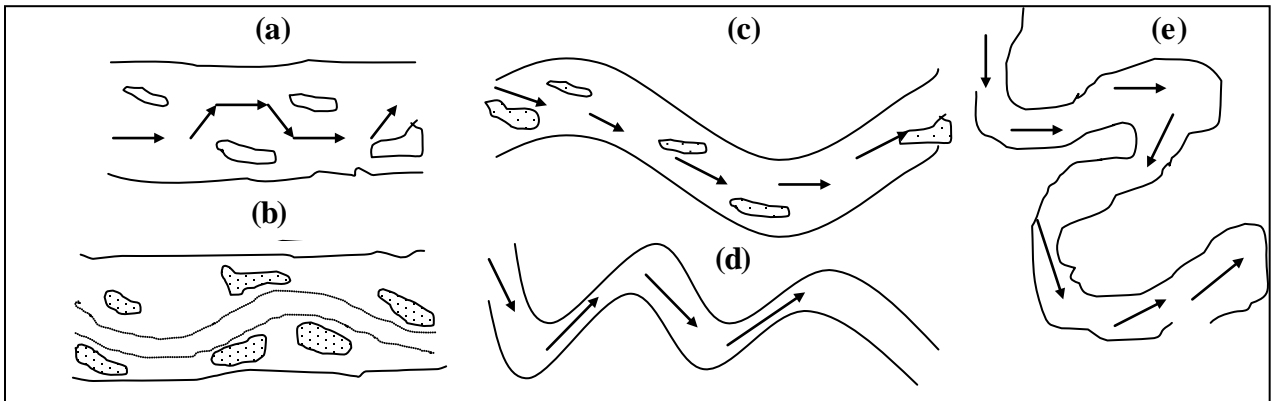


Fig: 2.2 Sequence of Channel Changes with Decrease in Discharge and Sediment

Primarily concerning to the Longitudinal bed profile it is found customary to mention the hydraulic characteristics of river flow dynamics with sediment discharge which constitutes and imparts dynamism to river streambed and other river morphological parameters. It is spontaneous to understand that a river originates from its watershed at higher altitudes of mountainous slopes which relatively receive high intensity rainfalls. Mainly, large river streams all around the world starts its voyages from higher mountainous elevation towards the sea. In the beginning the path of the flow is so steep that it has enormous potential to erode the bed in the vertical direction by virtue of which it develops V-shaped river section deep gorge or canyons. It has no flood plains and covers full width of its valley at all stages. A river at its young stage is characterized by presence of rapids, water falls, steep and varying gradients and presence of lakes.

At this stage the river is said to become mature after its youth stage. The slope at this stage is so reduced that it can no more cut the bed but starts widening. The sediment transportation capacity is just adequate to transport the sediments in the flow from upstream and the sediment material is derived from bank widening.

If the sediment content in the flow is above the transporting capacity heavier sediments are settled on the bed upstream the profile slope. Conversely, if the transporting rate capacity is yet to be satisfied, the bed material picked up and the stream slope is reduced. Hence, matured streams adjust its profile slope delicately. It is in the stage of maturity that the stream flows sinusoidal or meandering path in plan.

2.3 STREAM SLOPE

In general the longitudinal slope of a stream shows a continual decrease along its length. Examination of stream profiles would show that the slope is greatest near the source, decreasing more or less regularly as the river follows its course. Such reduction in slopes corresponds to a longitudinal profile which is concave upwards (Garde and Raju 2000). Several factors are responsible for this. The reasons put forward by different scientists and engineers have been summarized in the following lines.

Firstly, size of bed material being transported decreases in downstream direction due to abrasion (Garde and Raju 2000). Hack (1962) found slope varied as $d^{0.60}$ for stream in Virginia and Maryland (USA). Shulits (1941) assumed that the stream slope is proportional to the size of the bed material and accordingly proposed a slope reduction equation (Eq: 2.1)

$$S = S_0 e^{-\alpha x} \quad (2.1)$$

S_0 and S are the slopes at $x=0$ and at any distance x being measured in downstream direction and α a slope reduction coefficient. Brush (1961) and Hack (1962) have shown that the stream slope is proportional to a negative power of the length of the stream up to that point indicating there by a decrease in slope along the length in conformity with the equation.

Low water profiles of the river Mississippi between Fort Jackson and Cairo of the Ohio between Cairo- Pittsburg (USA) and of several rivers in Europe are found to confirm the Eq: (2.1) (Garde and Raju 2000).

Secondly, in humid regions, the discharge in a stream increases in the downstream direction due to inflow from the tributaries. Unless there is a corresponding increase in the sediment inflow, the stream would necessarily flatten to the extent required by the increased sediment and water discharge (Garde and Raju 2000).

Thirdly, the sediment contribution of the upper region of a drainage basin is large compared to the run-off contribution to the stream flow. Which mean higher sediment contribution necessitating higher slope. While the lower region of the same drainage basin contributes smaller sediment quantity compared to its run-off discharge contribution signifying flatter slope requirement (Garde and Raju 2000).

Fourthly, on lower part of river sediments are usually finer and the streams are narrow with greater depth to width ratio leading to higher hydraulic efficiency requiring flatter slope (Garde and Raju 2000).

Garde (1982) presented an analysis considering the change in the bed material size, discharge and sediment load in the direction of flow.

He gave following relationships.

$$d = d_0 e^{\alpha_1 x} \quad [\text{Variation in sediment size in the downstream direction}] \quad (2.2)$$

$$Q = Q_0 e^{\alpha_2 x} \quad [\text{Variation in discharge } \alpha_2 \text{ between } 0.001 \text{ to } 0.0078/\text{ km for Indian rivers}] \quad (2.3)$$

$$Q_T = Q_{T0} e^{\alpha_3 x} \quad [\text{Variation in Total sediment load discharge } \alpha_3 \text{ between } 0.0006 \text{ to } 0.002/\text{ km for Indian rivers}] \quad (2.4)$$

Where d =sediment size; d_0 =Sediment size at $x=0$; x =Distance measured in flow direction; Q =Discharge; Q_0 =Discharge at $x=0$; Q_T =Total sediment load discharge; $Q_{T0} = Q_T$ at $x=0$; $\alpha_1, \alpha_2, \alpha_3$ are coefficients.

Combining the Eqs. 2.2), (2.3) and (2.4) with Kondap's relation for width & depth and a sediment transport law, Garde (1982) showed that;

$$S = S_0 e^{(0.178\alpha_3 - 0.426\alpha_2 - 0.713\alpha_1) x} \quad (2.5)$$

Where S_0 and S are slopes at x equal to zero and at any value x .

Thus, depending on the relative values of α_1, α_2 and α_3 it is possible to get a decreasing, increasing, or constant slope in a long reach. The fact has been observed by investigators such as Hack (1962).

2.4 STREAMBED CHANGES DURING THE FLOODS

On several alluvial streams, the stream bed elevation was seen to rise during flood while the bed was lower after the flood receded. On few other streams exactly opposite happenings have been recorded. These changes can be very rapid for example on the Missouri river at Omaha, Nebraska (USA), the bed was found to be scouring at a rate of 0.3 m per minute during a flood. (Garde and Raju 2000).

In the simplest form to understand the process of bed profile variation one has to assess the inflow out flow of sediment discharge in the reach under the consideration.

- a) If the incoming amount or the rate of the sediment upstream of the reach is higher than outgoing from the reach downstream it is obvious that the difference of the two quantities must have been dropped within the length of the reach. This process of rising of the bed level is called Aggradation.
- b) Conversely, if the incoming amount or the rate of the sediment upstream of the reach is lower than outgoing from the reach downstream then the difference of the two quantities must have been fulfilled by picking up the bed materials from within the length of the reach. This process of lowering of the bed level is called Degradation.

2.5 OCCURRENCES OF AGGERADATIONS AND DEGRADATION

2.5.1 AGGRADATION

2.5.1.1 Occurrence of Aggradation

Occurrence of aggradation is the most often observed phenomena on the upstream side of Dams, Barrages and any other disturbances caused by man made features or natural activities like barricade due to land slide. Because of disturbance in the equilibrium state of sediment flow in the stream causing reduction in the bed profile slope the sediment carrying capacity of the flow is weakened, which leads to settling of the sediment contained in the flow (Basically bed load) is retained in the zone upstream to such features.

Other instance of aggradation of river bed is rising of the water level in the Lake or the sea which causes to reduce the slope of the water surface of river leading to a drop in the sediment transporting capacity and the result is aggradation. The situation of aggradation involves lower rate of sediment outflow than the inflow so that temporal gradient of bed level is positive.

In the sediment continuity equation

$$\frac{\partial z}{\partial t} + \frac{1}{(1-\lambda)} \frac{\partial q_t}{\partial x} = 0 \quad (2.6)$$

Where λ = Porosity of the bed; q_t = Rate of sediment inflow per unit width; z = Bed elevation.

The consequences of aggradation more often reduce the conveyance capacity of the channel due to reduction in the flow area.

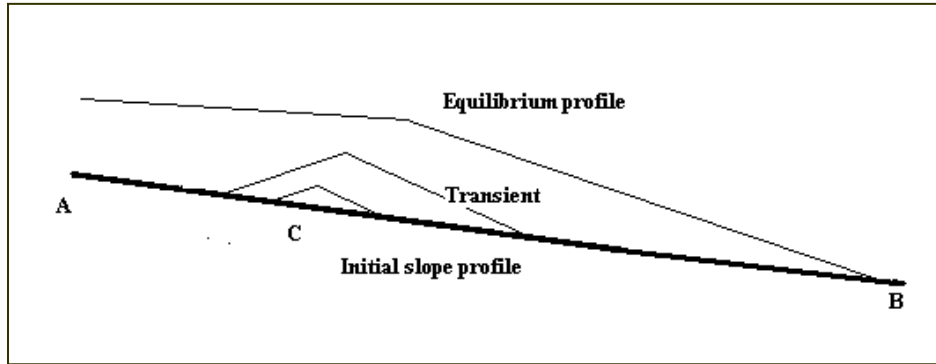


Fig: 2.3 Aggradation and Equilibrium L-Profile

Fig.: 2.3 shows how the process of aggradation reaches to final equilibrium condition. Where the aggradation takes place because of increase in the sediment load in the flow above its transport capacity part of the sediment of the bed load is disposed on the bed of the channel which gradually extends upstream and downstream (as shown in the figure continues) till new profile is attained. This new profile is the equilibrium state of the profile adequate to transport the incoming sediment discharge.

2.5.1.2 Effects of Aggradation

- a) Firstly, aggradation shrinks the active flow area of the river. Consequently, the flow is pushed to spread to wider coverage extending the flood affected area.
- b) In the reservoirs behind the storage dams, the filling up of the reservoir leads to decrease in the depth of the usable water. This necessitates fixing a dead level in the design of such structures.
- c) Bank erosion and river migration problems are more pronounced in the aggrading rivers like lower reaches of the river Brahmaputra.
- d) Aggradation of the river bed restricts the navigational opportunities of the river courses.
- e) The effect of aggradation extends the flood detention period over the flood plain during wet season causing water table to raise causing water logging (Garde and Raju 2000).

2.5.2 DEGRADATION

2.5.2.1 Occurrence of Degradation

Most often degradation of streambed is observed to be lowered downstream of Large Capacity Reservoirs and Pools. Such degradation was observed in Cherry Creek USA where

the extent of lowering being measured was 4.9m. But wherever sound rock exposures are encountered the process of degradation have found retarded (Garde and Raju 2000).

Another prominent location of occurrence of degradation is confluence of two or more rivers. Tributaries, generally steeper than the main stream but carry less run-off cause to lower the bed. At the instances, where the water discharges in the stream increases due to mixing of tributaries with relatively sediment free water discharge enhances the sediment transport capacity degradation occurs subsequently. And one another cause of degradation is because of increase in water surface profile slope as the result of fall in level of a lake. This type of degradation was noted in White river in California USA (Garde and Raju 2000).

Another location of degradation is where river has been started to flow along the cut-off developed in the meandered river (Fig: 2.4). The cut-off shortens the length of the river. In the beginning the cut-off has narrow width which gradually opens to accommodate the discharge through the channel.

In the meandered rivers, the meandering process advances to a stage that the river no more can negotiate a long serpentine path which impose more resistance and take a shortest channel route at an incidence of high flow.

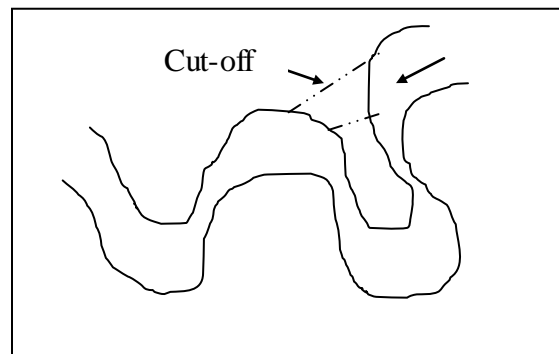


Fig: 2.4 Shortening of the River Flow Path due to Cut-off Development

2.5.2.2 Effect of Degradation

Followings are some of the much pronounced effects both harmful as well as beneficial in the study of River Engineering.

- a) Formation of Hydraulic Jump is apparently pushed downstream in spillways and Barrages due to downstream bed level lowering jeopardizing the stability of the structure. This situation was faced in the Wisconsin River at downstream of Prairie Du San Dam (USA).
- b) Dams constructed in pervious strata exhibit increase seepage head due to increase in level difference between upstream and downstream water. The effect of this could be more uplift and seepage.

- c) While in case of lowering of tail water level downstream of a Power Generation point due to degradation leads to increase in available effective heads for more power generation. This has occurred at Paraire Du Sac Dam in the Wisconsin river USA. And also at Upperborn power house at Munich on the Saalach River.
- d) Lowering of river bed by degradation process increases the capacity of the river channel to carry the flood flow, by lowering the high flood level of the river. Creating an artificial degradation by construction of a big reservoir was a method that had been suggested as a possible solution to the flood problem of the Yellow river in China and Kosi River in the Indian Territory. Lowering of water level due to degradation reduces the height of the ground water table in the adjoining areas.
- e) Lowering of water level may expose pile foundation of bridges abutments and other structures to air and this may lead to deterioration of piling & stability endangering the whole structure. This problem has also been observed in many of the river bridges around on their downstream due to increased flow intensities aggravated by the construction of the bridges.
- f) Degradation also causes lowering of water level at the existing irrigation intakes and thus makes the diversion of water for irrigation more difficult.
- g) Degradation may cause substantial lowering of bed in navigable rivers and in extreme cases locks may become inoperative. Such difficulties have been encountered on a lock at the Wisconsin River (USA) and on the Mause River (Holland) (Garde and Raju 2000).

2.6 MATHEMATICAL MODELLING OF ALLUVIAL RIVERS

Mathematical modelling of fluvial flow, sediment transport and morphological evolution started half a century ago and, to date, a variety of mathematical models have been developed and are in widespread use. However, the quality of mathematical river modelling remains uncertain because of: (a) poor assumptions in model formulations; (b) simplified numerical solution procedure; (c) the implementation of sediment relationships of questionable validity; and (d) the problematic use of model calibration and verification as assertions of model veracity.

The ability to make accurate calculations of fluvial flow, sediment transport, the associated morphological evolution processes and water quality is vital in a period when the concern

over the river environment and the influence of human intervention is increasing. The interaction between sediment and turbulent flow is of fundamental interest in the field of two-phase flow, and modelling the strongly coupled flow– sediment–morphology system provides a problem of considerable interest in computational fluid dynamics. Fluvial sediment transport process has been an increasingly important subject in the fields of water resources engineering, hydrology, geographical, geological, and environmental sciences, and more fundamentally fluid dynamics.

Fluvial sediment transport poses great challenges for river scientists and engineers. The essence of the discipline is the interaction between the fluid (water) and the solid (dispersed sediment particles) phases. The exposure of the fluvial systems to the natural and variable environment (climatic, geological, ecological and social, etc.) adds to the complexity of the process of sediment transport and the resulting morphological evolution of rivers.

The earlier efforts in mathematical river modelling were almost exclusively built on traditional fluvial hydraulics—that is, one-dimensional (1D) and two-dimensional (2D) Saint-Venant equations. The 1D and 2D models are at present widely used in engineering practice; yet the future of mathematical river modelling will undoubtedly be the more advanced full 3D computational fluid dynamics (Cao and Carling 2002).

2.6.1 MAJOR ISSUES OF MATHEMATICAL MODELS FOR ALLUVIAL RIVERS

Mathematical models of alluvial rivers can be categorized into two types: academic and applied. Academic models often deal with ‘how and why’ problems, being devoted to the conceptualization, mathematical formulation, solution (analytical or numerical) and interpretation of the flow, sediment transport, and morphological reaction. Improving the understanding of the mechanism of interaction among water, sediment and morphology is the major purpose of academic models. On the other hand, applied models are entirely concerned with quantitative modelling of the river systems in response to natural changes and human activities (e.g. construction of dams, bridges and flood control works). Currently, the most extensively used fluvial models are either 1D or depth-averaged (shallow) 2D, which are built upon traditional hydraulics principles—that is, Saint-Venant equations (Cao and Carling 2002).

2.6.2 1D AND 2D COMPUTATIONAL HYDRAULICS MODELS

This section mainly focuses on 1D hydraulic model, while most aspects examined here are pertinent to depth-averaged 2D cases. Based on cross-section-averaged variables, 1D numerical modelling of alluvial rivers has been most widely used in the fields of river training, hydropower generation, flood control and disaster alleviation, water supply, navigation improvement, as well as environment enhancement. HEC-6, ISIS-Sediment, GSTAR3D, CCHED, HEC-RAS and Mike11 are examples of a number of mathematical river models developed for fluvial water–sediment–morphology systems. The outputs of these models usually include sediment transport rates, changes in bed elevation and amounts of erosion and deposition throughout the river system considered. It has been recognized that 1D models are appropriate primarily for long-term and long-reach situations, whereas these models have been less successful for local flow–sediment–morphology problems as can be anticipated. Prior studies in this connection have focused on such aspects as flow resistance relations (including parameter identification and optimization), grain sorting, non-equilibrium modules, numerical techniques, and effects of vertical distributions. In the present state of the art, it is a common practice to tune the friction factor and sediment transport formulae to reconcile the computational results with measurements. In this section the fundamental components of 1D model are examined. In particular the effects of simplified continuity equations and the asynchronous solution procedure are addressed, which have rarely been studied before except for a formative comparison by Krishnappan (Cao and Carling 2002).

2.6.3 SIMPLIFIED CONTINUITY EQUATION FOR WATER-SEDIMENT MIXTURE

Alluvial flows over erodible beds can be distinguished from those over fixed beds in that the flow may entrain sediment from the bed or in contrast render the sediment carried by the flow to be deposited on the bed, which usually causes riverbed degradation or aggradation. This aspect is referred to as the bottom mobile (free) boundary problem. At the same time, the water–sediment mixture may have properties (density, etc.) different from clear water. In spite of these apparently known features of erodible-bed alluvial flows, it is often assumed that the rate of bed morphological evolution is of a lower order of magnitude than flow changes with adequately low sediment concentration. Accordingly, in existing 1D and 2D models, the water–sediment mixture continuity equation is almost exclusively assumed to be identical to that for a clear-water flow over a fixed bed without considering the alluvial riverbed mobility. This simplified mixture continuity equation is, in its form, the same as that

in the traditional Saint-Venant equations. The effect of this treatment appears to have been quantitatively addressed only by Correia et al(1992) and discussed by Rahuel(1993) Stevens(1988) claimed that bed mobility is important for complete coupling of water and sediment in discussing Lyn's(1987) analysis. Worm leaton and Ghumman(1994) compared the performance of several simplified models, but exclusive of a fully coupled model on a rigorous basis. Therefore the effect of bed mobility on model performance has not been apparent (Cao and Carling 2002).

2.6.4 SIMPLIFIED EQUATIONS IN ANALYTICAL MODELS

It is interesting to note that there have been several analytical models for channel aggradation and degradation. Whereas providing an easy-to-use approach to evaluating the response of channels to the changing of a simple water and sediment hydrograph or base lowering, these models are based heavily on assumptions. First, the flow is assumed to be quasi-steady, leading to the elimination of local derivatives in the water-sediment mixture continuity and momentum equations. Second, in the momentum equation the nonlinear convective acceleration term is ignored, yielding a diffusion model for bed elevation evolution. A slightly modified type of models, namely hyperbolic models have been developed by partly including the non-linear convective effect using a perturbation technique. Finally in the sediment continuity equation the temporal concentration term is almost exclusively not taken into account in order to make the analytical solution tractable. One of the major difficulties in using these analytical models is the determination of the model coefficients involved. Additionally, it appears not encouraging to use these analytical models with highly variable hydrographs (complicated boundary conditions). More comments on these analytical models can be found in Zanre and Needham (1996). It is necessary to recognize that the momentum equation for the mixture flow over erodible bed differs from that of fixed-bed clear water flow. However, it seems a common practice to reduce it to a clear water flow momentum equation, recognizing the uncertainty inherent in the resistance relationship that must be incorporated to close the momentum equation (Cao and Carling, 2002).

2.6.5 SEDIMENT TRANSPORT FUNCTIONS

A function is necessary to determine sediment transport rate and, for heterogeneous sediments, the size distribution of bed material being transported. A large number of functions have been developed. However, most, if not all, of these functions have been

confirmed using specific laboratory and/or field measurement datasets, and none has been proved to be universally correct. Also it cannot be stated which function is the ‘best’ to use for a given situation. Distinct sediment transport functions will yield different answers, and normally the sediment rates/discharges are more sensitive to the choice of sediment function than the changes of river morphology. The latter concurs with the known feature that the time-scale of changes in flow variables (velocity, depth and sediment discharge, etc.) is normally significantly less than that of bed evolution. This aspect will be recalled later with respect to the asynchronous solution procedure commonly used in current mathematical river modeling practice. Therefore model developers and end-users have to judge the computational results based on their experience and their understanding of the basis on which existing sediment transport functions were derived and validated. Undoubtedly the modelling output is still subject to model developers and end-users—the lack of objectiveness is apparent. Using both laboratory and river datasets, Yang and Wan(1991) compared the performance of several sediment transport functions that are popularly used, and showed that, for river datasets considered, the accuracy in ascending order was Engelund–Hansen(1967), Laursen(1958), Colby(1964), Ackers–White(1973), Einstein(1950), Toffaletti(1969), and Yang(1973). At the same time Yang and Wan (1991) claimed that the rating does not guarantee that any specific function is better than others under all hydraulic and sediment cases. For gravel-bed rivers, the formulae of Einstein, Parker, and Ackers– White were shown to perform reasonably well(Gomez and Church,1989).To measure the applicability of sand transport functions, an ‘applicability index’ was proposed by Williams and Julien(1989) on the basis of river characteristics. These authors argue that developing a universal (at least to a certain extent) procedure to help choose the ‘optimum’ sediment transport function among the large pool of candidates will be one of the most realistic strategies to cope with the uncertainty due to sediment transport functions (Cao and Carling ,2002).

2.6.6 MODEL CALIBRATION AND VERIFICATION/VALIDATION

2.6.6.1 Model calibration

A mathematical river model encompasses a number of parameters to be determined. One primary question is whether there is a unique combination of these parameters. From time to time the same (or similar) results are produced using different sets or combinations of model parameters. Usually there is no way to choose between these sets of parameters, other than to invoke extra-evidential considerations such as symmetry, simplicity, flexibility, personal,

political or metaphysical preferences as well as prejudices and financial considerations. A secondary question arises as to how the overall performance of modeling can be objectively judged in comparison with measurement. This is especially critical for 3D modeling as normally there are many megabytes of numbers (typically with over 50 000 nodes for a real river problem), and it is almost impossible for model developers and end-users to view, assimilate, interpret and present even a small fraction of the output. That way, the judgment of acceptable agreement with measured data is virtually on a basis of a limited portion of information, for example some selected verticals and cross-sections, etc. Known too many model developers and end-users is the fact that it is fairly feasible to reconcile the computed results to measurements within a local area by tuning the various parameters. Thirdly, it is hard to specify the initial conditions, whereas the computation can be sensitively influenced by the initial status in the non-linear systems; therefore the agreement between computed and measured results in general is largely not unbiased but subjective (Cao and Carling, 2002).

2.6.6.2 Model verification and validation

A verified model is useful as a prediction tool because of its demonstrated truth, and implies its reliability as a basis for decision-making. Equally correct is the term 'validation', which usually connotes legitimacy. It can, but does not necessarily denote an establishment of truth. Instead, it indicates the establishment of legitimacy, generally in terms of contracts, arguments, and methods. Validation means making legally valid, granting official sanction to or confirming the validity of something. A valid model contains no known errors or detectable flaws and is internally consistent. Verification is only possible in closed, rather than open systems, in which all components of the system are established independently, and are correct. Its application to natural systems is misleading. Alluvial river models are never closed systems, and therefore it is incorrect to use the term 'verification' for such models. Below are two specific reasons that make alluvial river models open. First, the model requires a number of input parameters that are not completely known. These input parameters are often embedded in turbulent closure modules, boundary conditions, sediment transport and entrainment functions as well as numerical discretization schemes, etc. Second, the observation and measurement of both independent and dependent quantities are laden with inferences and assumptions. Although many inferences and assumptions can, in some cases, be justified with experience, the degree to which the assumptions hold in new and complicated studies can never be established a priori. Alluvial river systems are complicated

in that turbulence is one of the last problems in classic physics, which remains to be solved, and this is further aggravated due to the presence of sediments. It is essential to recognize the restricted sense of the term ‘validation’. Legitimacy, official sanction, or being free of apparent errors and inconsistency does not necessarily mean truth or correctness, although truth or correctness is not precluded. It is misleading if the term validation is used to refer to actual modeling results in any particular realization. It is fairly popular for river modelers to use interchangeably the terms verification and validation. Thus they misleadingly imply that validation establishes model veracity. Even more critically, the term validation is used to suggest that the physical river phenomenon is accurately represented by numerical models. As stated above, there exist a lot of critical problems with the model calibration–verification/validation phases, both logically and practically. The most significant problem comes with the verification/validation phase, where the model is claimed a success. This is, as a matter of fact, committing the basic logic error of affirming the model output. Oreskes et al. describe this as follows ‘To claim that a proposition (or model) is verified because empirical data match a predicted outcome is to commit the fallacy of affirming the consequent. If a model fails to reproduce observed data, then we know that the model is faulty in some way, but the reverse is never the case. Confirming observations do not demonstrate the veracity of a model or a hypothesis, they only support its probability.’ The misuse of the terms verification and validation in mathematical river modeling can be risky with respect to public interests. Often the decision-makers may not be experts in river hydraulics. It is the responsibility of model developers and end-users to correctly inform the decision-makers of what mathematical Models can realistically reflect, and more essentially the degree to which the modeling results can be relied upon (Cao and Carling, 2002).

2.7 REVIEW OF THE EXISTING MODELS PERTAINING TO ALLUVIAL STREAMS

2.7.1 DELFT HYDRAULIC LABORATORY MODEL

DE Varies (1973) developed a mathematical model combining continuity and momentum equations along with Chezy’s equations for alluvial streams. In this model, the two dependent variables $U(x, t)$ and $Z(x, t)$ are computed in two separate steps. In this model, Cunge et al (1980) commented that computational time step cannot be chosen arbitrarily. This model is true for coarse sediment only.

2.7.2 CHEN'S MODEL

Chen (1973) formulated a model based on Saint Venant's continuity and momentum equations of unsteady flow of sediment-laden water. This model is capable of flood and sediment routing in a gradually varied flow channel. He used sediment load functions from Einstein's Bed load function as well as Toffaleti's function. Chen for the first time formulated a mathematical model that included sediment transport for generalized use. His works have proved to be a landmark in the field of open channel modeling for sediment-laden flow (Chen, 1973).

2.7.3 DASS MODEL

Dass (1975) developed multi-stream flow and compound stream flow models by adopting the uncoupled solution procedure to rout water and sediment in non-uniform channels with the capability to simulate bed level changes. The governing equations adopted by Dass are:

$$\frac{\partial Q}{\partial x} + \frac{\partial A}{\partial t} + \frac{\partial A_d}{\partial t} - q_l = 0 \quad (2.7)$$

$$\frac{\partial Q_s}{\partial x} + p \frac{\partial A_d}{\partial t} + \frac{\partial A_s}{\partial t} - q_s = 0 \quad (2.8)$$

$$\frac{\partial Q}{\partial t} + \frac{\partial(\rho QV)}{\partial x} + gA \frac{\partial y}{\partial x} + gAS_f - M_c = 0 \quad (2.9)$$

Where; x =Horizontal distance along the channel; t = Time; Q =Total discharge of sediment laden water; A = Area of available flow; A_d = Area of deposit; q_l = lateral inflow; A_s =Volume of sediment concentration in flow; ρ = Density of sediment laden water; p = Porosity of bed material; q_s = Lateral inflow of sediment; Q_s = Sediment Discharge. S_f = Energy slope; M_c =Factor dependent on bed slope; V = Mean velocity of flow;

However, the validation of the model has been done in a hypothetical channel case (Dass, 1975).

2.7.4 FLUVIAL MODELS (1978 and 1984)

Chang and Hill (1976) developed this model in 1976. The same equations of St. Venant are solved. In the case of aggradation, the deposition is made starting from the lowest point in horizontal layers. A four point implicit finite difference schemes with uncoupled solution procedure is used to solve the equations. Channel width adjustments are used to reflect lateral migration. Manning's equation is used to represent resistance to flow.

He also developed FLUVIAL 11 Model in 1984 which employs a space-time domain in which space domain is represented by the discrete cross-sections along the river reach and the time domain is represented by discrete time steps. The model uses the concept enunciated by Langbein and Leopold that the equilibrium channel represents a state of balance with a minimum rate of energy expenditure along the channel. Chang has considered the bank erodibility or coefficient of bank erosion to predict the bank changes. Fluvial 11 is undoubtedly a promising model for channel changes prediction. However the adoption of empirical bank erodibility factor appears to have constrained its universal applicability and may require considerable calibration efforts. This model cannot be applicable for a river of multi-channel configuration.

2.7.5 HEC-6 MODEL

This model has been developed by W.A. Thomas at Hydrologic Engineering Centre, U.S.A. in 1977. There are five different options provided for the transport of sediment, viz Lausen's equation, Toffaleti's equation, Yang's stream power function, Duboy's equation and $Q_t = f(Q,S)$. The flow equation is the Manning's equation. For numerical solution, uncoupled explicit finite difference scheme is used. Simulation of reservoir sedimentation using HEC-6 was reported to be successful (HEC 2004).

2.7.6 WATER RESOURCES MODELLING FROM DHI WATER AND ENVIRONMENT

MIKE 11 - River and Channel Hydraulics

MIKE 11 is a one-dimensional hydrodynamic software package including a full solution of the St. Venant equations, plus many process modules for advection-dispersion, water quality and ecology, sediment transport, rainfall-runoff, flood forecasting, real-time operations, and dam break modelling.

The software can simulate flow and water level, water quality and sediment transport in rivers, irrigation canals, reservoirs and other inland water bodies. It is an engineering tool

with capabilities provided in a modular framework. It can be applied on numerous applications - from simple design tasks to large forecasting projects including complex structure operation policies. It allows you to integrate your river and floodplain modelling with watershed processes, detailed floodplain representation, sewer systems and coastal processes. MIKE 11 offers links to groundwater codes (Mike 11 User Guide, 1993).

2.7.7 HEC-RAS - (Version-4.0, 2006)

This is the latest version developed by US Army Corps of Engineers at Hydrologic Engineering Center. This is Next Generation of hydrologic engineering software which encompasses several aspects of hydrologic engineering including; river hydraulics; reservoir system simulation; flood damage analysis; and real time river forecasting for reservoir operations. The system is comprised of a graphical user interface (GUI), separate hydraulic analysis components, data storage and management capabilities, graphics and reporting facilities. The HEC-RAS system will ultimately contain three one dimensional hydraulic analysis components (i) Steady flow water surface profile (ii) Unsteady flow simulations (iii) movable boundary sediment transport computations. Apart from this software contains several hydraulic design features. This is capable of importing GIS data or HEC-2 data (Brunner, 2002; HEC-RAS Manual, 2006).

It is an integrated system of software, designed for interactive use in a multi-tasking environment. The system is comprised of a graphical user interface, separate hydraulic analysis components, data storage and management capabilities, graphics and reporting facilities.

The HEC-RAS system will ultimately contain three one-dimensional hydraulic analysis components for:

- Steady flow water surface profile computations
- Unsteady flow simulation
- Movable boundary sediment transport computations

A key element is that all three components will use a common geometric data representation and common geometric and hydraulic computation routines. In addition to the three hydraulic analysis components, the system contains several hydraulic design features that can be invoked once the basic water surface profiles are computed (HEC-RAS Manual, 2006).

The review of existing models indicates that several models are available with different features. All the models use St. Venant's equations and have different sediment predictors, energy slope relations and distribution of aggradation/degradation equations. A natural river has many complexities due to its size, flow variations, concentration of sediment and its properties, engineering works carried out on the river and other geographical, meteorological, social factors. Due to these reasons, no model can claim to have considered all the factors. Therefore, the models cannot have universal applicability. Hence, for modelling a particular river one should be very careful to choose a model, which is applicable according to the characteristics of that river.

Hec-Ras (version 4.0) is latest in the family of the existing models for sediment transport & mobile bed modeling, so in this dissertation it has been envisaged to initiate work on this model to figure out the suitability for the specific purpose as well for specific applicability.

2.8 GENERAL PHILOSOPHY OF THE MODELLING SYSTEMS IN HEC-RAS

HEC-RAS is an integrated system of software, designed for interactive use in a multi-tasking, multi-user network environment. The system is comprised of a graphical user interface (GUI), separate hydraulic analysis components, data storage and management capabilities, graphics and reporting facilities. The system contains three one-dimensional hydraulic analysis components for: (1) steady flow water surface profile computations; (2) unsteady flow simulation; and (3) movable boundary sediment transport computations. A key element is that all three components use a common geometric data representation and common geometric and hydraulic computation routines. In addition to the three hydraulic analysis components, the system contains several hydraulic design features that can be invoked once the basic water surface profiles are computed (Brunner, 2002; Warner, 2002).

2.8.1 OVERVIEW OF HYDRAULIC CAPABILITIES

HEC-RAS is designed to perform one-dimensional hydraulic calculations for a full network of natural and constructed channels. The following is a description of the major hydraulic capabilities of HEC-RAS.

Steady Flow Water Surface Profiles: This component of the modeling system is intended for calculating water surface profiles for steady gradually varied flow. The system can handle a single river reach, a dendritic system, or a full network of channels. The steady flow

component is capable of modeling subcritical, supercritical, and mixed flow regime water surface profiles.

The basic computational procedure is based on the solution of the one-dimensional energy equation. Energy losses are evaluated by friction (Manning's equation) and contraction/expansion (coefficient multiplied by the change in velocity head). The momentum equation is utilized in situations where the water surface profile is rapidly varied. These situations include mixed flow regime calculations (i.e., hydraulic jumps), hydraulics of bridges, and evaluating profiles at river confluences (stream junctions).

The effects of various obstructions such as bridges, culverts, weirs, spillways and other structures in the flood plain may be considered in the computations. The steady flow system is designed for application in flood plain management and flood insurance studies to evaluate floodway encroachments. Also, capabilities are available for assessing the change in water surface profiles due to channel improvements, and levees.

Unsteady Flow Simulation: This component of the HEC-RAS modelling system is capable of simulating one-dimensional unsteady flow through a full network of open channels. The unsteady flow equation solver was adapted from Dr. Robert L. Barkau's UNET model (HEC, 2004). This unsteady flow component was developed primarily for subcritical flow regime calculations.

The hydraulic calculations for cross-sections, bridges, culverts, and other hydraulic structures that were developed for the steady flow component were incorporated into the unsteady flow module. Additionally, the unsteady flow component has the ability to model storage areas and hydraulic connections between storage areas, as well as between stream reaches.

Sediment Transport/Movable Boundary Computations: This component of the modeling system is intended for the simulation of one-dimensional sediment transport/movable boundary calculations resulting from scour and deposition over moderate time periods (typically years, although applications to single flood events will be possible).

The sediment transport potential is computed by grain size fraction, thereby allowing the simulation of hydraulic sorting and armoring. Major features include the ability to model a full network of streams, channel dredging, various levee and encroachment alternatives, and the use of several different equations for the computation of sediment transport.

The model will be designed to simulate long-term trends of scour and deposition in a stream channel that might result from modifying the frequency and duration of the water discharge

and stage, or modifying the channel geometry. This system can be used to evaluate deposition in reservoirs, design channel contractions required to maintain navigation depths, predict the influence of dredging on the rate of deposition, estimate maximum possible scour during large flood events, and evaluate sedimentation in fixed channels (Brunner, 2002 ; Warner 2002; Manual HEC-RAS,2006).

2.8.2 THEORETICAL BASIS FOR ONE- DIMENSIONAL FLOW CALCULATION

HEC-RAS is currently capable of performing one-dimensional water surface profile calculations for steady gradually varied flow in natural or constructed channels. Subcritical, supercritical, and mixed flow regime water surface profiles can be calculated.

Equations for Basic Profile Calculations

Water surface profiles are computed from one cross section to the next by solving the Energy equation with an iterative procedure called the standard step method. The Energy equation is written as follows:

$$Y_2 + Z_2 + \frac{\alpha_2 V_2^2}{2g} = Y_1 + Z_1 + \frac{\alpha_1 V_1^2}{2g} + h_e \quad (2.10)$$

Where: Y1, Y2 = depth of water at cross sections; Z1, Z2 = elevation of the main channel inverts; V1, V2 = average velocities (total discharge/ total flow area); α_1 , α_2 = velocity weighting coefficients; g = gravitational acceleration; h_e = energy head loss; a diagram showing the terms of the energy equation is shown in Fig: 2.5.

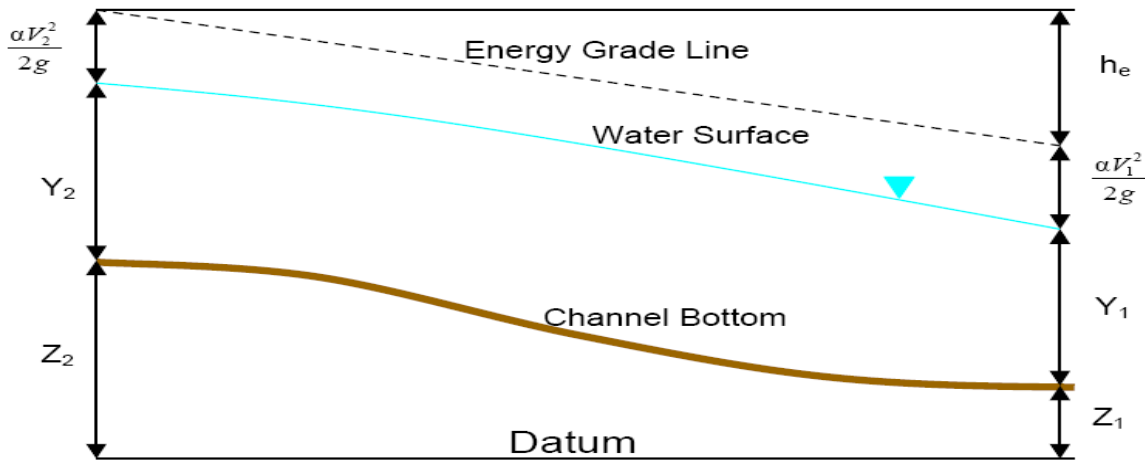


Fig: 2.5 Representations of Terms in the Energy Equation

The energy head loss (h_e) between two cross sections is comprised of friction losses and contraction or expansion losses. The equation for the energy head loss is as follows:

$$h_e = L\overline{S_f} + C \left| \frac{\alpha_2 V_2^2}{2g} - \frac{\alpha_1 V_1^2}{2g} \right| \quad (2.11)$$

The distance weighted reach length, L , is calculated as:

$$L = \frac{L_{lob} \overline{Q_{lob}} + L_{ch} \overline{Q_{ch}} + L_{rob} \overline{Q_{rob}}}{\overline{Q_{lob}} + \overline{Q_{ch}} + \overline{Q_{rob}}} \quad (2.12)$$

Where: L_{lob} , L_{ch} , L_{rob} = cross section reach lengths specified for flow in the left overbank, main channel, and right overbank, respectively ; $\overline{Q_{lob}}$, $\overline{Q_{ch}}$, $\overline{Q_{rob}}$ = arithmetic average of the flows between sections for the left overbank, main channel, and right overbank, respectively

Cross Section Subdivision for Conveyance Calculations

The determination of total conveyance and the velocity coefficient for a cross section requires that flow be subdivided into units for which the velocity is uniformly distributed. The approach used in HEC-RAS is to subdivide flow in the overbank areas using the input cross section n-value break points (locations where n-values change) as the basis for subdivision. Conveyance is calculated within each subdivision from the following form of Manning's equation (based on English units):

$$Q = KS_f^{1/2} \quad (2.13)$$

$$K = \frac{1.486}{n} AR^{2/3} \quad (2.14)$$

Where: K = conveyance for subdivision; n = Manning's roughness coefficient for subdivision
A = flow area for subdivision; R = hydraulic radius for subdivision (area / wetted perimeter)

The program sums up all the incremental conveyances in the overbanks to obtain a conveyance for the left overbank and the right overbank. The main channel conveyance is normally computed as a single conveyance element. The total conveyance for the cross section is obtained by summing the three subdivision conveyances (left, channel, and right).

In general, it is felt that the HECRAS default method is more commensurate with the Manning equation and the concept of separate flow elements (Brunner, 2002).

Composite Manning's n for the Main Channel

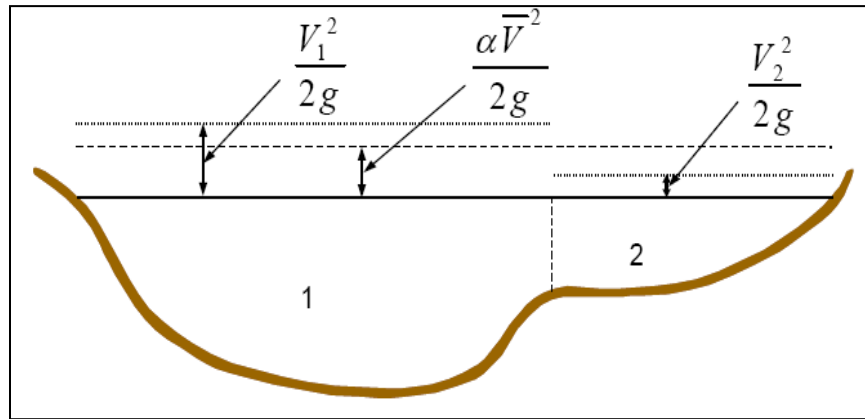
Flow in the main channel is not subdivided, except when the roughness coefficient is changed within the channel area. HEC-RAS tests the applicability of subdivision of roughness within the main channel portion of a cross section, and if it is not applicable, the program will compute a single composite n value for the entire main channel. The program determines if the main channel portion of the cross section can be subdivided or if a composite main channel n value is utilized.

The computed composite n_c should be checked for reasonableness. The computed value is the composite main channel n value in the output and summary tables.

Evaluation of the Mean Kinetic Energy Head

Because the HEC-RAS software is a one-dimensional water surface profiles program, only a single water surface and therefore a single mean energy are computed at each cross section. For a given water surface elevation, the mean energy is obtained by computing a flow weighted energy from the three subsections of a cross section (left overbank, main channel,

and right overbank). Figure 2.6 below shows how the mean energy would be obtained for a cross section with a main channel and a right overbank (no left overbank area).



V_1 = mean velocity for sub area 1, V_2 = mean velocity for sub area 2

Fig: 2.6 Example of How Mean Energy is Obtained

To compute the mean kinetic energy it is necessary to obtain the velocity head weighting coefficient alpha. Alpha is calculated as follows:

Mean Kinetic Energy Head = Discharge-Weighted Velocity Head

$$\alpha \frac{\bar{V}^2}{2g} = \frac{Q_1 \frac{V_1^2}{2g} + Q_2 \frac{V_2^2}{2g}}{Q_1 + Q_2} = \alpha = \frac{2g \left[Q_1 \frac{V_1^2}{2g} + Q_2 \frac{V_2^2}{2g} \right]}{(Q_1 + Q_2) \bar{V}^2}$$

$$\alpha = \frac{[Q_1 V_1^2 + Q_2 V_2^2]}{(Q_1 + Q_2) \bar{V}^2}$$

In general:
$$\alpha = \frac{[Q_1 V_1^2 + Q_2 V_2^2 + \dots + Q_N V_N^2]}{Q \bar{V}^2} \quad (2.15)$$

The velocity coefficient, α , is computed based on the conveyance in the three flow elements: left overbank, right overbank, and channel. It can also be written in terms of conveyance and area as in the following equation:

$$\alpha = \frac{(A_t)^2 \left[\frac{K_{lob}^3}{A_{lob}^2} + \frac{K_{ch}^3}{A_{ch}^2} + \frac{K_{rob}^3}{A_{rob}^2} \right]}{K_t^3} \quad (2.16)$$

Where: A_t = total flow area of cross section; A_{lob} , A_{ch} , A_{rob} = flow areas of left overbank, main channel and right overbank, respectively; K_t = total conveyance of cross section; K_{lob} , K_{ch} , K_{rob} = conveyances of left overbank, main channel and right overbank, respectively.

Friction Loss Evaluation

Friction loss is evaluated in HEC-RAS as the product of S_f and L (Eq: 2.11), where S_f is the representative friction slope for a reach and L is defined by Eq: (2.12). The friction slope (Slope of the energy grade line) at each cross section is computed from Manning's equation as follows:

$$S_f = \left[\frac{Q}{K} \right]^2 \quad (2.17)$$

Alternative expressions for the representative reach friction slope (S_f) in HEC-RAS are as follows:

Average Conveyance Equation

$$\overline{S_f} = \left[\frac{Q_1 + Q_2}{K_1 + K_2} \right]^2 \quad (2.18)$$

Average Friction Slope Equation

$$\overline{S_f} = \frac{S_{f1} + S_{f2}}{2} \quad (2.19)$$

Geometric Mean Friction Slope Equation

$$\overline{S_f} = \sqrt{S_{f1} \times S_{f2}} \quad (2.20)$$

Harmonic Mean Friction Slope Equation

$$\overline{S_f} = \frac{2(S_{f1} \times S_{f2})}{S_{f1} + S_{f2}} \quad (2.21)$$

Equation (2.21) is the “default” equation used by the program; that is, it is used automatically unless a different equation is requested by input. The program also contains an option to select equations, depending on flow regime and profile type (e.g., S1, M1, etc)

Contraction and Expansion Loss Evaluation

Contraction and expansion losses in HEC-RAS are evaluated by the following equation:

$$h_{ce} = C \left| \frac{\alpha_1 V_1^2}{2g} + \frac{\alpha_2 V_2^2}{2g} \right| \quad (2.22)$$

Where: C = the contraction or expansion coefficient

The program assumes that a contraction is occurring whenever the velocity head downstream is greater than the velocity head upstream. Likewise, when the velocity head upstream is greater than the velocity head downstream, the program assumes that a flow expansion is occurring.

Steady Flow Program Limitations

The following assumptions are implicit in the analytical expressions used in the current version of the program:

1. Flow is steady.
2. Flow is gradually varied. (Except at hydraulic structures such as: bridges; culverts; and weirs. At these locations, where the flow can be rapidly varied, the momentum equation or other empirical equations are used.)
3. Flow is one dimensional (i.e., velocity components in directions other than the direction of flow are not accounted for).
4. River channels have “small” slopes; say less than 1:10.

Flow is assumed to be steady because time-dependent terms are not included in the energy equation (Eq: 2.10). Flow is assumed to be gradually varied because Eq: (2.10) is based on the premise that a hydrostatic pressure distribution exists at each cross section. At locations where the flow is rapidly varied, the program switches to the momentum equation or other empirical equations. Flow is assumed to be one-dimensional because Eq: (2.11) is based on the premise that the total energy head is the same for all points in a cross section. Small

channel slopes are assumed because the pressure head, which is a component of Y in Eq: (2.10), is represented by the water depth measured vertically.

The program has the capability to deal with movable boundaries (i.e., sediment transport) and requires that energy losses be definable with the terms contained in Eq: (2.11).

Uniform Flow Computations

For preliminary channel sizing and analysis for a given cross section, a uniform flow editor is available in HEC-RAS. The uniform flow editor solves the steady-state, Manning's equation for uniform flow. The five parameters that make up the Manning's equation are channel depth, width, slope, discharge, and roughness.

$$Q = f(A, R, S, n) \tag{2.23}$$

Where: Q = Discharge; A = Cross sectional area; R = Hydraulic radius; S = Energy slope
n = Manning's n value

When an irregularly shaped cross section is subdivided into a number of sub areas, a unique solution for depth can be found. And further, when a regular trapezoidal shaped section is used, a unique solution for the bottom width of the channel can be found if the channel side slopes are provided. The dependant variables A, and R, can then be expressed in the Manning equation in terms of depth, width and side slope as follows:

$$Q = f(Y, W, z, S, n) \tag{2.24}$$

Where: Y = Depth; W= Bottom width; z = Channel side slope

By providing four of the five parameters, HEC-RAS will solve the fifth for a given cross section. When solving for width, some normalization must be applied to a cross section to obtain a unique solution, therefore a trapezoidal or compound trapezoidal section with up to three templates must be used for this situation.

Cross Section Subdivision for Conveyance Calculations

In the uniform flow computations, the HEC-RAS default Conveyance Subdivision Method is used to determine total conveyance. Sub areas are broken up by roughness value break points and then each sub area's conveyance is calculated using Manning's equation. Conveyances are then combined for the left overbank, the right overbank, and the main channel and then further summed to obtain the total cross section conveyance.

Bed Roughness Functions

Because Manning's n values are typically used in HEC-RAS, the uniform flow feature allows for the use of a number of different roughness equations to solve for n. HEC-RAS allows the user to apply any of these equations at any area within a cross section; however, the applicability of each equation should be noted prior to selection. Manning equation method, one n value or a range of n values is prescribed across the cross section and then the Manning's equation is used to solve for the desired parameter.

Sediment Transport Capacity

The sediment transport capacity function in HEC-RAS has the capability of predicting transport capacity for non-cohesive sediment at one or more cross sections based on existing hydraulic parameters and known bed sediment properties. It does not take into account sediment inflow, erosion, or deposition in the computations. Classically, the sediment transport capacity is comprised of both bed load and suspended load, both of which can be accounted for in the various sediment transport predictors available in HEC-RAS. Results can be used to develop sediment discharge rating curves, which help to understand and predict the fluvial processes found in natural rivers and streams.

Sediment Gradation

Sediment transport rates are computed for the prescribed hydraulic and sediment parameters for each representative grain size. Transport capacity is determined for each grain size as if that particular grain size made up 100% of the bed material. The transport capacity for that size group is then multiplied by the fraction of the total sediment that that size represents. The fractional transport capacities for all sizes are summed for the total sediment transport capacity.

$$g_s = \sum_{i=1}^n g_{si} P_i \quad (2.25)$$

Where: g_s = Total sediment transport; g_{si} = Sediment transport for size class i; P_i = Fraction of size class i in the sediment; n = Number of size classes represented in the gradation.

Because different sediment transport functions were developed differently with a wide range of independent variables, HEC-RAS gives the user the option to select how depth and width

are to be computed. The HEC-6 method converts everything to an effective depth and width. However, many of the sediment transport functions were developed using hydraulic radius and top width, or an average depth and top width. For this reason, HEC-RAS allows the user to designate which depth/width method to use. If the default selection is chosen, then the method consistent with the development of the chosen function will be used. For irregular cross section shapes, HEC-RAS uses the effective depth/effective width or hydraulic radius/top width as the default. Also available for use is the hydraulic depth, which is used to represent the average depth and is simply the total area of the section divided by the top width.

Sediment Transport Functions

Because different sediment transport functions were developed under different conditions, a wide range of results can be expected from one function to the other. Therefore it is important to verify the accuracy of sediment prediction to an appreciable amount of measured data from either the study stream or a stream with similar characteristics. It is very important to understand the processes used in the development of the functions in order to be confident of its applicability to a given stream.

Typically, sediment transport functions predict rates of sediment transport from a given set of steady-state hydraulic parameters and sediment properties. Some functions compute bed-load transport, and some compute bed-material load, which is the total load minus the wash load (total transport of particles found in the bed). In sand-bed streams with high transport rates, it is common for the suspended load to be orders of magnitude higher than that found in gravel-bed or cobbled streams. It is therefore important to use a transport predictor that includes suspended sediment for such a case.

The following sediment transport functions which are also available in HEC-RAS:

- Ackers-White (1973)
- Engelund-Hansen (1967)
- Laursen (1958)
- Meyer-Peter Müller (1948)
- Toffaleti (1969)
- Yang (1973)

These functions were selected based on their validity and collective range of applicability. All of these functions, except for Meyer-Peter Müller(1948), are compared extensively by Yang and Wan (1991) over a wide range of sediment and hydraulic conditions. Results varied, depending on the conditions applied. The Meyer-Peter Müller(1948) and the bed-load portion of the Toffaleti(1969) function were compared with each other by Amin and Murphy (1981). They concluded that Toffaleti(1969) bed-load procedure was sufficiently accurate for their test stream, whereby, Meyer-Peter Müller(1948) was not useful for sand-bed channels at or near incipient. A short description three main sediment predictors is summarized below. (Brunner, 2002; Karamisheva(2006).

Ackers-White(1973): The Ackers-White transport function is a total load function developed under the assumption that fine sediment transport is best related to the turbulent fluctuations in the water column and coarse sediment transport is best related to the net grain shear with the mean velocity used as the representative variable. The transport function was developed in terms of particle size, mobility, and transport.

A dimensionless size parameter is used to distinguish between the fine, transitional, and coarse sediment sizes. Under typical conditions, fine sediments are silts less than 0.04 mm, and coarse sediments are sands greater than 2.5 mm. Since the relationships developed by Ackers-White are applicable only to non-cohesive sands greater than 0.04 mm, only transitional and coarse sediments apply. Original experiments were conducted with coarse grains up to 4 mm; however the applicability range was extended to 7 mm.

This function is based on over 1000 flume experiments using uniform or near-uniform sediments with flume depths up to 0.4 m. A range of bed configurations was used, including plane, rippled, and dune forms, however the equations do not apply to upper phase transport (e.g. anti-dunes) with Froude numbers in excess of 0.8. The general transport equation for the Ackers-White function for a single grain size is represented by:

$$X = \frac{G_{gr} s d_s}{D \left(\frac{u^*}{V} \right)^n} \quad \text{and} \quad G_{gr} = C \left(\frac{F_{gr}}{A} - 1 \right) \quad (2.26)$$

Where: X = Sediment concentration, in parts per part; G_{gr} = Sediment transport parameter ; s = Specific gravity of sediments ; d_s = Mean particle diameter ; D = Effective depth ; u^* = Shear velocity ; V = Average channel velocity ; n = Transition exponent, depending on

sediment size ; C = Coefficient ; F_{gr} = Sediment mobility parameter ; A = Critical sediment mobility parameter

A hiding adjustment factor was developed for the Ackers-White method by Proffitt and Sutherland (1983), and is included in RAS as an option. The hiding factor is an adjustment to include the effects of a masking of the fluid properties felt by smaller particles due to shielding by larger particles. This is typically a factor when the gradation has a relatively large range of particle sizes and would tend to reduce the rate of sediment transport in the smaller grade classes (Brunner, 2002).

Engelund-Hansen(1967): The Engelund-Hansen function is a total load predictor which gives adequate results for sandy rivers with substantial suspended load. It is based on flume data with sediment sizes between 0.19 and 0.93 mm. It has been extensively tested, and found to be fairly consistent with field data.

The general transport equation for the Engelund-Hansen function is represented by:

$$g_s = 0.05\gamma_s V^2 \sqrt{\frac{d_{50}}{g\left(\frac{\gamma_s}{\gamma} - 1\right)}} \left[\frac{\tau_0}{(\gamma_s - \gamma)d_{50}} \right]^{3/2} \quad (2.27)$$

Where: g_s = Unit sediment transport; γ = Unit wt of water; γ_s = Unit wt of solid particles; V = Average channel velocity; τ_0 = Bed level shear stress; d_{50} = Particle size of which 50% is smaller

Yang(1973): Yang's method (1973) is developed under the premise that unit stream power is the dominant factor in the determination of total sediment concentration. The research is supported by data obtained in both flume experiments and field data under a wide range conditions found in alluvial channels. Principally, the sediment size range is between 0.062 and 7.0 mm with total sediment concentration ranging from 10 ppm to 585,000 ppm. Channel widths range from 0.44 to 1746 ft, depths from 0.037 to 49.4 ft, water temperature from 0o to 34.3°Celsius, average channel velocity from 0.75 to 6.45 fps, and slopes from 0.000043 to 0.029 (Yang and Wan ,1991).

Yang (1984) expanded the applicability of his function to include gravel-sized sediments. The general transport equations for sand and gravel using the Yang function for a single grain size is represented by: (Garde and Raju, 2000; Brunner, 2002)

$$\log C_t = 5.435 - 0.286 \log \frac{\omega d_m}{\nu} - 0.457 \log \frac{u^*}{\omega} + \left(1.799 - 0.409 \log \frac{\omega d_m}{\nu} - 0.314 \log \frac{u^*}{\omega} \right) \log \left(\frac{VS}{\omega} - \frac{V_{cr}}{\omega} \right) \quad (2.28)$$

For sand $d_m < 2mm$

$$\log C_t = 6.681 - 0.633 \log \frac{\omega d_m}{\nu} - 4.816 \log \frac{u^*}{\omega} + \left(2.784 - 0.305 \log \frac{\omega d_m}{\nu} - 0.282 \log \frac{u^*}{\omega} \right) \log \left(\frac{VS}{\omega} - \frac{V_{cr} S}{\omega} \right) \quad (2.29)$$

For gravel $d_m \geq 2mm$

Where: C_t = Total sediment concentration, ω = Particle fall velocity, d_m = Med. particle diameter
 ν = Kinematic viscosity, u^* = Shear velocity, V = Average channel velocity,
 S = Energy gradient

2.8.3 THEORETICAL BASIS FOR SEDIMENT CALCULATIONS (HEC, 1981)

Sediment transport rates are calculated for each flow in the hydrograph for each grain size. The transport potential is calculated for each grain size class in the bed as though that size comprised 100% of the bed material. Transport potential is then multiplied by the fraction of each size class present in the bed at that time to yield the transport capacity for that size class. These fractions often change significantly during a time step; therefore an iteration technique is used to permit these changes to affect the transport capacity. The basis for adjusting bed elevations for scour or deposition is the Exner equation.

2.8.3.1 Equation for Continuity of Sediment Material Control Volume

Each cross section represents a control volume. The control volume width is usually equal to the movable bed width and its depth extends from the water surface to the top of bedrock or other geological control beneath the bed surface. In areas where no bedrock exists, an arbitrary limit (called the "model bottom") is assigned (Fig: 2.7). The control volume for cross section 2 is represented by the heavy dashed lines. The control volumes for cross sections 1 and 3 join that for cross section 2, etc.

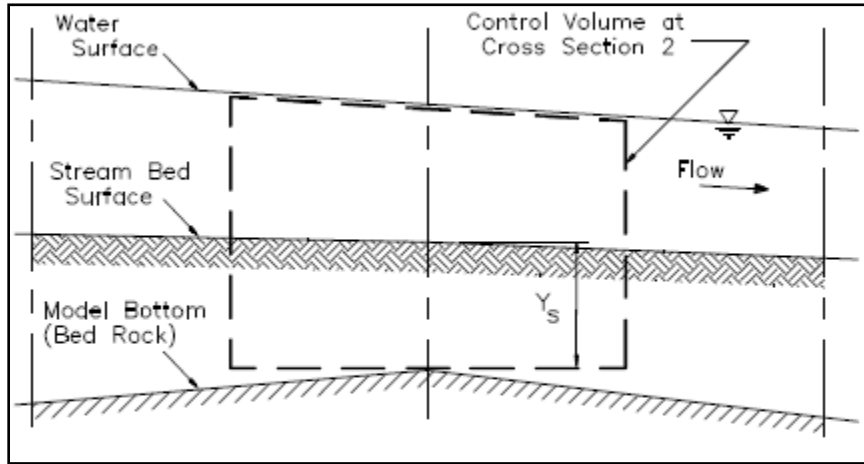


Fig: 2.7 Control Volume for Bed Material

2.8.3.2 Exner Equation

The above description of the processes of scour and deposition must be converted into numerical algorithms for computer simulation. The basis for simulating vertical movement of the bed is the continuity equation for sediment material (Eq: 2.30)

$$\frac{\partial G}{\partial x} + B_0 \frac{\partial Y_s}{\partial t} = 0 \quad (2.30)$$

Where: B_0 = width of movable bed; t = time; G = average sediment discharge rate during time step Δt ; x = distance along the channel; Y_s = depth of sediment in control volume

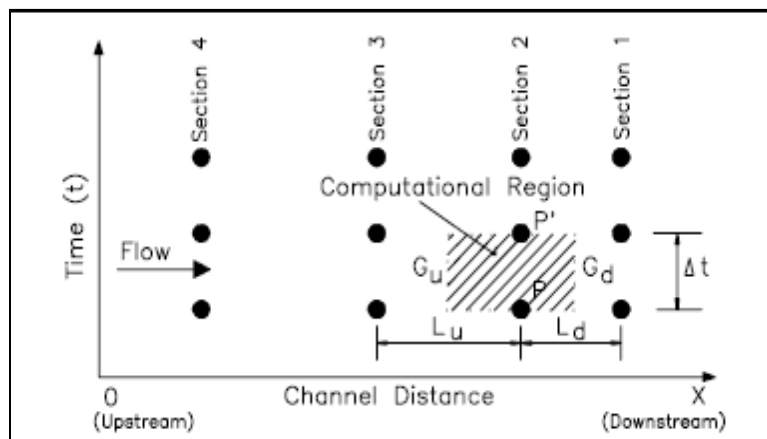


Fig: 2.8 Computation Grid

Equations (2.31) and (2.32) represent the Exner Equation expressed in finite difference form for point P using the terms shown in Fig: 2.8.

$$\frac{G_d - G_u}{0.5(L_d - L_u)} + \frac{B_{sp}(Y'_{sp} - Y_{sp})}{\Delta t} = 0 \quad (2.31)$$

$$Y'_{sp} = Y_{sp} - \frac{\Delta t}{(0.5)B_{sp}} \cdot \frac{G_d - G_u}{L_d + L_u} \quad (2.32)$$

Where: B_{sp} = width of movable bed at point P; G_u , G_d = sediment loads at the upstream and downstream cross sections, respectively; L_u , L_d = upstream and downstream reach lengths, respectively, between; cross sections Y_{sp} , Y'_{sp} = depth of sediment before and after time step, respectively, at point P; 0.5 = the "volume shape factor" which weights the upstream and downstream reach lengths; Δt = computational time step.

The initial depth of bed material at point P defines the initial value of Y_{sp} . The sediment load, G_u , is the amount of sediment, by grain size, entering the control volume from the upstream control volume. For the upstream-most reach, this is the inflowing load boundary condition provided by the user. The sediment leaving the control volume, G_d , becomes the G_u for the next downstream control volume. The sediment load, G_d , is calculated by considering the transport capacity at point P, the sediment inflow, availability of material in the bed, and armoring. The difference between G_d and G_u is the amount of material deposited or scoured in the reach labeled as "computational region" on Fig: 2.8, and is converted to a change in bed elevation using Eq: 2.32.

The transport potential of each grain size is calculated for the hydraulic conditions at the beginning of the time interval and is not recalculated during that interval. Therefore, it is important that each time interval be short enough so that changes in bed elevation due to scour or deposition during that time interval do not significantly influence the transport potential by the end of the time interval. Fractions of a day are typical time steps for large water discharges and several days or even months may be satisfactory for low flows. The amount of change in bed elevation that is acceptable in one time step is a matter of judgment. Good results have been achieved by using 10% of the water depth, whichever is less, as the allowable bed change in a computational time interval. The gradation of the bed material, however, is recalculated during the time interval because the amount of material transported is very sensitive to the gradation of bed material. If transport capacity is greater than the load entering the control volume, available sediment is removed from the bed to satisfy continuity (HEC, 1981).

CHAPTER -3

DESCRIPTION OF STUDY AREA

DESCRIPTION OF STUDY AREA

3.1 INTRODUCTION

Stretching within the basin periphery of 82°E to 97° 50' E longitudes and 25° 10' to 31° 30' N latitudes the river Brahmaputra envelopes a drainage area of 580,000 sq.km and recognized to be one of the most braided channel river. The hugeness of the river system in terms of the drainage area and the lengths it encompasses may be realised from its aerial extent as under.

Table: 3.1 The Aerial Distribution of the Total Drainage Basin.

Country	Basin area	Channel Length
	(Km ²)	(Km)
1. Tibet (China)	293,000	1,625
2. Bhutan	45,000	-
3. India	194,413	918
(a) Arunachal Pradesh	81,424	278
(b) Assam	70,634	640
(c) Nagaland	10,803	-
(d) Meghalaya	11,667	-
(e) Sikkim	7,300	-
(f) West Bengal	12,585	-
4. Bangladesh	47,000	337

Originating in a great glacier mass at an altitude of 5,300 m just south of the lake Konggyu Tso in the Kailas range, about 63 km southeast of Mansarovar lake in southern Tibet at an elevation of 5300m, the Brahmaputra flows through China (Tibet), India and Bangladesh for a total distance of 2880 km, before emptying itself into the Bay of Bengal through a joint channel with the Ganga. It is known as the Tsangpo in Tibet (China), the Siang or Dihang in Arunachal Pradesh (India), the Brahmaputra in Assam (India) and the Jamuna, Padma, and Meghana in Bangladesh.

Before entering India, the river flows in a series of big cascades as it rounds the Namcha-Barwa peak. The river forms almost trough receiving the flows of its tributaries both from North and South. The river, with its Tibetan name Tsangpo in the uppermost reach, flows through

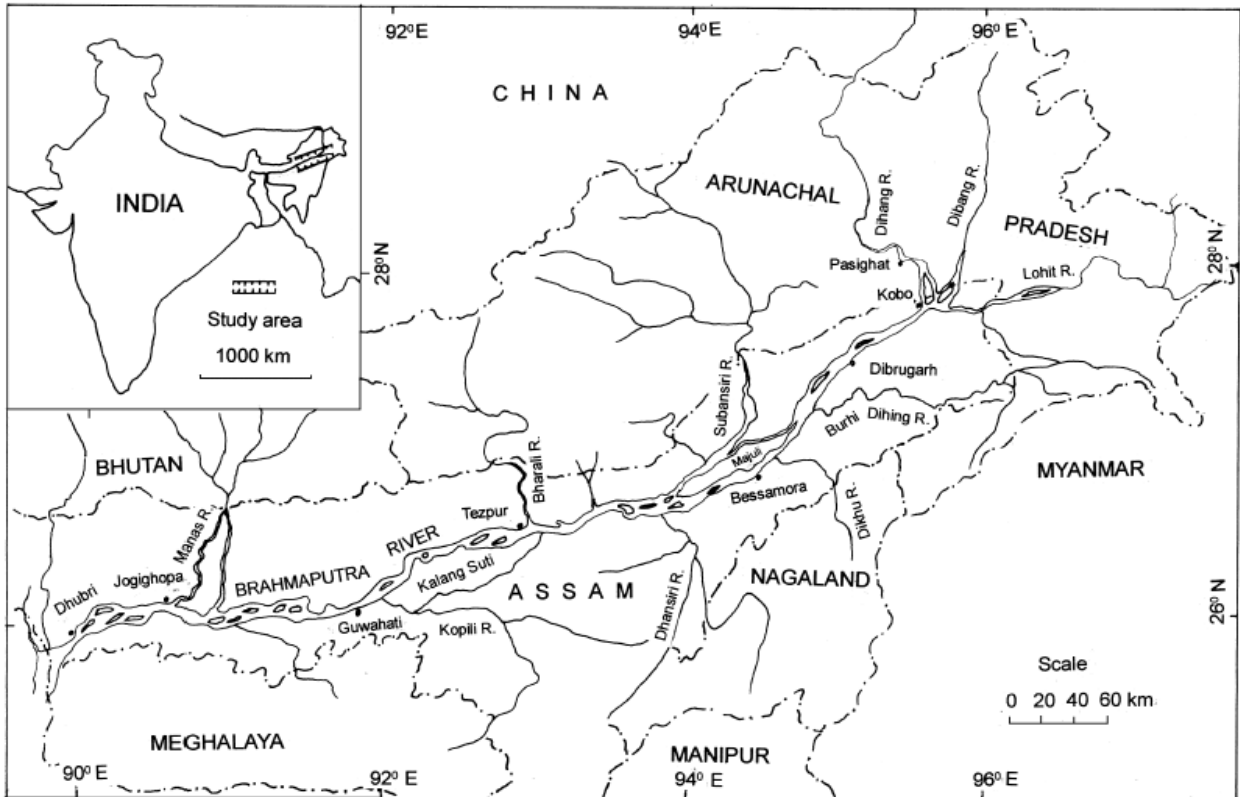


Fig: 3.1 Location Map of the Brahmaputra River in Assam, India (Sarma, 2005)

southern Tibet for about 1,625 km eastward and parallel to tributaries, viz., the Nau Chhu, the Tsa Chhu, the Men Chhu, the Charta Tsangpo, the Raga Tsangpo, the Tong Chhu, the Shang Chhu, the Gya Chhu, the Giamda Chhu, the Po Tsangpo and the Chindru Chhu and the right bank tributaries, viz. the Kubi, the Kyang, the Sakya Trom Chhu, the Rhe Chhu, the Rang Chhu, the Nyang Chhu, the Yarlung Chhu, and the Trulung Chhu join the river along its uppermost reach. At the extreme eastern end of its course in Tibet the Tsangpo suddenly enters a deep narrow gorge at Pe, where in the gorge section the river has a gradient ranging from about 4.3 to 16.8 m/km (Fig. 3.2).

The river enters in India near Tuning in Arunachal Pradesh. After travelling for a distance of 278 km up to Kobo, it meets with two rivers the Dibang and the Lohit in Assam near Kobo. Below this confluence point, the river is known by the name of the Brahmaputra. It passes through Assam into Bangladesh and at last it meets with the Ganga near Goalundo in Bangladesh before joining the Bay of Bengal. Its total length is 2,880 km comprising of 1,625 km in Tibet, 918 km in India and 337 km in Bangladesh. It is also one of the most braided rivers in the world with width variation from 1.2 km at Pandu near Guwahati to about 18.13 km near Gumi few km distances downstream to this point.

Traversing through deep narrow gorges of the Himalayan terrain the Tsangpo takes a southward turn and enters Indian Territory at an elevation of 660 m. The river then enters the State of Assam (India) taking two important tributaries the Dibang and the Lohit. At the exit of the gorge the slope of the river is only 0.27 m/km. At the head of the valley near Dibrugarh the river has a gradient of 0.09-0.17 m/km, which is further reduced to about 0.1 m/km near Pandu (Fig: 3.1). The mighty Brahmaputra rolls down the Assam valley from east to west for a distance of 640 km up to Bangladesh border (Table 3.1).

3.2 LONGITUDINAL SECTION OF THE BRAHMAPUTRA RIVER

The longitudinal section of the Brahmaputra River from its origin to the outfall point is depicted in Fig: 3.2.

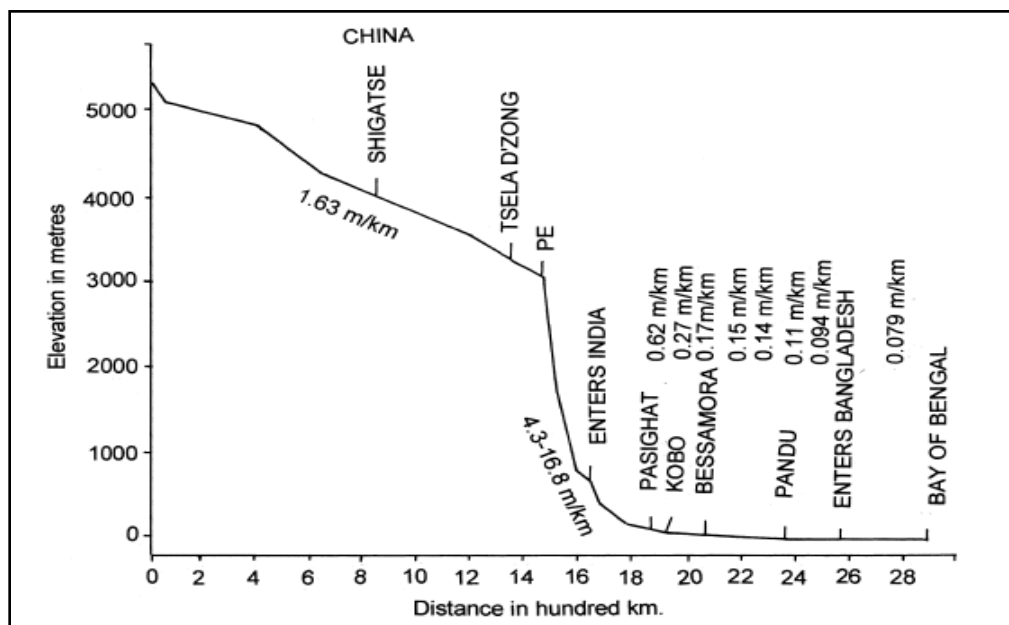


Fig: 3.2 longitudinal profile of the Brahmaputra River (Sarma, 2005)

3.3 THE BRAHMAPUTRA RIVER SYSTEM

The Brahmaputra River, termed as a moving ocean (Wapcos, 1993), is an antecedent snow-fed large Trans-Himalayan river which flows across the rising young Himalayan range. Considerable variations in width, gradient, discharge and channel pattern occur throughout its course. Geologically, the Brahmaputra is the youngest of the major rivers of the world and unique in many respects. It happens to be a major river for three countries, viz., China, India and Bangladesh. The river basin of the Brahmaputra is bounded on the north by the Kailas and Nyen- Chen-Tanglha ranges of mountains; on the east by the Salween river basin and the Patkai range running along the Indo-Myanmar border; on the south by the Nepal Himalayas,

the Naga and Barail ranges and the Meghalaya Plateau; and on the west by the Ganga river basin (Sarma, 2005).

The maximum meridional extent of the basin is 1,540 km along 29°30' N latitude and maximum latitudinal extent is 780 km along 90° E longitude. The total length of the river is 2,880 km (Table 3.1). Several tributaries join the river all along its length. The average annual runoff of the Brahmaputra at Pasighat, Pandu and Bahadurabad in Bangladesh is 186,290,494,357 and 589,000 million cubic metre respectively. The monsoon flow of the Brahmaputra at Tesla Dzong in Tibet is 36.27% of the flow at Pasighat (Wapcos, 1993).

Throughout its course within India, the Brahmaputra is braided with some well defined nodal points where the river width is narrow and restricted within stable banks. All along its course in the valley, abandoned wetlands and back swamps are common. The river carries about 735 million metric tons of suspended sediment loads annually.

The Indian section of the Brahmaputra River receives innumerable tributaries flowing down the northern, north-eastern and southern hill ranges. The mighty Brahmaputra along with the well-knit network of its tributaries controls the geomorphic regime of the entire region, especially the Brahmaputra valley. In the north, the principal tributaries are the Subansiri, the Jia Bhareli, the Dhansiri, the Puthimari, the Pagladiya, the Manas and the Champamati. Amongst these, the Subansiri, the Jia Bhareli and the Manas are the Trans-Himalayan Rivers. The principal south bank tributaries are the Burhi Dehing, the Disang, the Dikhow, the Dhansiri (south), the Kopili and the Krishnai.

It is observed that three Trans-Himalayan tributaries, the Subansiri, the Jia Bhareli and the Manas on the north have a basin more than 10,000 km², i.e., only two south bank tributaries namely the Dhansiri and the Kopili form a basin area more than 10,000 km². The Manas River combined with the Aie and the Beki rivers drains biggest area of 41,350 km². The 442 km long Subansiri River and the 360 km long Burhi Dehing River are considered longest, respectively, among the north-bank and south bank tributaries (Water Year book, CWC, 2002). In terms of the average annual discharge, the Subansiri carries a discharge of 755-771 m³/sec, which ranks first among all the important tributaries. The Jia Bhareli and the Manas in the north carrying an average annual suspended sediment load of 2,013 ha.m and 2,166 ha.m, respectively, are the leading rivers in the case of sediment discharge (11). Of all the north and south bank tributaries, as many as fourteen have sediment yields in excess of 500 tons/ km²/year, the highest being 4,721 tons/km² /year (Sankhua,2006).

3.4 HYDROLOGIC AND PHYSIOGRAPHIC CHARACTERISTICS OF THE BRAHMAPUTRA RIVER

The statistical details of the river are described below (Sankhua, 2006):

(a) Total basin area from its source to its confluence with Ganga at Goalundo in Bangladesh	580,000 km ²
(i) Basin area within Tibet	293,000 km ²
(ii) Basin area in Bhutan and India	240,000 km ²
(iii) Basin area in Bangladesh	47,000 km ²
(b) Length from its source to outfall in Bay of Bengal	2,880 km
(c) Gradient	
(i) Reach within Tibet	1 in 385
(ii) Reach between Indo-China border and Kobo in India	1 in 515
(iii) Reach between Kobo and Dhubri	1 in 6,990
(iv) Reach within Bangladesh	
First 60 km from Indian Border	1 in 11,340
Next 100 km stretch	1 in 12,360
Next 90 km stretch	1 in 37,700
(d) Observed discharge	
(i) Maximum observed discharge at Pandu (on 23.8.1962)	72,727 m ³ /sec
(ii) Minimum observed discharge at Pandu (on 20.2.1968)	1,757 m ³ /sec
(iii) Average dry season discharge at Pandu	4,420 m ³ /sec
(iv) Normal annual rainfall within basin ranges between 2,125 mm in Kamrup District of Assam and 4,142 mm in Tirap district of Arunachal Pradesh.	

3.5 GEOLOGY AND GEOMORPHOLOGY

The Brahmaputra basin in India, comprising of varying geologic and geomorphic characteristics, represents its peculiar physiographic make-up. The basin is bounded by the eastern Himalayas on the north and east, the Naga-Patkai ranges on the northeast and Meghalaya Plateau and Mikir hills on the south. The region can be geologically and tectonically divided into four major zones, viz. the Himalayan folded and Tertiary hills and mountains, the Naga-Patkai ranges, the Meghalaya Plateau and Mikir hills and the Brahmaputra valley in Assam.

The Himalayan zone comprises of three topographic units that rise progressively to the north. The lowermost ranges, called sub-Himalayas with an average elevation of 1,000 m, consist mainly of Tertiary sand stones, and are conspicuous by the presence of many raised, relatively young terraces (Goswami and Das, 2000). The middle Himalayas, having an

average elevation of 4,000 m are underlain by lower Gondwana (Palaeozoic) deposits comprising shales, slates, and phyllites overlain by a thick horizon of basaltic rocks. The greater Himalayas with an average elevation of 6,000 m consist primarily of granites and gneisses (Goswami and Das, 2000). The Himalayan Mountains with their syntaxial N-E bends originated out of the Tethyan Geo-synclin) and are essentially composed of loose sedimentary rocks. The sub Himalayas and the lower Himalayas are characterized by piedmont zones, low discontinuous ridges, low linear ridges, high rugged hills and upland valley depressions.

The Patkai-Naga ranges stand on the eastern and south-eastern border of the Brahmaputra valley in Assam. These ranges, with an average elevation of 1,000 m, are composed of Tertiary sediments and characterized by the presence of a large number of active faults. This zone consists of piedmont plains, anticlinal ridges and synclinal valleys with terraced alluvial fills, undifferentiated sharp ridges and narrow valleys, upland valley depressions and plateau remnants. The Meghalaya plateau and the Mikir hills attaining an elevation ranging from 600 m to 1,800 m are made up primarily of gneisses and schist. This part, being a rigid mass, belongs to the Deccan plateau of the stable Indian peninsular block of Pre-Cambrian age. It is characterized by plateau remnants, inselbergs, deeply dissected uplands with faulted monoclines of Tertiary cover, denuded hills, basement controlled structural ridges covered with Tertiary rocks and upland valley depressions (Sankhua, 2000).

The Brahmaputra valley in Assam, on the other hand, is underlain by recent alluvium approximately 200-300 m thick, consisting of clay, silt, sand, and pebbles. The valley is developed over the fore deep in between the peninsular mass and the Tethyan geosynclines. The fore deep is characterized by some complicated tectonic features represents a series of faults and thrust extending in the NE-SW direction from the eastern margin of the Meghalaya plateau across the North Cachar Hills to Tirap District of Arunachal Pradesh. These thrusts are originated at the time of the late Himalayan-Patkai-Naga Hills orogeny and pushed the tertiary deposits into folds and faults. The fore deep is believed to be under the sea till the sub-recent period received deposits during all the periods of the tertiary and quaternary ages. The tertiary deposits consist mainly of sand stones, shale, grit, conglomerate and lime stones (Sankhua, 2000).

Towards the close of the Pleistocene period, alluvium began to be deposited in the form of sand, pebbles and gravels especially along the northern foothills of the Brahmaputra valley. These valley deposits of reddish brown sandy clay with some pockets of unasserted pebble,

cobble, sand and silt have been identified as older alluvium. The tertiary beds of the valley are overlain by a thick layer of newer alluvium composed of sand, silt and clay, which are being brought down from the rising Himalayas in the north, the Patkai Naga ranges in the east and south-east and the Meghalaya plateau in the south by numerous tributaries of the Brahmaputra. The characteristic geological and tectonic framework coupled with structural complexities has rendered the Brahmaputra basin geo-morphologically a most complicated one. A variety of landform under varied climatic conditions has formed over the geologic and tectonic base of the region. The peri-glacial, glacio-fluvial, and fluvial processes are dominantly operative in the basin at varying altitudes (Sankhua, 2006).

The higher elevations of the Himalayas experience peri-glacial and glacio-fluvial erosion and deposition. The bare relief of the sub-Himalayas and greater Himalayas suffer from immense sheet erosion owing to peri-glacial solifluction. The low hill ranges with hot and humid climate and heavy rainfall concentrated to a few months of the year experience solifluction, sheet erosion and landslides.

The incidence of landslides is high in the Himalayan foothills, where heavy rainfall, high seismicity and toe cutting of hill slopes by the streams are most frequent. Heavy rains often loosen soil and the soft rocks of the young Himalayan ranges. Rainwater percolates through joints, fractures, foliations, and pores of rocks and soils and finally makes them loose and heavy, which cause heavy slope failure. Fluvial processes are, on the other hand, significantly dominant on the valley bottoms and plains where alluvial deposition takes place due to erosion of the higher surface by rivers and flooding in the valleys. The Erosional and depositional processes conspicuously intensified by copious rainfall and frequent seismic movements, however, play a dominant role in creating various fluvial-geomorphic environments in the basin (Sankhua, 2006).

3.6 CHANNEL PROCESS

The Brahmaputra River in India forms a complex river system characterized by the most dynamic and unique water and sediment transport pattern. The Brahmaputra is the fourth largest river in the world (Goswami and Das, 2000). The water yield from per unit basin area is among the highest of the major rivers of the world. The Jia Bhareli, a major tributary, carries a mean annual water discharge in the order of $0.0891 \text{ m}^3/\text{sec}/\text{km}^2$. As estimated by Goswami (1982), the Brahmaputra yields $0.0306 \text{ m}^3/\text{sec}/\text{km}^2$ at Pandu. As regards sediment transport, the river has also set records in carrying large volumes of sediment. The high

intensity of monsoon rains, easily erodible rocks, steep slopes, and high seismicity contribute a lot by rendering the river a heavily sediment-laden one. Thus, the Brahmaputra becomes one of the leading sediment carrying rivers of the world. Amongst the large rivers of the world, it is second only to the Yellow river in China in the amount of sediment transport per unit of basin area (Goswami and Das, 2000).

The Brahmaputra is a uniquely braided river of the world. Although braiding seems to be best developed in rivers flowing over glacier outwash plains or alluvial fans, perfect braiding is also found to occur in large alluvial rivers having low slope, such as the Brahmaputra in Assam (India) and Bangladesh or the Yellow River in China. The Assam section of the Brahmaputra River is in fact, highly braided and characterized by the presence of numerous lateral as well as mid channel bars and islands (Goswami and Das, 2000).

The high degree of braiding of the Brahmaputra channel near Dibrugarh and downstream of Guwahati is indicated by the calculated braiding indices of 5.3 and 6.7 respectively for the two reaches, following the method suggested by Brice (1964). A braiding Index of 4.8 for the entire Assam section of the river calculated on the basis of satellite data of 1993 also suggests a high degree of braiding of the Brahmaputra River (Sankhua, 2006).

The basin with varied terrain characteristics and being an integral part of the monsoonal regime of south-east Asia shows a marked spatial variation in the distribution of precipitation. The rainfall in the Teesta valley varies from 164 cm in the south to 395 cm in the north. The average annual rainfall in the lower Brahmaputra valley is 213 cm while the same in the north-eastern foothill belt is 414 cm. The basin as a whole has the average annual rainfall of 230 cm with a variability of 15-20%. The Himalayan sector receives 500 cm of rainfall per year, the lower ranges receiving more than the higher areas (Goswami and Das, 2000). During the monsoon, months of May to October receive about 12% of the annual total.

In the sub-Himalayan belt soils with little depth developed over the Tertiary sand stones generally belong to red loam, laterite, and brown hill soil type with admixtures of cobbles and boulders. The greater part of the Brahmaputra valley is made up of new alluvium of recent deposition overlying Tertiary, Mesozoic and Archaean bedrocks. Along the piedmont zone, there occur some patches of older alluvium extending along the interfluves of the tributaries flowing from the Himalayan foothills. The soils of the Meghalaya plateau and the Mikir Hills in the south are of laterite and loamy silt and fine silt types.

In general, braiding in the Brahmaputra follows the mechanism of central bar type of braid

formation. During high flow, a central bar is deposited in the channel and gradually the bar accretes vertically to the level of the floodplain. It also builds on the downstream end through deposition of bed load material due to the slack water occurring behind the bar. The bar growth causes a decrease in total cross-sectional area leading, thereby, to the instability of the channel. Lateral erosion then follows on one or both the banks. Through repetition of this process in the divided reach, a well developed braided reach with multiple sandbars and islands is produced (Sankhua, 2006).

In the Assam section of the river, the presence of such nodes of stable banks is found to effect the formation and location of the bars. There are nine nodal reaches of narrow constriction at various locations along the Brahmaputra, which are at Murkongselek (4.8 km), Disangmukh (5.10 km), downstream of Jhanjimukh (3.75), upstream of Dhansiri north (4.0 km), downstream of Dhansirimukh (4.4 km), upstream of Tezpur (3.6 km), Pandu, Guwahati (1.2 km), Sualkuchi (2.4 km) and Pancharatna (2.4 km). Since banks are relatively stable in these reaches, the river scours deeper to accommodate the flood discharge. The scoured debris is then deposited in the channel immediately downstream from the narrow section. As a result, the channel becomes wider and bars and islands are produced. Formation of bars causes reduction in cross sectional area and the river, therefore, cuts its banks laterally to accommodate the discharge. Thus, the downstream of the nodes intense braiding develops resulting in channel widening through continuous migration of both banks of the Brahmaputra (Sankhua, 2006).

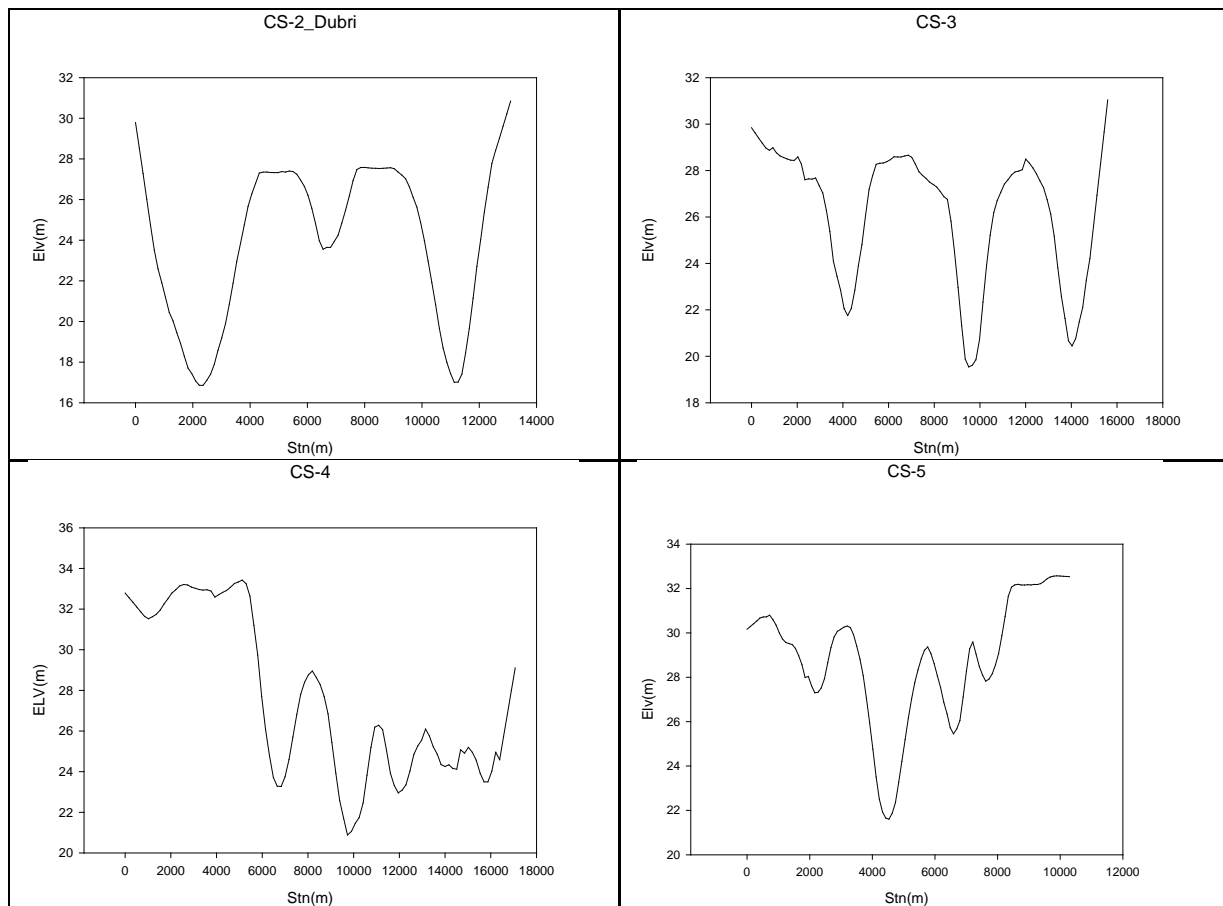
As reported from the studies carried out on braided rivers of the world, the major factors thought to be responsible for braiding and bar formation are steep channel gradient, high erodibility of bank materials, great variability in discharge, overabundance of load, and aggradation of the channel bed. In case of the Brahmaputra River in Assam bar formation and channel division are owing to a combination of factors like high variability in discharge, excessive sediment transport, easily erodible bank materials and aggradation of the channel. Being the fourth largest river in the world with an average discharge of 19,830 m³/sec at its mouth, the Brahmaputra carries 82% of its annual flow at Pandu (Assam) only during the rainy season from May to October. The maximum and minimum mean monthly flows in the river during 1990-2002 are 48,160 m³/sec and 3,072 m³/sec, respectively. On an average, therefore, the maximum flow is more than fifteen times the minimum (Goswami and Das, 2000).

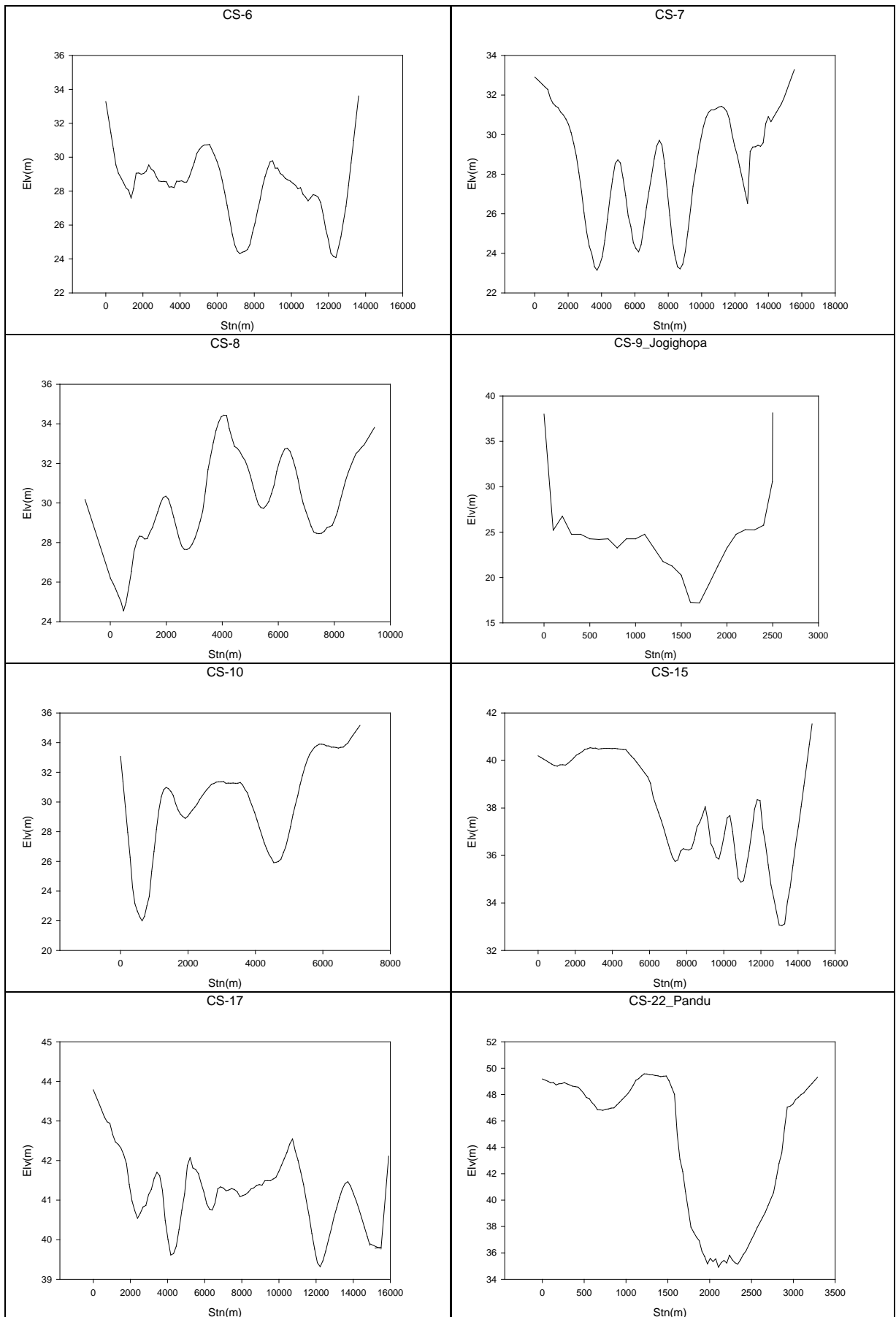
High variability in discharge of the river is mainly caused by seasonal rhythm of the monsoon

and the freeze-thaw cycle of the Himalayan snow. As regards the pattern of sediment transport, the river has the record of carrying excessive sediment load which is believed to be one of the important factors responsible for braiding.

3.7 STUDY AREA

The area under Indian Territory encloses a 622.73 km river stretch encompassing 64 no. Of different cross section with kobo on the northern **most (65no.)** To Dhubri on the south (2no.). The cross-section no 1. In the series lies in the territory of Bangladesh. The area under the consideration for the present study encloses a 622.73 km river stretch of Brahmaputra encompassing 64 no. Of different cross section with Kobo on the northern most (65no.) to Dubri on the south (2no.).The plan of River Brahmaputra with depiction of study reach has been shown in Fig: 3.4.





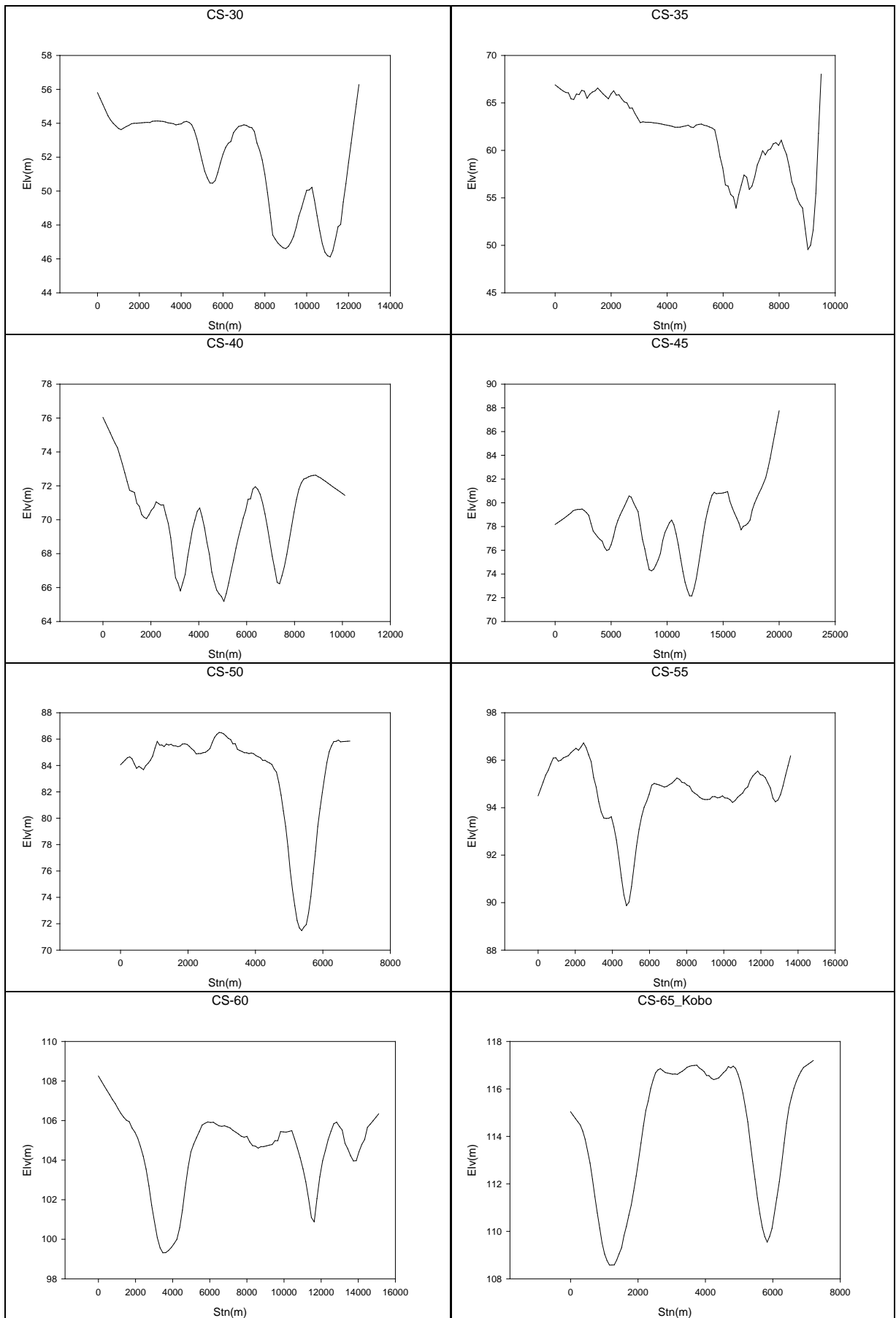


Fig: 3.3. Measured cross section for different cross sections along the 622 km river reach taken between the year 1982 to 1997

One can easily figure out the significant variations in width as well as bed configuration in general. Widths of the channel vary ranging from 3 km to 20 km. In an average width is around 6 km in the study reach. Visualizing the cross-sections in Fig: 3.3 , it is evident that some cross-sections are exhibiting incised channel forms whereas some showing wide shallow river pattern indicating that bed configurations of the study reach are highly irregular ranging from rock outcrops to fine alluvial bed. The hydraulic geometry data of 64 number of cross section were plotted to view the general tendencies of variation of the cross section profile in the temporal increments. The plotting reveal a very drastic changes in the cross profiles for some of the sections. Since, the successive stations along a cross section are very widely apart compared to the vertical variation of the ground levels the non submergible banks are not easily discernible. The longitudinal profile (Thalweg) for the study reach gives the idea that the reach is by a large aggrading in nature. The bed level variations from Year-1993 to Year -1997 are highly irregular which suggests that 1 D hydraulic modelling should be applied only for relatively long stretch of the river. In this case it should be at least above 100 km to predict longitudinal thalweg profiles.

At Pandu, the river carries an average suspended load of 402 million metric tons. A river with such gigantic water and sediment discharge magnitudes represents its most dynamic fluvial regime. Its large alluvial channel having a width of 6 to 17 km is, therefore, marked by braiding, rapid aggradation and bank line changes (Sankhua, 2006). The longitudinal slope of reach Pandu to Jogighopa is 0.11m/km (Sarma, 2006)

CHAPTER -4
FORMULATION AND DEVELOPMENT
OF FLOW SIMULATION MODEL

FORMULATION AND DEVELOPMENT OF FLOW SIMULATION MODEL

4.1 INTRODUCTION

The global hierarchal rank of the river Brahmaputra is recognized to be third in sediment discharge, fifth in fluvial discharge and eleventh in size of the total drainage area (Sarma, 2005). Being one of the youngest river system with varied nature of drainage areas from snow peak mountains to lower flood valley of the Assam and the complexity exuberated by high sediment yielding geological surfaces it has been a very formidable task to quantify all the embodied “fluvial-river-morphological characteristics” to explain the ever changing characteristics of the river. The high degree of braiding(Goswami and Das, 2000) of the parent channel, more emphatically, when it open to the Assam valley because of still a steep valley gradient the fall in the hydraulic competency due to braiding is reflected to sediment transportation and downstream aggradation. Very unstable hydraulic geometry and hence the river channel morphology in the spatial and temporal space hinders the formulation of an idealised hydraulic models. Moreover, the researches and the literatures on braided channels are less compared to single channel in alluvium region. Due to high non linearity involved in the interdependencies of the hydrological – morphological and hydraulic parameters, majority of relationships developed relating hydrological and hydraulic parameters are empirical.

The river Brahmaputra is one of the rivers which are well under the observation of different stake holders. The sediment discharges and flood discharges at certain locations have been continuingly recorded and the river cross sections surveyed. Still, the limitation in the human capacity, instrumentation, the ambience of the measurement and the risk involved, the actual data acquisition often remain off-set by errors. The importance of the information that could be derived from the analysis of the data is very high in the design, management and future risk and hazard strategies.

Taking in to account the situation as described above, the present study is a formative attempt to implement a flow simulation model HEC-RAS for the study reach. The algorithms established by the researchers /modellers in the various literatures advocate success of flow simulation model application depends on the size of the data covering wide patterns of

phenomena .More the data sets better is the results' reliability. In the assessment of the available data, data sorting, data generation supporting further analysis, modelling and deriving inferences HEC-RAS has been known to be robust. As the technique is a data driven model requiring gamut of data patterns representing the actual phenomena to accommodate all the possibilities within the patterns of independent and dependent variables.

In the near future, more work with more expertise on this line would be enhancing the dependability on the strength of the technique in the more complex analysis.

The study has been carried out on the following data sets and the area.

- a) Study Stretch of the river channel (from Kobo to Dhubri) 622.73 km
- b) No. of the river cross sections (year 1988, 1992, 1993 and 1997) 65.no
- c) Hydrological Data(Jogighopa-Pandu) 2003 to 2007

4.2 DATA SOURCES AND DATA TYPES

4.2.1 HYDROGRAPHIC DATA

Morpho-metric data: the reduced levels of the river cross-sections of post-monsoon period of 64 stations have been collected from the Brahmaputra Board, Government of India. The surveying time varies from 1957 to 1997. But for the present modeling, the most current available cross sectional data for the year 1988, 1992, 1993 and 1997 has been adopted. This data assumed to represent the most recent cross section configuration.

4.2.2 DISCHARGE AND STAGE DATA

Discharge and stage data of the river Brahmaputra collected for two along the main river channel cross-sections from Central Water Commission (CWC), Assam Flood Control Department and Brahmaputra Board have constituted main data resource to the model implementation. The length of data record used was from year 2003 to 2007.

4.2.3 SEDIMENT DATA

Sediment data obtained from the monthly suspended sediment data in respect of Jogighopa and Pandu for the years from 2003 to 2007 and average monthly discharge (cumecs) and monthly average suspended sediment yield of major tributaries processed for all the years from 1993 to 1997 have been used in the study. Characteristic sediment particle size distribution at the cross-sections was collected from CWC.

4.3 PRE- PROCESSING OF HYDRO GRAPHIC DATA

As a certain degree of uncertainty is associated with hydrologic frequency distributions on relative time scales, the sensitive response function of the river / stream as Stage - Discharge (G-Q) relationships , Sediment discharge Rating ($Q_t - Q$) curves, Stream flow Hydrographs, etc needs to adequately represented from the observed field data. The Brahmaputra River Basin in terms of its complexity calls for well-defined response models. In the study, some of the significant steps followed are outlined as:

- (i) The first step is the abstraction of outliers and errors in the data sets. Conceptual or statistical tools as regression and curve fitting were implemented on the variables pertaining to specific river / stream to identify the irrational points; they were either discarded or rectified based on the earlier trends or pattern of the data.
- (ii) The datasets are then sorted strictly on a base time scale. Monthly average record data sets pertaining to the main river are chosen for the study, the period between November 2003 and October 2007 has been adopted as the base time scale for the framing of the channel response parameters and the model formulation.

4.4 DATA GENERATION

In numerical river modelling one of the most important parameter is upstream river boundary condition. For the Brahmaputra River the only available flow data are located in the middle reach of the main river (Pandu, at river cross section 22 and Jogigopa cross section 9).

The upstream river location is located at a river cross section 65 place called Kobo. Therefore, using the drainage-area ratio method, flow measured at Pandu site was transferred to Kobo site. The remaining flow at Pandu was used as internal boundary in the numerical model.

In this process, with the help of ARCHYDRO 9 extension of ARCGIS 9.3, the drainage area of the two gauging sites has been delineated; i.e. drainage area which is contributing for gauging station at Pandu and drainage areas contributing for gauging site at Kobo. See Fig. For both station the contributing drainage area has been calculated and used for generation of upstream boundary condition. The drainage area contributing for station at Kobo has been found to be 175862 km² and for Pandu 345667 km².

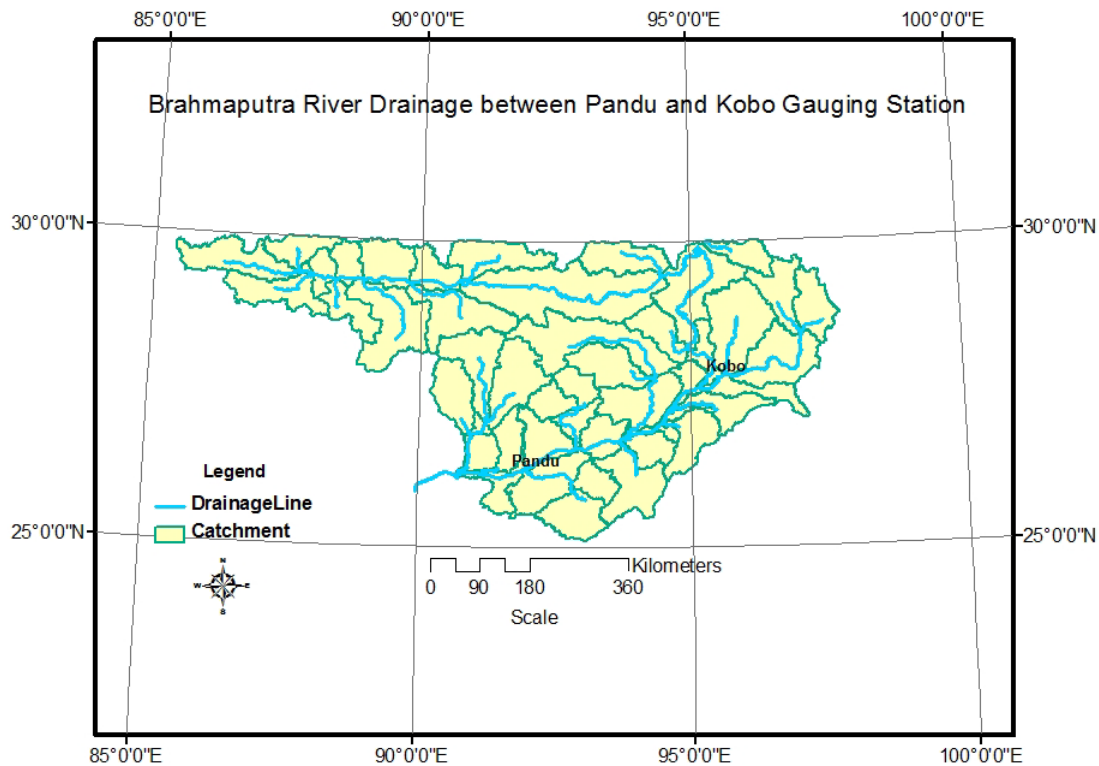


Figure showing the contributing area for Pandu and Kobo gauging stations; Developed from 90m resolution SRTM DEM.

4.5 DEVELOPMENT OF FLOW SIMULATION MODEL IN ‘HEC-RAS’

The system contains three one-dimensional hydraulic analysis components for: (1) steady flow water surface profile computations; (2) unsteady flow simulation; and (3) movable boundary sediment transport computations. A key element is that all three components will use a common geometric data representation and common geometric and hydraulic computation routines. In addition to the three hydraulic analysis components, the system contains several hydraulic design features that can be invoked once the basic water surface profiles are computed.

HEC-RAS is designed to perform one-dimensional hydraulic calculations for a full network of natural and constructed channels. Theoretical basis for one-dimensional calculation in HECRAS is briefed in chapter-2.

4.5.1 DATA REQUIREMENTS AND INPUT

The basic input data required for sedimentation analysis by HEC-RAS model can be grouped into four categories as below.

4.5.1.1 Geometric Data

Geometry of the physical system is represented by cross sections, specified by coordinate points (stations and elevations), and the distance between cross sections. Hydraulic roughness is measured by Manning's n-values and can vary from cross section to cross section. At each cross section n-values may vary vertically and horizontally. The program raises or lowers cross-section elevations to reflect deposition or scour and thus generates data during the course of its execution.

The River System Schematic

The river system schematic is required for any geometric data set within the HEC-RAS system. The schematic defines how the various river reaches are connected, as well as establishing a naming convention for referencing all the other data. The river system schematic is developed by drawing and connecting the various reaches of the system within the geometric data editor (Fig: 4.1). It is required to develop the river system schematic before any other data can be entered.

Each river reach on the schematic is given a unique identifier. As other data are entered, the data are referenced to a specific reach of the schematic. For example, each cross section must have a "River", "Reach" and "River Station" identifier. The river and reach identifiers defines which reach the cross section lives in, while the river station identifier defines where that cross section is located within the reach, with respect to the other cross sections for that reach.

[Brahmaputra River Schematic plot\(c/s2-c/s65\)](#)

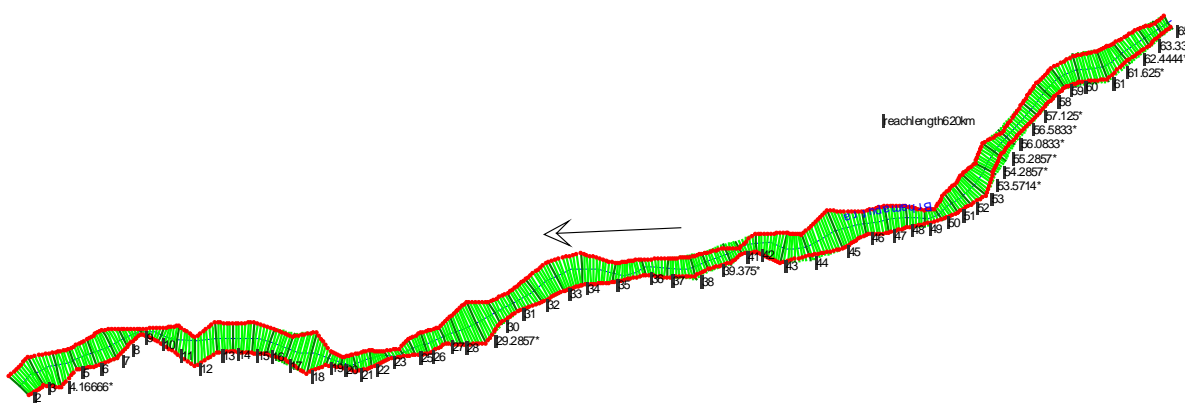


Fig: 4.1 Schematic Plot of the Study Reach of Brahmaputra River in the Program Module.

The connectivity of reaches is very important in order for the model to understand how the computations should proceed from one reach to the next. It is required to draw each reach from upstream to downstream, in what is considered to be the positive flow direction.

Cross Section Geometry

Boundary geometry for the analysis of flow in natural streams is specified in terms of ground surface profiles (cross sections) and the measured distances between them (reach lengths). Cross sections are located at intervals along a stream to characterize the flow carrying capability of the stream and its adjacent floodplain. They should extend across the entire floodplain and should be perpendicular to the anticipated flow lines. Occasionally it is necessary to layout cross-sections in a curved or dog-leg alignment to meet this requirement. Every effort should be made to obtain cross sections that accurately represent the stream and floodplain geometry.

Cross sections are required at representative locations throughout a stream reach and at locations where changes occur in discharge, slope, shape, or roughness, at locations where levees begin or end and at bridges or control structures such as weirs. Where abrupt changes occur, several cross sections should be used to describe the change regardless of the distance. Cross section spacing is also a function of stream size, slope, and the uniformity of cross section shape. In general, large uniform rivers of flat slope normally require the fewest number of cross sections per km. The purpose of the study also affects spacing of cross sections. For instance, navigation studies on large relatively flat streams may require closely spaced (e.g., 200 feet) cross sections to analyze the effect of local conditions on low flow depths, whereas cross sections for sedimentation studies, to determine deposition in reservoirs, may be spaced at intervals on the order of km.

The choice of friction loss equation may also influence the spacing of cross sections. For instance, cross section spacing may be maximized when calculating an M1 profile (backwater profile) with the average friction slope equation or when the harmonic mean friction slope equation is used to compute M2 profiles (draw down profile). The HEC-RAS software provides the option to let the program select the averaging equation.

Each cross section in an HEC-RAS data set is identified by a River, Reach, and River Station label. The cross section is described by entering the station and elevation (X-Y data) from left to right, with respect to looking in the downstream direction. The River Station identifier may correspond to stationing along the channel, mile points, or any fictitious numbering

system. The numbering system must be consistent, in that the program assumes that higher numbers are upstream and lower numbers are downstream.

Each data point in the cross section is given a station number corresponding to the horizontal distance from a starting point on the left. Up to 500 data points may be used to describe each cross section. Cross section data are traditionally defined looking in the downstream direction. The program considers the left side of the stream to have the lowest station numbers and the right side to have the highest. Cross section data are allowed to have negative stationing values. Stationing must be entered from left to right in increasing order. However, more than one point can have the same stationing value. The left and right stations separating the main channel from the over bank areas must be specified on the cross section data editor. End points of a cross section that are too low (below the computed water surface elevation) will automatically be extended vertically and a note indicating that the cross section had to be extended will show up in the output for that section. The program adds additional wetted perimeter for any water that comes into contact with the extended walls.

Other data that are required for each cross section consist of: downstream reach lengths; roughness coefficients; and contraction and expansion coefficients. These data will be discussed in detail later in this chapter. Numerous program options are available to allow easily adding or modifying cross section data.

Reach Lengths

The measured distances between cross sections are referred to as reach lengths. The reach lengths for the left over bank, right over bank and channel are specified on the cross section data editor. Channel reach lengths are typically measured along the thalweg. Over bank reach lengths should be measured along the anticipated path of the center of mass of the over bank flow. Often, these three lengths will be of similar value. There are, however, conditions where they will differ significantly, such as at river bends, or where the channel meanders and the over banks are straight. Where the distances between cross sections for channel and over banks are different, a discharge-weighted reach length is determined based on the discharges in the main channel and left and right over bank segments of the reach. In the selected reach of Brahmaputra, all three lengths were taken similar values. Downstream reach lengths as well as reach length with respect to extreme downstream station (Jogighopa) are given in Table: 4.1

Table 4.1 Reach Length of Study All Reaches

S.no.	Channel name	D/S reach length	Distance from base station
1	dhubri 2	0	0
2	3	107170.1	107170.1
3	4	10199.98	214340.2
4	5	8669.99	321510.3
5	6	9690.02	428680.4
6	7	9690.02	535850.5
7	8	7140	643020.6
8	9	9180	750190.7
9	10	10199.98	857360.8
10	11	8160	964530.9
11	12	8669.99	1071701
12	13	10199.98	1178871
13	14	8160	1286041
14	15	9690.02	1393211
15	16	8669.99	1500381
16	17	9690.02	1607552
17	18	11219.99	1714722
18	19	8669.99	1821892
19	20	6550.01	1929062
20	21	6551.01	2036232
21	22	8160	2143402
22	23	9180	2250572
23	24	6630.01	2357742
24	25	5610	2464912
25	26	6120	2572082

26	27	9690.02	2679253
27	28	6630.01	2786423
28	29	10719.98	2893593
29	30	10199.98	3000763
30	31	10199.98	3107933
31	32	11729.99	3215103
32	33	12750	3322273
33	34	13270	3429443
34	35	15800	3536613
35	36	15309.96	3643783
36	37	11729	3750954
37	38	12240	3858124
38	39	6630	3965294
39	40	11219.99	4072464
40	41	11219.99	4179634
41	42	8669.99	4286804
42	43	13759.99	4393974
43	44	11219.99	4501144
44	45	16320.09	4608314
45	46	14280	4715484
46	47	11219.99	4822655
47	48	9690.02	4929825
48	49	8669.99	5036995
49	50	7140	5144165
50	51	7140	5251335
51	52	7140	5358505
52	53	7140	5465675
53	54	9690	5572845

54	55	9180	5680015
55	56	9180	5787185
56	57	17850	5894356
57	58	11219.99	6001526
58	59	9690.02	6108696
59	60	9690.02	6215866
60	61	12750	6323036
61	62	11219.99	6430206
62	63	13260.01	6537376
63	64	8160	6644546
64	Kobo 65	5610	6751716

Energy Loss Coefficients

Several types of loss coefficients are utilized by the program to evaluate energy losses: (1) Manning's n values or equivalent roughness "k" values for friction loss, (2) contraction and expansion coefficients to evaluate transition (shock) losses.

Manning's n: Selection of an appropriate value for Manning's n is very significant to the accuracy of the computed water surface profiles. The value of Manning's n is highly variable and depends on a number of factors including: surface roughness; vegetation; channel irregularities; channel alignment; scour and deposition; obstructions; size and shape of the channel; stage and discharge; seasonal changes; temperature; and suspended material and bed load.

In general, Manning's n values should be calibrated whenever observed water surface profile information (gage data, as well as high water marks) is available. As water surface profile information is adequately available for the study reach, so Manning's n values were calibrated in fixed bed module with spatial as well as based on discharge variation and values fed into sediment module of flow simulation for further analysis.

There is a difference in Manning's n between fixed and movable bed situations. Fixed bed n's are values which do not depend on the characteristics of the movable boundary, movable bed

n's are values which may depend on the rate of sediment transport and, hence, the discharge. Appropriate values for Manning's n were initially determined by executing HEC-RAS in fixed bed mode, i.e., as a step-backwater program. This is necessary to properly compare calculated water surface elevations with observed water surface profiles, with established rating curves, during the analysis of geometric data and calibration of n values, many program executions were required. Study reach has been subdivided into separate segments, cross-section were interpolated to appropriate numbers and program is executed for different value of n until computed water surface profiles at approximately matched with observed ones. Finally, calibrated n with discharge variation and spatial variation obtained.

Changing n values with distance should be justified based on changes in vegetation, channel form, structures, or sediment size. The technique assumes that the entire bed of the river is stationary and does not move or change roughness during a flood event. Before focusing on sediment transport, however, Manning's n value for the channel is appropriate for a movable boundary analyzed and whatever required minor adjustments, were made to ensure that the n value for the movable portion of the cross section is in reasonable agreement with that obtained from bed roughness predictors.

Selection of Contraction and Expansion Coefficients

Information for contraction and expansion losses is sparser than that for n values. King and Brater (1963) give values of 0.5 and 1.0 respectively for a sudden change in area accompanied by sharp corners, and values of 0.05 and 0.10 for the most efficient transitions. Design values of 0.1 and 0.2 are suggested. They cite Hinds (1928) as their reference. Values often cited by the Corps of Engineers (HEC, 1990a) are 0.1 and 0.3, contraction and expansion respectively, for gradual transitions .So in the present study, contraction and expansion coefficient are by default taken as 0.1 and 0.30.

4.4.1.2 Hydrologic Data

The hydrologic data consist of water discharges, temperatures and flow durations. The discharge hydrograph is approximated by a sequence of steady inflow discharges each of which occurs for a specified numbers of days. Water surface profiles are calculated by using the standard step method to solve the energy equation. Friction loss is calculated by Manning's equation, and expansion and contraction losses will be included if the representative loss coefficients are specified.

The monthly discharges at the site for the period Nov. 1993 to Nov. 1997 are used to obtain a discharge frequency hydrographs and the gauges respective.

Steady Flow Data

Steady flow data were required in order to perform a steady water surface profile calculation and consequently calibration of 'n' worked out. Steady flow data consist of flow regime, boundary conditions and discharge information.

Boundary conditions are necessary to establish the water surface at the ends of the river system (upstream and downstream). A starting water surface is necessary in order for the program to begin the calculations. In a sub critical flow regime, boundary conditions are only necessary at the downstream ends of the river system. If a supercritical flow regime is going to be calculated, boundary conditions are only necessary at the upstream ends of the river system. If a mixed flow regime calculation is going to be made, then boundary conditions must be entered at all ends of the river system. Observed monthly flow profile were fed as input in different cross-section segmental reach and program were run separately to compute water surface elevation at d/s and compared with observed one to estimate n .

Quasi-unsteady Flow Data

Current sediment capabilities in HEC-RAS are based on quasi-unsteady hydraulics. The quasi-unsteady approach approximates a flow hydrograph by a series of steady flow profiles associated with corresponding flow durations. Boundary conditions were flow series (flow hydrograph) at upstream boundary(c/s-65 Kobo). At downstream boundary(c/s-2 at Dubri site), stage time series /rating curve applied. The stage -time series boundary condition allows inputting a time series of stages at the downstream boundary.

As sensitive inputs to the Model boundary values, the Stage-Discharge relations, the G-Q relations of the major rivers/ streams under consideration needs to sufficiently dictate the hydraulic behavior,.

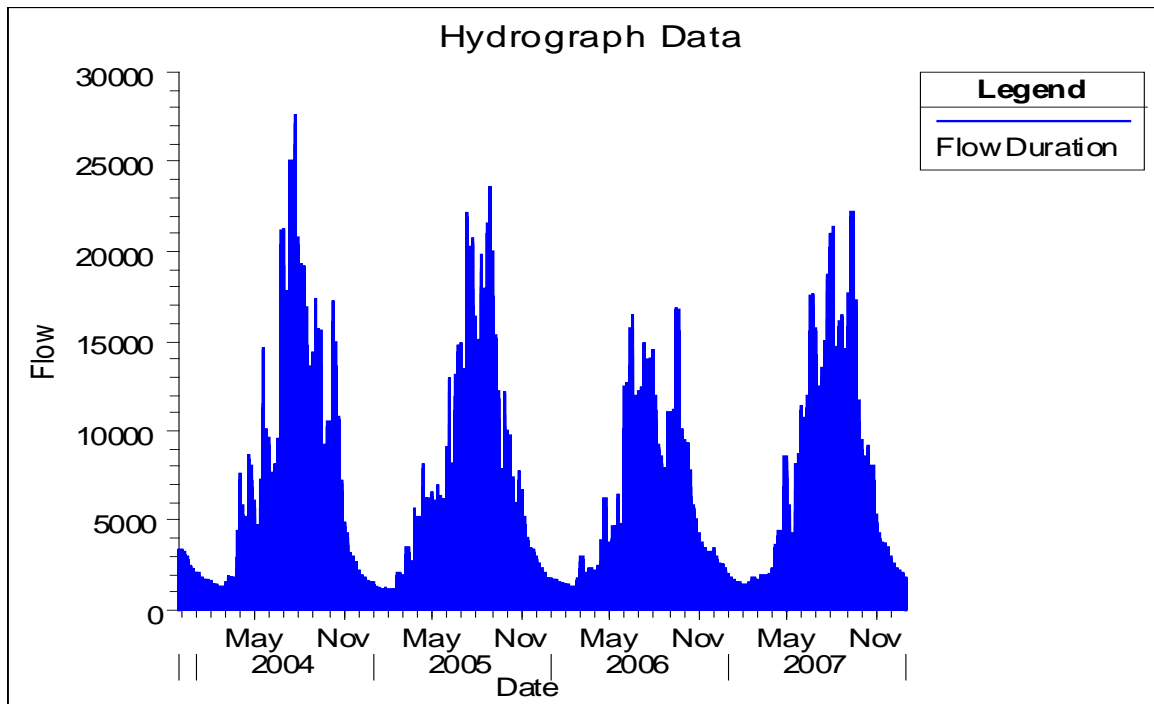


Fig 4.2 Simulation Hydrograph generated at c/s-65 (Kobo Site)

Stage-Discharge Relation at extreme d/s boundary of reach is plotted in Fig: 4.4, similarly Discharge hydrograph at extreme u/s boundary is also plotted in Fig 4.3 which has also been taken as inputs for simulating flow for specific period. Lateral flow series at Jogighopa site shown in Fig 4.4.

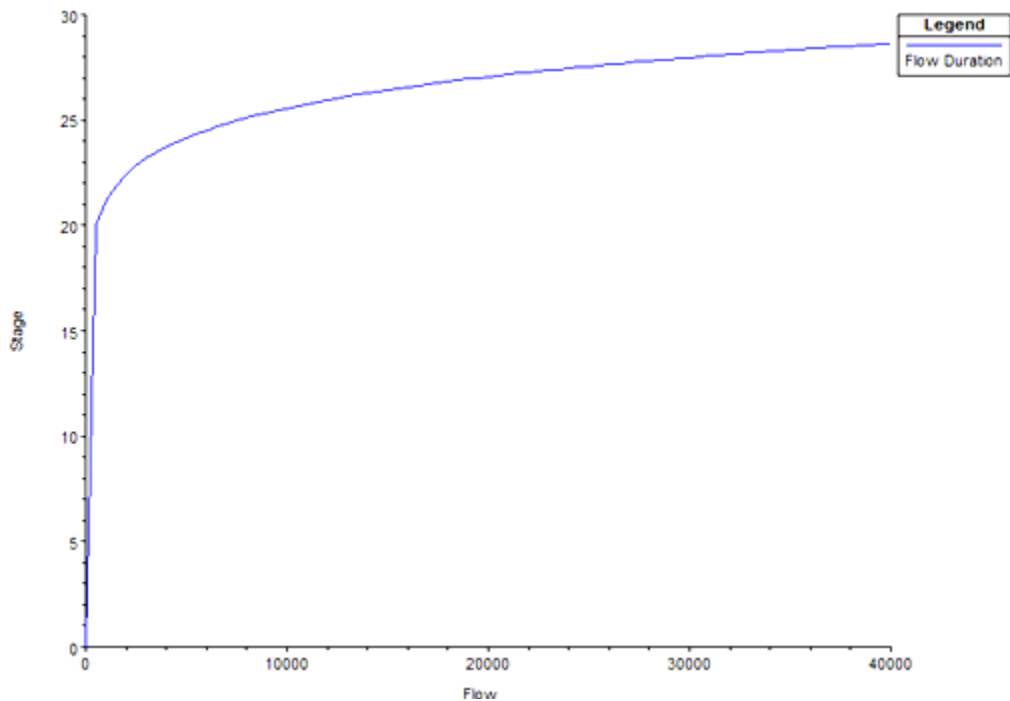


Fig: 4.3 Stage – Discharge Relation at c/s-9(Jogighopa site)

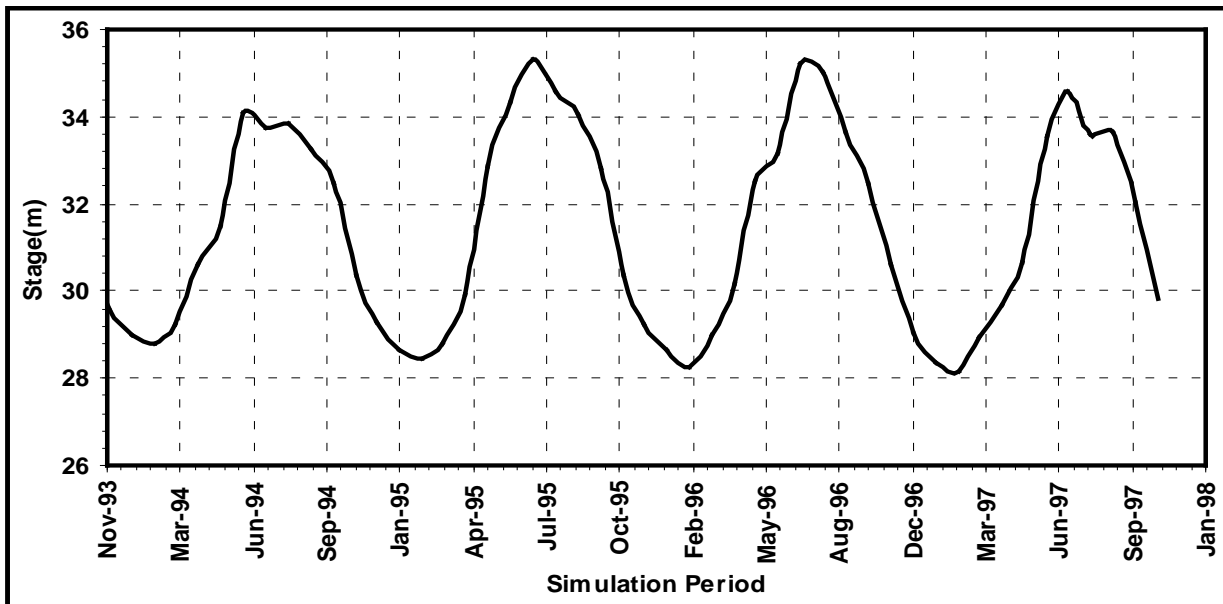


Fig 4.4 Stage Series at c/s-9(Jogighopa site)

4.4.1.3 Sediment Data

The sediment data consist of inflowing sediment load data, gradation of material in the stream bed and information about sediment properties. The inflowing sediment load is related to water discharge by a rating table at the upstream end of the model.

Sediment mixtures are classified by grain size using the American Geophysical union scale. The program accommodates clay (up to 0.004 mm), four classes of silt (0.004 – 0.0625 mm), five classes of sand (very fine sand 0.0625 mm to very course sand 0.2 mm) and five classes of gravel (very fine gravel 0.2mm to very coarse gravel 0.64mm).Sediment transport capacity is calculated at each cross section by using hydraulic data obtained during the calculation of water surface profiles and the gradation of bed material for that cross section.

The variations in the sediment load discharge with the flow is calibrated from the Sediment Discharge Rating Curves and entered to the model input.

Each cross-section must have an associated bed gradation. Possession of data in regard to bed material for all cross section couldn't be done. But character of bed material within the study reach can presumed to be similar in nature so far sediment transport is concerned. Bed material gradation at cross section -2 (Dhubri) is taken as representative bed gradation (Fig: 4.5) through out the alluvial study reach except where outcrops were present.

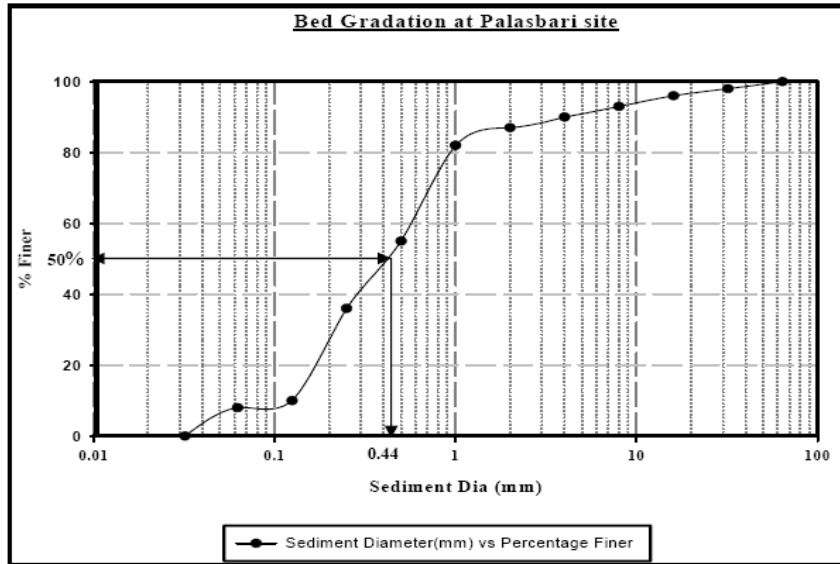


Fig: 4.5 Representative Bed Gradation (semi-log) Plot of the Study Reach

Sediment Boundary Conditions

For sediment transport analysis sediment boundary conditions must be applied. Usually boundary conditions are applied at extreme u/s and d/s cross sections .Internal boundary conditions were applied where flow change is occurring i.e. where tributaries are meeting the main stream. In model formulated sediment rating curves were applied for simulating sediment transport. Sediment rating curve at c/s-65 were plotted and depicted in Figs. 4.6. A rating curve determines a sediment inflow based on water flow.

Besides the hydrologic data, sediment data and roughness coefficients, other bound values accorded are the depth of sediment bed control volume (adopted as 5.0 meter wherever necessary) and the water temperature. The sensitivity of the variation in water temperature (C) over the sediment transport rates and water surface is also simulated as presented in the result summary tables. Average monthly variation of temperature as per field data (Based on average. Temperature record in the period 1931 -1960 at Guwahati) is adopted (Table 4.2).



Fig: 4.6 Sediment Rating Curve at c/s-22 (Pandu Site)

Table: 4.2 Average Monthly Temperature Variations

S.N.	Month	Average Temperature(°C)
1	January	17.5
2	February	19.55
3	March	23.35
4	April	25.95
5	May	26.9
6	June	28.1
7	July	28.95
8	August	29
9	September	28.65
10	October	26.25
11	November	22.3
12	December	18.7

4.4.2 PROGRAM ORGANISATION

The HEC-RAS program in its present form has been organized into two major modules. Modules run with various sub-programs where data have been transferred for specific output generation. The functional flowchart of the program is shown in Fig. 4.8

4.4.2.1 Hydrodynamic modeling and calibration of 'n'. (Steady flow analysis)[First Module]

Roughness Coefficients

Roughness coefficients are one of the main variables used in calibrating a hydraulic model. Generally, for a free flowing river, roughness decreases with increased stage and flow. However, if the banks of a river are rougher than the channel bottom (due to trees and bushes), then the composite n value will increase with increased stage. Sediment and debris can also play an important role in changing the roughness. More sediment and debris in a river will require the modeler to use higher n values in order to match observed water surfaces.

4.4.2.2 Sediment Transport Analysis (Quasi-unsteady flow analysis) [Second Module]

The outputs obtained from first module were to be applied in this module for calibration and testing of the model. Calibrated value of roughness parameter n from first module gave the idea of n and its relation with discharge and also its variation with distance. With slight processing the calibrated set of Manning's n were fed into sediment module. In this module the whole study reach were taken as geometric data i.e. Cross-section-65 (Kobo) to cross-section -2 (Dhubri). Some intermediate cross-sections were linearly interpolated to assure stability to running of the module.

Other sediment data like representative bed gradation at each cross-section /sediment inflow at u/s locations as well as flow change locations were fed into the module. Flow series at u/s boundary and lateral flow series at internal boundaries as well as stage series at d/s is fed into the module. Simulation plans for varying sediment predictors as well as different time series were designated and executed and outputs were obtained. A detailed discussion on outputs will be done in the consecutive chapter.

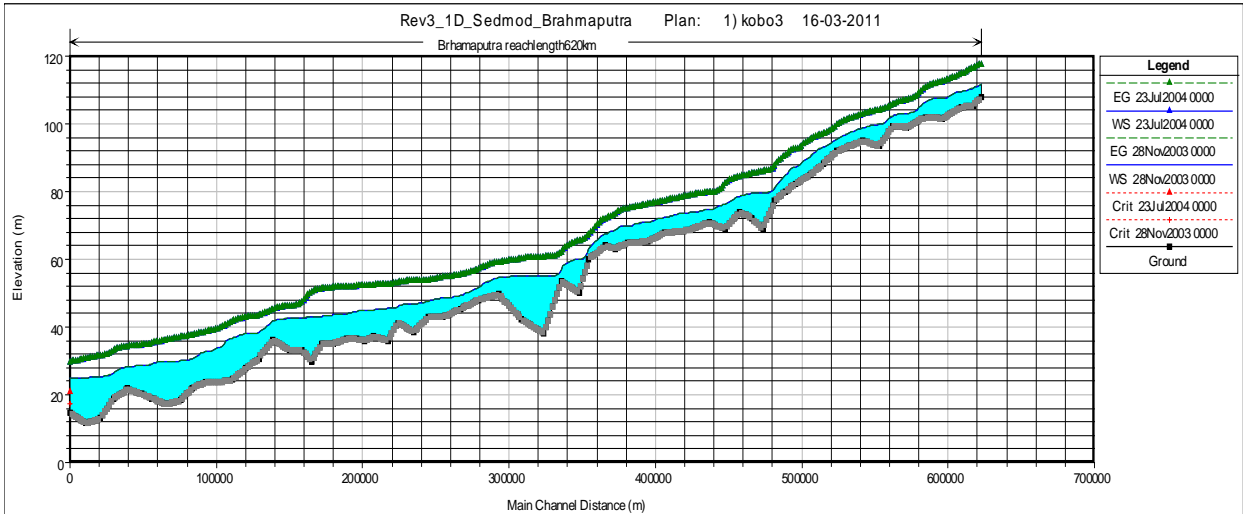


**Fig 4.7 Sediment Transport Analysis and Prediction of water surface profile for
Nov2003 and July2004 (C/s-2 to C/s-65)**

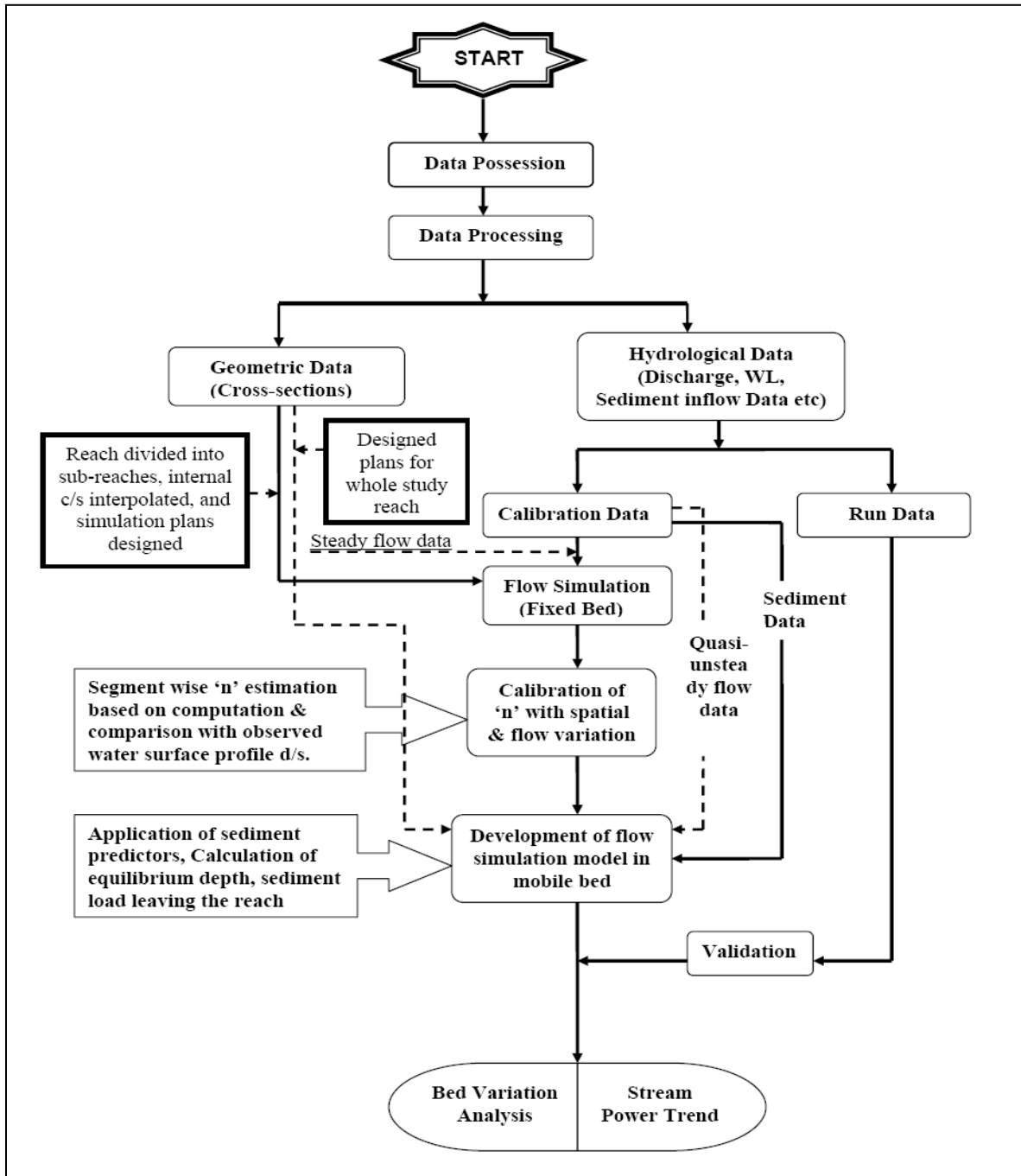


Fig: 4.8 Schematic Flow Chart of Adopted Methodology

CHAPTER -5

RESULTS AND DISCUSSIONS

RESULTS AND DISCUSSIONS

5.1 INTRODUCTION

Flow simulation is done on the 1D mathematical model HEC-RAS in the study reach of Brahmaputra Rive. The manning's roughness coefficient is calibrated and assessment of stream power, rating curves and consequently sediment transport analysis is done with application of various available sediment predictors to assess aggradations/degradations within the reach. Temporal unit stream power variations with correlation to slope variation are also dealt. The results obtained are discussed in detail herein after.

5.2 BED ROUGHNESS CALIBRATION

Observed flow series of year 2004 at Jogighpa and Pandu is used to calibrate manning's roughness coefficient. The calibration is done for range of flows for each month. And hence roughness variation for high and low flows is accounted for (Fig. 5.1). For this process steady flow condition is used and observed water surface is matched with calculated one.

It can be observed that, the seasonal variation of manning's roughness is higher in non monsoon period (low flow) and lower monsoon period (high flow). This trend is in agreement with observed results in major alluvial rivers (Fig. 5.2.).

It is also observed that roughness varies within the same month; but since the seasonal variation is more pronounced, seasonal value is adopted for qausi-unsteady sediment transport analysis in HEC-RAS model.

The capability of HEC-RAS to accommodate seasonal roughness variation within a one full year cycle is applied. The subsequent sediment transport analysis will be discussed in the coming topics.

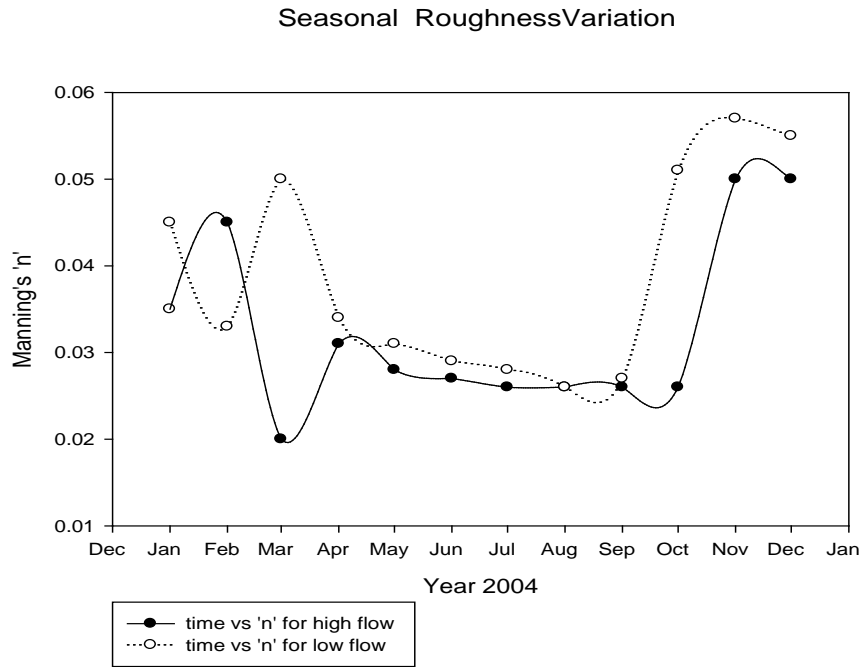


Fig.5.1. Seasonal roughness variation after model calibration

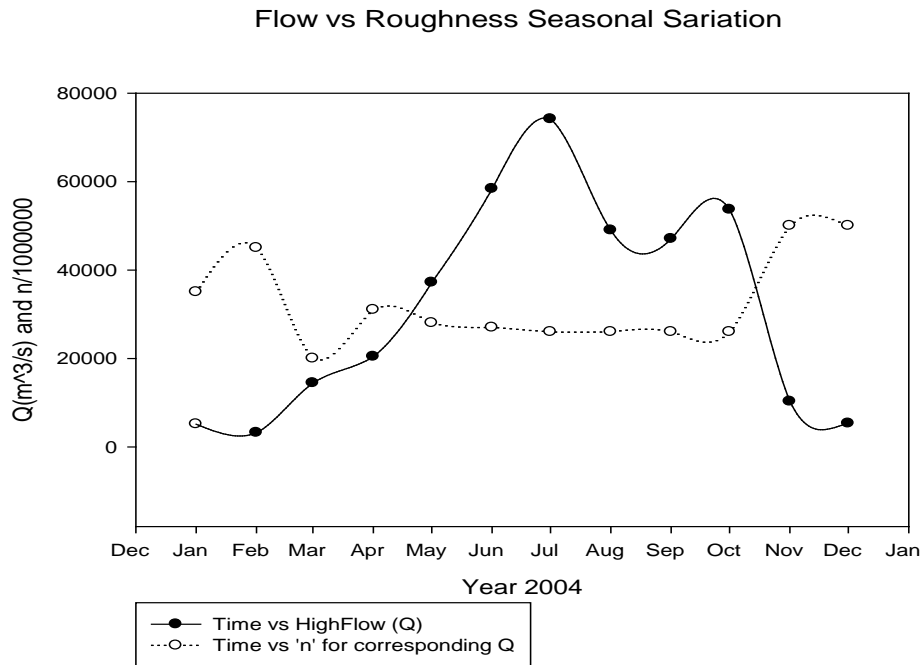


Fig.5.2. Seasonal roughness variation vs. high flow used for calibration.

5.3 SEDIMENT TRANSPORT ANALYSIS, HEC-RAS

Using the calibrated Manning's roughness value, mobile bed sediment transport is done for the year Nov28, 2003 to Sept30, 2007. The analysis is performed using Ackers – White, Engelund-Hansen and Yang's sediment transport function. The reason these functions are

selected is that the range of input values they used in developing their equations encompass the situation in Brahmaputra River and also due to their wide range of applicability. Ackers – White is developed in flume for overall particle diameter of 0.04-7mm and Yang developed his equation based on field observation of overall particle diameter of 0.15-1.7mm, which bases transport on Stream Power, the product of velocity and shear stress. Engelund-Hansen is developed based on flume data for particle mean diameter of 0.19mm to 0.93mm. It has been extensively tested and found to be fairly consistent with field data (HEC-RAS, manual, 2010). To see the comparison for this study average mean particle diameter of 0.44mm is used. The Ackers-White transport function is a total load function developed under the assumption that fine sediment transport is best related to the turbulent fluctuations in the water column and coarse sediment transport is best related to the net grain shear with the mean velocity used as the representative variable. The transport function was developed in terms of particle size, mobility, and transport. See Chapter 2 for further discussion.

It should be noted that the value adopted here is based on sediment gradation data collected in the middle reach of the river (Plasibari). Hence it is assumed that it represents the whole reach.

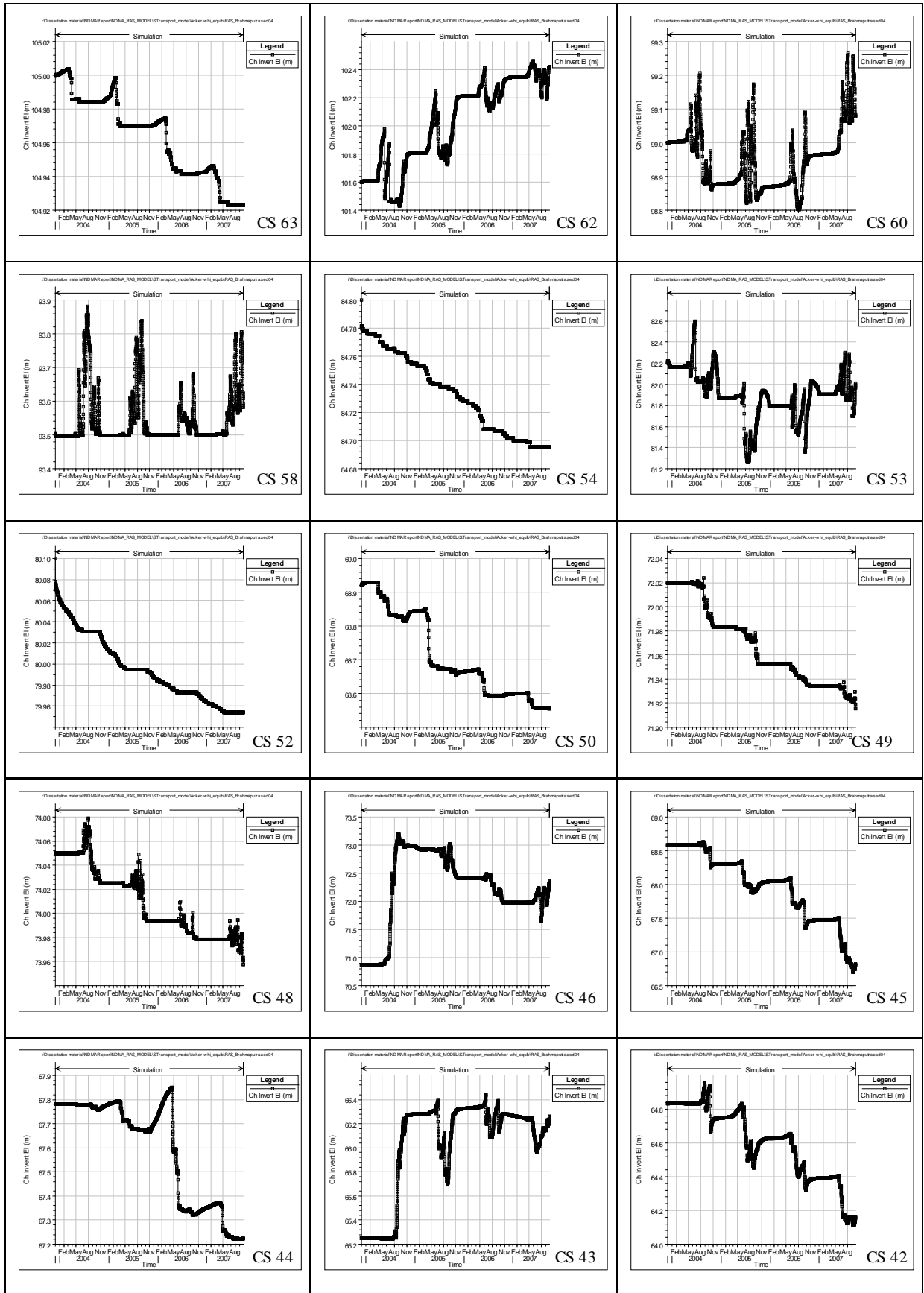
The analysis is performed using upstream boundary condition of Equilibrium Load option; this is due to lack of verified rating curve at Cross Section 65. HEC-RAS computes sediment transport capacity, for each time step, at this cross section and this will be used as the sediment inflow. Since load is set equal to capacity for each grain size, there will no be aggradation or degradation at this cross section.

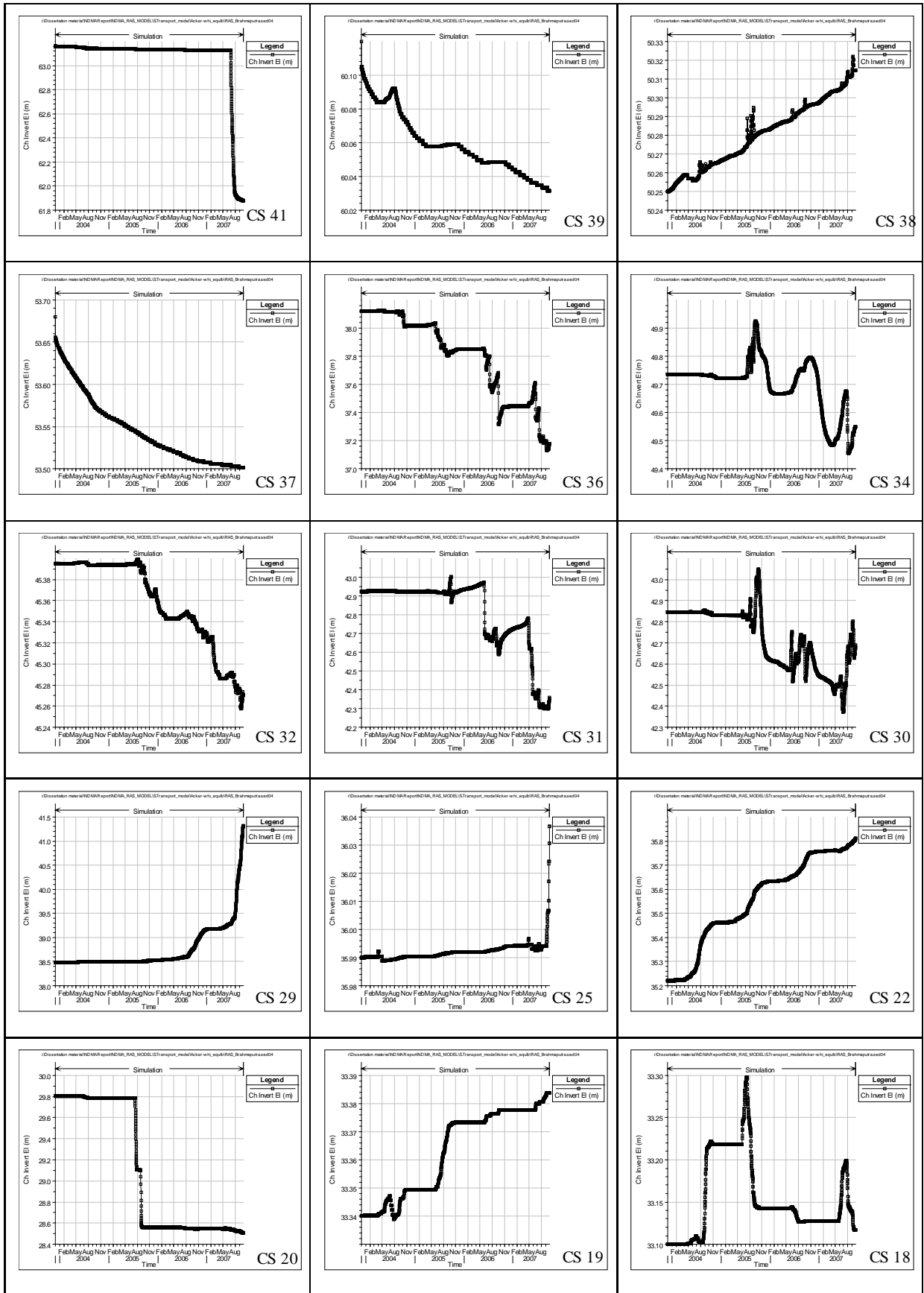
The output from the above three sediment transport function will be discussed here under. The discussion will focus on the overall sediment deposition or erosion and hence the aggradation and degradation of bed level over the analysis period of 2003 to 2007.

Bed level change of ± 5 cm will be considered as fairly stable cross section in this analysis.

5.3.1 ACKERS – WHITE SEDIMENT TRANSPORT ANALYSIS OUTPUT

As can be seen in the figure below, the river bed is exhibiting variation in time in the pattern of aggradation or degradation. The output of this analysis clearly shows that aggradation and degradation occurring simultaneously in different portion of the river reach. And also it can be observed that in some cross sections there is pure aggradation or degradation trend over the year 2003 to 2007; where as in some there is occurrence of both aggradation(e.g. CS62) and degradation(e.g. CS63) over the simulation period (e.g. CS 60, 58, 53, 46) for example.





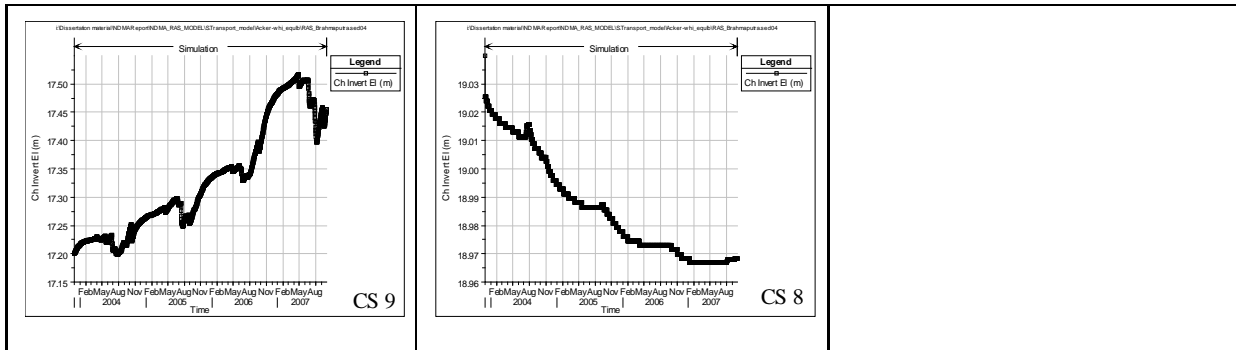


Fig.5.3. variation of bed change for individual cross section over the simulation period based on Acker-White sediment transport function

Sediment transport function is directly dependent on parameters like mean sediment particle size, velocity, shear stress and flow pattern in the channel. Figure 5.4 shows that bed change over high flow and low flow. It is observed that the bed is eroding in high flow period and deposition is taking place over low flow periods.

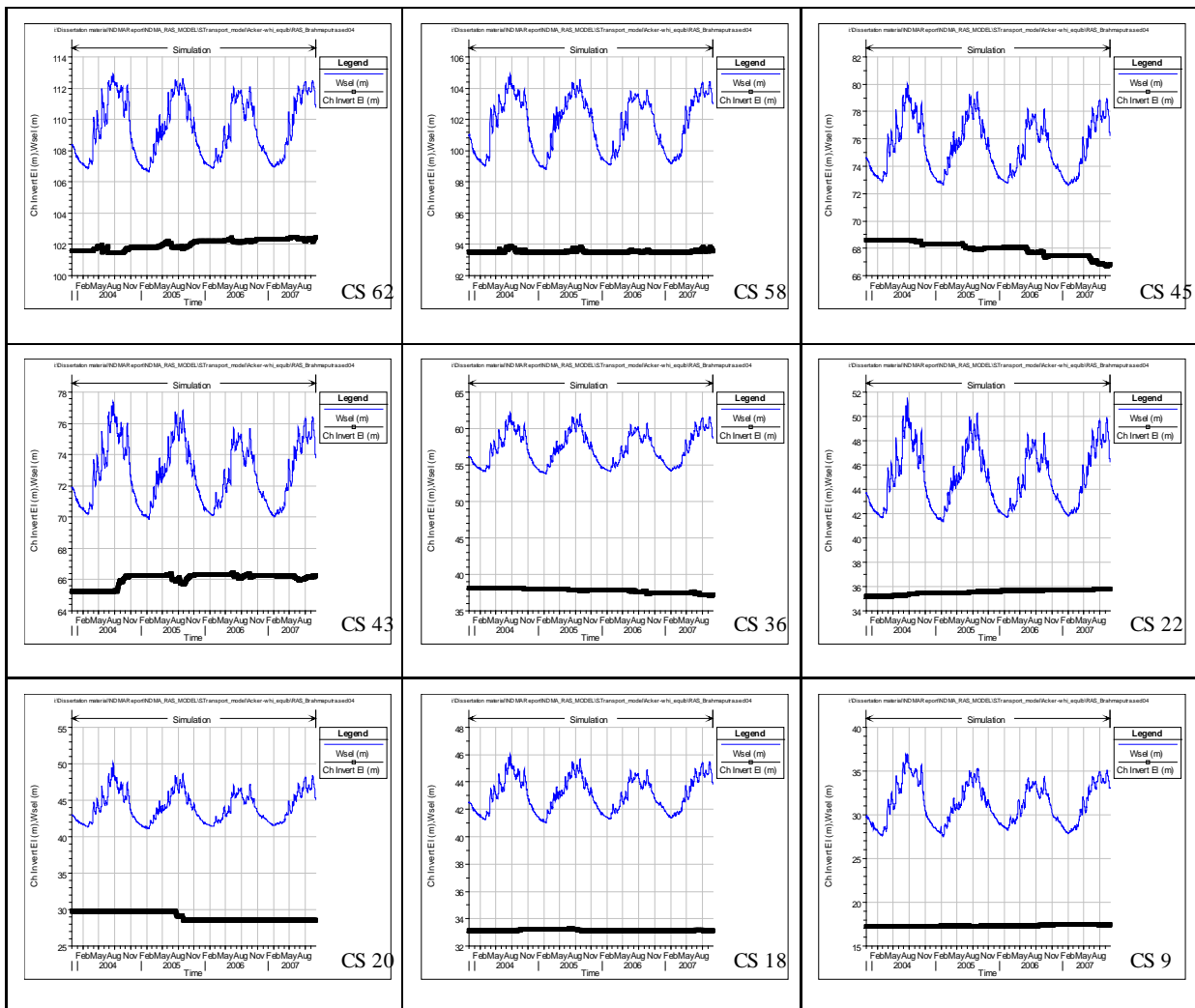


Fig. 5.4 bed level change vs water surface elevation

And it is also observed that when the discharge increases, velocity and shear stress in the channel increase and hence bed level change is the result (Fig. 5.5). In figure 5.5, velocity, flow and shear stress pattern changing in tandem is shown.

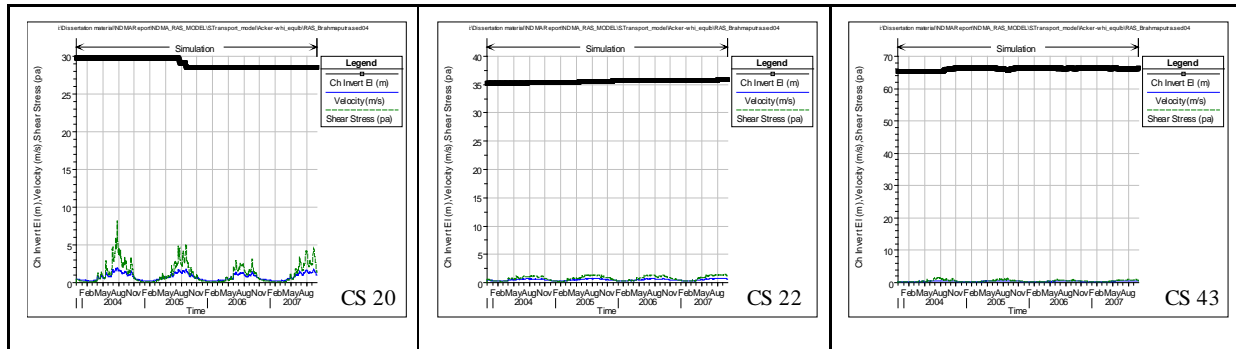
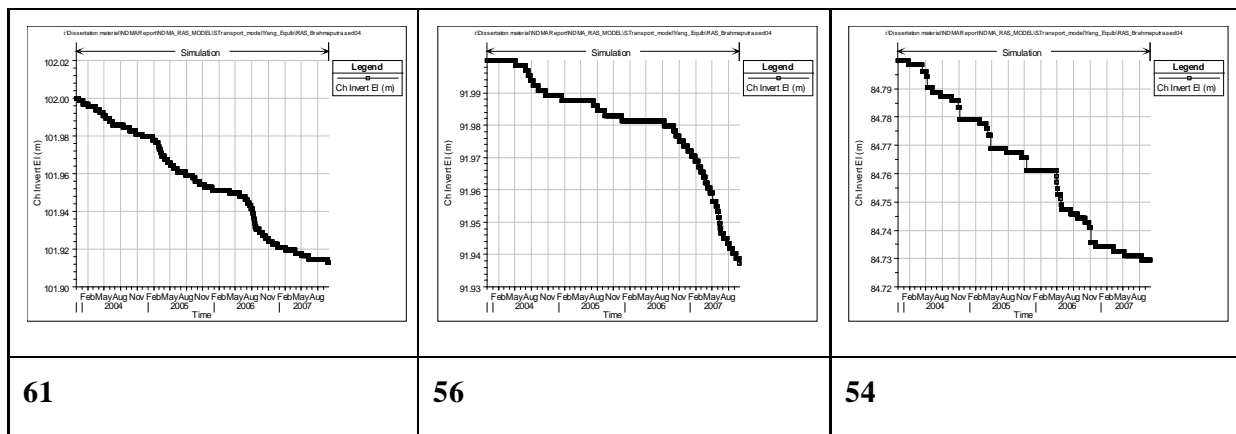


Fig. 5.5 bed level change vs channel shear stress and velocity

5.3.2 YANG TRANSPORT ANALYSIS OUTPUT

Similarly the sediment analysis is performed using Yang's sediment transport function. Here also the general trend is more or less the same as that of result obtained from Acker-White sediment transport function. But the major difference is observed in the extent of aggradation and degradation observed.

In Yang's sediment transport function the observed bed change variation is minimal compared to the above method. As can be observed in figure 5.6, the number of cross section which shows bed change variation in the range of ± 5 cm has greatly decreased. 12 compared to 32 observed in Acker-White sediment transport predictor.



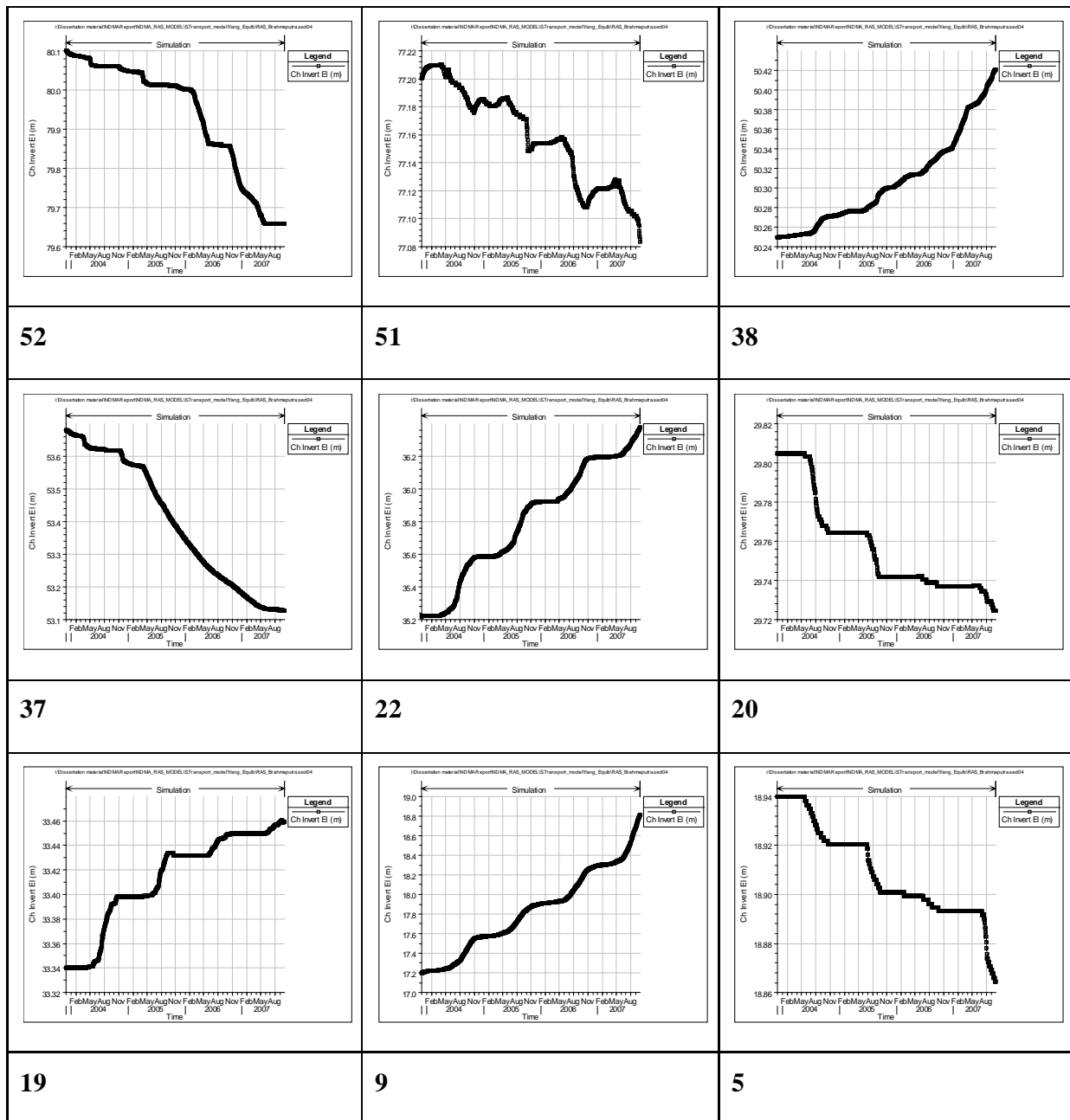


Fig.5.6. variation of bed change for individual cross section over the simulation period based on Yang sediment transport function

In this sediment transport function, the variation of bed change is minimal to the variation of magnitude of flow (fig. 5.7).

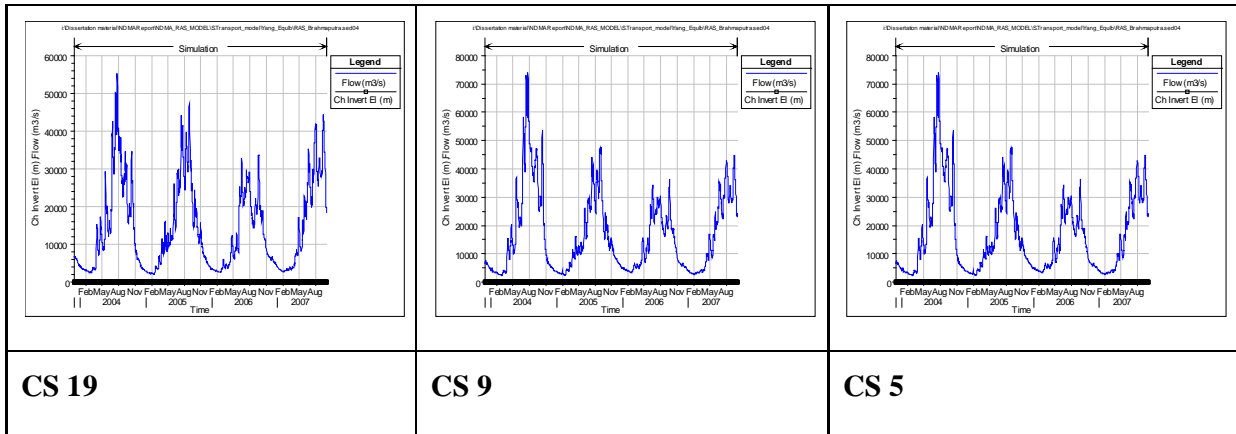


Fig. 5.7 bed level change vs water surface elevation

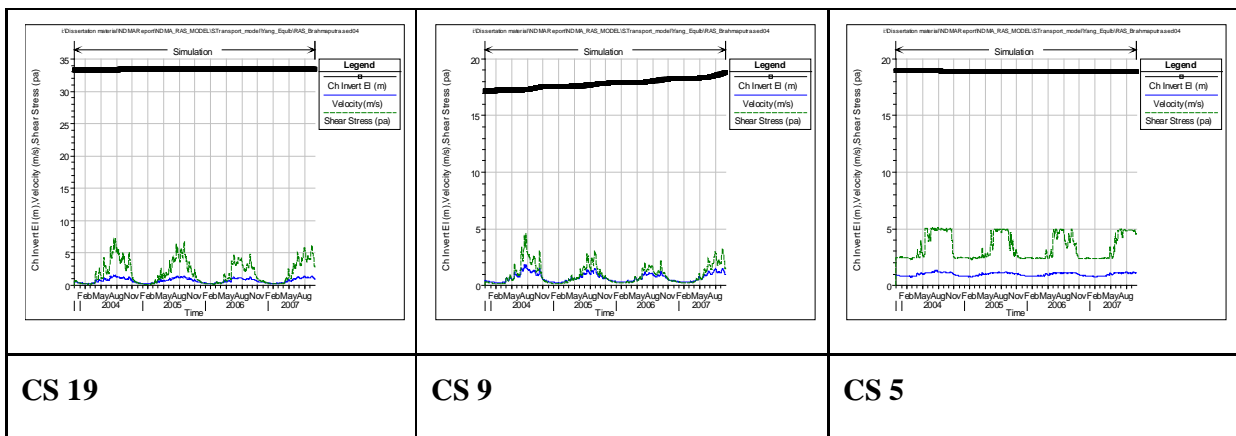
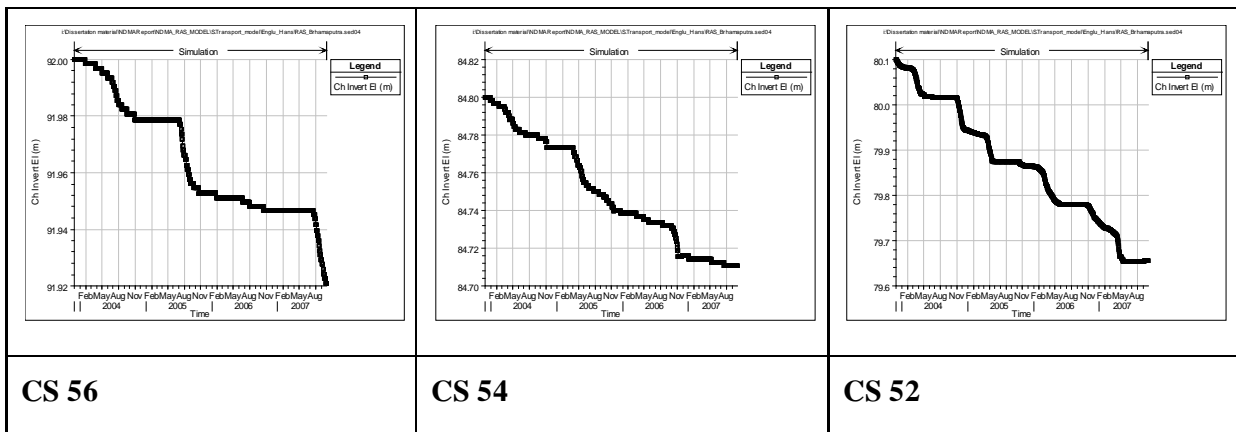
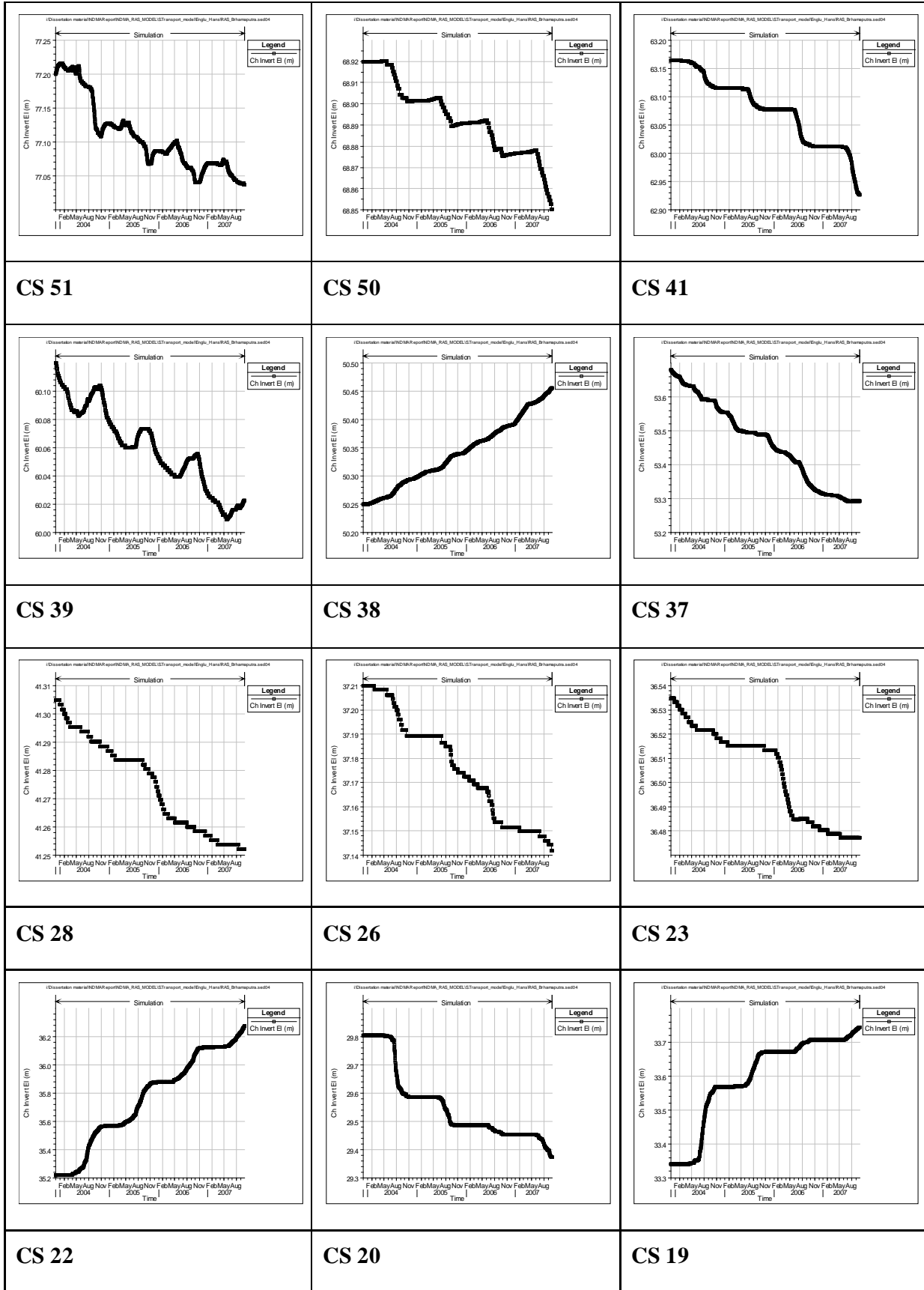


Fig. 5.8 bed level change vs channel shear stress and velocity

5.3.3 ENGULEND-HANSEN TRANSPORT ANALYSIS OUTPUT

Here the number of cross section more than or equal to five centimeter has increase from 12 (Yang's method) to 22. Yet the extent of bed change variation over the simulation period is closer to Yang's method than Acker-White. Some cross sections where there was observed aggradation or degradation in the other methods has exhibited the reverse trend in this method.





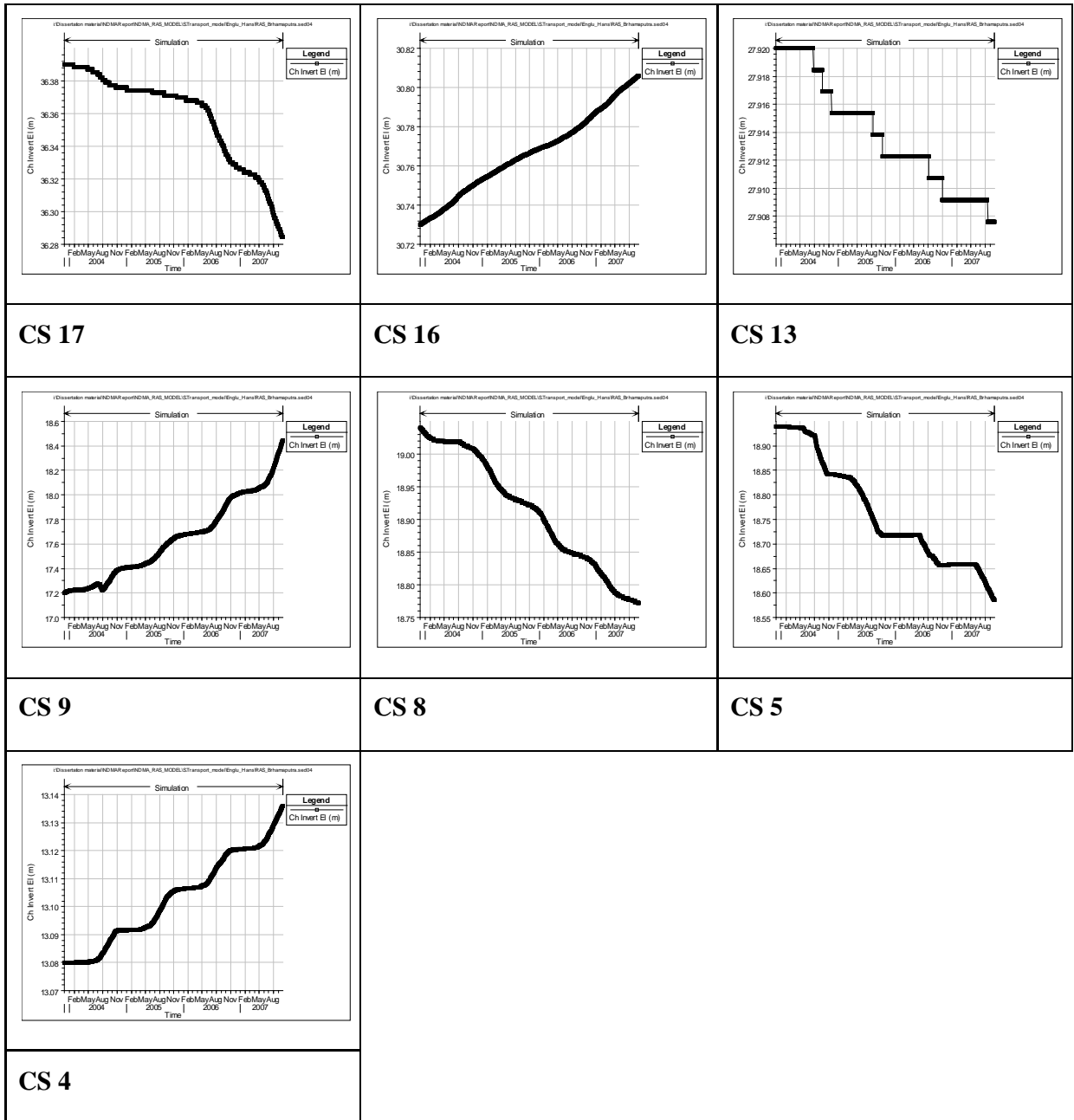


Fig.5.9. variation of bed change for individual cross section over the simulation period based on sediment transport function Engulend-Hansen

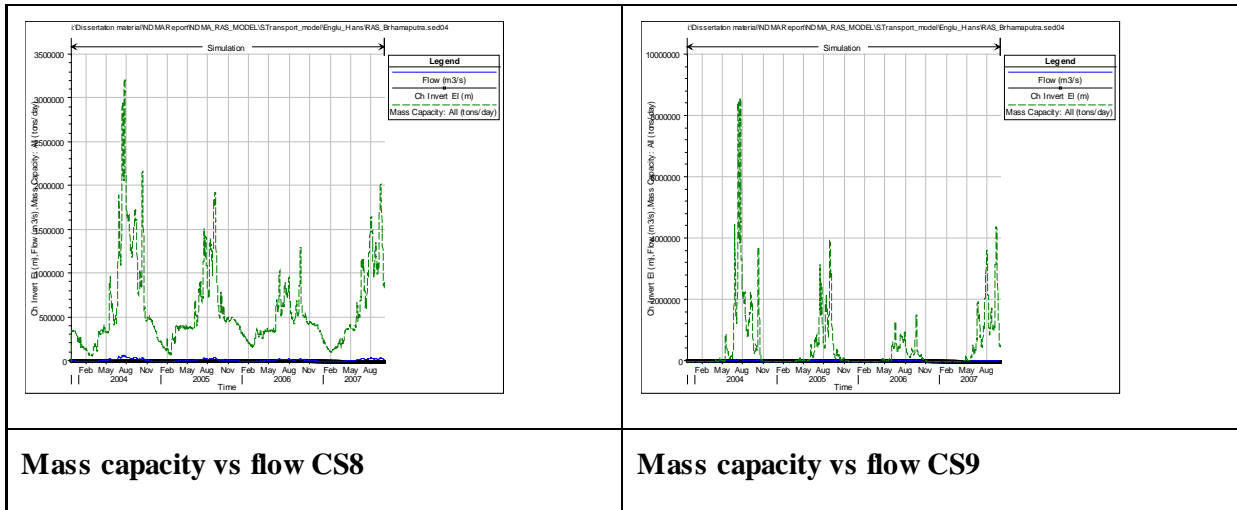


Fig. 5.10 Mass capacity vs flow

In the above figure it can be seen that, at cross sections where there is low mass capacity (transport capacity in total mass at computational step) (CS9) there is a tendency for deposition. Where there is high mass capacity (CS8) erosion is occurring. Therefore this clearly shows the correlation between sediment transport capacity and bed level change.

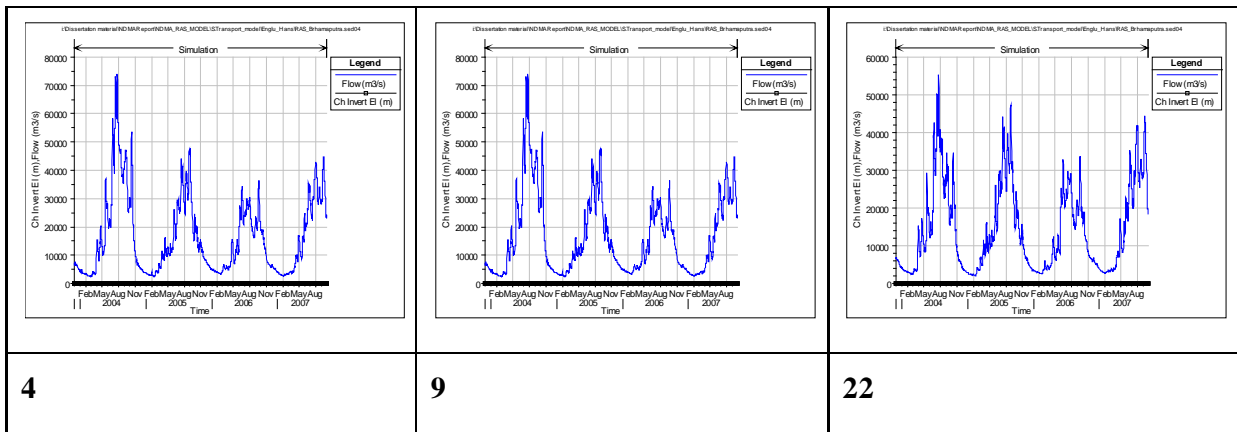


Fig. 5.11 bed level change vs water surface elevation

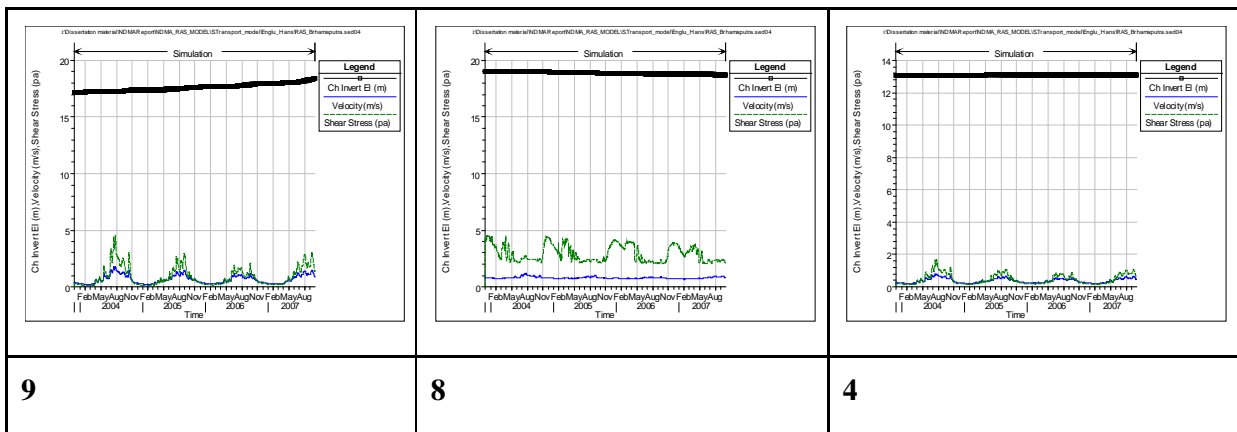


Fig. 5.12 bed level change vs channel shear stress and velocity

The above figure (5.11 and 5.12) also shows the same trend that is explained in the above topics.

Figure 5.13 shows that the average bed variation comparing the three methods used in this study. All of the methods have their own bed level prediction, Acker-White methods gives very high bed level variation compared to the other two methods.

In terms of the magnitude of bed level change, Yang and Engulend-Hansen functions are in agreement.

From this figure, it can be concluded that generally the pattern of aggradation and degradation is distributed throughout the 620km of the reach. The localities that aggradation is predominant are in the vicinity of Cross Section 62,58,50,47,43,28,22,18,and 9.

It should be bear in mind that in some cross sections one function is predicting and the other degradation or relatively stable bed level condition. And the use of any particular method is very much dependent on the applicability of the function for the given river. To suggest any one of the above method for sediment transport predication, it requires the use of intensive data for model verification; which in this case could not be available for the simulation period.

Average river bed level change over the simulation period

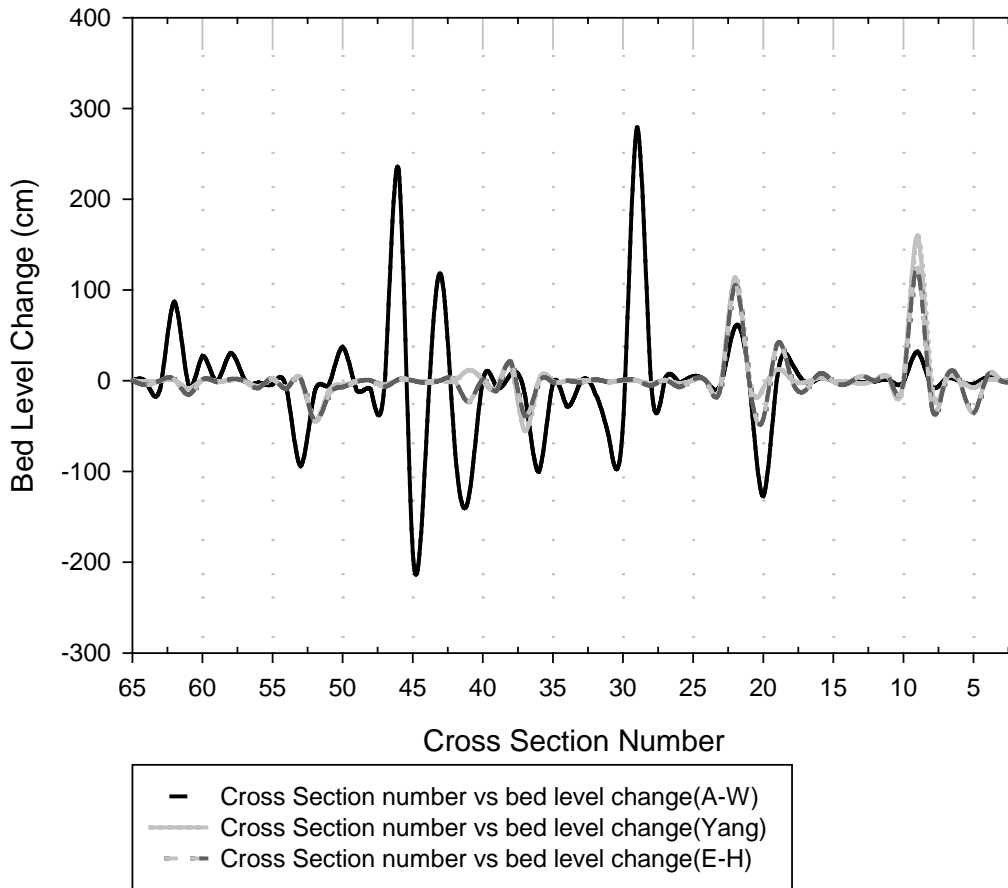


Fig. 5.13 Average bed level variation for the three transport functions over the simulation period

The sediment transport functions are, to varying degrees, the results of theoretical and empirical science. Even the most theoretically detailed was fit to data using empirical coefficients. These coefficients represent the central tendencies of the data considered but will not likely reflect the transport of the specific site precisely, even if an appropriate transport function is selected. Hence at the end of the day field verification is a must.

CHAPTER – 6

PILOT STUDY SCHEMES FOR EROSION

CONTROL ON THE BRAHMAPUTRA

RIVER FOR MORIGAON SITE;

AND NEAR GUWAHATI AIRPORT OF

BRAHMAPUTRA RIVER

**PILOT STUDY SCHEMES FOR EROSION CONTROL ON THE
BRAHMAPUTRA RIVER FOR MORIGAON SITE;
AND NEAR GUWAHATI AIRPORT OF BRAHMAPUTRA RIVER**

**6.1 PILOT STUDY SCHEME FOR EROSION CONTROL ON THE
BRAHMAPUTRA RIVER FOR MORIGAON SITE**

The Water Resources Department of Assam communicated to IIT Roorkee the partial cross-sectional data survey data of the left bank side of the Brahmaputra in the study area in Morigaon site at the vicinity of 61th KM of the left Dyke, along with stage data. In addition the latest satellite data (2007) of the pilot study area has been procured by IIT Roorkee. Making use of the above data, a scheme for pilot study has been formulated. A schematic diagram of the arrangement of erosion control structures is depicted in Fig. 62.

The underlying concept behind the pilot scheme is centred on breaking-up the incoming erosion vortex current by using framed structures like RCC Kellner Jetty, and reversal of the erosion secondary flow towards the away from the bank through use of emerging technique of submerged vane to induce sedimentation. Furthermore, to afford protection to the critical toe of the bank line. Polymer Rope Gabions filled with Geo-Synthetic bags has been proposed along with and additional protection by RCC Kellner Jetty.

The rationale of using the above new techniques for the Brahmaputra is based on the fact that the RCC Kellner Jetty field is expected to trap sediment and debris and thereby effectively weaken the eroding flow vortices. The RCC Kellner Jetty field technique in due course will create sediment deposits as the heavy sediment laden flow will be adequately slowed down the part with bed material load.

The detailed estimate of the pilot study scheme is given in the following pages along with the layout of the river training structures their structural details.

Total estimated cost of the scheme stands of Rs. 1.644 crores for the one Kilometer bank length of the pilot study area.

6.1.1 ABSTRACT OF TOTAL APPROXIMATE COST AT MORIGAON SITE

1.

Cost of Polymer Rope Gabion Submerged Vane

Total No. of submerged vane = 3 no. x 7 array

= 21 no.

Cost of one submerged vane = 93650

Total Cost of Submerged vane = 21 x 93650 = **Rs.1966650**

Cost of Polymer Rope Gabion along the bank

Total length = 500m

Cost of Polymer Rope Gabion 9365/m

Cost Polymer Rope Gabion along the bank = 500 x 9365

= **Rs.4682500**

2. No. RCC Kellner Jetty along the bank = $(500/2.5) \times 3$ rows = 600 no.

No. of RCC Kellner Jetty in retards along the bank

= $(10/2.5) \times 3$ rows x 7 lines = 84 no.

No. of RCC Kellner Jetty in diversion line

= $(510/2.5) \times 5$ line = 1020 no.

No. of RCC Kellner Jetty in retard line $(50/2.5) \times 5$ line + $(50/2.5) \times 3$ line +

$(45/2.5) \times 3$ line x 2 no. + $(40/2.5) \times 3$ line x 2 no. + $(35/2.5) \times 3$ line + $(30/2.5) \times 3$ line + $(20/2.5) \times 3$ line + $(20/2.5) \times 5$ line = 506

Total No. of RCC Kellner Jetty in retard and diversion

= 600 + 84 + 1020 + 506 = 2210 no.

Cost of one RCC Kellner Jetty Rs. 4040

Total cost of RCC Kellner Jetty = 2210 x 4040 = **Rs.8928400**

3. Cost of 26mm PP Rope

Total length = 510×5 rows + 50×5 + 50×3 + 45×3 + 45×3 + 40×5 + 35

$\times 3$ + 30×3 + 20×3 + 20×5 + 500×3 + $7 \times 10 \times 3$ = 5485m

Add 5% extra for tie, anchorage and wastage = 1.05×5485 = 5760m

Cost of pp rope = Rs.150/m

Total cost of pp rope = 5760×150 = **Rs.864000**

Total cost of Submerged Vane + RCC Kellner Jetty + PP Rope

= **Rs.1966650 + Rs.4682500 + Rs.8928400 + Rs.864000**

= Rs.16441550/-

= **Rs.1.644 Crore**

6.1.2 APPROXIMATE ESTIMATE FOR R.C.C. KELLNER JETTY

Size of RCC Kellner Jetty = 3.0 m

Section – 15 cm x 15 cm

6.1.2.1 Quantity of Concrete for one No. RCC Kellner Jetty

(a) Volume of Concrete

$$= 0.15 \text{ m} \times 0.15 \text{ m} \times 3.0 \text{ m} \times 3 \text{ nos.}$$

$$= 0.2025 \text{ m}^3$$

(b) Providing haunch at the junction of

RCC Kellner jetty of size = 0.15 m x 0.15 m

No. of haunch = 12 Nos.

Quantity of Concrete for haunch

$$= \frac{1}{2} \times 0.15 \times 0.15 \times 0.15 \times 12$$

$$= 0.02025 \text{ m}^3$$

Total volume of concrete (a+b)

$$= (0.2025 + 0.02025) \text{ m}^3$$

$$= 0.22275 \text{ m}^3$$

$$= 7.867 \text{ cft} = 0.223 \text{ m}^3$$

6.1.2.2 Quantity of steel for one RCC Kellner Jetty

(a) For longitudinal bars

No of bars = 4 nos

Dia of bars = 8 mm

Volume of longitudinal bar

$$= 4 \text{ nos} \times \frac{\pi}{4} \times 8^2 \times 3000 = 602880 \text{ mm}^3$$

$$= 6.0288 \times 10^{-4} \text{ m}^3$$

Density of steel = 7.85 t/m³

Wt. of longitudinal bars = 7.85 x 6.0288 x 10⁻⁴ x 3 nos.

$$= 0.01420 \text{ t}$$

$$= 14.20 \text{ kg}$$

(b) For stirrups

Length of one stirrups rod = (120 mm x 4 + 50 mm) = 530 mm

$$= 0.53 \text{ m}$$

$$\text{No of stirrup} = \left(\frac{3000}{150} + 1 \right) = 21 \text{ nos}$$

Total length of stirrup rod = 21 x 0.53 x 3

$$= 33.39 \text{ m}$$

Volume of stirrup rod = $\pi/4 \times 6^2 \times 33.39 \times 10^3$

$$= 943601.4 \text{ mm}^3$$

$$= 9.4360 \times 10^{-4} \text{ m}^3$$

Wt of stirrup rod = 7.85 x 9.4360 x 10⁻⁴ t

$$= 7.4072 \times 10^{-3} \text{ t}$$

$$= 7.40 \text{ kg}$$

$$\begin{aligned} \text{Total wt (a+b)} &= (14.20 + 7.40) = 21.60 \text{ kg} \\ \text{Add 5\% extra for wastage} &= 21.60 \times 1.05 = 22.68 \text{ kg} \\ &= 0.02268 \text{ MT} \end{aligned}$$

6.1.2.3 Quantity of G. I. wire of dia 4 mm

Providing hole at the spacing of 30 cm c/c

No of hole for one member

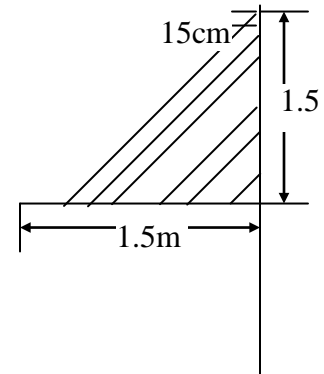
$$\left[\frac{(300 - 60)}{30} + 1 \right] = 9 \text{ nos}$$

Provide 10 nos hole, 5 nos of each side

Then spacing of hole = 25 cm c/c

Length of wire

$$\begin{aligned} &= \sqrt{125^2 + 125^2} + \sqrt{100^2 + 100^2} + \sqrt{75^2 + 75^2} \\ &\quad + \sqrt{50^2 + 50^2} + \sqrt{25^2 + 25^2} + 5 \times 15 \\ &= 176.77 + 141.42 + 106.06 + 70.71 + 35.355 + 75 \\ &= 605.315 \text{ CM} \end{aligned}$$



Total no of force = 12 nos

$$\text{Total length} = 12 \times 605.315 = 7263.75 \text{ cm}$$

$$= 72.64 \text{ m}$$

Add 5% extra for wastage

$$= 3.64$$

$$= 76.28 \text{ m}$$

Using 4 mm G. I wire

$$\text{Volume of total wire} = \pi/4 \times 4^2 \times 76.28 \times 10^3$$

$$= 958076.8 \text{ mm}^3$$

$$= 9.58 \times 10^{-4} \text{ m}^3$$

$$\text{Wt of wire} = 7.85 \times 9.58 \times 10^{-4} = 7.52 \times 10^{-3} \text{ t}$$

$$= 7.52 \text{ kg}$$

6.1.2.4 Quantity of Shuttering

$$\text{Total length of shuttering} = (0.15 + 0.15 + 0.15) \times 3 + 0.15 \times 0.15 \times 2$$

$$= 1.395 \text{ m}^2 \text{ for 1 no.}$$

$$\text{For 3 no.} = 1.395 \times 3 = 4.185 \text{ m}^2$$

6.1.3. ABSTRACT OF COST FOR ONE RCC KELLNER JETTY

Sl. No.	Items	Quantity	Rate	Amount (Rs.)
1.	Casting of RCC M-15 with nominal mix of (1:2:4) RCC Kellner Jetty consisting of 3 member of length 3m with 15cm x 15cm square cross-section and having the reinforcement as per detail drawing	0.223 m ³	Rs. 3255/m ³	725.86
2	Providing M.S. reinforcement (Tor steel) as per approved design drawing removal of rust, cutting, bending, binding including supplying annealed wire placing Ms rod in position complete job	0.02268 MT	Rs.42871.00/MT	972.30
3.	Cost of G. I. Wire of 4 m.m dia. including carriage and labour	7.52 kg	Rs.40/kg	300.80
4.	Proving centering including structing proping etc. And remvoign after use	4.185 m ²	Rs.283.30/m ²	1185.61
5.	PVC Pipe of dia 10mm for making hole	L.S.	-	100.00
6.	Labour charge for placing of RCC Kellner Jetty at site	1 Nos.	750/each	750.00
				4034.57 Say 4040

6.1.4 APPROXIMATE ESTIMATE FOR POLYMER ROPE GABION FILLED WITH NEW GEO SYNTHETIC BAGS OF SIZE 0.75M X 0.45 M (CEMENT BAG SIZE)

6.1.4.1 Total volume of structure

$$= 10 \text{ m} \times 2.0 \times 2.5 \text{ m}$$

$$= 50\text{m}^3$$

Assuming one bag occupy 1 cft

$$\text{Volume} = 0.0283\text{m}^3$$

No. of bags for 30m^2 volume

$$= 50 / 0.0283$$

$$= 1766.28 \text{ nos} \simeq 1770\text{nos}$$

6.1.4.2 Quantity of Bamboo

Assuming length of bamboo = 6m and average dia 8 cm

(a) No of bamboo for vertical bamboo

$$= 20 \text{ nos}$$

$$\text{Total length of Bamboo Pile} = 20 \times 3.5 = 70 \text{ m}$$

(b) No of bamboo for horizontal bamboo as runner

$$\text{Total length of runner} = 21\text{m}$$

$$= \frac{(2.23 \times 2 + 6) \times 2}{6} = 3.40 \text{ nos} \simeq 4 \text{ nos.}$$

(c) No of bamboo for lateral ties

$$\text{Length of one ties} = 2 + 0.3 = 2.3 \text{ m}$$

$$\text{Total Length tie} = 9 \times 2.3 = 20.7$$

$$\text{No of ties} = 9 \text{ nos}$$

$$\text{Total Length tie + Runner} = 21 + 21 = 42\text{m}$$

$$\text{No of Bamboo} = \frac{2.30 \times 9}{6} = 3.45 \simeq 4 \text{ nos}$$

$$\text{Total no of bamboo (a+b+c)} = (20 + 4 + 4) = 28 \text{ nos}$$

6.1.4.3 Size of Polymer rope gabion

Providing 10m x 2.0m x 2.5m polymer rope gabion of 10mm dia rope having mesh size 200mm x 200mm

6.1.5 ABSTRACT OF COST OF ONE POLYMER ROPE GABION FILLED WITH NEW GEO SYNTHETIC BAG GABION

Sl. No.	Items	Quantity	Rate	Amount (Rs.)
1.	Supply of new Geo synthetic bags of size 0.75 m x 0.45 m	1770 nos	Rs.15 each	26,550
2	Supply of Bamboo of average dia of 8 cm	28 nos	Rs.80 each	2240
3.	Labour charge of piling of Bamboo	70 m	Rs.8.9/m	623
4.	Labour charges for fitting and fixing of horizontal Bamboo as runner and lateral ties	42 m	Rs.1.90/m	79.80
5.	Labur charge for filling empty new synthetic bag with local sand, stiching the bags and placing polymer rope gabion in water with a carrage of filled bag by boat including loading unloading and stacking with lead of ½ km all complete job as per approve design specification and direction of E/I	1770	Rs. 8.0/each	14160
6	Supply of polymer rope gabion of size 10m x 2.0m x 1.5 m of 10mm dia rope and having mesh size of 200mm x 200mm	1 nos.	50000	50000
				93,652.80 Say 93,650 for 10 m length 9365 m for 1 m length

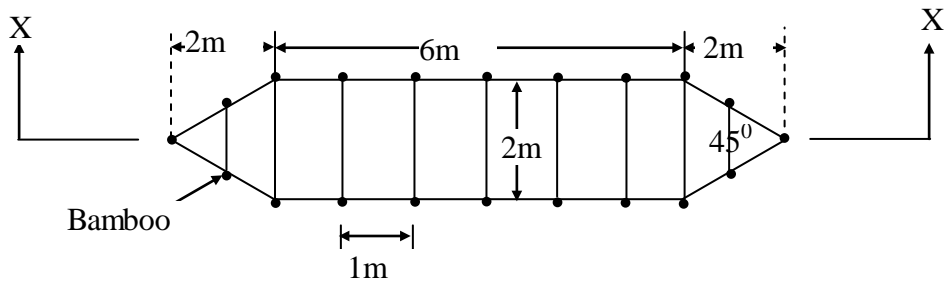


Fig. 6.1 Plan of Polymer Rope Gabion

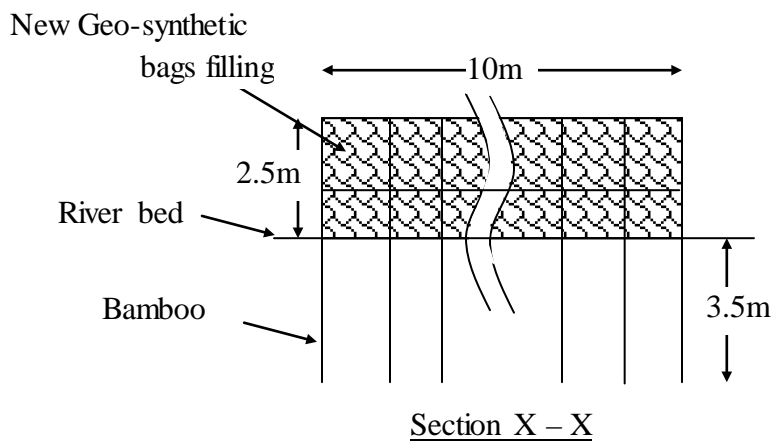


Fig. 6.2 Typical Drawing of Polymer Rope Gabion Submerged Vane

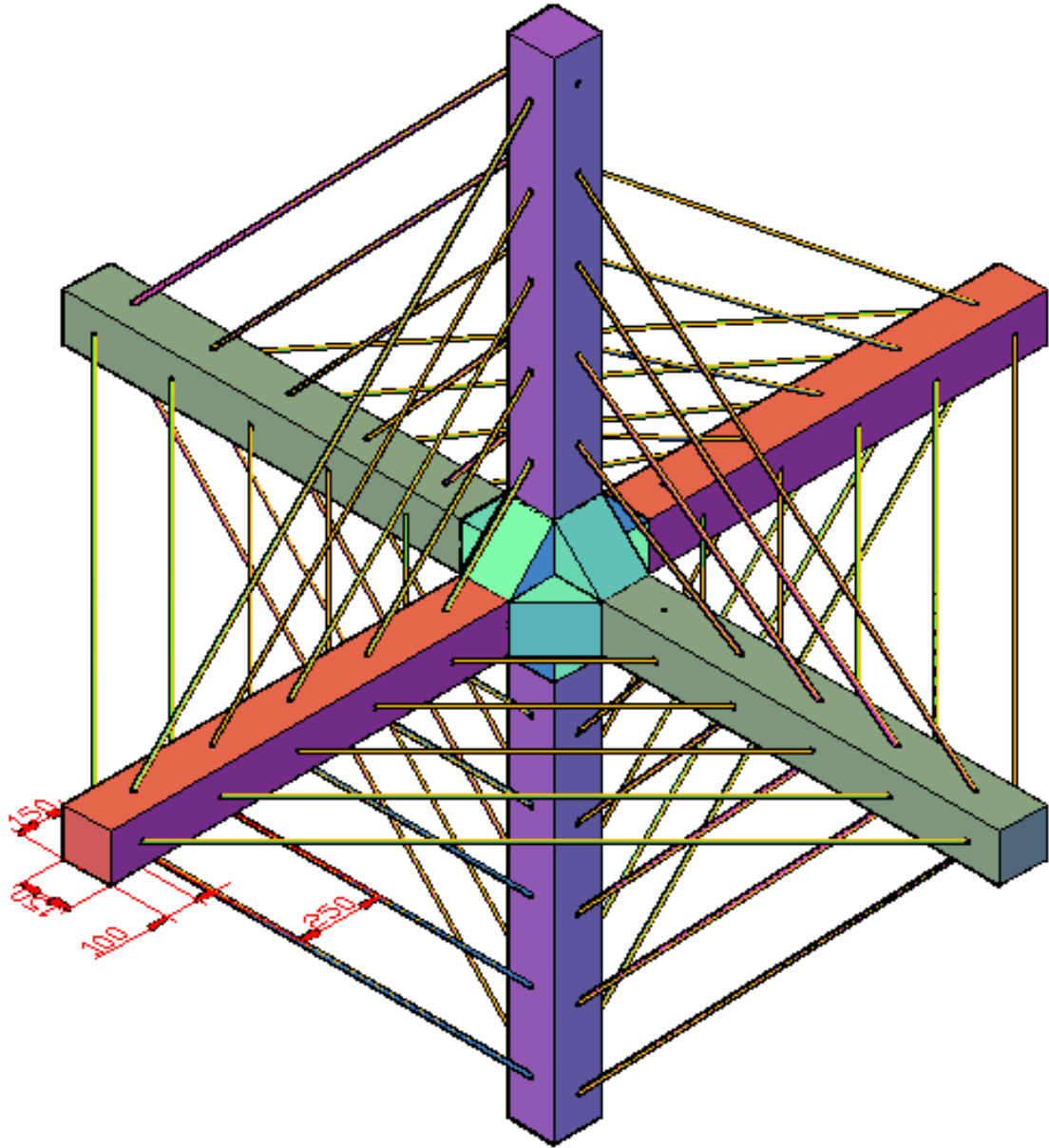
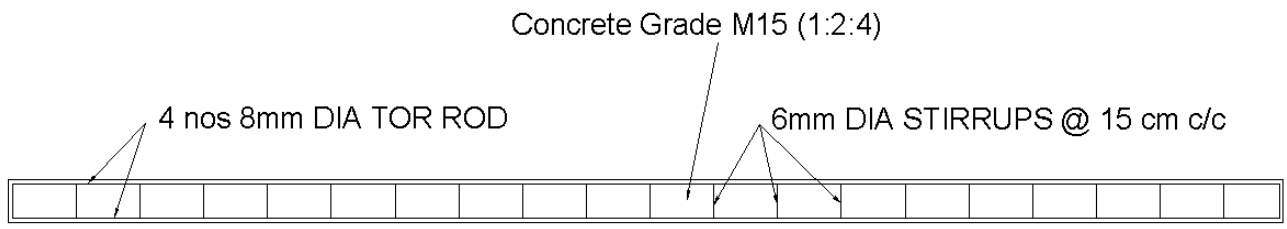
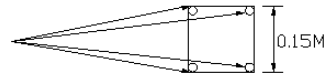


Fig. 6.3 Typical Layout of RCC Kellner Jetty of 3m length and 15cm thickness with 15cm x 15cm haunch at junction mesh with 4mm GI Wire



DETAILS OF LONGITUDINAL REINFORCEMENT
IN RCC KELLNER JETTY

4 nos 8mm DIA TOR ROD

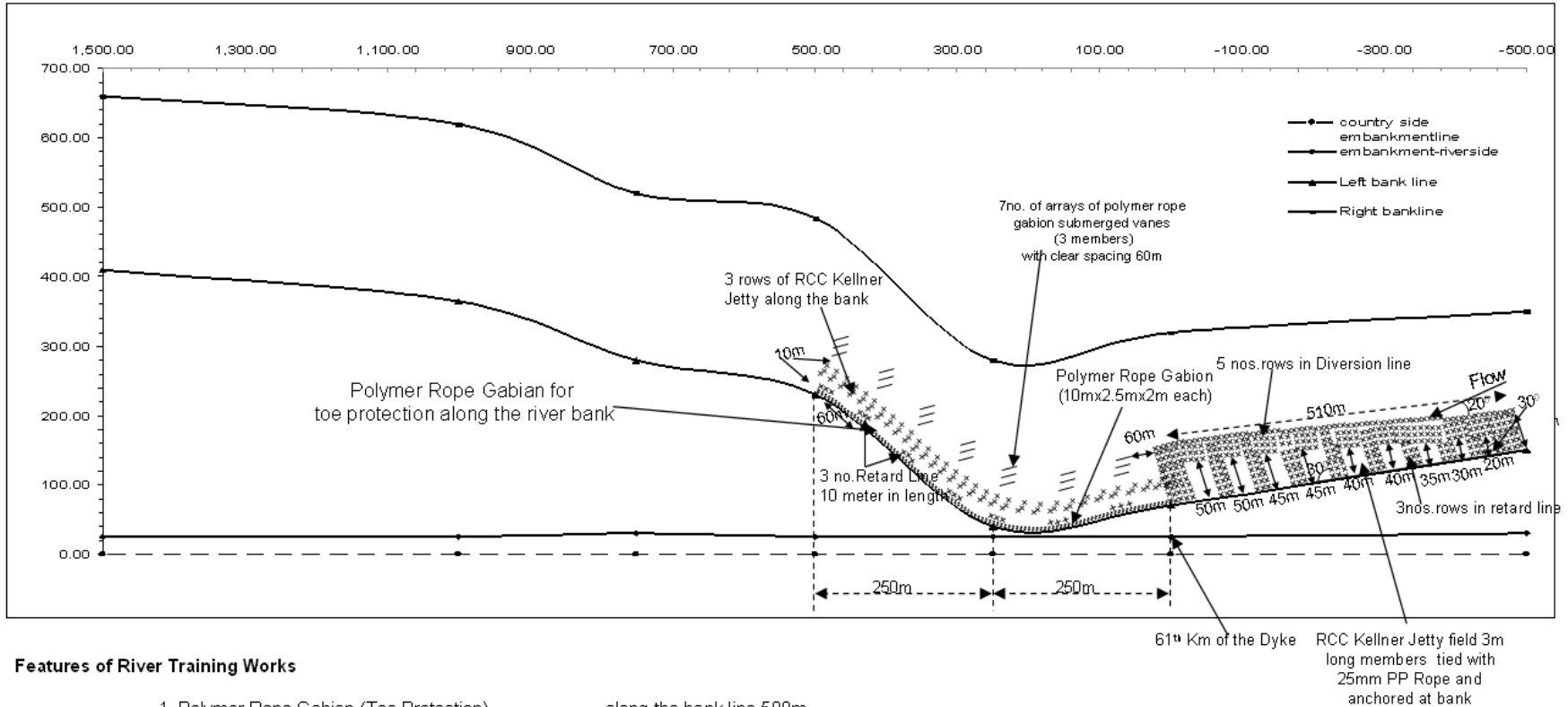


CROSS SECTION

Note: For other relevant details refer IS: 456-2000

Fig. 6.4 Details of Longitudinal Reinforcement in RCC Kellner Jetty

SCHEME FOR PILOT STUDY FOR EROSION CONTROL NEAR MORIGAON SITE



Features of River Training Works

- | | |
|---|--|
| <ol style="list-style-type: none"> 1. Polymer Rope Gabion (Toe Protection) 2. RCC Kellner Jetty 3. Submerged Vanes using Polymer Rope Gabion | <ul style="list-style-type: none"> - along the bank line 500m - along the bank line 500 m - 7 no. of arrays with 60m spacing along the channel lateral spacing 7 m C-C with striking angle 20° with dominant flow direction Clear spacing from vanes to RCC Kellner Jetty - 10 m |
|---|--|

Note: RCC Kellner jetty must be tied with 26mm Polypropylene Rope to each other through 3 inch 10 mm dia U type hook which is prefixed

Fig. 6.5 Detail Layout of Erosion Control Structures at Morigaon Site in the vicinity of 61st Km of the left Dyke

6.2 DESIGN PHILOSOPHY TO EVOLVE COST EFFECTIVE RIVER TRAINING MEASURES IN SITE OF THE BRAHMAPUTRA NEAR GAUWAHATI AIRPORT

6.2.1 PREAMBLE

For the purpose of experimental field study a drifting subsidiary channel of the Brahmaputra river hugging the Gauwahati airport(shown in the enclosed satellite imagery) has been adopted to test the river response as well as to effect required fine tuning to achieve efficacious results.

6.2.2 OBJECTIVES

The basic goal of the proposed field experimental study with very limited intervention is broadly spelt out below

1. To simulate the Brahmaputra river reach based on one dimensional numerical model developed by United States Hydrologic Engineering Center (USHEC) called HEC- RAS 4.1. The reach length span from Dubri, (Cross section 2) and Kobo, (Cross-section 65). Simulation of flow includes the analysis of stream bed aggradation and degradation behavior of the critical reach of the Brahmaputra River. Based on this flow simulation findings and experimental study, training measure are given below
2. to observe the effect of Jack Jetty Screen for effecting limited siltation and partial channel closure.
3. to test and evaluate the combined action of the package of measures comprising bamboo submerged vanes, RCC Jack Jetty field and bamboo board fencing on bank protection / near bank modification of fluvial parameter and near bank sedimentation. Obviously any limited achievement of near bank sedimentation is expected to facilitate & contribute towards land reclamation with the help of subsequent consolidation of sediment deposits.

6.2.3 HYDRAULICS OF PROPOSED TRAINING MEASURES

1. The submerged vane systems made of Jati bamboo is expected to generate desired secondary circulation in the stream flow to deflect the heavy sediment

laden bottom flow filaments towards the stream bank side resulting in sedimentation. The upper flow layers deficient in requisite sediment load are forced by the vane generated swirling vortices to move towards the channel centerline, thereby causing deepening of the streambed away from the bank. This radical modification of stream flow characteristics due to presence of submerged vanes acts as a catalyst in desired reshaping of channel topography. It may be highlighted here that the above radical transformation involving reversal of flow vortex direction cannot possibly be achieved through the conventional spur/ groyne system or any other flow retarding devices such as porcupine screens or permeable spur.

2. The deflected heavy sediment laden flow layers coming from the submerged vanes will be intercepted by the jack jetty field comprising the diversion lines & the retards to further assist in the dissipation of residual flow energy. Obviously the slowed down sediment carrying flow will be induced to deposit its sediment load within the compartments of the jack jetty field.
4. To further help in the desired aim of sedimentation within the jetty field, improvised board fencing method will be put in place behind the jack jetty system & these improvised board fencing is proposed to be made of Jati bamboo which is locally available in abundance in Assam.

The above new river training structures presented through the attached four numbers of typical drawings which may be further modified appropriately at the time of implementation. The layout of the above river training systems can also be seen from the attached satellite imageries which also depict the channel changes occurring in the study area covering a period from 2005 – 2011.

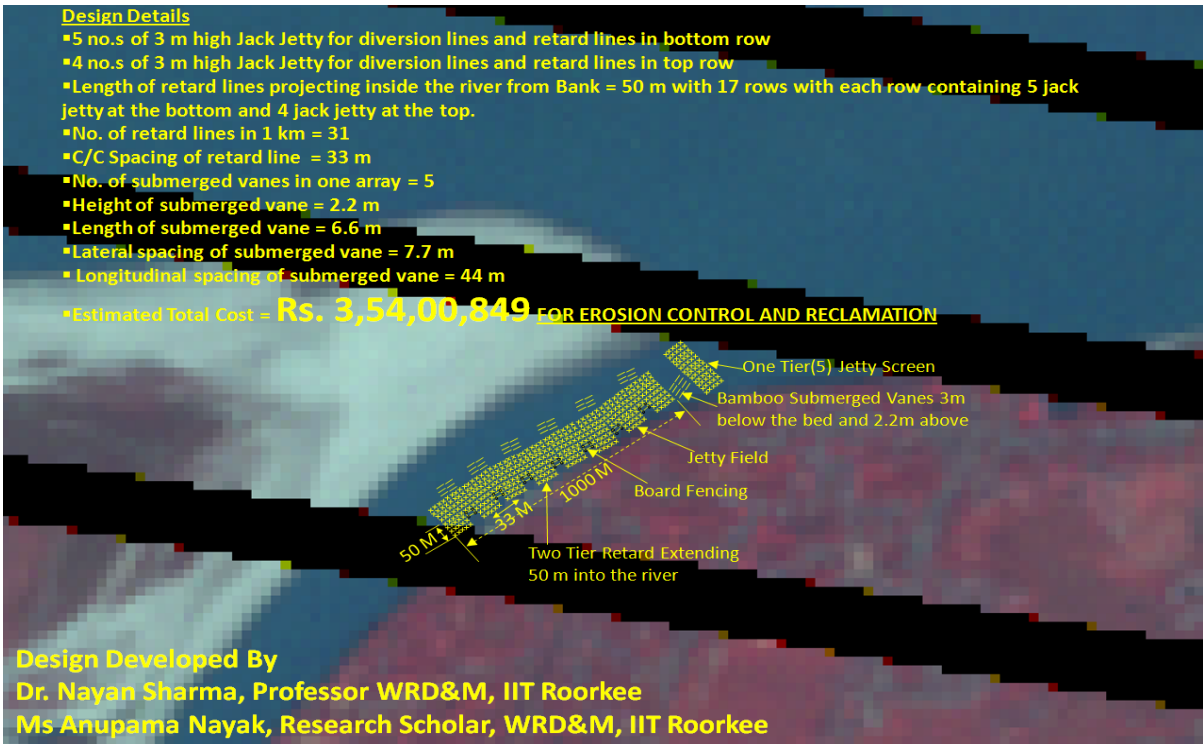


Fig. 6.6 Detail Layout Of River Erosion Control Structures At Proposed Site Of The Brahmaputra Near Gauwahati Airport

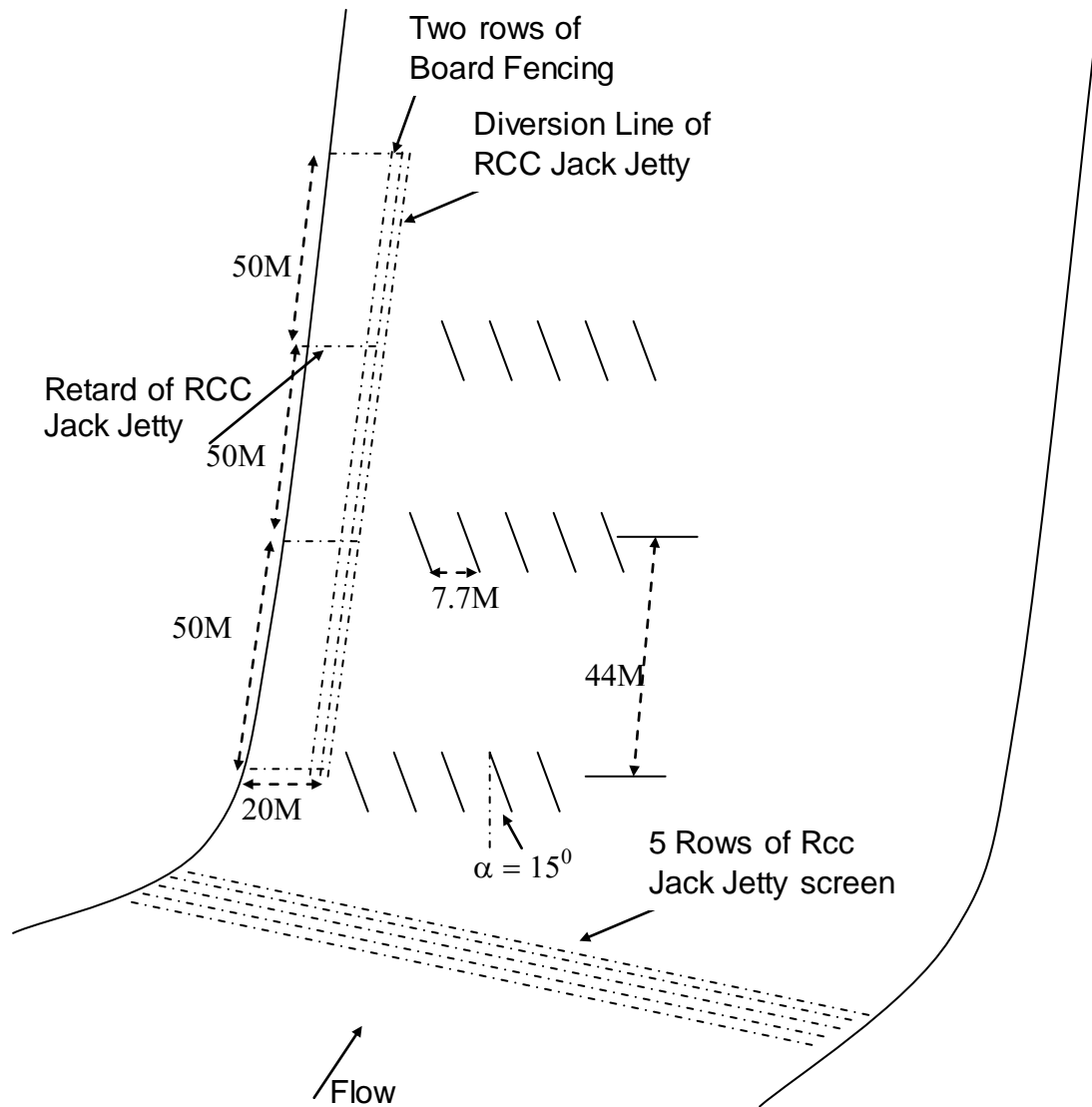


Fig. 6.7 Typical Drawings Of Submerged Vanes Board Fencing And RCC Jack Jetty For Brahmaputra River Near Guwahati Bridge

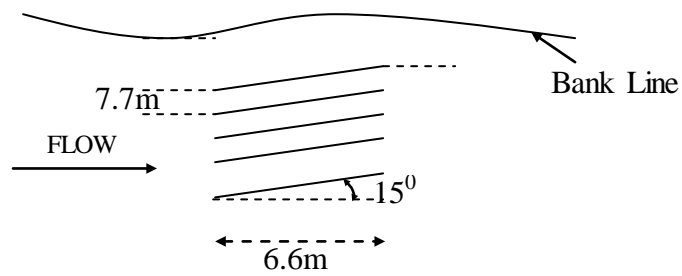
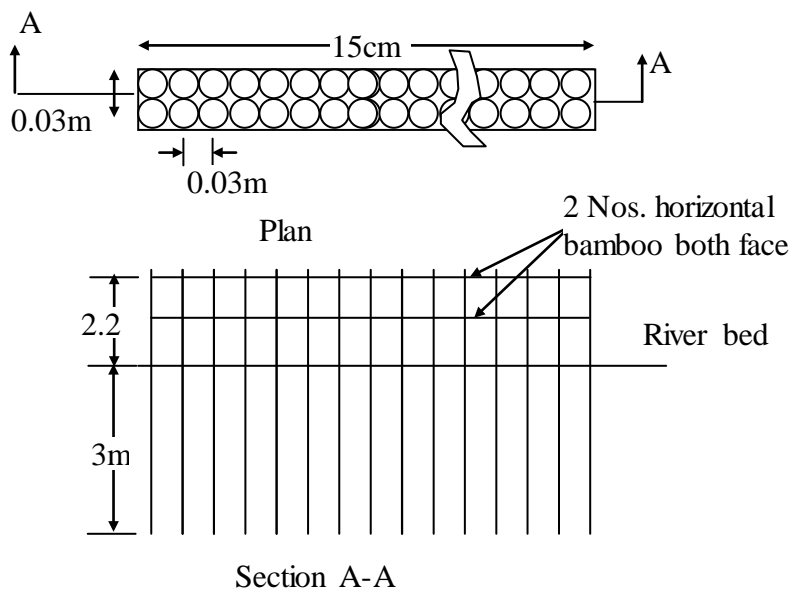
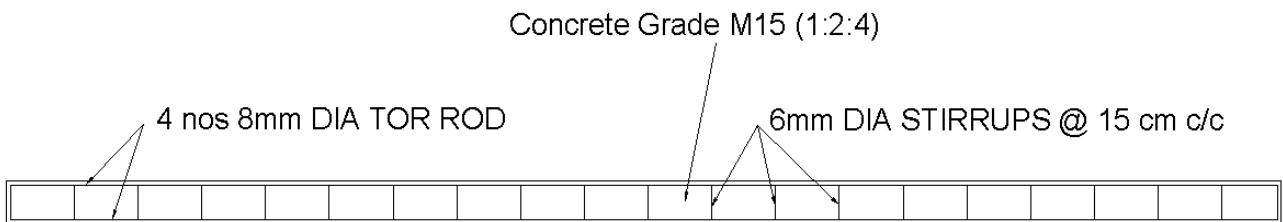
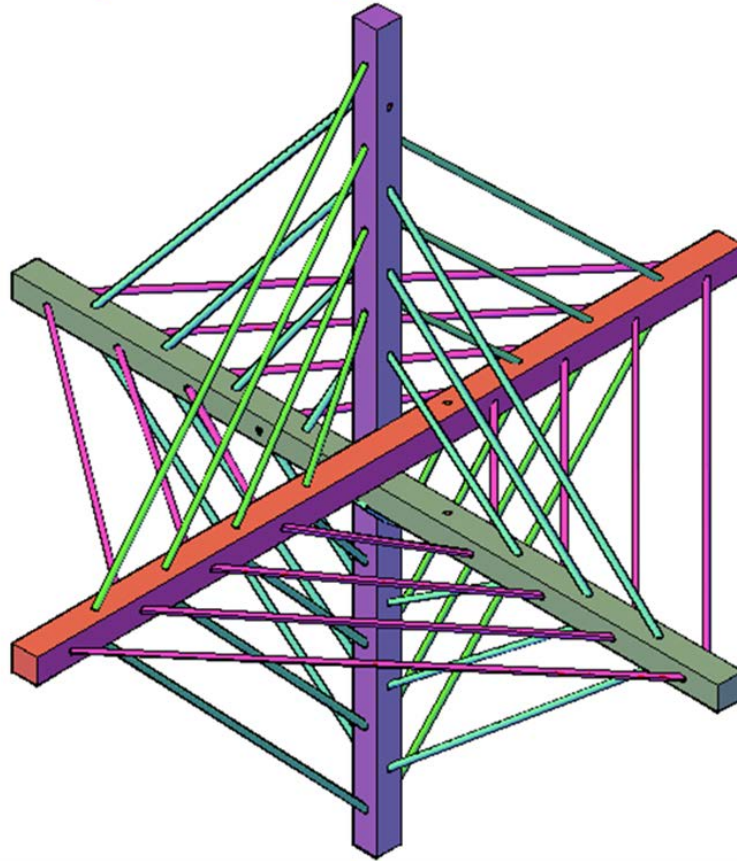


Fig. 6.8 Typical Layout of Bamboo Submerged Vane

Kellner Jetty of 3m length and 10 cm thickness



DETAILS OF LONGITUDINAL REINFORCEMENT IN RCC JACK JETTY



CROSS SECTION

Fig. 6.9 Typical Layout of RCC Kellner Jetty of 3m length and 15cm thickness with 4mm GI Wire

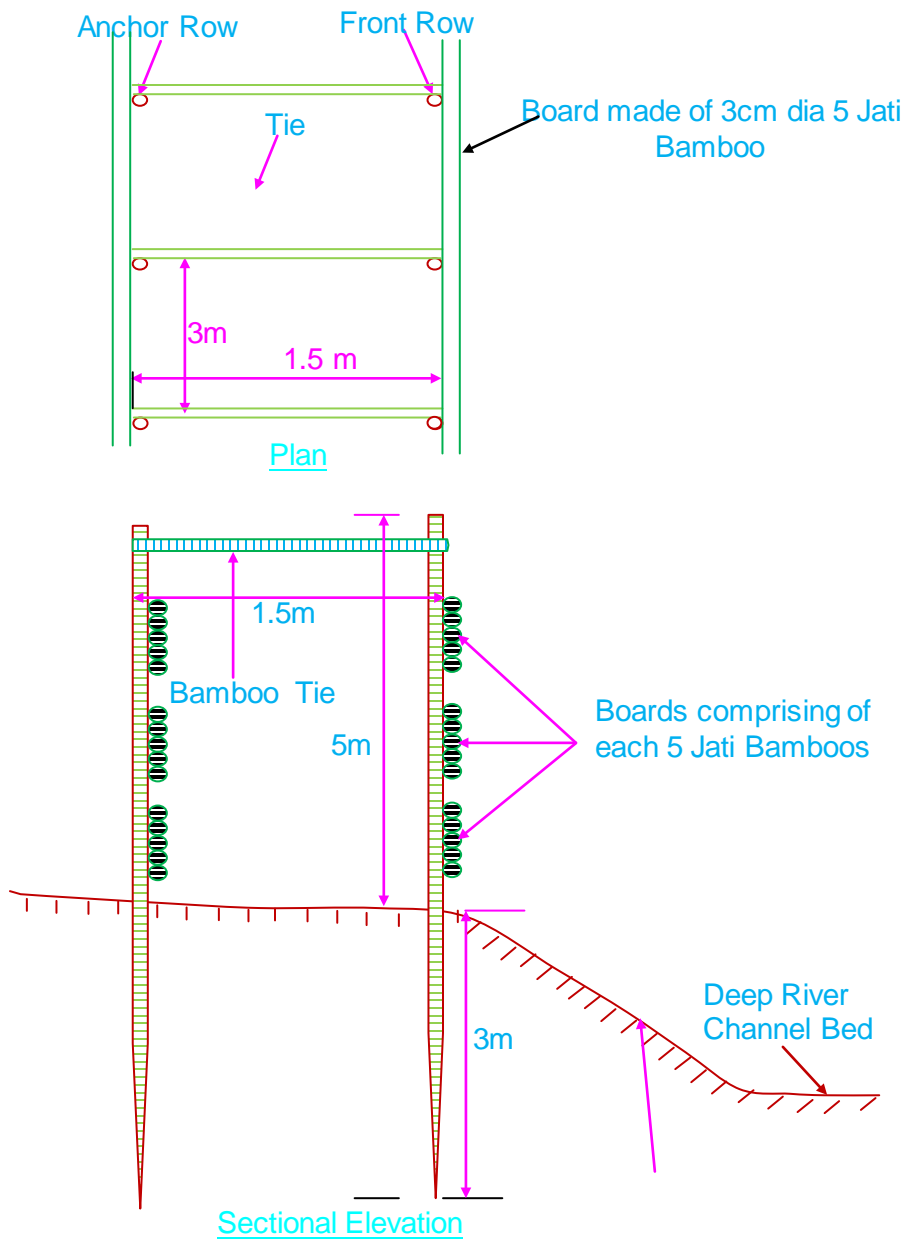


Fig. 6.10 Typical Layout of Board Fencing

6.2.4 COST ESTIMATE OF PROPOSED SITE OF THE BRAHMAPUTRA NEAR GAUWAHATI AIRPORT

6.2.4.1 Approximate Estimate of Jack Jetty

Width of river at left channel =	350	m
Size of one jack jetty =	3	m
No of jetties required in one row to cover the whole width of the river =	117	
No of jetties required in 5 row to cover the whole width of the river =	585	
No of jetties required in 4 rows in the second tier =	468	
Total no of jetties required to cover the whole width of the river =	1053	
Length of the river that is being protected by jetty field =	1000	m
No of jetties required in one row to cover the 1000m length of the river =	333	
No of jetties required in 5 row to cover the 1000m length of the river =	1665	
No of jetties required in one row on the second tier to cover the 1000m length of the river =	333	
No of jetties required in 4 row on the second tier to cover the 1000m length of the river =	1332	
Length of retard =	50	m
No of jetties required in one row of retard =	17	
No of jetties required in 5 rows of retards =	85	
No of jetties required in one row of retard on the second tier =	17	
No of jetties required in 4 rows of retards on the second tier =	68	
No of jetties required in one retard =	153	
Spacing of retards =	33	m
No of retards required to cover 1000m width of the river =	31	
Totals no of jetties required for the retards =	4743	
Total number of jack jetties required for jetty screen and jetty field =	8793	
Length of rope required for jetty screens in front =	3150	m
10%=	315	m
Length of rope required to tie each jack unit in diversion line jetty fields =	9000	m
10%=	900	m
Length of rope required to tie each jack unit in retard jetty fields =	13950	m
10%=	1395	m
Total length of rope to tie jack jetties =	28710	m
10% for dead man anchor =	2871	m
Total length of rope =	31581	m
Cost of one prestressed member =	950	RS
Cost of three prestressed members =	2850	RS
Apprx. Cost of one jack jetty is =	2850	RS
Cost of jack jetties is =	25060050	RS
Cost of rope per metre =	140	RS
Total Cost of rope =	4421340	RS
Total cost of jack jetties =	29481390	RS

6.2.4.2 Approximate Cost Estimate of Submerged Vane

Width of river covered by vanes =	35	m
-----------------------------------	----	---

Average depth of water just downstream of Brahmapitra bridge =	5	m
Height of vane =	2.2	m
Length of vane =	6.6	m
Vane to vane distance =	7.7	m
No of vanes in an array =	5	m
Distance between two arrays =	44	m
Total no of arrays in 1000m =	23	Nos
Total number of vanes =	115	Nos
No of vanes at entry =	10	Nos
Total number of vanes in the study site =	125	Nos
Depth of bamboo below river bed =	3	m
Height of bamboo above river bed =	2.2	m
size of one Jati bamboo =	7.6	m
Cost of one Jati bamboo =	60	Rs
No of bamboo in one vane =	5	
Cost of one Vane =	300	RS
Cost of submerged Vanes =	37500	RS
	Rs	37,500

6.2.4.3 Approximate Cost Estimate for Board Fencing

Length of river to be covered =	1000	m
Length of one bamboo =	7.6	m
Dia of one bamboo=	3	cm
Dia of cluster of 5 bamboos =	15	
Depth of bamboo below river bed =	3	m
Height of bamboo above river bed =	5	m
Noof bamboo clusters required for anchor to cover the required length of river =	466	
No of bamboo clusters required for main to cover the required length of river =	466	
No of horizontal bamboo clusters required along depth =	17	
No of bamboo clusters required horizontally to cover the entire required length of river both for main and anchor =	4474	
No of ties required =	1564	
Total number of bamboo clusters required =	6970	
Cost of one bamboo cluster =	300	RS
Cost of board fencing =	2091000	RS
	Rs	20,91,000
Rate for driving the bamboo by water jetty technique=	425700	RS
Expense for site visit =	147000	RS
Approximate total cost =	32182590	RS
	Rs	2,70,59,790
10%=	3218259	RS
Approximate total cost =	35400849	RS
	Rs	3,54,00,849

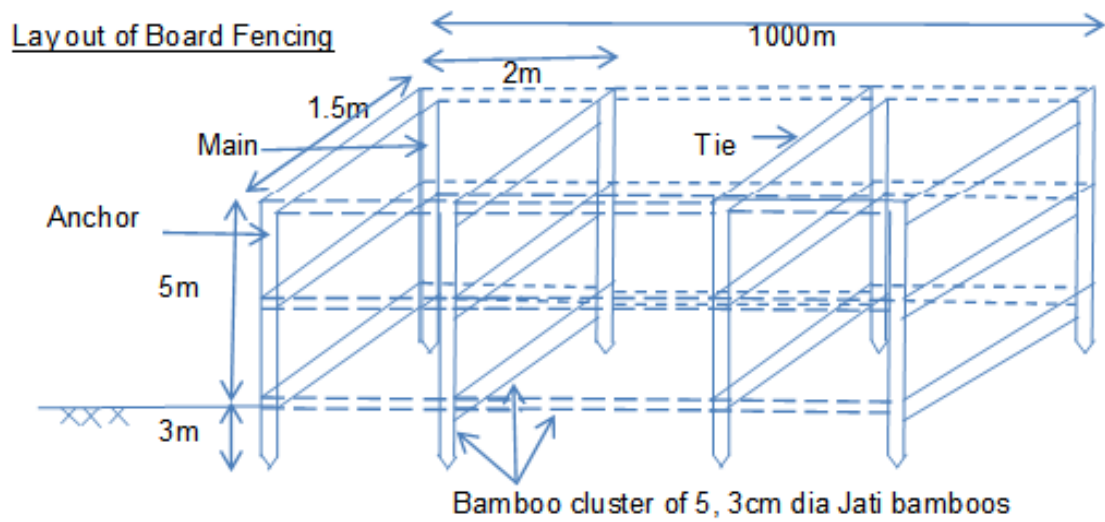
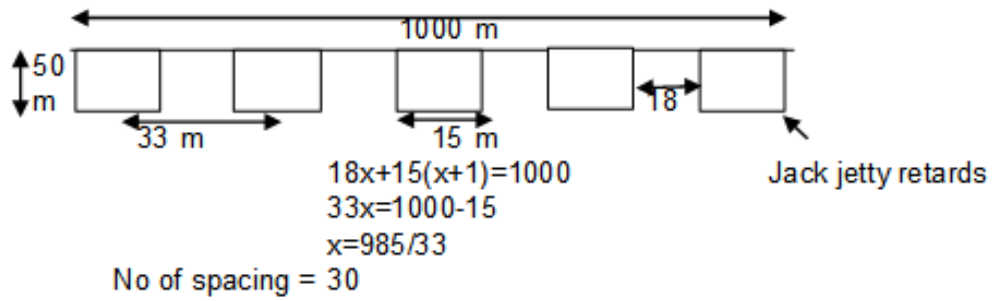


Fig. 6.11 Layout of Board Fencing

CHAPTER – 7

SUMMARY

SUMMARY

Using HEC-RAS 4.1 latest version of 'River Analysis System' whole reach of Brahmaputra River from Dhubri(Cross section 2) to Kobo(Cross section 65)extending a length of 622km is modeled and flow in simulation is done. The model is calibrated for seasonal variation of roughness coefficient. Based on the output of this one dimensional numerical model, analysis of stream bed aggradation and degradation behavior of critical reach of the Brahmaputra River is performed. Model output is used as supplementary information for river training work for erosion studies. This model can also be used for flood propagation study with unsteady flow analysis option and for specific bed configuration.

River training works is proposed for two pilot areas on Brahmaputra River. Those pilot areas are, near Airport of Guwahati Bridge and Morigaon site. The proposed river training work includes observing the effect of Jack Jetty Screen for effecting limited siltation and partial channel closure and to test and evaluate the combined action of the package of measures comprising bamboo submerged vanes, RCC Jack Jetty field and bamboo board fencing on the bank protection/ near bank modification of fluvial parameter and near bank sedimentation.

Obviously any limited achievement of near bank sedimentation is expected to facilitate and contribute towards land reclamation with the help of subsequent consolidation of sediment deposits.

The submerged vane systems made of Jati bamboo is expected to generate desired secondary circulation in the stream flow to deflect the heavy sediment laden bottom flow filaments towards the stream bank side resulting in sedimentation. The deflected heavy sediment laden flow layers coming from the submerged vanes will be intercepted by the jack jetty field comprising the diversion lines and the retards to further assist in the dissipation of residual flow energy.

To further help in the desired aim of sedimentation within the jetty field, improvised board fencing method will be put in plane behind the jack jetty system and these improvised board fencing is proposed to be made of Jati bamboo which is locally available in abundance in Assam.

REFERENCES

REFERENCES

1. Ackers, P. and White, W. R. (1973), "Sediment Transport: New Approach and Analysis", *Journal of Hydraulics Division, ASCE* Vol. 99 No. HY.11.
2. Amin, M.I. and P. J. Murphy. (1981), Two Bed Load Formulas. *JHD, Proc. ASCE*, Vol. 107, No. HY-8.
3. Bagnold, R.A. (1966), "An approach to the sediment transport problem from general physics", *Geological survey professional paper 422-1 (USA)*.
4. Brunner Gary W. (2002), "HEC-RAS, River Analysis System Hydraulic Reference Manual" The U.S. Army Corps of Engineers' (HEC) 609 Second Street Davis, CA 95616-4687.
5. Brush, L. M. (Jr.) (1961), "Drainage Basins, channel and flow characteristics of selected streams in central Pennsylvania" *USGS Professional Paper 282F*.
6. Cao Z. and Carling P. A. (2002), "Mathematical modelling of alluvial rivers: reality and myth. Part 1: General review" *Proceedings of the Institution of Civil Engineers, Water & Maritime Engineering* 154, Issue 3 Pages 207-219.
7. Cao Z. and Carling P. A. (2002), "Mathematical modelling of alluvial rivers: reality and myth. Part 2: General review" *Proceedings of the Institution of Civil Engineers, Water & Maritime Engineering* 154, Issue 4 Pages 297-307.
8. Correia L. R. P., Krishnappan B. G. and Graf W. H. (1992), "Fully coupled unsteady mobile boundary flow model". *Journal of Hydraulic Engineering, ASCE*, 1992, 118, No. 3, 476-494.
9. Chang H.H. (1979), "Stream Power and River channel patterns", *ASCE Journal of Hydrologic Engineering*, Vol. 41, pp. 303-311.
10. Chang, H.H. "Modelling of River Channel Changes", *Journal of Hydraulics Division, ASCE*, Vol. 110, No. 2, February, 1984.
11. Chang, H.H. and Hill, J.C. (1976), "Computer Modelling of Erodible Flood Channels and Deltas, Model for erodable channel" *J. Hydraulics Division, ASCE*, 102(HY10), pp. 1461-1477

12. De Vries M. (1973), "River bed variations—aggradation and Degradation". Proceedings of an International Seminar on the Hydraulics of Alluvial Streams, IAHR, Delft, 1973, pp. 1–10.
13. Chen, Y.H., "Mathematical Modeling of water and Sediment Routing in Natural Channels", Dissertation presented to the department of Civil Engineering, Colorado State University, Fort Collins, Colorado, in partial fulfillment of the requirements for the degree of Doctor of Philosophy, 1973.
14. Colby, B. R. (1964), "Practical Computations of Bed Material Discharge". JHD, Proc. ASCE, Vol.90, HY-2.
15. Cunge, J. A., Holly, F. M., and Verwey, A. (1980), "Practical Aspects of Computational River Hydraulics", Pitman, London.
16. Dass, P., "Water and Sediment routing in non- uniform channels" Doctoral Dissertation submitted to Colorado State University, Fort Collins, Colorado, 1975.
17. Einstein H. A. (1950), "The Bed –Load Function for Sediment Transportation in Open Channel Flows" USDA, Tech. Bull. No. 1026.
18. Engelund, F., "Hydraulic Resistance of Alluvial Streams", Journal of Hydraulics Division, ASCE, Vol. 92, No. HY, February, 1966.
19. Engelund, F. and E. Hansen. (1967), "A Monogram on Sediment Transport in Alluvial Streams", Teknisk Forlag, Denmark, 1967.
20. Garde, R. J. (1982), "Longitudinal profile on an alluvial Stream in" Engineering Geoscience Ed. B.B.S. Singhal. Sarita Prakashan, New Delhi.
21. Garde R.J. and Ranga Raju K.G. (2000), "Mechanics of Sediment Transportation and Alluvial Stream Problems" (3e), New Age International Publishers, pp. 14-178, 271-308, 366-384, 381-406, 614-644.
22. Gerald C. Nanson and He Qing Huang (2007), "Least action principle, equilibrium states, iterative adjustment and the stability of alluvial channels", earth surface processes and landforms 2007, pp 923-942.
23. Gomez B. and Church M. (1989), "An assessment of bed load sediment transport formulae for gravel bed rivers". Water Resource Research, 1989, 25, No. 6, 1161–1186.
24. Gordon E. Grant (1997), "Critical flow constrains flow hydraulics in mobile-bed streams: A new hypothesis water resources research", vol. 33, no.2 pp. 349-358.

25. Graf W.H (1971). "Hydraulics of sediment transport", McGraw-Hill, New York.
26. Goswami, D.C., (1985), "Brahmaputra River, Assam, India: Physiography, Basin Denudation, and Channel Aggradation", Water Resources Research, V-21, pp. 959-978
27. Goswami, D.C. and Das, P.J., (2000), "Report on some characteristics of high flow and low flow in the Brahmaputra River", India, Guwahati University.
28. Guidelines for the calibration and application of computer program HEC-6, (1981), US Army Corps of Engineers, Training doc. No 13.
29. Hack,J.J (1962) "Study of Longitudinal Stream Profiles in Virginia and Maryland",USGS Prof. Paper 500-A.
30. Hec-Ras River Analysis System User's Manual Version 4.0 beta (2006), US Army Corps Of Engineers Institute of Water Resources, HEC, CA- 95616.
31. Hinds, Julian. (1928), "The Hydraulic Design of Flume and Siphon Transitions," Transactions of the American Society of Civil Engineers, vol. 92, New York, NY.
32. Karamisheva et al (2006), "Sediment transport formulae for compound channel flow", proceeding of institution of civil engineering, Water Management 159, Issue WM3 pp.183-193.
33. King, Horace W. and Brater, Ernest F. (1963), Handbook of Hydraulics, McGraw-Hill Book. Company, Inc., New York, NY.
34. Laursen,E.M,(1958), "Total Sediment Load of Streams. JHD,Proc. ASCE,Vol.84, N0.HY- 1.
35. Lyn D. A. (1987), "unsteady sediment transport modelling", Journal of Hydraulic Engineering, ASCE, 1987, 113, No. 1, 1-15.
36. Meyer-Peter,E and R. Müller.(1948), "Formulas for Bed Load Transport", Proc. IAHR,2nd Congress , Stockhom.
37. Mike-11 user guide (2003), Edition, June 2003.
38. Sarma J. N. (2005), "Fluvial process and morphology of the Brahmaputra River in Assam, India", Science Direct, Geomorphology 70 (2005) p-226- 256.
39. Shankua R.N (2006), "ANN based Spatio-Temporal Morphological Model of the river Brahmaputra", Ph.D Thesis I.I.T Roorkee.
40. Sinha Rajiv (2005), "Why do Gangetic Rivers aggrade or degrade?" Current Science, VOL. 89, No. 5.

41. Toffaleti, F. B. (1969), "Definitive Computations of Sand Discharge in rivers", JHD, Proc. ASCE, Vol.95, No. HY-1.
42. U.S. Army Corps of Engineers, Hydrologic Engineering Center (HEC), (1990a), "HEC-2, Water Surface Profiles User's Manual," Davis, CA.
43. WAPCOS, (1993), "Morphological studies of river Brahmaputra", New Delhi.
44. Warner et al (2002), "HEC-RAS, River Analysis System Applications Guide", US Army Corps of Engineers Hydrologic Engineering Center (HEC) 609 Second Street Davis, CA 95616-4687.
45. Wu W., Rodi W. and Wenka T. (2000), "3D numerical modelling of flow and sediment transport in open channels", Journal of Hydraulic Engineering, ASCE, 2000, 126, No. 1, 4-15.
46. Yang, C.T. (1973), "Incipient Motion and Sediment transport". JHD, Proc. ASCE, Vol.99, No HY-10.
47. Yang C. T. and Wan, S., (1991), "Comparisons of Selected Bed-Material Load Formulas," ASCE Journal of Hydraulic Engineering, Vol. 117, No. 8, pp. 973-989.
48. Yang C.T., (1976), "Minimum Unit Stream Power and Fluvial Hydraulics" ASCE Journal of Hydraulic Division, Vol.102 NO. HY7, pp.919-933.

**FINAL
RECOMMENDATIONS**

1. Data analysis and computer simulation studies conducted in the present study have succinctly brought out that the prime causative factor of stream bank erosion vis-à-vis channel instability processes of the Brahmaputra can be attributed to inherent “sediment overloading” of the river fluvial system. In the light of aforesaid observation, it is recommended to effectively control sediment ingress into the Brahmaputra river system through comprehensive watershed management as well as development programme.
2. In view of the fact that extensive extent of stream bank-line is under grip of unabated erosion process, it is recommended to deploy cost-effective erosion control measures, namely single or multiple tier *Jack Jetty system* along with *submerged vanes* as per site condition feasibility. The required layout of *Jack Jetty* field may be appropriately devised by carefully considering the suitable *Jack Jetty Density Index (JJDI)* and *Jack Jetty Submergence Index (JJSI)* at the time of implementation of field pilot schemes after duly accounting for the prevailing river configuration.
3. The braiding phenomenon of the Brahmaputra has displayed a sharply increasing trend in the recent decades giving rise to highly disturbing incidence of channel instability in the wake of stream bank erosion process. It is recommended to urgently undertake measures to control the rise of braiding intensity through effective closures of subsidiary channels with the help of *Jack Jetty Screen* and *submerged vanes* protected by *Reno Mattress*.
4. To start with, field pilot studies may be undertaken at two sites – one near *Morigaon (Bhuragaon)* and the other near *Guwahati Airport* for which preliminary designs have been evolved. The preliminary design may be fine tuned at the time of implementation as mentioned at para 2 above, as well as after critically reviewing their performance in the post flood season.
5. The R&D endeavour of the present study to evolve *ANN* models for simulating watershed hydrologic response for runoff and sediment is found to be quite encouraging. It is recommended to use and periodically improve these models with availability of more field data in future.
6. The mathematical model developed with the help of *HEC-RAS 4.1* may be used on trial basis to start with for flood forecasting and preliminary channel improvement purposes. However, an exclusive comprehensive study is recommended to develop a fully moveable

bed and bank erosion model which duly accounts for complex flow phenomena such as secondary flow, vortex formation, turbulence & mass dispersion, fluvial transients of water and sediment, and morphodynamic fluxes as per state-of-the-art.

7. On account of the prevalent inadequacy of reliable and consistent field data, modelling in relation to erosion, sediment inflow and flood forecasting may have certain elements of inconsistencies and discrepancies, resulting in fallacious prediction of future scenario. It urgently warrants strengthening and upgrading of existing data acquisition and processing infrastructure at the ground level of the concerned agencies. Following equipment/data should urgently be procured for the existing or proposed data acquisition establishments of the field agencies / organizations.

(i) Data acquisition instruments –

a. Acoustic Doppler Current Profilers (ADCPs)

b. Ultrasonic Flow Meter / Fluorometer

c. Latest Sediment Sampler

d. Portable Suspended Sediment Analyzer

e. Laser Particle Size Analyzer

f. Total Station and GPS

g. Automatic Gauge Level Recorder

(ii) Upgrading of Surveyed Hydrographic Data

a. Survey of cross sectional data interval should be of the order of 500m at least between two given sections for good quality mathematical model development and analysis.

b. The cross-sections survey should be updated regularly (at say every five years interval) depending on observed hydrological events

c. Flow measurements for high flood events

(iii) Optical and Microwave Satellite Data Procurement

a. For monitoring and change detection of spatial and temporal features in the river and in the basin including flood plain.

(iv) Improving the spatial density of hydro-meteorological data acquisition network

- a. Hydrological data (Stage, Discharge & Sediment) observation stations may be increased by including / restoring sites near Tezpur (Koliabhomora Bridge) , Bessamara (Majuli), Bogibeel (New Bridge near Dibrugarh), in addition to the existing sites at Pandu & Jogighopa
 - b. The spatial density of Meteorological stations requires to be significantly upgraded along with installation of the latest data acquisition and data logging systems.
- (v) Development of Management Information System (MIS) for main stem Brahmaputra along with the flood plain / catchments, tributaries
8. Capacity building of the technical manpower associated at various levels of river management is recommended through periodic professional training on latest advances in the technology
 9. Creation of a comprehensive data base comprising all pertinent data & information using latest data management system.
 10. Establishment of an autonomous well-equipped R&D Centre to be manned by highly competent manpower for conducting applied research at state-of-the-art level.
